Mechanism of How Plants Sense Cold in Natural Environments

Hayato HIRAKI

Division of Thermo-Biosystem Relations,
Specialty of Cryobiosystems Science,
The United Graduate School of Agricultural Sciences,
Iwate University

2019.03

Contents

Chapter 1

Summary

General introduction **8**

Biotic and abiotic stresses, and Ca^{2+} signals 8

Physiology of freezing stress and cold acclimation 9

Transduction of Ca^{2+} signals in cold acclimation 10

Encoding and decoding of the Ca^{2+} signals 11

Crosstalk of Ca^{2+} signal 12

Cold acclimation treatment: views from Ca^{2+} signals 12

Goal of this study 13

Chapter 2

Development of the Observation System of Ca^{2+} Signals under the Cooling in Intact Plant

Abstract **16**

Introduction **17**

Materials **18**

Development of the experimental system 18

Sample preparation 18

Ca^{2+} signal measurement, correction for temperature, and data analysis 19

Discussion **20**

Importance of temperature corrections for the Ca^{2+} sensor proteins 20

Advantages of the observation systems 21

Chapter 3

Calcium Signaling-Linked *CBF/DREB1* Gene Expression Was Induced Depending on the Temperature Fluctuation in the Field: Views from the Natural Condition of Cold Acclimation

Abstract **29**

Introduction **30**

Materials and Methods **31**

Results and Discussion **33**

Cold-induced Ca^{2+} signals of root cells in simple cooling conditions 33

Effect of temperature fluctuation on Ca^{2+} signals 36

Comparison of Ca^{2+} signals between leaf and root cells 37

Expression of *CBF/DREB1* genes in the field and Ca^{2+} signals 40

Conclusion 43

Chapter 4

Effect of the Temperature Cycle and Fluctuation during Cold Acclimation Treatment on Gene Expressions and Freezing Tolerance in Arabidopsis

Abstract **68**

Introduction **69**

Materials and Methods **71**

Results **73**

Freezing tolerance in the three Arabidopsis accessions 73

Temperature changes of the three cold acclimation treatments in Col-0 74

Effect of temperature cycle and fluctuation on the electrolyte leakage values 75

Gene expressions induced by three kinds of cold acclimation treatments 75

Inhibition of gene expressions by Ca^{2+} channel blockers in three acclimation treatments 76

Discussion **77**

Freezing tolerance in the three Arabidopsis accessions after conventional cold acclimation and temperature fluctuating cold acclimation treatment 77
Three acclimation settings and natural environment 77
Effect of temperature cycle and temperature fluctuation on freezing tolerance 78
Effect of temperature cycle and temperature fluctuation on gene expressions 79
Conclusion 81

Chapter 5
Season Specificity in the Cold-Induced Calcium Signal and the Volatile Chemicals in the Atmosphere
Abstract 99
Introduction 100
Materials and Methods 101
Results 102
Discussion 105
Seasonal changes in Ca^{2+} signals and cold acclimation 105
Estimation of candidate factors which cause the seasonal changes of Ca^{2+} signal 106
Ethylene is one of the candidate substances 107
Conclusion 108

Chapter 6
Soft X-ray Spectromicroscopy: A Versatile Tool to Probe Plant Ion Distribution
Abstract 121
Introduction 122
Materials and Methods 123
Results and Discussion 124
Role of Ca^{2+} accumulation in the extracellular space and the vacuole 124
The experimental system 125
Conclusion 125

Chapter 7
General discussions 133
Advantage and originality of Ca^{2+} signal observation 133
Small range of cooling and slow cooling rate 133
Direct observation of the effect of the Ca^{2+} channel blockers 133
Eighteen facts in cold-induced Ca^{2+} signal in plant cells 134
Detailed explanation of the 18 facts of cold-induced Ca^{2+} signal in plant cells 135
Ca^{2+} signal and the balance of Ca^{2+} channel and Ca^{2+} pump 139
Ca^{2+} signal in several plant species 141
Role of the Ca^{2+} signal in cold acclimation process: from the aspect of the gene expression and freezing tolerance 143

Conclusion 150
Acknowledgements 151
Copyright 152
References 153

Chapter 1

Summary

Plants enhance their freezing tolerance by exposure to low-temperature. This phenomenon is known as cold acclimation (CA). Transient concentration change in cytosolic Ca^{2+} (i.e., Ca^{2+} signal) is widely accepted as a second messenger in CA process, especially in the response to the cooling. Several reports have shown the characteristics of the Ca^{2+} signal, and signal transduction. On the other hand, these studies were based on the artificial cooling and CA treatment, which hardly happens in the field. Therefore, it was difficult to conclude that Ca^{2+} signals could be used in response to small and slow temperature changes in the field.

To observe the Ca^{2+} signal which may be induced in the field condition, I developed the experimental system of cryomicroscope with Yellow Cameleon 3.60 expressing Arabidopsis. The cryomicroscope consists of laser scanning confocal microscope and cryostage / cryochamber. Since the fluorescent intensities of fluoresce protein are affected by the low-temperature, the correction formula was also established to compare the peak value of Ca^{2+} signal in different temperature. Using this system, I investigated the Ca^{2+} signal under several temperature conditions by combining the cooling rate, the start temperature and the cooling time duration. Although the clear Ca^{2+} signal has not been observed by the cooling with 3°C min^{-1} of cooling rate in root in the previous study, I succeeded in observing the Ca^{2+} signal with about 0.5°C min^{-1} of cooling rate in leaf. Since leaf is less responsive to cooling than root, the result updated our knowledge, and strongly supports the hypothesis that the Ca^{2+} signal is used as a messenger to relay the information of cooling from the cold receptor to transcriptional factors. Subsequently, in both root and leaf cells, Ca^{2+} signal rapidly disappear after stopping of the cooling and thereafter under a constant low-temperature; and no Ca^{2+} signal was observed after that. This result suggests that if the temperature is stable and constant, no Ca^{2+} signal is induced even during 2°C constant CA treatment except the initial temperature change from room temperature to the acclimation temperature. Thus, CA in the field, rich in temperature fluctuation, was performed in Morioka during the winter season to investigate the effect of the temperature changes during the CA process. In CA under field conditions, the expression patterns of *CBF/DREB1s* was distinctly different from in artificial CA. Pharmacological studies with Ca^{2+} channel blockers, $LaCl_3$ and ruthenium red, showed that the Ca^{2+}-induced expression of *CBF/DREB1s* was closely correlated with the amplitude of temperature fluctuation in minutes, suggesting that Ca^{2+} signals regulate *CBF/DREB1s* expression during CA under natural conditions.

To see the effect of the temperature fluctuation in minutes and the temperature cycle of day and night in the controlled environment, the special temperature settings of CA were established. I used the conventional CA at constant 2°C, 10°C-day and 2°C-night of temperature

cyclic CA (C–CA), and the 1°C range of temperature fluctuating cyclic CA (FC–CA). The Ca^{2+} channel blockers were used to examine the role of Ca^{2+} signal in each acclimation treatment. Freezing tolerance of the plants after C–CA and CA was almost same, and FC–CA resulted weakest freezing tolerance. On the other hand, the expression level of *CBF/DREB1s* was tended to be higher in order of CA, FC–CA and C–CA plants. In addition, the contribution of Ca^{2+} signal was higher in FC–CA and C–CA for freezing tolerance and FC–CA for gene expression. Furthermore, the Ca^{2+} signal enhanced *CBF1/DREB1B*, *CBF2/DREB1C* and *CBF3/DREB1A* in FC–CA, but suppressed the expression of *CBF2/DREB1C* and *CBF3/DREB1A* in C–CA. These results consistent with the results of experiments of the field CA described above. It had not been reported that Ca^{2+} signaling inhibited the gene expression level of *CBF/DREB1s* so far. Therefore, the experiments of FC–CA and C–CA suggested the existence of a novel Ca^{2+}-*CBF/DREB1s* pathway.

Surprisingly, Surprisingly, despite using Arabidopsis plants grown in a growth chamber, we observed a clear seasonal change in cold-induced Ca^{2+} signals only in roots. Ca^{2+} signals were captured using Arabidopsis expressing Yellow Cameleon 3.60. In winter, two Ca^{2+} signal peaks were observed during a cooling treatment from 20°C to 0°C, but in summer only one small peak was observed under the same cooling condition. In the spring and autumn seasons, an intermediate type of Ca^{2+} signal, which had a delayed first peak and smaller second peaks compared with the those of winter type, was observed. Volatile chemicals and/or particulates in the air from the outside may affect plants in the growth chamber; this idea is supported by the fact that incubation of plants with activated carbon changed the intermediate-type Ca^{2+} signal to the summer-type. There was also a weak correlation between the seasonal characteristics of the Ca^{2+} signal and the solar radiation intensity. It has been reported that the ethylene concentration in the atmosphere seasonally changes depending on the solar radiation intensity. Ethylene gas and 1-aminocyclopropane-1-carboxylic acid treatment affected the Ca^{2+} signals, the shape of which became a shape close to, but not the same as, the winter type from the intermediate type or the summer type, indicating that ethylene in the atmosphere may be one of several factors influencing the cold-induced Ca^{2+} signal.

Additionally, to study the change of the accumulation level of Ca^{2+} in the Ca^{2+} pools before and after the CA treatments, the soft X-ray spectromicroscopy beamline at the Canadian Light Source is equipped with a state-of-the-art scanning transmission X-ray microscope was used. CA treatment induced the Ca^{2+} accumulation in the extracellular space and vacuole, where is the main Ca^{2+} pools. It is considered that the Ca^{2+} influx through Ca^{2+} channels may be enhanced by increasing the osmolarity difference between cytosol and Ca^{2+} pools. In addition, when Ca^{2+} channel blockers, $LaCl_3$ and ruthenium red, were sprayed to investigate the role of Ca^{2+} signals for the Ca^{2+} accumulation, the blocker spray tended to decrease the Ca^{2+} accumulation after CA treatment, but increased after FC–CA. These results suggest that the

cooling without the Ca^{2+} signals may induce the Ca^{2+} accumulation in the extracellular space and the vacuole to fix the Ca^{2+} signaling. Taken together, plants might adapt Ca^{2+} signaling to the ambient temperature by regulating the Ca^{2+} concentration in the Ca^{2+} pools.

In conclusion, this study revealed that: (1) the Ca^{2+} signal is induced by the field-like cooling; (2) Ca^{2+} signals regulate the gene expression of *CBF/DREB1s* positively and negatively depending on the amplitude of temperature fluctuation; (3) the Ca^{2+} signal is suppressed during the summer and modified in the winter by exposure to volatile chemicals such as ethylene; and (4) there was the feedback between Ca^{2+} accumulation in the pools and Ca^{2+} signaling. Therefore, the Ca^{2+} signaling deeply contribute the sensing of the cold to regulate the physiological process of the CA, and will become a clue to understand how plant sense cold in natural environment.

General introduction

Calcium ion (Ca^{2+}) is common element of living organisms, and known as a second messenger in many responses. In mammal, it is famous fact that the transient cytosolic Ca^{2+} concentration change (i.e., Ca^{2+} signal) mediates the activity of a muscle and nerve system (Del Castillo and Stark, 1951; Hubbard, 1961; Shirokova *et al*., 1998). On the other hand, plants also regulate their physiological reaction via Ca^{2+} signals. Especially, the stomatal closure by the guard cells is controlled by the Ca^{2+} signals like a muscle (Allen *et al*., 2001; Nomura *et al*., 2008). Besides, it had been reported that the Ca^{2+} signal is one of the earliest responses for the stress (Knight *et al*., 1991, Knight *et al*., 1992). As plants do not have a nerve system, and temperature receptor have been not discovered, the Ca^{2+} signal in each cell becomes an important clue for "how plants accept stress such as temperature". Plants do not increase or sustain the tolerance under unstressed condition, because plants need to save the energy to grow and compete neighboring plants. Ca^{2+} signal may mediate the balance of growth and stress tolerance; and therefore, it is important to study the Ca^{2+} signals for not only plant's physiology understanding but also for improving agriculture production.

Biotic and abiotic stresses, and Ca^{2+} signals

Plants enhance their stress tolerance to survive the severe situation. Pathogen and wounding from insects are included in biotic stresses; and salt, drought, heat, strong light, cold and freezing are categorized to abiotic stresses (Sturz *et al*., 1997; Moffat, 2002; Mittler, 2006). Since plants are the sedentary, the environmental adaptability is essential function for plants. Among the several kinds of stresses, low-temperature stress has a devastating impact on crop productivity (Li and Sakai, 1982), because low-temperature limits plant growth and development (Thomashow, 1999). In addition, chilling and freezing include a few different kinds of stresses at the same time. Chilling and freezing stresses cause the osmic stress and the direct effect on metabolism in plant (Thomashow, 1999). The ice formation leads the transferring the intracellular water to the extracellular ice, and therefore extracellular freezing causes the dehydration stress (Steponkus, 1984).

It had been reported that Ca^{2+} signal was caused in several stresses (Trewaves and Knight, 1994; Bush, 1995; Braam *et al*., 1997; McAinsh *et al*., 1997; Sanders *et al*., 1999), and may act as a second messenger (Tuteja and Mahajan, 2007; Martí and Stancombe, 2013). The hypothesis that Ca^{2+} acts as a second messenger in cold sensing was supported by several reports which showed Ca^{2+} elevation induced by low-temperature stress and cold shock (Plieth *et al*., 1999; Knight and Knight, 2000). Knight *et al*. (1996) and Knight and Knight (2000)

revealed that there were two peaks in the cold-induced Ca^{2+} signal, and suggested that the first peak of the Ca^{2+} signal was mainly composed with the influx from extracellular space and the second peak was may be derived from the Ca^{2+} efflux from vacuole (i.e., intracellular organelles). Plieth *et al*. (1999) concluded that the temperature sensing was mainly dependent on the cooling rate whereas the absolute temperature was of less importance. Nagel-Volkmann *et al*. (2009) showed the similarity in the characteristics of cold-induced Ca^{2+} signals between the monocot (e.g., wheat) and dicot (e.g., Arabidopsis).

Furthermore, both the cold sensitive and insensitive plant can induce Ca^{2+} signal for the response to the cold (Knight *et al*., 1991; Campbell *et al.*, 1996; Plieth *et al.*, 1999; Nagel-Volkmann *et al*., 2009), but the cold sensitive plants cannot decrease Ca^{2+} concentration and restore quickly like the cold insensitive plants (Jian *et al*., 1999). Since Ca^{2+} has cytotoxicity (Kass and Orrenius, 1999), cell effuses Ca^{2+} using Ca^{2+} pumps which are activated by the specific concentration of Ca^{2+} (Keener and Sneyd, 1998). The prolonged increase of Ca^{2+} concentration causes the active oxygen species accumulation, metabolic dysfunction and structural damage (Monroy *et al*., 1993; Monroy and Dhindsa, 1995; Chen, 2000). These reports suggest that the formation of the Ca^{2+} signals under low temperature is involved in cold stress tolerance.

Taken together, the Ca^{2+} signals are closely involved in the low-temperature sensing of plants, and may influence in the cold and freezing tolerances.

Physiology of freezing stress and cold acclimation

The freezing temperature may cause extracellular and intracellular freezing, and cell death. The ice in extracellular space could result in disruption of cells and tissues, because the ice adheres directly to cell wall and cell membrane (Levitt, 1980). The ice formation also causes the mechanical stress and dehydration due to the transferring of intracellular water to extracellular ice (Steponkus, 1984). On the other hand, intracellular freezing is a lethal event for plant cells (Steponkus, 1984). Since chemical potential of ice is lower than that of water at the same subzero temperature, ice formation in extracellular space leads the water transfer from intracellular to extracellular. This is the cellular dehydration which is caused under the freezing stress (Levitt, 1980; Steponkus and Webb, 1992). The low-temperature inhibits the photosynthetic electron transport and enzymatic reactions. Under the condition of photoinhibition caused by the low-temperature, the reactive oxygen species (ROS) are released from PS II, and ROS damage chloroplast (Asada, 1996). These physiological stresses lead the cell death in sensitive plants and non-cold-acclimated plants.

Plants survive under the subzero temperature condition in winter by enhancement of

low temperature and freezing tolerance occurring during non-freezing temperature season. This phenomenon is known as cold acclimation (CA) (see Levitt, 1980; Thomashow, 1999). The process of the CA may start after plant cells sense low temperature. Arabidopsis increased in freezing tolerance from an initial 50% lethal temperature (LT_{50}) of about −3°C to LT_{50} of approximately −6°C after 1 day at 4°C, and achieved −8°C to −10°C LT_{50} value after 8 to 9 days at 4°C (Gilmour *et al*., 1988). Through CA process, plants change plasma membrane composition (Steponkus, 1984). For example, it has been reported that the CA induced the increase of fatty acid desaturation in membrane phospholipid and changes of membrane sterols and glucocerebrosides (Uemura and Yoshida, 1984; Yoshida and Uemura; 1984; Lynch and Steponkus 1987; Thomashow 1998). CA treatment also caused accumulation of compatible solute such as glycinebetaine, proline, soluble sugars (Koster and Lynch, 1992), and accumulated late embryogenesis abundant (LEA) proteins which protect protein higher-order structure (Welin *et al*., 1994). These extensive changes were regulated by transcription factors, such as C-repeat (CRT)-binding factor/dehydration-responsive element-binding protein 1 (CBF/DREB1) transcription factors (Liu *et al*., 1998; Thomashow, 1999).

Transduction of Ca^{2+} signals in cold acclimation

To sense the temperature changes, plants may use actin cytoskeleton and/or cell membrane fluidity. It is reported that membrane fluidization prevented Ca^{2+} influx and a cold acclimatization (CA)-specific gene expression at 4°C (Örvar *et al*., 2000). Conversely, membrane rigidification induced Ca^{2+} influx and a CA-specific gene expression even at 25°C in alfalfa (Örvar *et al*., 2000). In *Brassica napus*, the activity of cold-activation *BN115* promoter was suppressed by benzyl alcohol which caused membrane fluidization (Sangwan *et al*., 2001). They infer that the membrane fluidity was the important factor for temperature sensing and opening the Ca^{2+} channels.

Ca^{2+} signals are relayed by Ca^{2+}-binding proteins that act as Ca^{2+} sensors, which have Ca^{2+} specific binding domains such as EF hands (Luan *et al*., 2002). Calmodulin (CaM), Calmodulin B-like protein (CBL) and Ca^{2+} dependent protein kinases (CDPK) are the candidates of Ca^{2+} sensors (Luan *et al*., 2002; Batistic and Kudla, 2004). In fact, the cold responsive genes *KIN1* and *LTI78* were suppressed in CaM3 overexpression plant (Townley and Knight, 2002). In addition, the Ca^{2+} chelators, Ca^{2+} channel blockers, CaM inhibitor W7, and CDPK inhibitor H7, suppressed the expression level of *KIN1* and *KIN2* in Arabidopsis (Tähtiharju *et al*., 1997). Those kinds of inhibitors also suppressed the cold induced gene expression level of *CAS15* and *CAS18* in alfalfa (Monroy *et al*., 1993). These reports suggesting that CaMs and CDPK regulate gene expressions through Ca^{2+} signals. In consequence,

transgenic *Arabidopsis* plants overexpressing CDPK showed enhanced freezing tolerance (Chen *et al*., 2013). Furthermore, calcium/calmodulin-regulated receptor-like kinase (CRLK) knock-out mutants exhibited an increased sensitivity to chilling and freezing temperatures (Yang *et al*., 2010). Besides, it had been reported that calmodulin binding transcription activator (CAMTA) is the positive regulator of *CBF2/DREB1C* expression, and the double *camta1* and *camta3* mutant showed weak freezing tolerance compare with the wild-type (Doherty *et al*., 2009). Kidokoro *et al*. (2017) also reported that CAMTA3 and CAMTA5 function as transcriptional activator of *CBF1/DREB1B* and *CBF2/DREB1C*.

Transient changes in Ca^{2+} concentration also affects protein phosphorylation (Monroy *et al*., 1993; Monroy *et al*., 1998). Therefore, Ca^{2+} signals may contribute to a MAP kinase cascade. Janak *et al*. (1996) found that low-temperature and drought stress increased the activity of a MAP kinase in alfalfa. In addition, Teige *et al*. (2004) reported that the map kinase MKK2 mediate the cold and salt stress signals. They found that *mkk2* plant was hypersensitive to freezing and hardly germinated in salted medium, but MKK2 overexpressing plant showed hardiness to freezing and high salt.

Taken together, Ca^{2+} signals may be transduced to the information which regulate the CA process through the several pathways.

Encoding and decoding of the Ca^{2+} signals

Ca^{2+} signals are just the pattern of the increase and decrease of Ca^{2+} concentration, but induce specific responses in plants. It means that the primary stimulus must be encoded and decoded like a “language” in plant cells. For example, it has been reported that the Ca^{2+} signal controls stomatal closure depending on the frequency, transient number, duration and amplitude of the signal (Allen *et al*., 2001; Nomura *et al*., 2008). Furthermore, artificial Ca^{2+} signals which were caused by the abscisic acid (ABA) and extracellular Ca^{2+} concentration abolished stomatal closure in *Arabidopsis gca2* mutant which exhibits aberrant guard cell ABA signaling (Allen *et al*., 2001). When plants receive a stimulus, they response specifically to each stimulus. Most stimuli induces the Ca^{2+} signals, but the Ca^{2+} signals are specific in each stimulus (McAinsh *et al*., 1995; Allen *et al*., 2001; Love *et al*., 2004; Miwa *et al*., 2006; McAinsh and Pittman, 2009; Dodd *et al*., 2010; Short *et al*., 2012). Thus, it had been proposed that the Ca^{2+} signals encode information to identify the stimulus (Liu *et al*., 2015).

In fact, the three kinds of Ca^{2+} oscillations, a strong spike, high-frequency spikes, and weak prolonged elevation, activated different gene expression profiles (Whalley *et al*., 2011; Whalley and Knight, 2013). They used the artificial Ca^{2+} signals which were caused by the electric stimulation, and suggested that Ca^{2+} signals regulate the specific downstream reactions. The

approach combining experimental data with mathematical modelling revealed that Ca^{2+} signal was decoded, and regulate the expression of CAMTA-regulon genes depending on the history of the Ca^{2+} signal and Ca^{2+} accumulation during all the lifetime (Liu *et al*., 2015).

On the other hand, some researchers reviewed that Ca^{2+} signal acts as just a chemical switch. It means that Ca^{2+} signal itself does not encode specific information but is an essential switch in signaling (Scrase-Field and Knight, 2003). Sometimes, researchers tend to expect that plant also have the Ca^{2+} signaling in the muscle and nerves in animals. In particular, the Ca^{2+} signal related to stomatal closure resembles the Ca^{2+} signal in animal (Scrase-Field and Knight, 2003). Therefore, we should calmly examine the Ca^{2+} signal and the phenomenon which caused by the Ca^{2+} signal.

Crosstalk of Ca^{2+} signal

Crosstalk between Ca^{2+} signals and stimuli including Ca^{2+} concentration change was reported by many studies. The effect of ABA on the downstream responses via Ca^{2+} signals had been shown by several studies (Hamilton *et al.,* 2000; Rudd and Franklin-Tong, 2001; Finkelstein *et al*., 2002). Blue light also causes the transient Ca^{2+} increase via phototropins (phot1 and phot2) (Zhao *et al*., 2013). Ryanodine receptor (RyR) on the surface of endoplasmic reticulum and vacuole acts as a Ca^{2+} release channel. Slow vacuole channel (SV channel) also acts as a Ca^{2+} release channel. The calcium-sensing protein (CAS) of thylakoid membrane (Peltier *et al*., 2004; Vainonen *et al*., 2008; Nomura *et al*., 2008) induces extracellular Ca^{2+}-induced cytosolic Ca^{2+} increase process (Han *et al*., 2004; Nomura *et al*., 2008; Rocha and Vothknecht, 2012). In addition, it has been reported that chloroplast has ion channels such as ACA1, HMA1, MSL2/3 and GLR3.4 including the putative Ca^{2+} channels (Huang *et al*., 1993; Seigneurin-Berny *et al*., 2005; Haswell and Meyerowitz, 2006; Teardo *et al*., 2011; Hochmal *et al*., 2015).These Ca^{2+} release channels were activated by cytosolic Ca^{2+} increase so that Ca^{2+} signal was affected by itself (Wang *et al*., 2001; Haak *et al*., 2001; Sanders *et al*., 2002).

Cold acclimation treatment: views from Ca^{2+} signals

Researchers who work on cold acclimation use artificial CA treatment such as 2°C constant, but each research group uses a slightly different CA treatment. For example, there are reports using the following conditions: 2°C constant under a 12-h photoperiod (Yamazaki *et al*. 2008), 2°C constant at 8-h photoperiod (Uemura *et al*. 1995), 4°C constant under an 8-h photoperiod (Doherty *et al*. 2009), 4°C constant under a 12-h photoperiod (Dong *et al*. 2011), and 5°C-day and 2°C-night under a 12-h photoperiod (Uemura and Yoshida 1984). From the aspect

of Ca^{2+} signal, since Ca^{2+} signal always is induced by the cooling, constant temperature or small temperature differences in a day does not induce the Ca^{2+} signal during CA treatment. On the other hand, several Ca^{2+} signal pathways in CA process were revealed by using the constant low-temperature treatment. This is because every CA treatment include the rapid cooling from the room temperature to the acclimation temperature such as 2°C and 4°C when the CA treatment starts. The rapid cooling surely induces the Ca^{2+} signal, and the Ca^{2+} signal acts as a messenger. Therefore, the previous studies mainly focused on the roles of Ca^{2+} signal which was induced by the rapid cooling as an initial step of cold acclimation. For the next step of the study on Ca^{2+} signal involved in CA process, we need to focus on the role of Ca^{2+} signals which are induced by the small temperature fluctuation and slow cooling during CA.

Goal of this study

Research on Ca^{2+} signals has been reported as described above. On the other hand, there are many experiment conditions that are distinctly separated from the natural conditions and it is still unclear how the Ca^{2+} signal plays a role in the cold acclimation process in actual field. It is important to clarify the role of Ca^{2+} signal in cold acclimation process based on correct understanding of the characteristics of Ca^{2+} signal and how it works in the field, in other words, "how plants sense cold in the field." The research will deepen the understanding of the cold acclimation process and become an important step to consider agricultural application.

The research on Ca^{2+} signals in plants was actively done a few decades ago. Knight *et al*. (1991) succeeded in observing the Ca^{2+} signal in living cells by using Arabidopsis expressing aequorin. After establishing this method, mainly Dr. Knight's group worked on and developed the study of the cold-induced Ca^{2+} signal. They found several characteristics of the Ca^{2+} signals at low temperature. However, there are a few questions and points which should be answered and improved. Plieth *et al*. (1999) used a 3°C min^{-1} as the slowest cooling rate. However, such a fast cooling is not occurred often in the field (Figure 3.12c and 4.13b). They mentioned that the cooling with a 3°C min^{-1} of the cooling rate induced only prolonged Ca^{2+} signal without any peaks. Therefore, it is difficult to conclude that the Ca^{2+} signal is used as a second messenger in CA process in the field. In addition, in the report of Plieth *et al*. (1999), the authors observed cold-induced Ca^{2+} signals after the root part was cut and then cooled. Besides, in the report of Knight and Knight (2000), intact plants were observed, but were maintained floating in a solution. Furthermore, in many studies including Dr. Knight's group, the temperature correction of cold-induced Ca^{2+} signals has not performed even though Ca^{2+}-sensing aequorin protein is an enzyme and its reactions are affected by temperature.

To obtain the evidence which indicates that the Ca^{2+} signal is induced in the field and

acts as a messenger for inducing the gene expression related to cold acclimation, I conducted the following experiments.

1) Establishing the method to observe the Ca^{2+} signal with accurate temperature changes in root and leaf cells (Chapter 2).
2) Measurement of Ca^{2+} signal in root and leaf cells with the small and slow cooling (Chapter 3).
3) Analysis of the gene expression under CA treatment in the field with or without Ca^{2+} channel blockers (Chapter 3).
4) Determination of the effect of temperature cycle of day and night and temperature fluctuation in minutes during CA process and the role of the Ca^{2+} signals induced by the two temperature changes using the Ca^{2+} channel blockers (Chapter 4).
5) Exploration of the factor which causes the seasonal changes of Ca^{2+} signals discovered during my research (Chapter 5).
6) Consideration of the relationship between Ca^{2+} pools and Ca^{2+} signaling (Chapter 6).

Chapter 2

Development of the Observation System of Ca^{2+} Signals under the Cooling in Intact Plant

Abstract

For the sensing of the intracellular Ca^{2+} concentration change in plants, Ca^{2+}-sensitive luminescent protein, aequorin expressing plants were used in previous studies. Aequorin and CCD camera system can observe the wide area but the sensitivity and resolution are low. Here, to detect the Ca^{2+} in the plant cells in high sensitivity and resolution, fluorescence resonance energy transfer (FRET)-based Ca^{2+}sensor, Yellow Cameleon 3.60 expressing Arabidopsis was used. I developed the experimental system which can cool the intact plant under the confocal microscope by two types of cooling unit. One is cryostage which can control the temperature of small aluminum stage by using liquid N_2 and heater following by the computer program and used for root observation. Root part of the plant was sealed between two slide grasses with 100 μL of buffer and put on the stage. The other is cryochamber. It consists of the ethanol circulator and jacked beaker. The temperature of the ethanol is controlled by the circulator following the computer program and the ethanol goes through the jacketed beaker. The air temperature around the plant in the bottom of the beaker changes depending on the temperature of surrounding ethanol. The cryochamber was used for leaf observation. These two types of observation system allow us to know the cold induced-Ca^{2+} signals under the microscopic level in intact plant. In addition, since the FRET efficiency is affected by the temperature, I established the temperature correction formula. By using this formula, we can compare the Ca^{2+} signals at different absolute temperatures. Thus, this observation system is optimal for the time laps Ca^{2+} signals observation in intact plant with temperature changes.

Introduction

With the advent of the aequorin-expressing plants, the research on the live image of cytosolic Ca^{2+} has been developed. Aequorin is a Ca^{2+}-sensitive luminescent protein from jelly fish *Aequorea victoria* (Shimomura *et al.*, 1962). Knight *et al*. (1991) succeeded in establishing the plants expressing aequorin, and reported that touch, cold-shock, and fungal elicitors induced Ca^{2+} concentration change in the cytosol (Knight *et al*., 1991). Cold-induced Ca^{2+} signals have been studied mainly in the Knight's group in detail (Knight et al., 1991; Knight et al., 1996; Plieth *et al*., 1999; Knight and Knight, 2000; Nagel-Volkmann *et al*., 2009). Knight's group examined various temperature parameters affecting Ca^{2+} signals using their experimental systems based on the aequorin-expressing plants and a luminometer with a Peltier element.

In 2004, a novel fluorescence resonance energy transfer (FRET)-based Ca^{2+} sensor, Yellow Cameleon (YC) 3.60 was established (Nagai *et al.,* 2004). YC3.60 was based on GFP variants, known as fluorescence proteins (cpVenus and ECFP), and calmodulin (CaM). Two fluorescent proteins were bound with a glycylglycine linker, a CaM and a CaM-binding peptide of myosin light-chain kinase (M13). Usually, 408 nm laser exited only ECFP of YC3.60, but when CaM bind to Ca^{2+}, the fluorescence energy of ECFP transferred to cpVenus. The fluorescence changes of cpVenus and ECFP indicate the concentration change in Ca^{2+} (Figure 2.1). Krebs *et al*. (2012) provided the powerful tool: stable YC3.60-expressing Arabidopsis by the UBQ10 promoter. Since YC3.60 is a kind of fluorescence protein, microscopic analysis is available. This is the advantage of the YC3.60 compared to aequorin-based experimental system in the special and temporal resolution.

Although Knight's group has been studied on cold-induced Ca^{2+} signal in detail since a few decades ago, I think that their results are still not sufficient for three reasons. First, they did not perform temperature correction of luminescence. As long as the aequorin is an enzyme, temperature affects the intensity of the luminescence. Therefore, the effect of absolute temperature on Ca^{2+} signals cannot really be evaluated, and consequently, Ca^{2+} signals at different temperatures cannot be compared accurately. Second, cold-induced Ca^{2+} signals have been observed only at the extremely fast cooling rates that hardly happen in nature. To solve these problems, I developed the experimental system which can capture Ca^{2+} signals with accurate temperature control. Third, they did not observe the Ca^{2+} signals in natural state. For example, in the report of Plieth *et al*. (1999), the authors observed cold-induced Ca^{2+} signals using cut roots. In the report of Knight and Knight (2000), while intact plants were used, plants were observed in a state floating in a solution. Thus, I developed the observation system with the cryostage and cryochamber.

Materials

Development of the experimental system

Cryomicroscopy-based experimental systems were employed to observe samples at a microscopic level during temperature changes. The cryomicroscopy system for root analyses consisted of a confocal microscope (C2si; Nikon Co., Tokyo, Japan; http://www.nikon-instruments.jp/jpn/bioscience-products/confocal/c2/index.html), cryostage (THMS600; Linkam Scientific Instruments, Ltd., UK; http://www.linkam.co.uk/thms600-features/; Figure 2.2c), objective inverter (300T; LSM TECH, USA; http://lsmtech.com/our-products/#InverterScope), and an iron plate to attach the equipment to the microscope and adjust the height. The temperature of the cryostage was regulated by a heater and liquid N_2 following the program edited by Linksys for Windows (Linkam Scientific Instruments). The cryostage was covered with a plastic bag filled with dry air to prevent the misting of the lens and cover glass (Figure 2.2d) (Hiraki *et al*., 2014).

The cryomicroscopy system for leaf analyses consisted of a confocal microscope, cooling circulator (Figure 2.3b) (Ministat 230 with Pilot ONE; Huber Kältemaschinenbau GmbH, Germany; http://www.huber-online.com/en/product_datasheet.aspx?no=2015.0012.01), glass-jacketed beaker (Asahi Glassplant Inc.; http://www.asahiglassplant.com/products/) (as a cooling chamber), objective inverter, adjustment cylinder (to extend objective inverter), and an iron plate. The glass-jacketed beaker was covered with an expanded polystyrene box (to stabilize the internal temperature) and a plastic box containing a rubber sheet at the base (to enable the attachment of the iron plate) (Figure 2.3d-f). To monitor air and medium temperatures, four thermocouples were attached to the medium and the beaker. Temperature data were collected using a thermocouple data logger (MCR-4TC; T&D Co., Japan; https://www.tandd.co.jp/product/mcr-4_series.html).

Sample preparation

For Ca^{2+} signal observation in root cells, YC3.60-expressing *Arabidopsis* seedlings were placed on a 24 mm × 18 mm cover glass, with only the roots covered by an 18 mm × 18 mm cover glass. Silicone (Sin-Etsu Chemical Co., Ltd., Japan) was used to ensure that space was maintained between the cover glasses (i.e., a shallow well was constructed). The well was filled with 100 µL 1 mM MES/KOH buffer (pH 5.6). The aerial plant parts were covered with plastic wrap, and a drop of water was added to prevent the sample from dehydration (Figure 2.2a). The prepared samples were then placed on the cryostage (Figure 2.2c) and temporarily fixed with thin silicone to improve thermal conductivity. Before starting all experiments, samples were placed on the cryostage and maintained at a constant temperature for at least 10

min (i.e., starting temperature). Fluorescence images of the root elongation zone were observed at intervals of 1 to 15 s. The interval was mainly 1 to 2 s.

For leaf observation, YC3.60-expressing *Arabidopsis* seedlings were placed in a petri dish (diameter: 40 mm) containing modified Hoagland's nutrient medium and 1 mL 1 mM MES/KOH (pH 5.6) buffer. The surface of the medium was covered with plastic wrap (Figure 2.3a). The dish was attached to the bottom of a glass-jacketed beaker with silicone, and the samples were incubated at the starting temperature for at least 10 min. Fluorescence images of the fifth leaf (except cotyledon) were observed at 5 to 60-s intervals.

Ca^{2+} signal measurement, correction for temperature, and data analysis

The cryomicroscopy systems to analyze transgenic *Arabidopsis* plants expressing a FRET-based Ca^{2+} sensor (i.e., YC3.60) (Nagai *et al.,* 2004) enabled the observation of fluctuations cytosolic Ca^{2+} concentration. Fluorescence images were captured with a 32-channel spectral detector or 472/30 nm (for ECFP fluorescence) and 527/20 nm (cpVenus fluorescence) dichroic filters used for confocal laser scanning microscope. The fluorescence ratio was calculated according to the following equation using the fluorescence intensity values of cpVenus at t s [$VF(t)$] and ECFP at t s [$CF(t)$].

$$Ratio\ (t) = \frac{[VF(t)]}{[CF(t)]}$$

The normalized FRET value for each sample was determined using this equation by using the NIS-elements C program (Nikon). The data for the experiment assessing the effects of temperature changes needed to be corrected because the fluorescence intensities were influenced by temperature (Felber *et al*., 2004). I established correction formula for temperature changes in leaf and root cells. Leaf protoplasts and whole roots were used for making the correction formula. Since leaf is covered with the cuticle layer which prevent from entering the liquid chemicals into the cell, leaf protoplasts were prepared. Leaf protoplast and roots were treated with 2.5 µM ionomycin, 0.01% Triton X-100, and 250 nM $CaCl_2$ for 1 h to increase the intracellular Ca^{2+} concentration. The FRET values at 25°C, 20°C, 15°C, 10°C, 5°C, 0°C, and −5°C were measured (Figure 2.4a, 2.4b). The correction formulae for leaf and root cells were based on an approximation formula. Finally, the normalized FRET values indicating the Ca^{2+} concentration were calculated using the following equations and the smoothed FRET values at t s [$SR(t)$] and 0 s [$SR(0)$]:

$$Corrected\ Relative\ Ratio\ of\ Root\ Cells\ (t) = \frac{[SR(t)]/1.0772e^{0.0122\times T(t)}}{[SR(0)]/1.0772e^{0.0122\times T(0)}}$$

$$Corrected\ Relative\ Ratio\ of\ Leaf\ Cells\ (t) = \frac{[SR(t)]/3.147e^{0.0235\times T(t)}}{[SR(0)]/3.147e^{0.0235\times T(0)}}$$

where T represents the temperature at a specific time point.

The shape of Ca^{2+} signal varies greatly after performing the correction formula. The examples are shown in Figure 2.4. In the leaf cells, unless the correction formula is performed, the signal decreases as the temperature goes down and it is difficult to distinguish the peaks. However, by performing the correction formula, analysis of the peak became possible (Figure 2.4c). In the root cells, although it is easy to distinguish the peak compared to the leaves without performing the correction formula, the second peak seems to be smaller than first peak. After applying the correction equation, it turns out that the second peak tended to be larger than the first peak (Figure 2.4d). The temperature correction allowed us to correctly compare signals at different temperatures, and consequently, the parameters that generate calcium signal were qualitatively analyzed in our cryomicroscope in detail.

Additionally, each data set was subjected to binominal smoothing using the IGOR Pro 6.3.6.0 program (WaveMetrics, Inc.; https://www.wavemetrics.com/) to detect Ca^{2+} signal peaks. This program was also used for analyzing the Ca^{2+} signals and determining the timing and height of the peaks. The outliers caused by focus changes during microscopic analyses were replaced with values calculated with IGOR Pro.

Averaged rather than individual Ca^{2+} signals are presented in figures. Sometimes, the averaged Ca^{2+} signals do not show actual peak shape due to the differential signal initiation. To clearly visualize the data, I modified the x-axis (time) for the Ca^{2+} signals, and the first peak time was replaced with the averaged first peak time (Figure 2.5). This was performed only for visualizing the Ca^{2+} signals, but not for detailed analysis such as peak time and height. By this method, I prevented the Ca^{2+} signals from deforming due to the averaging treatment.

Discussion

Importance of temperature corrections for the Ca^{2+} sensor proteins

Despite the fact that Ca^{2+} sensor proteins of aequorin is an enzyme and its reaction is affected by the absolute temperature, the temperature correction of cold-induced Ca^{2+} signals has not performed in previous studies including Knight's group's work. Thus, I would like to emphasize that I introduced the temperature correction of Ca^{2+} signals (see Figure 2.4) and the cryomicroscope with cryostage or cryochamber with which the temperature in intact plant can be arbitrarily and accurately controlled (see Figures 2.2 and 2.3). Temperature correction

allowed us to correctly compare the Ca^{2+} signals at different temperatures, and consequently, the parameters that generate Ca^{2+} signal were qualitatively analyzed in our cryomicroscope in detail. If temperature correction is not performed, the Ca^{2+} concentration seems to decrease just by lowering the temperature even if the Ca^{2+} concentration does not actually decrease (see Figure 2.4c, d). In some cases, without temperature correction, it becomes difficult to distinguish signal and noise.

Advantages of the observation systems

Advantages of my observation system are three points: high sensitivity, accurate and fine control of cooling conditions, and observation with intact plants. First, with high sensitivity observation, quantitative analysis can be sufficiently performed even at a slow cooling-rate. It has been difficult to difficult to observe the Ca^{2+} concentration changes with slow cooling-rate so far. For example, the slowest cooling rate among the data shown in past references was 3°C min^{-1} and the signal at that time was also detected only slightly (Plieth *et al*. 1999). On the other hand, I performed quantitative analysis at a cooling rate of 2°C min^{-1} and also succeeded in analysis at a slow rate of 0.47°C min^{-1} (Figures 3.7 and 3.9 in chapter 3). The cooling rate of 0.5°C min^{-1} occurs very common in the field. Furthermore, I observed Ca^{2+} signals even when the temperature dropped and rose by 1°C (Figure 3.7).

Second, an observation system can keep a constant cooling rate accurately. The stopping of cooling instantaneously is very important. Under such observation system, for example, I am able to obtain the result of the effect of cooling stoppage. Stopping of the cooling is also important part of the cooling, but nobody has shown this before. The reason for this may be that no one could control the cooling rate accurately and freely.

Third, it is very important that plants are observed in a more natural state to reduce the possibility of artifacts from experimental results. In previous reports, there were some problems with this point. For example, in the report of Plieth *et al*. (1999), the authors observed cold-induced Ca^{2+} signals after cutting the root part and then cooled. There might have possibility that the Ca^{2+} signal behaves differently in separated root from intact plant. Besides, in the report of Knight and Knight (2000), intact plants were observed, but in a state floating in a solution. In natural environment, leaves are usually cooled via cooled air. Since the heat capacity differs between air and liquid, the cooling speed is also different. On the other hand, the aerial part of the plants does not attach to the agar medium or buffer solution in my experiment, and consequently, root was cooled by the water, and leaf was cooled via cooled air. Not only I used intact plants in both observation systems but also plants were observed in a more natural cooling state in the experiments (Figures 2.2a and 2.3a).

The above three points are the strong advantages of my experimental system, which

has never been available before. Taken together, the experimental system I developed in the current study brings us a new understanding of the role of Ca^{2+} signal in the cold sensing and cold acclimation process.

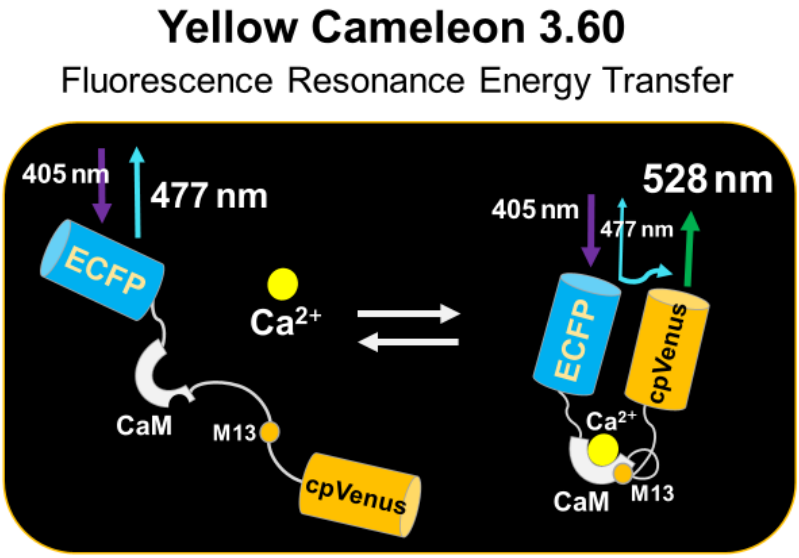

Figure 2.1. FRET-based Ca^{2+} sensor Yellow Cameleon 3.60.

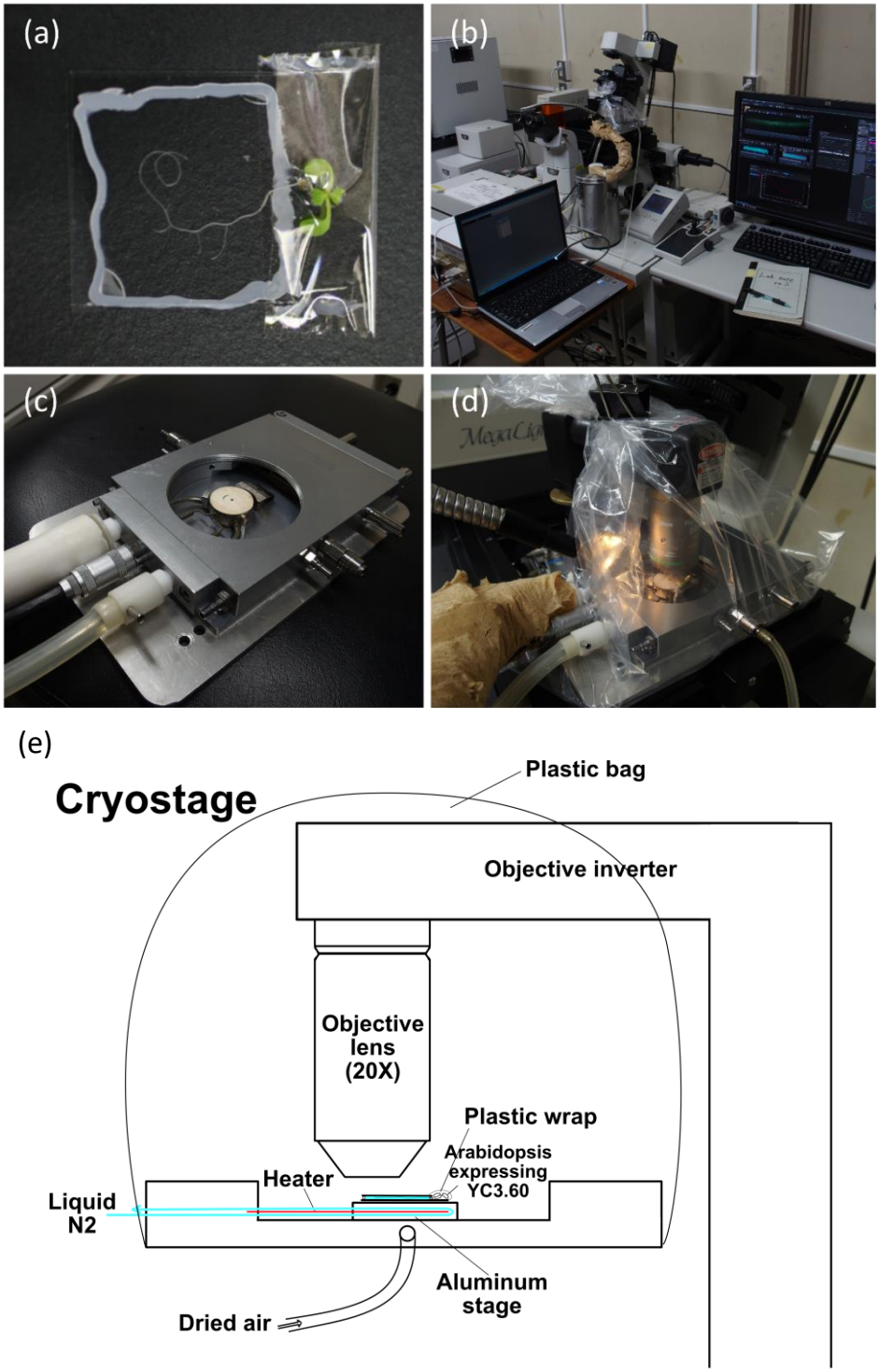

Figure 2.2. Ccryomicroscopy system for root observation. (a) Seven-day-old seedlings was put on a 24 mm × 18 mm size cover glass and only root part was covered with 18 mm × 18 mm cover glass. (b) Cryomicroscope was consisted with confocal microscope (C2si, Nikon Co., Tokyo, Japan), cryostage, and object inverter. (c) Cryostage (THMS600, Linkam scientific instruments, Ltd., UK) can control the temperature of the aluminum stage by using the heater and liquid N_2 following the program. (d) Objective inverter (300T, LSM TECH, USA) changes the optical path of the laser. By using this, it becomes possible to use an inverted microscope as upright microscope. (e) Schematic diagram of the cryostage. The sample was put on the cryostage, and then cryostage, objective inverter and objective lens were covered with plastic bag filled with dry air.

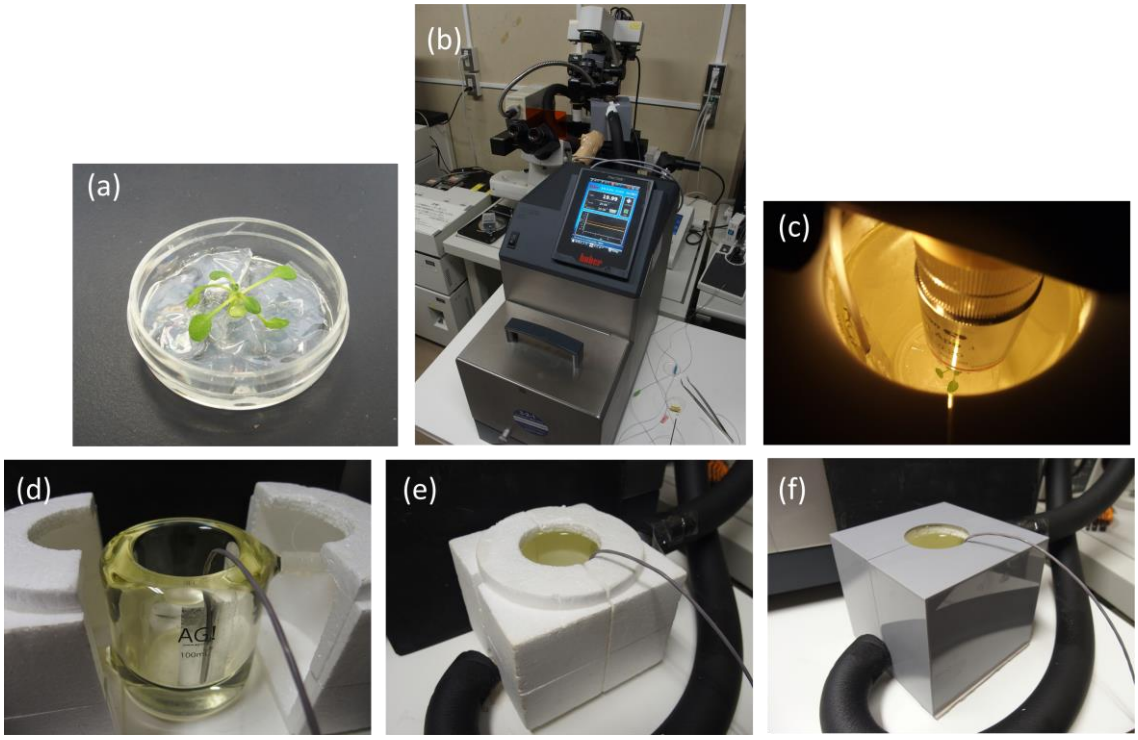

(g)

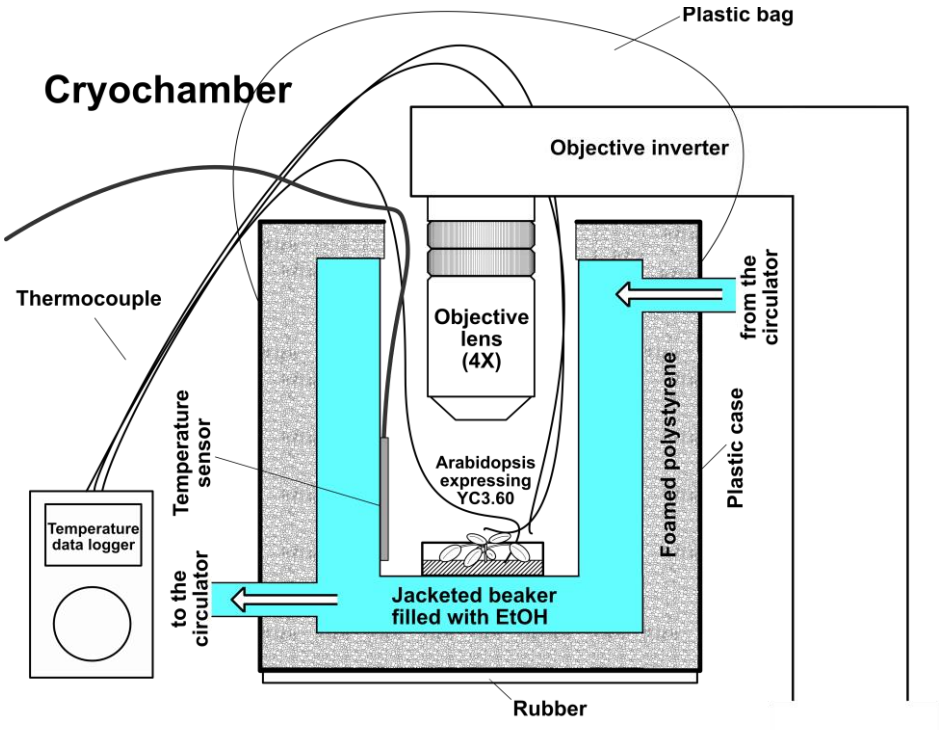

Figure 2.3. Cryomicroscopy system for leaf observation. (a) Plant was transferred to Petri dish with medium and 1 mL MES/KOH pH 5.6 buffer. (b) The Cooling circulator (Ministat 230 with Pilot ONE, Huber Kältemaschinenbau GmbH, Germany) controls the temperature of ethanol following the program. (c) Objective inverter with adjust cylinder was used to change the laser path (d) Glass jacketed beaker (Asahi Glassplant Inc.) is used as a cooling chamber. (e) Glass jacketed beaker was covered with expanded polystyrene box to stabilize inside temperature. (f) The box was covered with plastic box which has rubber sheet at the base to attach to the microscope. (g) Schematic diagram of the cryochamber.

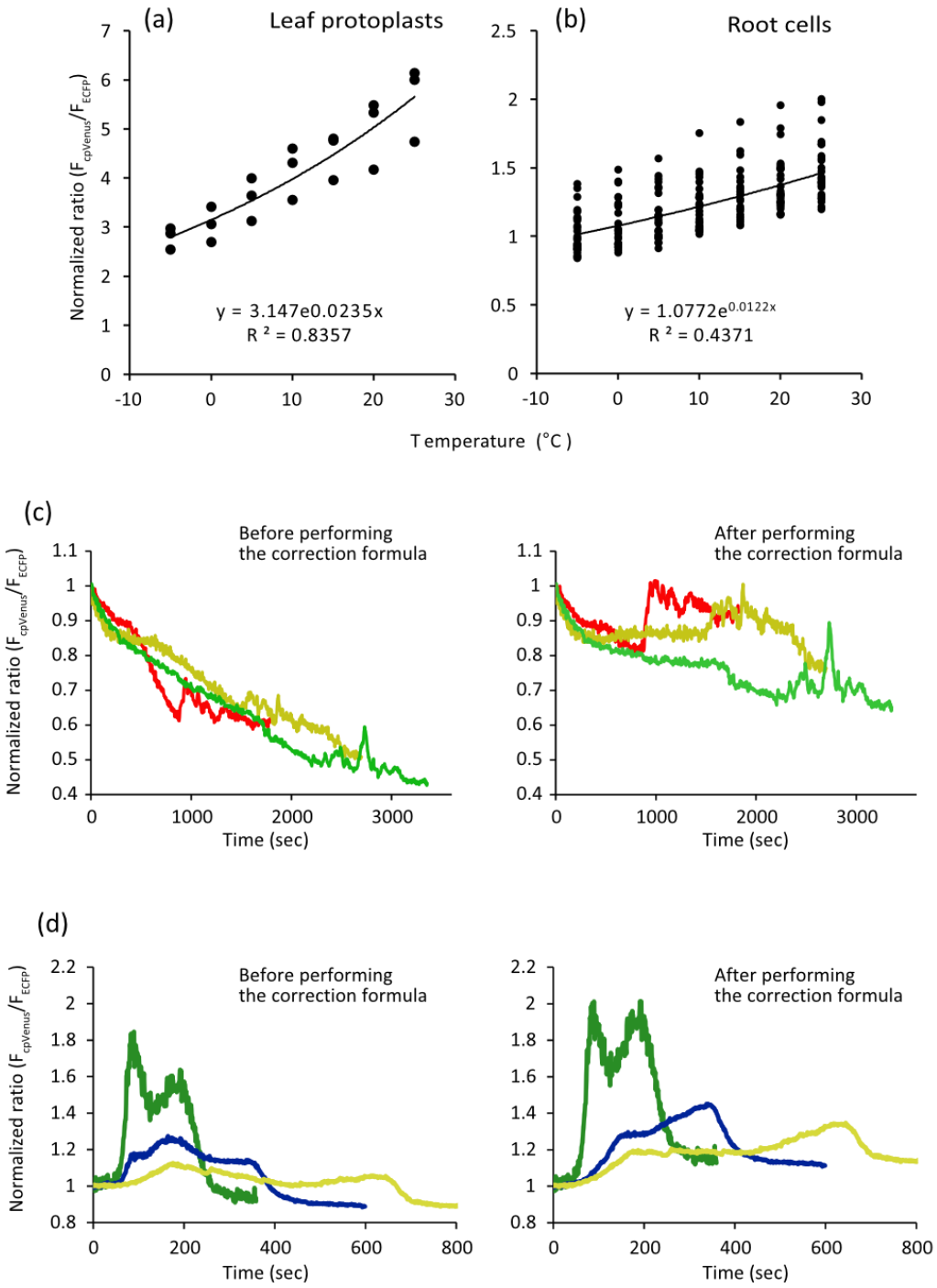

Figure 2.4. Effect of temperature changes on Yellow Cameleon 3.60 in leaf and root cells of Arabidopsis thaliana. (a) The FRET values of protoplasts of leaf cells were observed at at 25°C, 20°C, 15°C,10°C, 5°C, 0°C and -5°C. (b) The FRET values of root cells also observed at same temperature settings. (a and b) Protoplast and root were incubated with 2.5 µM ionomycin, 0.01% TritonX-100 and 250 nM $CaCl_2$ for 1 hour prior to the observation. The approximate formulas were calculated based on each result. (c) The example how Ca^{2+} signals were changed by performing the correction formula in leaf cells. (d) The example how Ca^{2+} signals were changed by performing the correction formula in root cells. Ratio values were normalized by the value at t = 0.

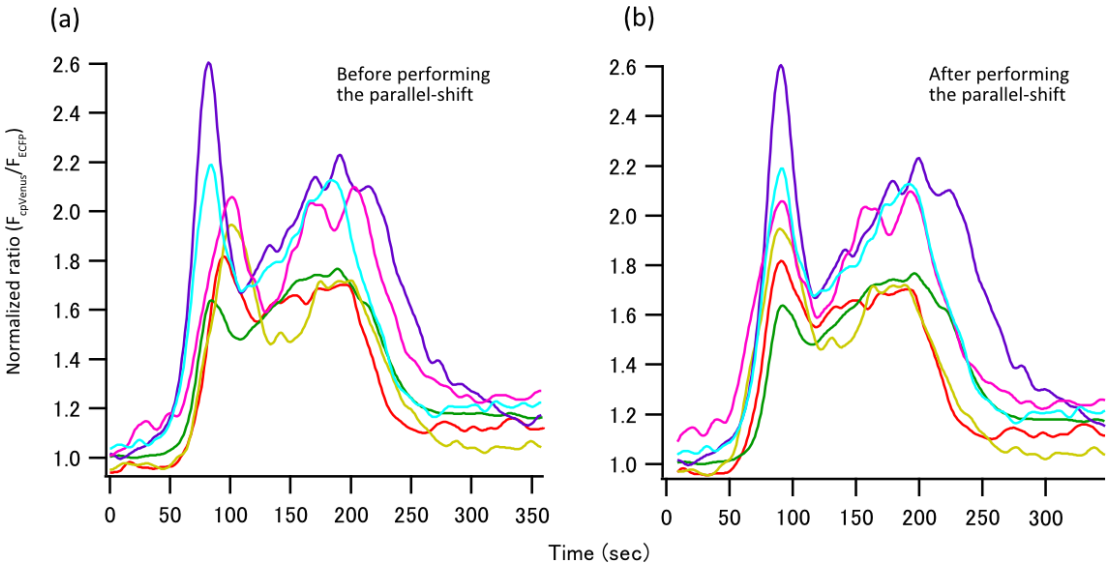

Figure 2.5. Example for parallel-shift among the x-axis of Ca^{2+} signals to visualize the averaged Ca^{2+} signal. (a) The left graph shows the data set which is not performed the parallel-shift. (b) Based on the averaged first peak time, the smoothed data were parallel-shifted along the x-axis and then averaged to show in the figures. Ratio values were normalized by the value at t = 0.

Chapter 3

Calcium Signaling-Linked CBF/DREB1 Gene Expression Was Induced Depending on the Temperature Fluctuation in the Field: Views from the Natural Condition of Cold Acclimation

Abstract

Environmental adaptability is essential for plant survival. Though it is well known that a simple cooling or cold shock leads to Ca^{2+} signals, direct evidence has not been provided that plants use Ca^{2+} signals as a second messenger in the cold acclimation (CA) process in the field. By developing a technique to analyze Ca^{2+} signals using confocal cryomicroscopy, I investigated Ca^{2+} signals under several temperature conditions by combining the start temperature, cooling rate and cooling time duration. In both root and leaf cells, Ca^{2+} signals rapidly disappeared after cooling stopped, and thereafter under a constant low temperature no Ca^{2+} signal was observed. Interestingly, under the cooling regime from 2°C to −2°C, non-acclimated plants grown at 23°C hardly showed Ca^{2+} signals, but cold-acclimated plants at 2°C were able to form Ca^{2+} signals in root cells. These findings suggest that plants sense temperature decreases with Ca^{2+} signals while adjusting the temperature sensitivity to their own temperature environment. Furthermore, if the temperature is constant, no Ca^{2+} signal is induced even during CA. Then, I also focused on the CA under field conditions, rich in temperature fluctuations. In CA under field conditions, the expression patterns of *CBF/DREB1* genes were distinctly different from those in artificial CA. Pharmacological studies with Ca^{2+} channel blockers showed that the Ca^{2+}-induced expression of *CBF/DREB1* genes was closely correlated with the amplitude of temperature fluctuation, suggesting that Ca^{2+} signals regulate *CBF/DREB1* gene expression during CA under natural conditions.

Introduction

Ca^{2+} is a common signaling element in living organisms. In plant cells, Ca^{2+} acts as a signaling element along with other ions, reactive oxygen species and phytohormones (Dat *et al*. 2000, Xiong *et al*. 2002, Wasternack 2007). Because biotic and abiotic stresses induce transient increases in the Ca^{2+} concentration in plant cells, Ca^{2+} signals are considered to be a secondmessenger during stress responses (McAinsh and Pittman 2009, Martí *et al*. 2013). Several characteristics of Ca^{2+} signals were reported using simple temperature changes (Knight *et al*. 1996, Plieth *et al*. 1999, Knight and Knight 2000). In this study, to understand the natural phenomenon of 'cold acclimation (CA)' in plants, I focused on the hypothesis that Ca^{2+} acts as a second messenger to induce C-repeat (CRT)-binding factor/dehydration-responsive element-binding protein 1 (CBF/DREB1) transcription factors in low-temperature sensing systems in thermal regimes found under field conditions.

CA is the phenomenon by which plants sense the cold at non-freezing low temperatures in the autumn and enhance freezing tolerance to survive severe winter (see Levitt 1980). In terms of gene expression, the transcriptional regulatory cascade during the CA process is mainly mediated by the CBF/DREB1 transcription factors, which bind to the DRE/CRT cis element and induce cold-responsive (COR) genes (Fowler and Thomashow 2002, Wang and Hua 2009). CBF/DREB1s are considered to be mediated by Ca^{2+} signals, for example through the calmodulin-binding transcription activator (Doherty *et al*. 2009, Kidokoro *et al*. 2017). In fact, rapid increases in intracellular Ca^{2+} levels induce the expression of *KIN1*, which is one of the CBF/DREB1 regulon genes (Knight *et al*. 1996).

Several studies have revealed that cooling or cold shock induces transient increases in Ca^{2+} levels (Plieth *et al*. 1999, Knight and Knight 2000, Kiegle *et al*. 2000, Krebs *et al*. 2012). The cold- induced Ca^{2+} signals were observed not only in Arabidopsis, but also in wheat (Nagel-Volkmann *et al*. 2009). Cooling treatments from room temperature to 0°C induce Ca^{2+} signals with two peaks (Knight and Knight 2000). In addition, the magnitude of Ca^{2+} signals is affected by the cooling rate rather than the absolute temperature, and no Ca^{2+} signal is observed by heating (Plieth *et al*. 1999, Nagel-Volkmann *et al*. 2009). Interestingly, several types of artificially induced Ca^{2+} signals at room temperature activate specific promoter motifs, including cold-responsive elements (Whalley *et al*. 2011, Whalley and Knight 2013). Thus, plants encode environmental information in Ca^{2+} signals, which are decoded to start and/or regulate the CA process (Chinnusamy *et al*. 2010, Miura and Furumoto 2013). However, when considering the field condition, it is not sufficiently clear which cooling factors (e.g., temperature at the start of cooling, cooling rate, cooling duration and their combination) cause and form the Ca^{2+} signals.

In almost all CA studies, the treatment has been conducted by placing plants at a

constant low temperature, such as 2°C. However, in the field, the air and soil temperatures are affected not only by the daily and seasonal sun movement, but also by cloud, rain and wind, and therefore the temperature change around plants is continuous and complex (Figure 3.1). Plants have evolved under the daily or seasonal temperature changes from several combinations of temperature factors, and the cold response Ca^{2+} signal has co-evolved in the context of these natural conditions. As the first step to understand this mechanism, the relationship between these cooling factors and Ca^{2+} signals must be quantified. In this study, I developed an experimental system that combined confocal cryomicroscopy and an Arabidopsis thaliana line expressing Yellow Cameleon 3.60 (YC3.60), which is a fluorescence resonance energy transfer (FRET)-based Ca^{2+} sensor (Nagai *et al*. 2004). Our cryomicroscope has a cryostage (Figure 2.2) or cryochamber (Figure 2.3) in which the temperature in intact plants can be arbitrarily and accurately controlled. The research with this newly developed system has three advantages over previous studies. First, this system has better resolution, and my mathematical analysis by the latest software provided a more in depth understanding of the Ca^{2+} signals than previous studies. Secondly, to quantify Ca^{2+} signals correctly in any absolute temperature, I corrected the temperature characteristic of YC3.60 (Figure 2.4). This is because the activities of Ca^{2+} sensor proteins are affected by temperature (Felber *et al*. 2004), although this temperature effect has not been accounted for in any previous reports. Thirdly, while a number of characteristics (e.g. peak number and response to the continuous temperature change) of Ca^{2+} were shown (Plieth *et al*. 1999, Knight and Knight 2000, Nagel-Volkmann *et al*. 2009), the cooling regimes found under natural conditions have not been investigated. Understanding of the Ca^{2+} behavior in the field is necessary to consider CA in the field. Here, my results showed that not only the cooling rate but also several cooling factors, plant conditions and their combination determine the final profile of Ca^{2+} signals. In addition, I provided a new aspect of the CA process in the field from the point of view of Ca^{2+} signals. Focusing on the Ca^{2+} signals under natural conditions, I pharmacologically analyzed the cold-responsive gene expression level under field CA conditions. Taken together, my results indicated that the expression of CBF/DREB1 genes may be differentially regulated by cold-responsive Ca^{2+} signals in the field compared with controlled-environment growth chambers at constant 2°C.

Materials and Methods

Plant materials

Arabidopsis thaliana (Col-0) plants were grown in Petri dishes containing modified Hoagland's nutrient solution solidified with 1% agar (Uemura *et al*., 1995), and grown at 23°C

under a 16 h photoperiod (photon flux rate: 80 μmol m^{-2} s^{-1}) for 7 d (for root samples) or 14 d (for leaf samples). Plants were incubated in a vertical position for the root study. Some plants were cold-acclimated at 2°C under a 12 h photoperiod (photon flux rate: 80 μmol m^{-2} s^{-1}) or in the field. The samples were covered with moistened paper and a plastic sheet to maintain humid conditions during CA treatment.

Sample preparation for microscopic observations

See "Sample Preparation for Microscopic Observations" in Chapter 2.

Cryomicroscope

See "*Cryomicroscope*" in Chapter 2.

Ca^{2+} signal measurement, correction for temperature, and data analysis

See "*Ca^{2+} Signal Measurement, Correction for Temperature, and Data Analysis*" in Chapter 2. Averaged rather than individual Ca^{2+} signals are presented in figures. Sometimes, the averaged Ca^{2+} signals do not show actual peak shape due to the differential signal initiation. To clearly visualize the data, I modified the x-axis (time) for the Ca^{2+} signals, and the first peak time was replaced with the averaged first peak time in Figures 3.2c, 3.6b, d, 3.9c and 3.13b. Untransformed data also shown in Figure 3.18. This was performed only for visualizing the Ca^{2+} signals, but not for detailed analysis such as peak time and height. By this method, I prevented the Ca^{2+} signals from deforming due to the averaging treatment.

Measurement of mRNA accumulation level

Total RNA was isolated from aerial parts of the Arabidopsis (Col-0) plant using ISOSPIN Plant RNA (NIPPON GENE CO., LTD., Japan). ReverTra Ace qPCR RT Master Mix (TOYOBO Co.) was used for the cDNA synthesis. Real-time PCR was performed on the corresponding cDNA synthesized from each sample. *PDF2* was used as a reference gene. The primers which were used for real-time PCR are listed (Table 3.1).

Cold acclimation treatment in the field

The samples were covered with moistened paper and a plastic sheet to maintain humid conditions during CA in the field. The field cold acclimation was performed on November 15–17 and December 6–8, 2016, and on March 21–23, 2017, in Morioka, Japan. Temperature data were

collected every 2 min using a thermocouple data logger (TR-55i; T&D Co., Japan). I avoided measuring the leaf temperature directly in order not to change the heat conductivity of the leaf. Also, I confirmed that there were few differences between leaf and air temperature in Figure 3.19.

Chemical treatments

A solution of 0.05% Triton X-100 was used as the control, and 0.05% Triton X-100 and 1.5 mM $LaCl_3$ or 50 μM RR, were used to inhibit the Ca^{2+} signaling during CA treatment or Ca^{2+} observation. About 200 μL of solution was sprayed on each plant 1 h prior to the experiment.

Results and Discussion

Cold-induced Ca^{2+} signals of root cells in simple cooling conditions

Several studies have reported that cold shock causes transient Ca^{2+} signals, and that the magnitude of Ca^{2+} signals is affected by the cooling rate rather than the absolute temperature (Plieth *et al*. 1999, Nagel-Volkmann *et al*. 2009). I constructed a confocal cryomicroscope with a cryostage on which the sample temperature can be arbitrarily and accurately controlled if samples are thin, as in the case of roots (Figures 3.2a and 3.3a). In this system, I confirmed that faster cooling rates resulted in higher Ca^{2+} signals (Plieth *et al*. 1999, Nagel-Volkmann *et al*. 2009). In addition, the correction formula of temperature for the YC3.60 fluorescence was established to compare the value 65 of the ratio [fluorescence value of cpVenus divided by that of enhanced cyan fluorescent protein (ECFP)] in any absolute temperature (see Chapter 2). Here, the combination of several parameters, such as temperatures at the start or end of cooling, the cooling rate and cooling duration, were studied.

First of all, to understand the effect of absolute temperatureon Ca^{2+} signals, I focused on the temperature at the start of cooling. At 30 s after starting to capture the image, roots ofnon-cold-acclimated (NA) plants were cooled from 20, 16 or 12 75
to 0°C at a cooling rate of 2°C min^{-1}, and then were maintained at 0°C (Figure 3.2b). From fluorescence images of ECFP (FRET donor) and cpVenus (FRET acceptor), the fluorescence ratio image, which is proportional to the concentration of free cytosolic Ca^{2+}, was obtained from the root cells (Figures 3.2a and 3.3a). The fluorescence ratio value at each time point (i.e. at the specified temperature) was temperature corrected, averaged and then was plotted (see Chapter 2). Ratio values were normalized by the value at t = 0. The normalized ratio was used as the y-axis to show small Ca^{2+} concentration changes. The temperature change from 20 to 0°C

produced two Ca^{2+} signal peaks, and the second peak appeared at about the 630 s point, the time orresponding to the end of cooling. When plants were cooled from 16 to 0°C, the Ca^{2+} signal profile was a flat peak, and the peak decreased quickly after the cooling treatment was stopped at about 500 s. This flat peak was formed by the overlap of two major peaks shown by analysis with the software IGOR Pro (Figure 3.3b). The temperature change from 12 to 0°C resulted in one sharp peak at about 400 s, and this peak also decreased just after stopping the cooling treatment (Figure 3.2c). In addition, the Ca^{2+} signals had one or two peaks (Figure 3.2c), and those signals consisted of four or five peaks (Figure 3.3b). While it has been reported that the apoplast and vacuole were the candidate Ca^{2+} pools for cold shock (Knight *et al.* 1996, Knight and Knight 2000), my results suggest that the Ca^{2+} signal is formed by release of Ca^{2+} from several Ca^{2+} pools and/or through several Ca^{2+} channels in the same Ca^{2+} pool.

Plieth *et al*. (1999) mentioned the importance of cooling rate. To see the effect of the cooling rate in my experimental setting, the plants were cooled from 20°C to 0°C with three different cooling rates: 2, 4 and 8°C min^{-1} (Figure 3.4a). These cooling induced different shape of the Ca^{2+} signals (Figure 3.4b). The peak times and the values of the Ca^{2+} signals of the first and the second peak in each Ca^{2+} signal was picked up and used for detailed analysis. There was the strong correlation between timing and amplitude both first and second peak (Figure 3.4c, d). Comparison with the three cooling rates, the timing of Ca^{2+} signal peak was significantly delayed in cooling rate-dependent manner. The fast cooling rate induced the fast Ca^{2+} signal peak (Figure 3.3b, e). The peak value of Ca^{2+} signal was significantly different between 8 and 4°C min^{-1}, also between 8 and 4°C min^{-1} of cooling rate. The faster cooling rate induced larger Ca^{2+} elevation (Figure 3.4b, f). In addition, the time between first and second peak were calculated in each cooling rate condition, and found that small cooling rate tended to induce the Ca^{2+} signal which had long time distance between first and second peak (Figure 3.4g). This may be the answer of the single peak Ca^{2+} signals which were induced by the rapid cold shock such as ice-cold water (Logan and Knight, 2003; Krebs *et al*., 2012).

To characterize the shape of the Ca^{2+} signals quantitatively, the following four technical terms were defined: (i) the latent phase, i.e. the period from the start of cooling until the Ca^{2+} increase; (ii) the increase phase, i.e. the period during the increase in the Ca^{2+} signal of the first peak; (iii) the decrease phase, i.e. the period during the decrease in the Ca^{2+} signal of the last peak; and (iv) the stable phase, i.e. the period after the Ca^{2+} signal (Figure 3.2d). In all conditions, the point when Ca^{2+} signals were in the decrease phase corresponded to the period just after stopping cooling or the time when the temperature reached approximately 0°C (Figure 3.2e). There were two possibilities for the cue for the decrease phase: (i) stopping cooling or (ii) absolute temperature (i.e. 0°C). To test these possibilities, plants were cooled (i) from 20 to 0°C or (ii) from 10 to −10°C (Figure 3.2h). In my experimental conditions, the buffer solution remained super-cooled even at −10°C. In both cases, two peaks of Ca^{2+} signal were observed

regardless of differences in the initial and nadir temperatures of cooling (Figure 3.2i), suggesting that 'stopping the cooling' decreases the Ca^{2+} signal. Besides, it should not be overlooked that the basic Ca^{2+} signal patterns such as the number of peaks did not change when the temperature decrease range was the same (Figures 3.2h, i and 3.4a, b). The temperature change from 12 to 0°C induced a Ca^{2+} signal with only one peak (Figure 3.2c). This means that if the cooling was stopped during the first increase of the Ca^{2+} signal, the first peak decreased, and no further Ca^{2+} increase was induced. Even in the case of cooling conditions from 10 to −10°C, the decrease phase was caused by stopping the cooling. This phenomenon seems to have the function of creating multiple Ca^{2+} signal peaks in the field. For example, the temperature fluctuations which are produced by the movement of the sun, clouds and wind may cause the sharp temperature decrease/increase of the leaves. The temperature decrease induces the increase phase of the Ca^{2+} signal, and the temperature increase (or stopping the cooling) causes the decrease phase of Ca^{2+} signals. Therefore, the temperature fluctuations may result in multiple Ca^{2+} signal peaks in the field. On the other hand, when the temperature decreased from 20°C to −10°C, plant showed the larger second peak of the Ca^{2+} signal and the peak decreased during the cooling (Figure 3.5). It indicates that if the cooling range is enough, the second peak of the Ca^{2+} signal start to decrease without stopping the cooling.

Although Plieth *et al*. (1999) mentioned that lower absolute temperature induced greater increases of Ca^{2+} signal, I showed that there were no significant differences among signal peak heights under different absolute temperatures (Figure 3.2g, k). Plieth *et al*. (1999) used step-wise cooling, which may have caused the larger Ca^{2+} increase depending on the absolute temperature. Furthermore, the luminescence of aequorin was not corrected by temperature in their studies. On the other hand, I carefully established a correction formula to compare the Ca^{2+} concentration level at different absolute temperatures. If temperature correction is not performed, the Ca^{2+} concentration seems to decrease just by lowering the temperature even if the Ca^{2+} concentration does not actually decrease in my experimental system (see Figure 2.4). In some cases, it becomes difficult to distinguish signal and noise without temperature correction. Thus, I would like to emphasize here that I introduced the temperature correction of Ca^{2+} signals (see Chapter 2). Furthermore, in the observation of root cells, I concluded that the absolute temperature affected the period from the start of cooling to the generation of the Ca^{2+} peak but did not affect the peak height (see Figure 3.2). These conclusions are quite important, given that Plieth *et al*. (1999) concluded that their results indicate that temperature sensing is mainly dependent on the cooling rate, dT/dt, whereas the absolute temperature T is of less importance. Without a temperature correction, it would be difficult to draw a valid conclusion. I also found that there was an effect of absolute temperature on the latent phase of Ca^{2+} signal. A lower start temperature resulted in a longer latent phase (Figure 3.2c, i). Similarly, the first peak time was delayed by lowering the start temperature. For

example, the first peak time when cooling from12°C caused at least a 100 s delay when compared with cooling from 20°C (Figure 3.2c, f). Thus, I concluded that the absolute temperature affects the time of the latent phase and peak time.

The cooling from 12 to 0°C induced a Ca^{2+} signal which had only one peak, but it was unclear whether the peak was the first or the second peak (Figure 3.2c). To clarify this, I determined the Ca^{2+} signal with $LaCl_3$, which is known to affect the appearance of the first peak but not that of the second peak due to the inhibition of Ca^{2+} influx from the extracellular space (Knight and Knight 2000). When plants were cooled from 20 to 0°C (Figure 3.6a), $LaCl_3$ mainly inhibited the appearance of the first peak in the roots but did not markedly inhibit the appearance of the second peak (Figure 3.6b). When cooled from 12 to 0°C when only one Ca^{2+} peak arose (Figure 3.6c), $LaCl_3$ almost eliminated the cold-induced Ca^{2+} peaks (Figure 3.6d). On the slope of the increase phase of Ca^{2+} signals and influx rate of Ca^{2+}, $LaCl_3$ significantly changed only the first peak in both cooling conditions from 20 and 12°C (Figure 3.6e). Thus, these results indicate that the Ca^{2+} source of the first peak is almost entirely the extracellular space regardless of absolute temperature.

Effect of temperature fluctuation on Ca^{2+} signals

To estimate the shape of Ca^{2+} signals which are caused by natural temperature changes in the field, I analyzed the influence of the small temperature fluctuations which generally occur in the field (Figure 3.1). Temperature change patterns with two different starting temperatures were tested: one was cooling from 20 to 19, 18, 17 or 16°C and then immediately increasing the temperature to 20°C (Figure 3.7a), and the other was cooling from 2 to 1, 0, −1 or −2°C and then immediately increasing the temperature to 2°C (Figure 3.7b). In all the patterns, cooling and warming rates were 2°C min^{-1}. In NA plants, the cooling from 20 to 19, 18 and 17°C induced Ca^{2+} signals with a small but significant peak, while only cooling from 20 to 16°C induced a sharper and larger Ca^{2+} signal peak (Figure 3.7c, e). In contrast, in the case of a starting temperature of 2°C, a distinct Ca^{2+} peak arose only when cooling from 2 to −1 or −2°C, and the peaks were smaller than when cooled from 20 to 17 or 16°C (Figure 3.7c–f). The statistical analysis of the height of the Ca^{2+} signal peak was based on the method used by Hiraki *et al*. (2016). Regardless of cooling from 20 or 2°C, warming did not cause a Ca^{2+} increase, but decreased the Ca^{2+} concentration.

The reaction of the NA plant to the cold is the first incidence of CA. NA plants showed a Ca^{2+} increase when cooled from 20 to 19°C (Figure 3.7c). Cooling from 20 to 18 or 17°C induced very similar Ca^{2+} signals, but these Ca^{2+} signals were larger than that induced by cooling from 20 to 19°C (Figure 3.7e). The Ca^{2+} signal induced by cooling from 20 to 16°C (4°C cooling), the lowest temperature of this experiment, was quantitatively and qualitatively

different from the others. The Ca^{2+} concentration was about double that of the 2 or 3°C cooling. Furthermore, the speed of the Ca^{2+} signal increase/decrease was faster compared with the other cooling conditions. In the field, the temperature rarely falls >4°C in a few minutes and, more often, the degree of a continuous temperature change is <2°C (e.g. see Figure 3.12b, c). Therefore, a sharp Ca^{2+} signal as observed may be a type of emergency alert for the plant cell.

Plants cold-acclimated for 7 d were also analyzed using the same patterns of temperature changes. In contrast to the results of NA plants, even when cooled from 20 to 16°C, the distinct Ca^{2+} signal was not observed (Figure 3.7g, i). In addition, a large Ca^{2+} signal peak arose when cooled from 2 to −2°C, and the peak was the highest among the temperature treatments for CA plants (Figure 3.7h, j). Thus, while cooling with a temperature difference of about 4°C is necessary to generate a distinct Ca^{2+} signal, its signal generation is dependent on the combination of absolute temperature and the plant CA condition.

It had been reported that CA treatment enhanced the 15 second peak of Ca^{2+} signals (Knight and Knight 2000). Here, I found a novel characteristic of the Ca^{2+} signal, i.e. CA changed the response of the first peak to cooling. It was confirmed by using $LaCl_3$ that this first peak was identical to the first peak of NA and CA plants (Figure 3.8). When NA plants were 20 cooled from 2°C, plants could not respond to 1 or 2°C cooling (Figure 3.7d). In contrast, CA plants did not show an increase in Ca^{2+} concentration when cooled from 20°C, but did when cooled from 2°C (Figure 3.7g, h). For NA plants, cooling from 2°C would be an unexpected temperature change and, thus, a Ca^{2+} signal is not induced unless the temperature change is large (e.g. greater than a few degrees). CA plants, in contrast, did not show an induction of Ca^{2+} signal even in the face of a large temperature drop from 20°C. These results may indicate that the Ca^{2+} signal is induced under conditions to which plants have been exposed for a certain period (i.e. at 20°C for NA plants and 2°C for CA plants). CA is known to induce the reconstruction of the plasma membrane (Uemura *et al*. 1995) and an increase in plasma membrane fluidity (Yoshida 1983). Ca^{2+} channels are regulated by membrane fluidity, which depends on the temperature (Örvar *et al*. 2000, Sangwan *et al*. 2001). Taken together with these studies, my results support the hypothesis that plants adjust their plasma membrane fluidity depending on the ambient temperature, and make the more distinct Ca^{2+} signal responses to regulate downstream activities during/after CA.

Comparison of Ca^{2+} signals between leaf and root cells

The environmental condition around leaves is quite different from that around roots. In fact, the temperature changes of the leaves were quite different from those of the soil (Figure 3.1). In addition, the temperature of the roots depends on the temperature of the soil that has a large heat capacity, and the temperature of the leaves is influenced by such factors as air

temperature, wind and sunlight. Thus, I assume that there is a difference between leaves and roots in their low temperature sensitivities. To test this assumption, I constructed a cryochamber for cryomicroscopy, in which an intact plant could be cooled in air (Figure 2.3), although accurate temperature control with this system is somewhat more difficult that with the cryostage (Figure 3.9a, b). The air temperature surrounding the leaves was cooled from 20°C to approximately 2.5°C at cooling rates of up to about 1.6°C min^{-1} (Figure 3.9a, b). In this case, leaf cells induced the Ca^{2+} signal with three peaks, while the Ca^{2+} signal of root cells induced by the temperature change of 20 to 0°C had only two peaks (Figure 3.9c). One of the differences between leaf cells and root cells is the presence or absence of chloroplasts. The calcium-sensing protein (CAS) of thylakoid membrane (Peltier *et al*. 2004, Nomura *et al*. 2008, Vainonen *et al*. 2008) induces an extracellular Ca^{2+}-induced cytosolic Ca^{2+} increase (Han *et al*. 2003, Nomura *et al*. 2008, Rocha and Vothknecht 2012). In addition, it has been reported that the chloroplast has ion channels such as ACA1, HMA1, MSL2/3 and GLR3.4 including the putative Ca^{2+} channels (Huang *et al*. 1993, Seigneurin-Berny *et al*. 2005, Haswell and Meyerowitz 2006, Teardo *et al*. 2011, Hochmal *et al*. 2015). Therefore, there is a possibility that the third Ca^{2+} peak observed only in leaf cells is formed by the Ca^{2+} influx from the chloroplast through the several Ca^{2+} channels. Ca^{2+} signals in leaf cells also decreased after stopping the cooling. When the cooling rate reached 0°C min^{-1} (Figure 3.9b, c: white arrow), the decrease phase of the Ca^{2+} signal was induced. In order to investigate whether this phenomenon occurs under other cooling conditions, the Ca^{2+} signals were observed by using three cooling rates (Figure 3.10a). Under all the cooling conditions, when the cooling was stopped during the third increase of Ca^{2+} signal, the third peak decreased immediately (Figure 3.10b, c: outlined arrowheads). While there were some differences in the Ca^{2+} signals between leaf and root cells, continuous cooling was required to sustain the Ca^{2+} signals in both types of cells. I found that in terms of responsiveness to cooling, the leaf cells were different from the root cells. In leaf cells, there was the longer latent phase of Ca^{2+} signal in leaf cells (Figure 3.9c). However, root cells showed a much shorter latent phase (Figure 3.9c). It is reported that the sensitivity to the cold is higher in root cells than in aerial parts in tobacco seedlings (Campbell *et al*. 1996). Thus, these factors may cause the delay in the decrease phase and the longer latent phase in leaf cells.

Furthermore, I found several Ca^{2+} characteristics related to cold response in leaf cells. I focused on the effect of the temperature at the start of cooling on Ca^{2+} signals as I tested in the root cells (Figure 3.2b, c). The three Ca^{2+} signal peaks were induced in leaf cells when the leaves were cooled from 12 to 1.5°C (Figure 3.9d–f), while only one Ca^{2+} signal peak was induced in root cells when cooled from 12 to 0°C, (Figure 3.2c). The reason why three peaks were observed on the leaves is that our cryochamber cannot stop the cooling immediately like the cryostage (Figure 3.9e). Additionally, the latent phase of the Ca^{2+} signal was shorter in leaf cells when cooled from 12 to 1.5°C than when cooled from 20 to 2.5°C (Figure 3.9d–f)

although lower temperature induced a longer latent phase in root cells (Figure 3.2c, f). In leaf cells, the increase in Ca^{2+} concentration appeared to begin immediately after the cooling rate started to decrease from the maximum value (Figure 3.9e, f). The time point where the cooling rate started to decrease from the maximum value was determined experimentally at about 520 s (Figure 3.9e: gray arrowhead) in the cooling from 12 to 1.5°C, and at about 740 s in the cooling from 20 to 2.5°C (Figure 3.9e: black arrowhead), which is consistent with the time at which the Ca^{2+} signal began to increase in both cases. In order to investigate whether this phenomenon is common in leaves, the cooling from 20 to 2.5°C with three kinds of cooling rate was tested (see Figure 3.10), and a strong correlation was found between the time point where the cooling rate started to decrease from the maximum value and the start time of the increase phase in Ca^{2+} signals (Figure 3.9g). Therefore, leaf cells may need a change in the cooling rate from fast to slow in order to induce the increase phase from the latent phase. On the other hand, at a slower cooling rate, after the time point where the cooling rate started to decrease from its maximum value, it tended to take more time until the time point where the Ca^{2+} signal began to increase (e.g. comparison among three cooling rates in Figure 3.10). It is difficult now for us to judge whether this is an essential phenomenon or not, because, at very slow cooling rates, there is a limit to the temperature control and measurement in our cryochamber system. In contrast, in root cells, any cooling rate induced the increase phase in Ca^{2+} signal, but the length of the latent phase was dependent on the absolute temperature (Figure 3.2c, f). The difference in factors necessary for the initiation of the Ca^{2+} increase may influence the length of the latent phase in Ca^{2+} signal to the same cooling in root and leaf cells (Figure 3.9a–c). This different initiation of the Ca^{2+} increase in root and leaf cells might be caused by the higher sensitivity to the same cooling of the Ca^{2+} increase to cold in root cells than in aerial parts (Campbell *et al*. 1996). It was noteworthy that Ca^{2+} signal peaks could be detected during cooling with a cooling rate of 0.47°C min^{-1} in leaf cells. In the root cells, the small difference (i.e. 1 to 4°C) and slower rate (i.e. 2°C min^{-1}) of cooling induced Ca^{2+} signals (Figure 3.7c, e). For accurate and stable control of the temperature in the cryochamber, the cooling and heating temperature cycle from 20 to 16 to 20°C with a 0.47°C min^{-1} cooling rate was used and repeated three times (Figure 3.9h). This setting was based on the temperature changes in the field in order to understand the behavior of Ca^{2+} signals in leaf cells in the field. While a previous study reported that the Ca^{2+} peak declined with each rapid cooling cycle (about 20 to 3.5°C with about 10°C min^{-1}) (Plieth *et al*. 1999), my slow cooling cycle (i.e. from 20 to 16°C with a 0.47°C min^{-1} cooling rate) induced a Ca^{2+} increase with constant peak heights (Figure 3.9i). It should be emphasized that I succeeded in the detection of the Ca^{2+} signal induced by the slow cooling (at 0.47°C min^{-1}). Plieth *et al*. (1999) also reported that the only prolonged Ca^{2+} signal without a peak was observed with a cooling rate of 0.03°C s^{-1} (i.e. 3°C min^{-1}), while a 3°C min^{-1} cooling rate is too fast under natural conditions (e.g. Figure 3.12c). On the other hand, I succeeded in observing the peaks in

the slow cooling cycle. Thus, my result clearly showed that Ca^{2+} signals could be used in response to small and slow temperature changes in the field.

Expression of CBF/DREB1 genes in the field and Ca^{2+} signals

Many researchers use the constant low temperature condition (e.g. 2 or 4°C) for CA treatment (Uemura *et al*. 1995, Knight and Knight 2000, Doherty *et al*. 2009). Since cooling was required for the generation of Ca^{2+} signals, conventional CA treatments, such as transfer of plants from 23°C to constant 2°C, caused the Ca^{2+} signals to occur only once (Figure 3.9j, k). In contrast, when plants are cold-acclimated in the field, the frequent rise and fall of temperature may induce the Ca^{2+} signals several times (Figure 3.9h, i). Therefore, I determined the role of Ca^{2+} signals in CA-associated gene expression of CA plants in the field during the winter with experimental control plants that were subjected to CA at constant 2°C. Experiments in the field were conducted during mid-November, early December and late March at Morioka, Japan, for 56 h using 2-week-old Arabidopsis (Figure 3.11). Since *KIN1* was down-regulated by the Ca^{2+} channel chelator (Knight *et al*. 1996), I focused on the expression of *CBF/DREB1* genes which regulate KIN and COR genes. The conventional CA treatment at constant 2°C induced the single and earliest expression peak of *CBF/DREB1* genes at 4 h (first day at 15:00 h) (Figure 3.12a: black line). In contrast, the field CA treatment tended to induce two peaks at 22 h (second day at 09:00 h) and 46 h (third day at 09:00 h) (Figure 3.12a: orange, gray and purple lines).

The maximum *CBF/DREB1* gene expression level was larger in the order of: the experiment in December, at constant 2°C, or in March (depending on the gene) and in November (Figure 3.12a). The highest/lowest air temperature in the field between 0 and 46 h in the experiment was 14/1.3°C, 5.1/−3.8°C and 10.7/−1.1°C in November, December and March, respectively. Thus, lower temperature tended to induce greater gene expression. Interestingly, the constant 2°C treatment does not have temperature oscillations in the day and night, but temperature fluctuations in minutes induced higher gene expression than that of November. Thus, absolute temperature itself may also affect the gene expression level.

The second expression peak of *CBF1/DREB1B* and *CBF2/DREB1C* was found only in CA in the field (Figure 3.12a). The *CBF/DREB1* genes are known to exhibit a transient expression pattern when exposed to low temperature (Fowler and Thomashow 2002, Agarwal *et al*. 2006). In the field, there were differences in absolute temperature, temperature fluctuation in minutes, and day length (Figure 3.12b, c). In particular, there were few temperature fluctuations in December (Figure 3.12c), but the second expression peak in *CBF/DREB1* genes was induced (Figure 3.12a). The only one difference between artificial CA at 2°C and the three field CA conditions was the temperature difference between day and night. This suggests that the

temperature difference of day and night is important for the second induction of *CBF/DREB1* gene expression.

The Ca^{2+} channel blockers, 1mM $LaCl_3$ and 50 mM ruthenium red (RR), were used to ascertain whether multiple and large expression levels of *CBF/DREB1* genes were induced by a Ca^{2+} signal. To visualize how the Ca^{2+} signals were inhibited by the Ca^{2+} channel blockers, a cryomicroscopy system was used. $LaCl_3$ strongly inhibited both the speed of increase and the height of the first Ca^{2+} signal peak, and the speed of increase in the second and third Ca^{2+} signal peaks (Figure 3.13). Since $LaCl_3$ inhibited Ca^{2+} influx from the extracellular space (Knight and Knight 2000), the cold-induced Ca^{2+} signal peaks in the leaf cells may be mainly composed of the Ca^{2+} influx from the extracellular space. However, it had been reported that the second peak was the Ca^{2+} release from internal sources (Knight and Knight 2000). Thus, another possibility is that the first Ca^{2+} influx from the extracellular space induces the release of Ca^{2+} from intracellular organelles, which forms the second and third Ca^{2+} signal peaks. In other words, $LaCl_3$ inhibited only the first peak, but it affects the second and the third peak in indirect ways. In fact, the slow vacuolar ion channels have been reported possibly to release Ca^{2+} from vacuoles depending on the increase in the cytosolic Ca^{2+} concentration (Ward and Schroeder 1994, Bewell *et al*. 1999). Another Ca^{2+} channel blocker, RR, was known as a putative inhibitor of mitochondrial and endoplasmic reticulum Ca^{2+} channels (Knight *et al*. 1992, Monroy and Dhindsa 1995). I observed that RR weakly inhibited all Ca^{2+} signal peaks in leaf cells (Figure 3.13). RR inhibited the speed of increase for the second and third Ca^{2+} signal peaks and the height and rate of increase for the first Ca^{2+} signal peak (Figure 3.13c, d), suggesting that all Ca^{2+} signal peaks included the Ca^{2+} influx from organelles. Besides, I confirmed that the Ca^{2+} channel blockers inhibited the Ca^{2+} signals induced by the field-like cooling (Figure 3.14).

Subsequently, I focused on the inhibition of gene expression levels by the Ca^{2+} channel blockers. I focused on the effect of Ca^{2+} channel blockers on the gene expression level of *CBF/DREB1* genes, in particular the second expression peak (i.e. at 46 h), because the first peak of the *CBF/DREB1* genes was possibly caused by the temperature change when plants were transferred from the chamber at 23°C to the CA treatment (e.g. outside or the 2°C chamber). In conventional CA at 2°C, there was no significant difference in the second expression peak of *CBF1/DREB1* between control and chemical-treated plants (Figure 3.15a). However, in the field CA in mid-November, the expression levels of *CBF1/DREB1B* and *CBF2/DREB1C* were significantly higher in the control than in the $LaCl_3$- and RR-treated plants, except for the expression of *CBF1/DREB1B* with $LaCl_3$. In contrast, the expression level of *CBF3/DREB1A* was not inhibited by the Ca^{2+} channel blockers (Figure 3.15b). In the CA under field conditions in early December, the expression levels of *CBF/DREB1* genes were also not inhibited by the Ca^{2+} channel blockers (Figure 3.15c). Conversely, in CA under field conditions in March, the expression level of *CBF1/DREB1B* was inhibited by both Ca^{2+} channel

blockers, but *CBF2/DREB1C* was inhibited only by $LaCl_3$ (Figure 3.15d).

Although the changes in temperature were similar in November, December and March, the extent of temperature fluctuation was larger in mid-November and late March than in early December (Figure 3.12c). The SDs of the temperature changes (Figure 3.12c; °C 2 min^{-1}) between 22 and 46 h of CA in three experimental months were calculated as an index of temperature fluctuation. The correlations between the SDs of temperature changes and the expression suppression rates by the Ca^{2+} channel blockers were calculated and plotted (Figure 3.16). I found a strong correlation between the suppression level of *CBF1/DREB1B* and *CBF2/DREB1C* at the second expression peak and the magnitude of temperature fluctuation (Figure 3.16). Therefore, this suggests Ca^{2+} signal induction in mid-November and late March as a result of the greater magnitude of temperature fluctuation than in early December.

$LaCl_3$ tended to inhibit *CBF2/DREB1C* and RR inhibited *CBF1/DREB1B*, which suggests that *CBF/DREB* genes may be regulated by different Ca^{2+} signal parameters. As shown in Figure 3.13, $LaCl_3$ and RR inhibited Ca^{2+} signals at different levels. Without an inhibitor, the first and second Ca^{2+} signal peaks were almost the same height, and the third Ca^{2+} signal peak was the smallest (Figure 3.13d). In the case of $LaCl_3$ treatment, the second Ca^{2+} signal peak became the highest because the first peak was inhibited more strongly. In the case of RR treatment, however, the first Ca^{2+} signal peak became the highest because the second and third peaks were inhibited more strongly. Previous reports have discussed Ca^{2+} signal decoding. In guard cells, the frequency, transient number, duration and amplitude of Ca^{2+} signals are important for controlling stomatal aperture (Allen *et al*. 2001). Three different amplitudes and frequencies of Ca^{2+} signals caused by electrical stimulation induce very different gene expression profiles (Whalley *et al*.2011, Whalley and Knight 2013). On the other hand, I demonstrated that Ca^{2+} channel blocker treatment affected the amplitude and ratio of Ca^{2+} signal peak heights (Figure 3.13). In particular, RR did not strongly decrease the amplitude of Ca^{2+} signal peaks (Figure 3.13), but inhibited *CBF1/DREB1B* expression significantly (Figures 3.15 and 3.16). This result indicates that the ratio of Ca^{2+} signal peak heights (e.g. ratio of first/second peak) and/or that of extracellular and intracellular influx may also be decoded to modulate gene expression.

It had been reported that calmodulin-binding transcription activator 3 (CAMTA3) and CAMTA5 respond to a temperature decrease, and induced the expression of *CBF1/DREB1B* and *CBF2/DREB1C* via the Ca^{2+} signaling pathway (Doherty *et al*. 2009, Kidokoro *et al*. 2017). These reports are consistent with my results showing that the gene expression of *CBF1/DREB1B* and *CBF2/DREB1C* was inhibited by the Ca^{2+} channel blockers only under conditions with temperature fluctuations (Figure 3.16). This suggests that Ca^{2+} signals induced by temperature regulate the gene expression of *CBF1/DREB1B* and *CBF2/DREB1C* in the field. In addition, $LaCl_3$ and RR tended to suppress the first expression peak of *CBF1/DREB1B* and

CBF2/DREB1C in each CA treatment, including conventional CA (Figure 3.17). Since the rapid temperature decrease occurred in all the conditions when plants were transferred outside or to the 2°C chamber, this suppression could be explained by the Ca^{2+}–CAMTA pathway.

The expression of *CBF3/DREB1A* was, however, not suppressed by $LaCl_3$ and RR (Figures 3.15 and 3.16). *CBF3/DREB1A* does not have a binding site for the CAMTA protein (Kidokoro *et al*. 2017). *CBF3/DREB1A* expression is also regulated by clock factors, such as CIRCADIAN CLOCK-ASSOCIATED 1 (CCA1) and LATE ELONGATED HYPOCOTYL (LHY) (Dong *et al*. 2011, Kidokoro *et al*. 2017). Therefore, I concluded that *CBF3/DREB1A* is controlled not only by Ca^{2+} signaling but also by many other factors. Moreover, the channel blockers tended to enhance the expression level of *CBF1/DREB1B* and *CBF2/DREB1C* under lower thermal amplitude fluctuations in December. These results suggest that different Ca^{2+} signals,

Conclusion

In this study, by using a newly developed Ca^{2+} signal determination system and carefully formulated temperature correction, I revealed several novel findings that (i) there was only one transient Ca^{2+} signal when plants are subjected to a rapid temperature drop at the beginning of conventional CA treatment (i.e. such as at constant 2°C), but multiple Ca^{2+} signals were induced in the temperature fluctuation during CA, which probably occurs under field-like CA conditions; (ii) Ca^{2+} signals were adapted to ambient temperatures and sensed temperatures even during or after CA; and (iii) the expression of *CBF/ DREB1* genes was regulated by the Ca^{2+} signals which were induced by the temperature fluctuation in the field during the winter. These results suggest that Ca^{2+} signals act as a messenger for temperature fluctuation in minutes in the field instead of large diurnal temperature changes from day to night.

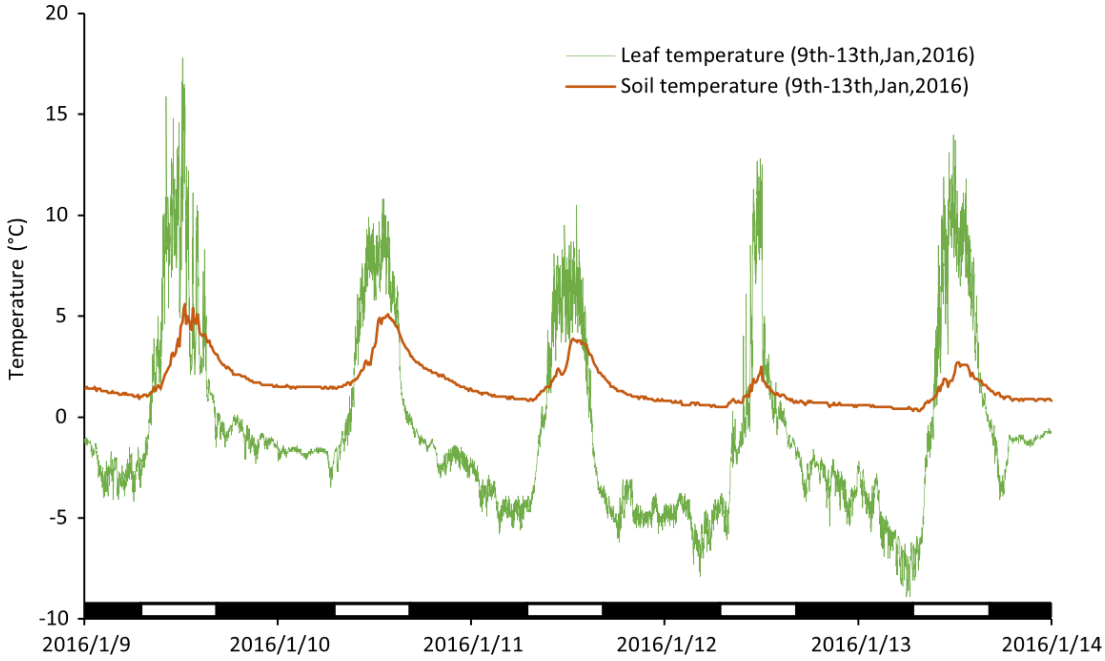

Figure 3.1. Temperature change of leaf and soil in Morioka on January. Green line shows the leaf temperature and brown line indicate the soil temperature. The temperature data were collected using a thermocouple data logger (TR-55i-TC, RTR-505-TC; T&D Co., Japan). The bar at the bottom the graph indicates daytime (white) and nighttime (black).

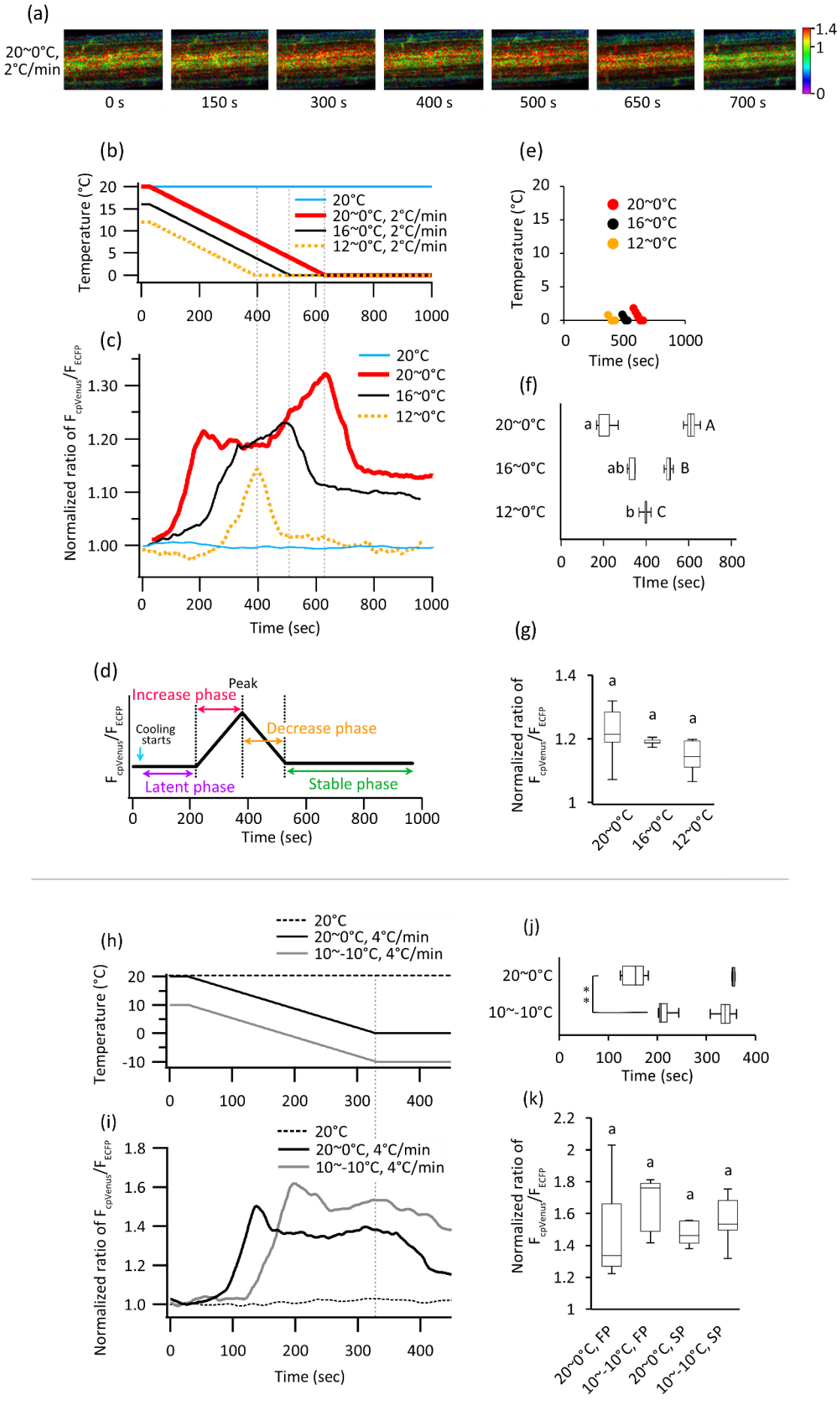
(a)
20~0°C, 2°C/min
0 s
150 s
300 s
400 s
500 s
650 s
700 s
1.4
1
0
(b)
Temperature (°C)
20°C
20~0°C, 2°C/min
16~0°C, 2°C/min
12~0°C, 2°C/min
Time (sec)
(c)
Normalized ratio of F cpVenus/F ECFP
20°C
20~0°C
16~0°C
12~0°C
Time (sec)
(d)
Increase phase
Peak
Decrease phase
Cooling starts
Latent phase
Stable phase
F cpVenus/F ECFP
Time (sec)
(e)
Temperature (°C)
20~0°C
16~0°C
12~0°C
Time (sec)
(f)
20~0°C
16~0°C
12~0°C
a
A
ab
B
b
C
TIme (sec)
(g)
Normalized ratio of F cpVenus/F ECFP
a
a
a
20~0°C
16~0°C
12~0°C
(h)
20°C
20~0°C, 4°C/min
10~-10°C, 4°C/min
Temperature (°C)
(i)
20°C
20~0°C, 4°C/min
10~-10°C, 4°C/min
Normalized ratio of F cpVenus/F ECFP
Time (sec)
(j)
20~0°C
10~-10°C
**
Time (sec)
(k)
Normalized ratio of F cpVenus/F ECFP
a
a
a
a
20~0°C, FP
10~-10°C, FP
20~0°C, SP
10~-10°C, SP

Figure 3.2. The effect of different starting and nadir temperature on Ca^{2+} signals in root cells. (a) An example of the ratio image of fluorescence of cpVenus divided by that of ECFP in Arabidopsis root expressing Yellow Cameleon 3.60. (b) The temperature settings. (c) Averaged Ca^{2+} signals when cooled from 20°C (red), 16°C (black) or 12°C (yellow) to 0°C at 2°C min^{-1} (n = 5 or 6). (d) Name of the Ca^{2+} signal phase. (e) The peak time (before the last decrease phase) of Ca^{2+} signal was plotted against the temperature. (f) Boxplots were used to indicate the timing of the Ca^{2+} signal peaks; or (g) the normalized FRET value which indicates the Ca^{2+} concentration changes. The boxplots present the first to third quartile values, and the bars represent the minimum and maximum values. Significant differences between each data set were analyzed using the Tukey–Kramer test [$p < 0.01$ (e), $p < 0.05$ (f)]. (h) Temperature settings. (i) Averaged Ca^{2+} signals when cooled from 20°C (black) or 10°C (gray) at a rate of 4°C min^{-1} (n = 5). (j) Boxplots were used to indicate the timing of the Ca^{2+} signal peaks (k) as well as the normalized FRET. The boxplots present the first to the third quartile values, and the bars represent the minimum and maximum values. Ratio values were normalized by the value at t = 0. The vertical broken lines in a to c or in h to i indicate the time point where cooling rate is 0°C min^{-1}. Significant differences between data sets were analyzed using the *t*-test (**$p < 0.01$).

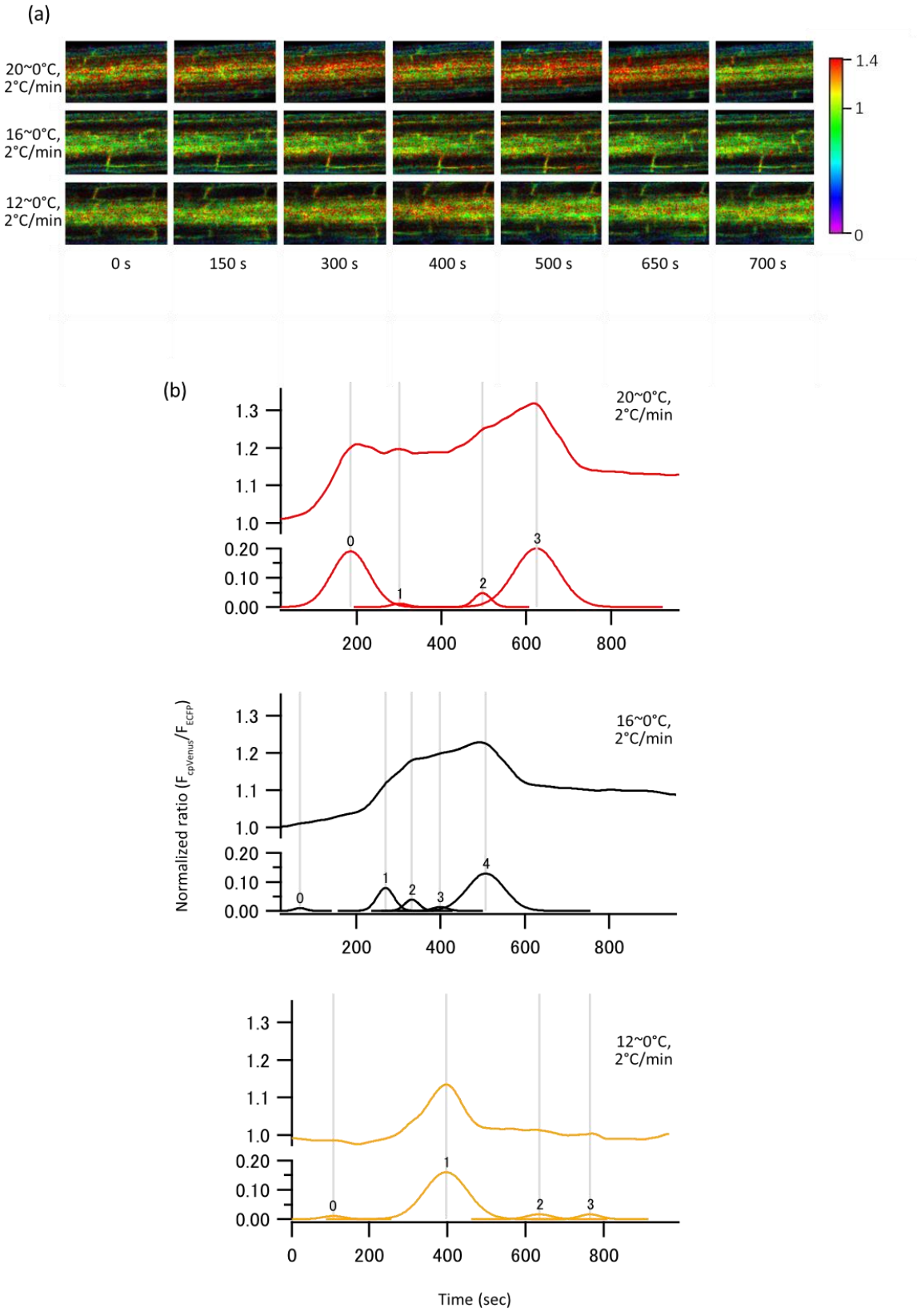

Figure 3.3. The ratio images of YC3.60 and peak analysis of the cooling from different start temperature. (a and b) The plants were cooled from 20°C, 16°C or 12°C to 0°C at a rate of 2 min. (a) The fluorescence image of cpVenus was devided with that of ECFP. (b) The Ca^{2+} signals were analyzed by using the software IGOR pro. This analysis shows that how many peaks make the Ca^{2+} signal.

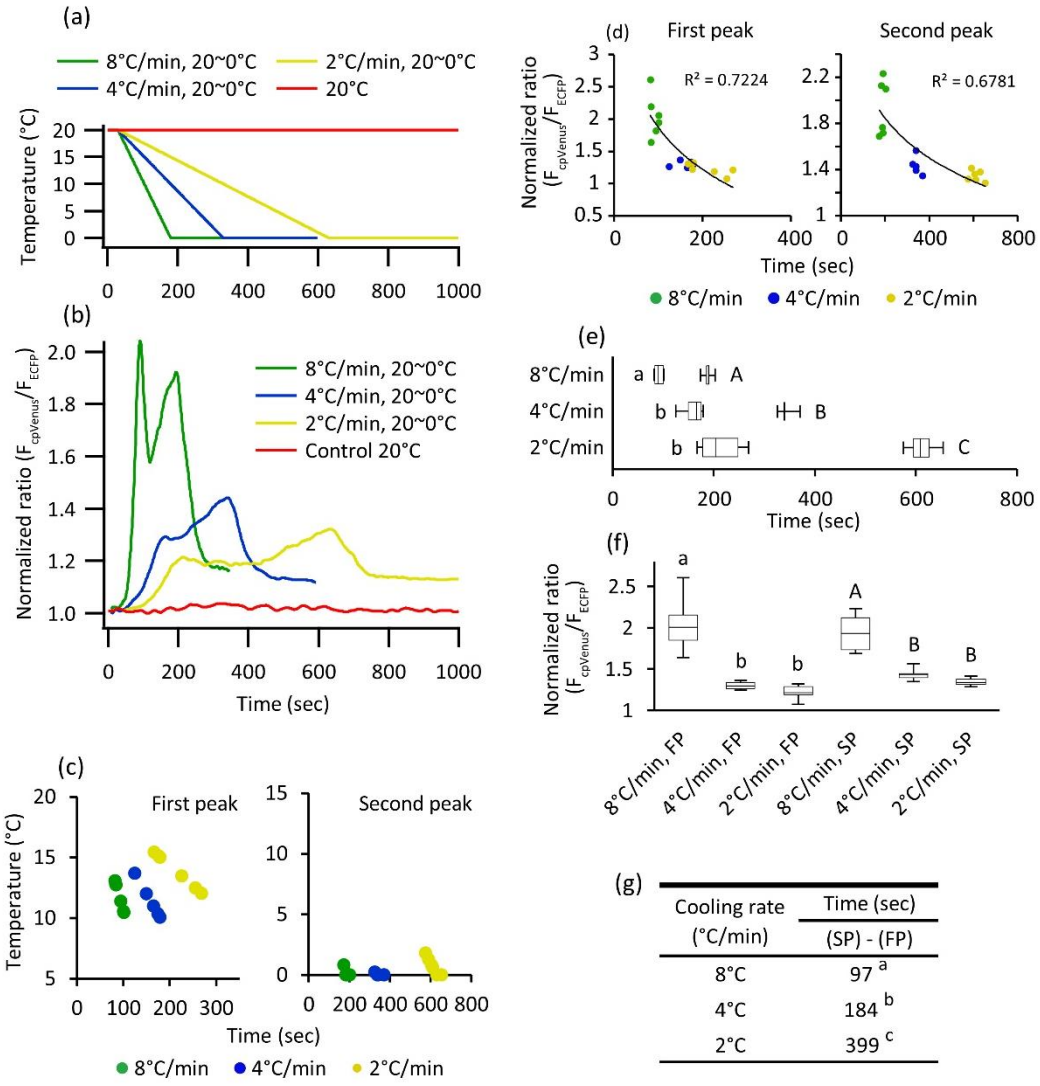

(g)

Cooling rate (°C/min)	Time (sec) (SP) - (FP)
8°C	97 [a]
4°C	184 [b]
2°C	399 [c]

Figure 3.4. Effect of the cooling rate on Ca^{2+} signals in the roots of Yellow Cameleon 3.60-expressing *Arabidopsis* plants. (a) Plants were cooled from 20°C to 0°C at 8°C min^{-1} (green), 4°C min^{-1} (blue), or 2°C min^{-1} (yellow). Constant 20°C treatment was also tested as a control (red). (b) The FRET values were calculated using the IGOR pro program and normalized against the initial values. Each plot of FRET ratios represents the mean of several independent experiments (n = 5 or 6). (c) The peak values were plotted against the temperature. (d) The timing of the first and second Ca^{2+} signal peaks and the corresponding concentrations were plotted to confirm the correlation. (e) Boxplots were used to indicate the timing of the Ca^{2+} signal peaks and (f) the relative ratio of Ca^{2+} concentration. The boxplots present the first to the third quartile values, and the bars represent the minimum and maximum values. (g) The time lags between the first peak (FP) and second peak (SP) were calculated. Ratio values were normalized by the value at t = 0. Significant differences between data sets were analyzed using the Tukey–Kramer test [$p < 0.05$ (e), $p < 0.01$ (f)].

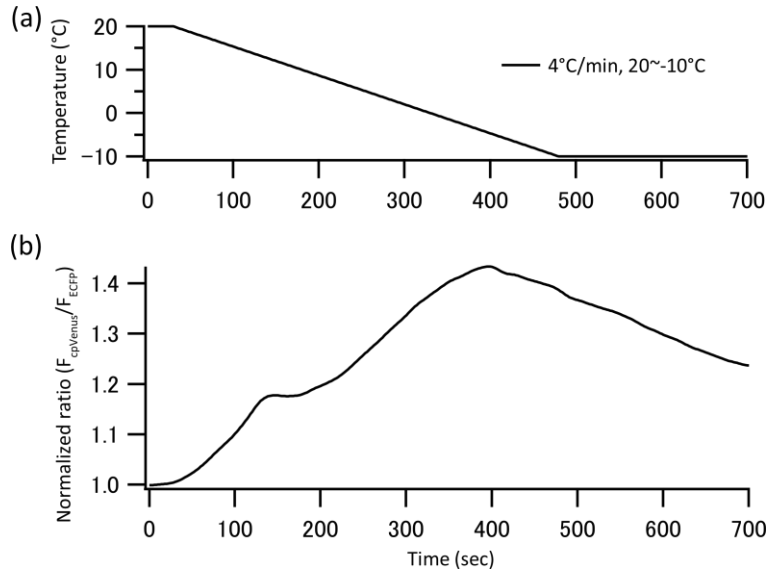

Figure 3.5. Ca^{2+} signals induced by the 30°C of cooling range. (a) The temperature was changed from 20°C to −10°C with 4°C min^{-1} of cooling rate. (b) The FRET values were calculated using the IGOR pro program and normalized against the initial values. Each plot of FRET ratios represents the mean of several independent experiments (n = 6).

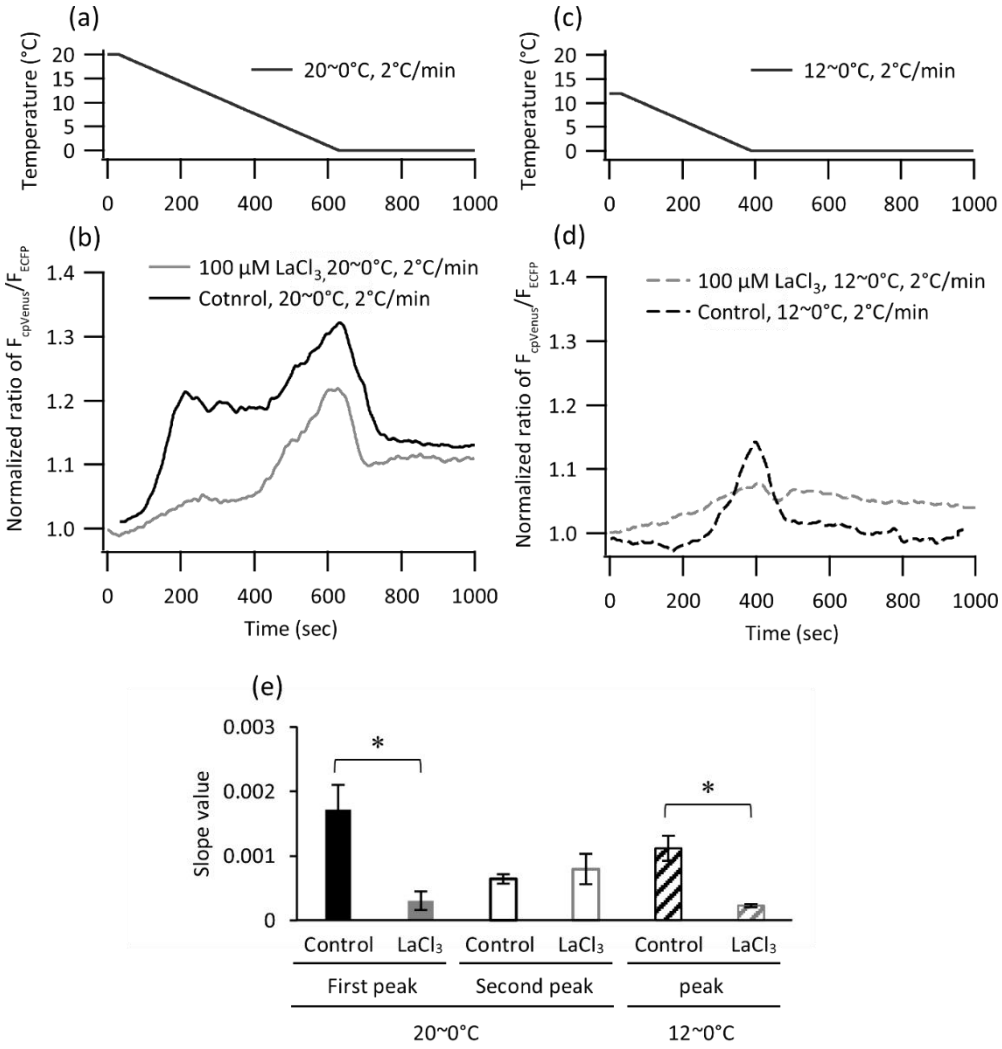

Figure 3.6. The source of Ca^{2+} signal under the low-temperature in root cells. (a and b) Averaged Ca^{2+} signals when cooled from 20°C to 0°C or (c and d) 12°C to 0°C at a rate of 2°C min^{-1} with/without $LaCl_3$ (n = 3 to 5). The black line indicates the Ca^{2+} signals of untreated plants (controls) and gray line indicates that treated with 100 µM $LaCl_3$ for 1 h prior to being analyzed. The FRET values were calculated and normalized against the initial values. (e) The slopes between 100 and 200 s, and between 500 and 600 s, were calculated for each first and second Ca^{2+} signal peak induced by a temperature change from 20°C to 0°C. The slope between 300 and 400 s for the temperature change from 12°C to 0°C was also calculated. Ratio values were normalized by the value at t = 0. Significant differences between each data set were analyzed using the *t*-test (*p< 0.05) (n = 3 to 5). The bars indicate the SE.

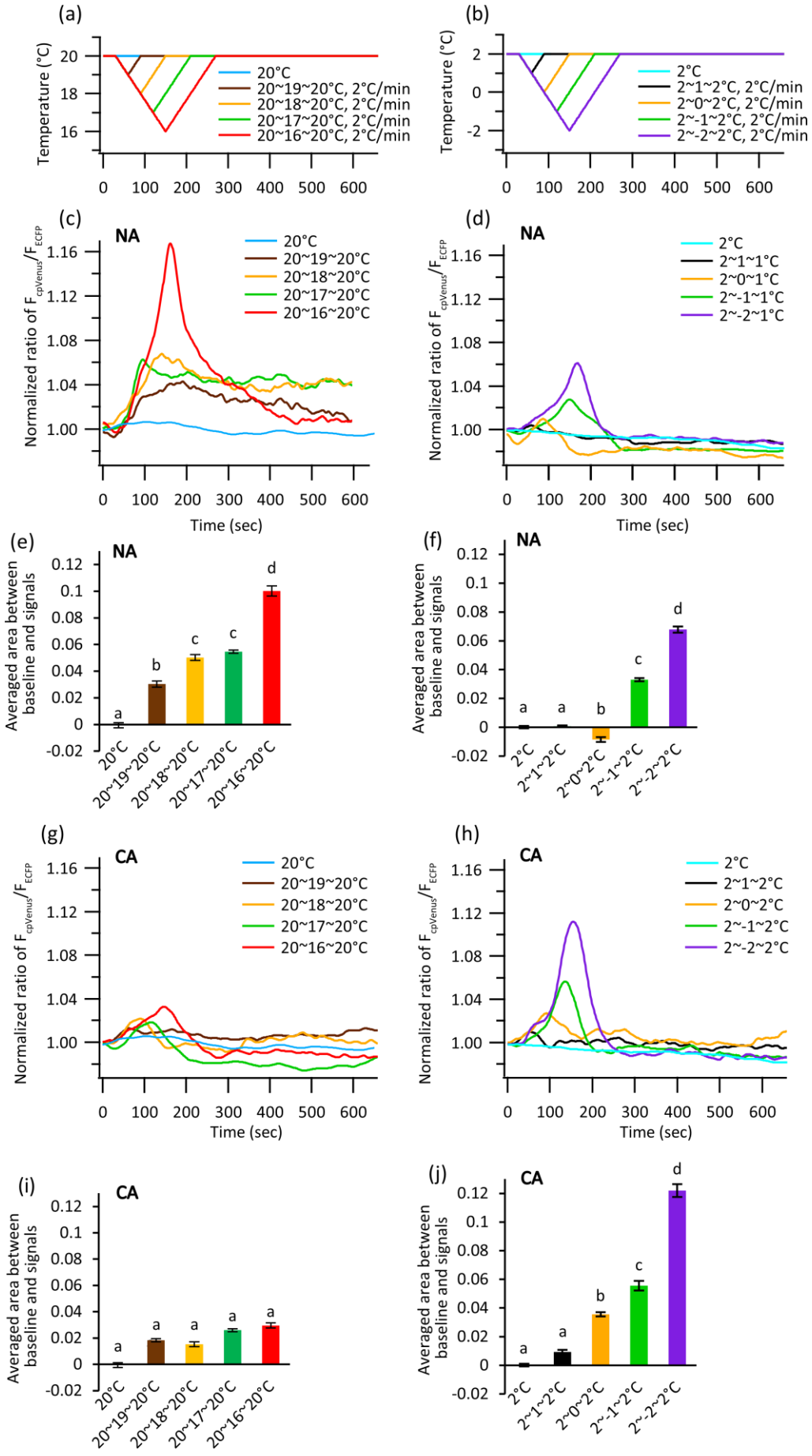
(a)
Temperature (°C)
20°C
20~19~20°C, 2°C/min
20~18~20°C, 2°C/min
20~17~20°C, 2°C/min
20~16~20°C, 2°C/min
(b)
Temperature (°C)
2°C
2~1~2°C, 2°C/min
2~0~2°C, 2°C/min
2~-1~2°C, 2°C/min
2~-2~2°C, 2°C/min
(c)
NA
Normalized ratio of F_cpVenus/F_ECFP
20°C
20~19~20°C
20~18~20°C
20~17~20°C
20~16~20°C
Time (sec)
(d)
NA
Normalized ratio of F_cpVenus/F_ECFP
2°C
2~1~1°C
2~0~1°C
2~-1~1°C
2~-2~1°C
Time (sec)
(e)
NA
Averaged area between baseline and signals
20°C
20~19~20°C
20~18~20°C
20~17~20°C
20~16~20°C
(f)
NA
Averaged area between baseline and signals
2°C
2~1~2°C
2~0~2°C
2~-1~2°C
2~-2~2°C
(g)
CA
Normalized ratio of F_cpVenus/F_ECFP
20°C
20~19~20°C
20~18~20°C
20~17~20°C
20~16~20°C
Time (sec)
(h)
CA
Normalized ratio of F_cpVenus/F_ECFP
2°C
2~1~2°C
2~0~2°C
2~-1~2°C
2~-2~2°C
Time (sec)
(i)
CA
Averaged area between baseline and signals
20°C
20~19~20°C
20~18~20°C
20~17~20°C
20~16~20°C
(j)
CA
Averaged area between baseline and signals
2°C
2~1~2°C
2~0~2°C
2~-1~2°C
2~-2~2°C

Figure 3.7. Ca^{2+} signals of non-acclimated or cold-acclimated YC3.60-expressing *Arabidopsis* roots. (a) Temperature conditions were from 20°C to 19°C and then to 20°C (brown), from 20°C to 18°C and then to 20°C (orange), from 20°C to 17°C and then to 20°C (green), and from 20°C to 16°C then to 20°C (red), and 20°C constant as a control (blue). (b) Other settings were from 2°C to 1°C and then to 2°C (black), from 2°C to 0°C and then to 2°C (orange), from 2°C to −1°C and then to 2°C (green), and from 2°C to −2°C to and then 2°C (purple), 2°C constant as a control (sky blue). Samples in all experiments were cooled/heated at a rate of 2°C min^{-1}. (c and d) The NA plants were analyzed using the cooling series of panel a. and panel b. (e and f) Statistical processing was performed based on the area formed between the baseline (i.e., Ca^{2+} signals of 20°C or 2°C constant) and Ca^{2+} signal induced by the cooling treatments from 50 to 200 s (n = 255~380). (g and h) CA plants were analyzed using the cooling series of panel a. and panel b. (i and j) Statistical processing was performed same way as e and f. The FRET values were calculated and normalized against the initial values (n = 4, 5). Ratio values were normalized by the value at t = 0. Significant differences between each data set were analyzed using the Tukey–Kramer test ($p < 0.05$).

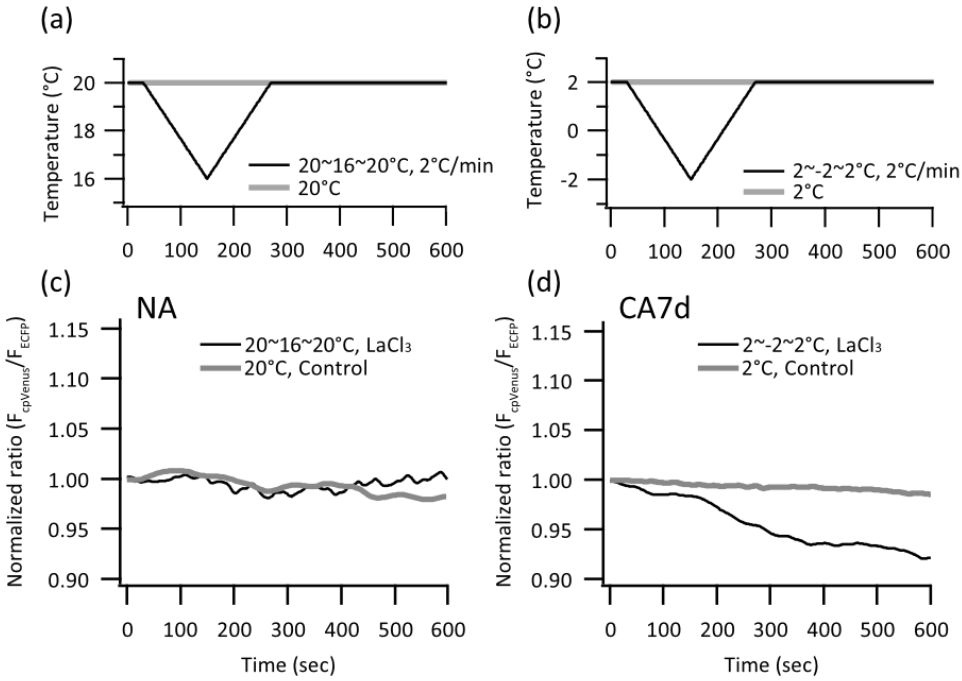

Figure 3.8. $LaCl_3$ test to nonacclimated (NA) and 7 days cold-acclimated (CA7d) Arabidopsis root cells. (a) The temperature was changed from 20°C to 16°C to 20°C at 2°C min^{-1}, or kept at 20°C for NA plants. (b) The temperature was changed from 2°C to −2°C to 20°C at 2°C min^{-1}, or kept at 2°C for CA7d plants (c and d) The FRET values of root cells were calculated and normalized against the initial values (n = 5). Ratio values were normalized by the value at t = 0.

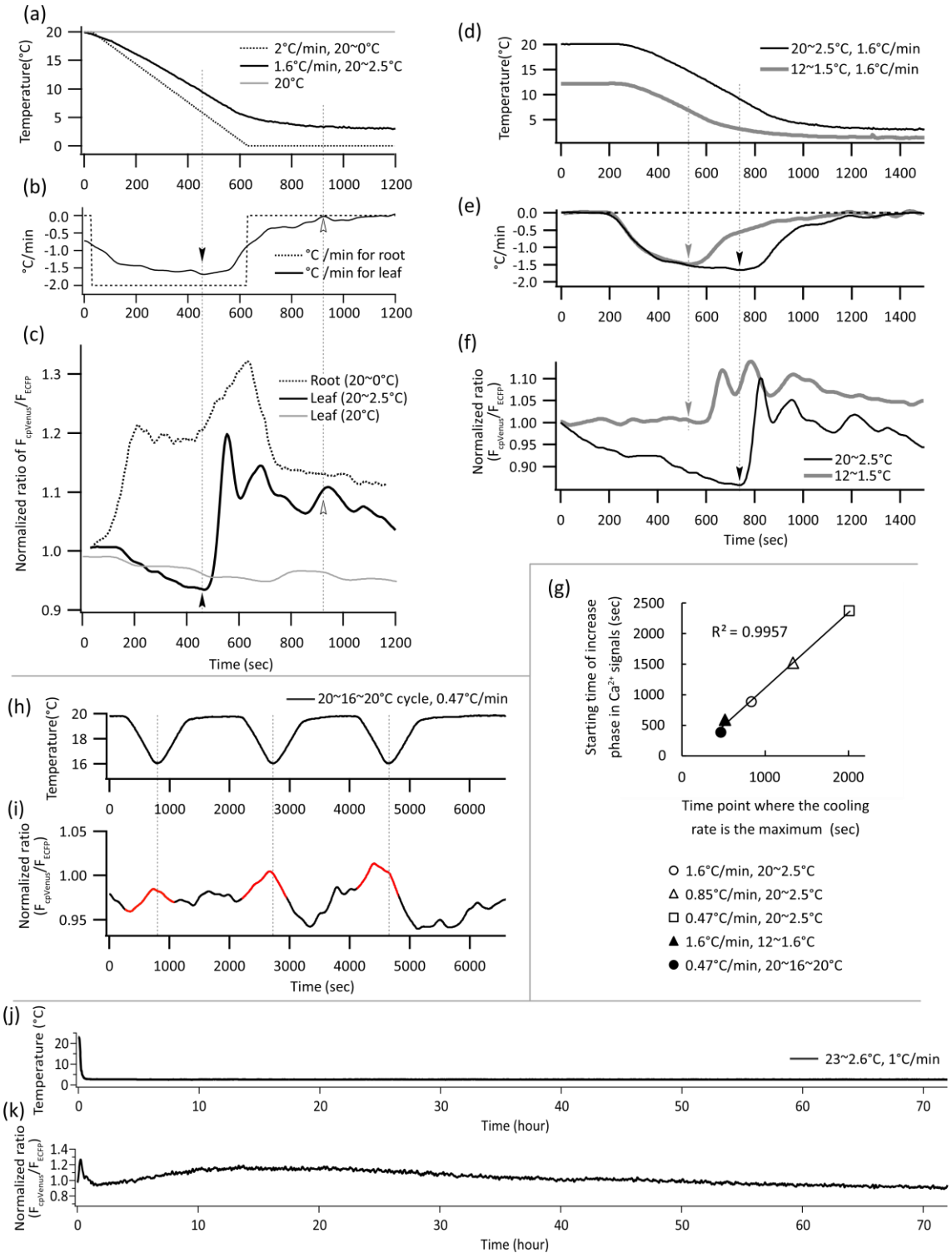

Figure 3.9. Ca^{2+} signal characteristics in leaf cells. (a) Comparison with the Ca^{2+} signal in leaf and root cells. Both leaf and root cells were cooled from 20°C to around 0°C at about 2°C min^{-1}, or kept at 20°C for leaf cells. (b) The cooling rate was calculated from the temperature setting (root) and temperature data (leaf). The temperature was measured every 5 s. The black arrow head indicates the time point where the cooling rate is the maximum and the white arrow head indicates the time point where cooling rate is 0°C min^{-1}. (c) Ca^{2+} signals induced by the cooling in the root (broken black line) and leaf cells (solid black line). Ca^{2+} signals at a constant 20°C are also shown as the baseline (gray line) (n = 4, 5). (d) Leaves were cooled from 20°C to about 2.5°C or from 12°C to about 1.5°C at 1.6°C min^{-1}. (e) The cooling rate was calculated from the temperature data. The temperature was measured every 5 s. The gray and black arrow head indicate the time point where the cooling rate is the maximum. (f) Ca^{2+} signals were observed in

each condition every 5 s (n = 4, 5). (g) The correlation between the time point where the cooling rate is the maximum and the starting time of increase phase in Ca^{2+} signals. Each plot was calculated from the results of Figure 3.9d-f (12°C to 1.5°C at 1.6°C min^{-1}), 3.9h, i (the first peak) and Figure 3.10 (h) Temperatures were changed from 20°C to 16°C to 20°C at 0.47°C min^{-1} for three cycles. (i) The Ca^{2+} signals were observed every 5 s (n = 5). The vertical broken lines in h to i indicate the time point where cooling rate is 0°C min^{-1}. (j) Temperatures were changed from 23°C to 2.6°C at 1°C min^{-1}, which mimicked CA treatment at a constant low temperature. (k) Fluorescence images were captured at intervals of 1 min for 72 h (n = 3). All ratio values were normalized by the value at t = 0. Each plot of normalized FRET values represents the average of independent experiments.

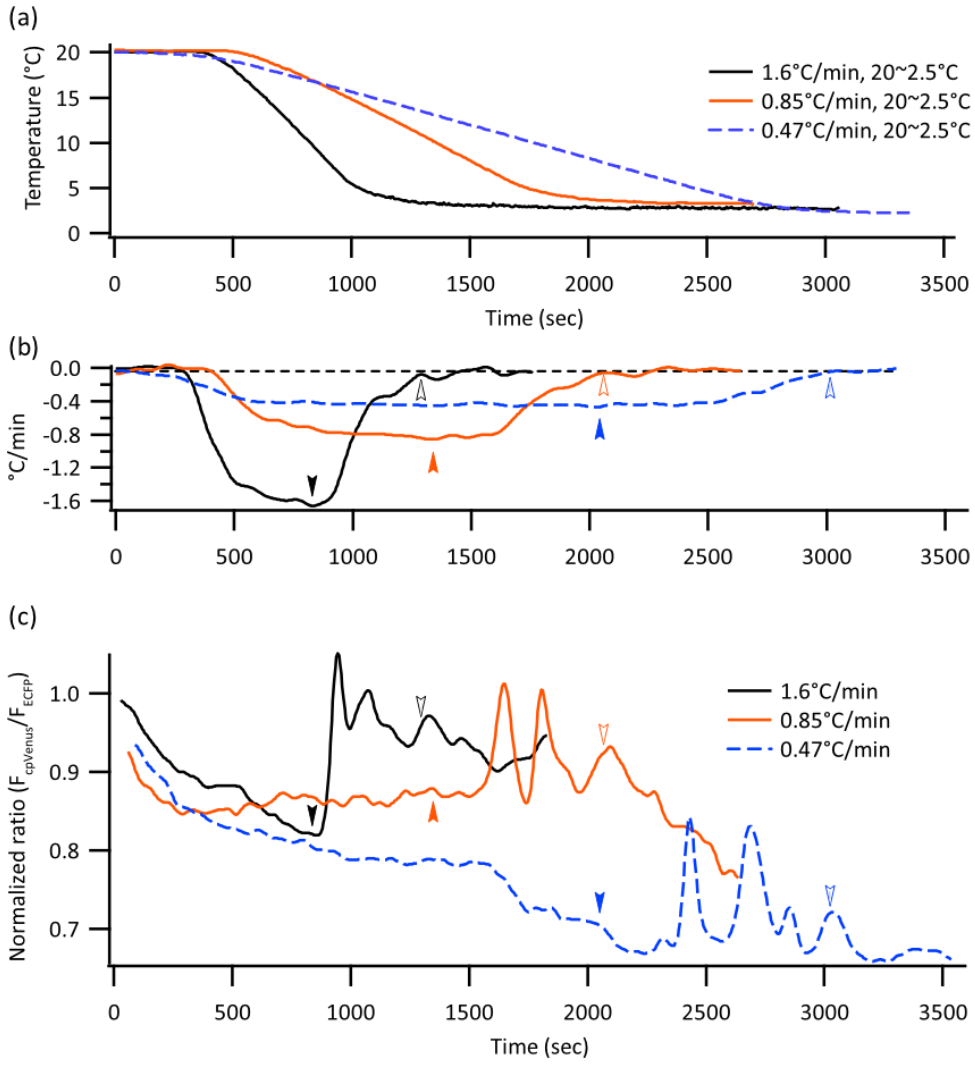

(d)

Cooling rate (°C/min)	Time (sec)		
	(SP) - (FP)	(TP) - (SP)	(TP) - (FP)
1.6°C	112 a	266 A	379 α
0.85°C	181 ab	335 A	517 α
0.47°C	250 b	240 A	490 α

Figure 3.10. Effect of the cooling rate on Ca^{2+} signals of YC3.60-expressing Arabidopsis leaves. (a) The temperature settings were as follows: from 20°C to 2.5°C at a rate of 1.6°C min^{-1} (solid black line), 0.85°C min^{-1} (solid orange line), or 0.47°C min^{-1} (dashed blue line). (b) The cooling rate was calculated from the temperature data. The black, orange and blue arrow heads indicate the time point where the cooling rate is the maximum in the cooling with the cooling rate of 1.6°C min^{-1}, 0.85°C min^{-1} and 0.47°C min^{-1}, respectively. Each color of outline arrow heads indicate the time point where the cooling rate became about 0. (c) The FRET values were calculated and normalized against the initial values (n = 4 to 5). (d) The time interval between the first peak (FP) and second peak (SP), between the FP and third peak (TP), and between the SP and TP were calculated. Significant differences between each data set were analyzed using by the Tukey–Kramer test ($p < 0.01$) (n = 4 to 5).

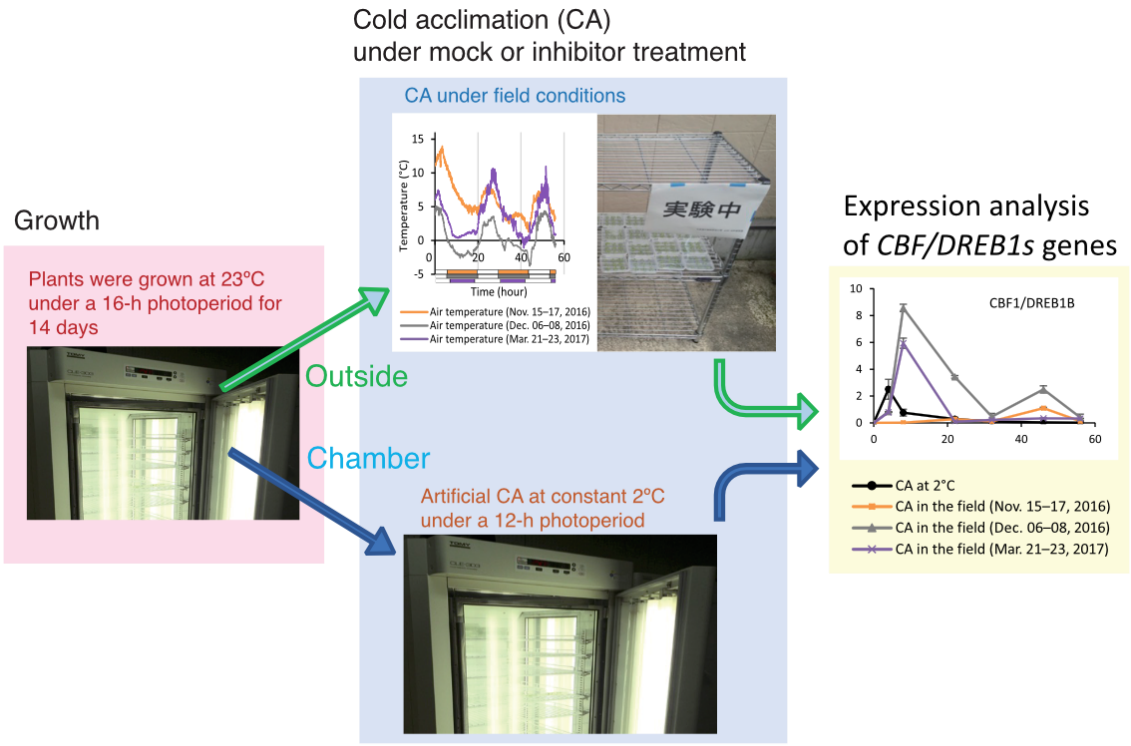

Figure 3.11. Expression of *CBF/DREB1s* during outside or artificial cold acclimation.

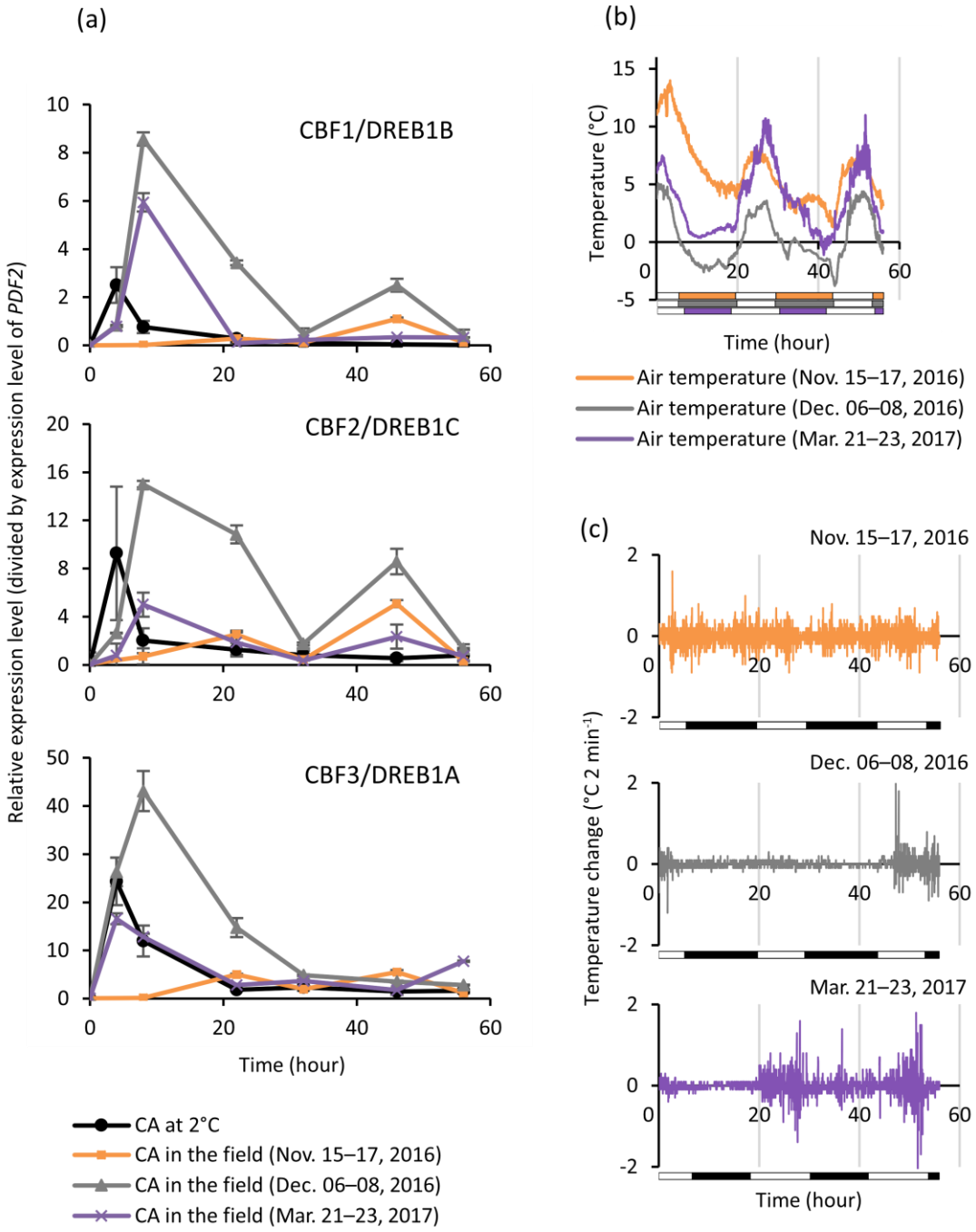

Figure 3.12. The expression levels of *CBF/DREB1s* during the CA treatment at 2°C or in the field. (a) The expression level of *CBF1/DREB1B*, *CBF2/DREB1C*, and *CBF3/DREB1A* were measured by real-time PCR at 0, 4 (except during November), 8, 22, 32, 46, and 56 h after starting the CA treatments (n = 3 or 4). Plants were cold acclimated in a constant 2°C chamber, or outside in November 15–17 and December 6–8, 2016, and March 21–23, 2017, in Morioka, Japan. The bar indicates the SE. (b) The air temperature was measured by the data loggers. The white and color bars indicate day and night time, respectively, during mid-November (orange), early December (gray), and late March (purple). (c) The rate of temperature change at °C 2 min^{-1} was calculated. The bars under the graph indicate day (white) or night (black) time.

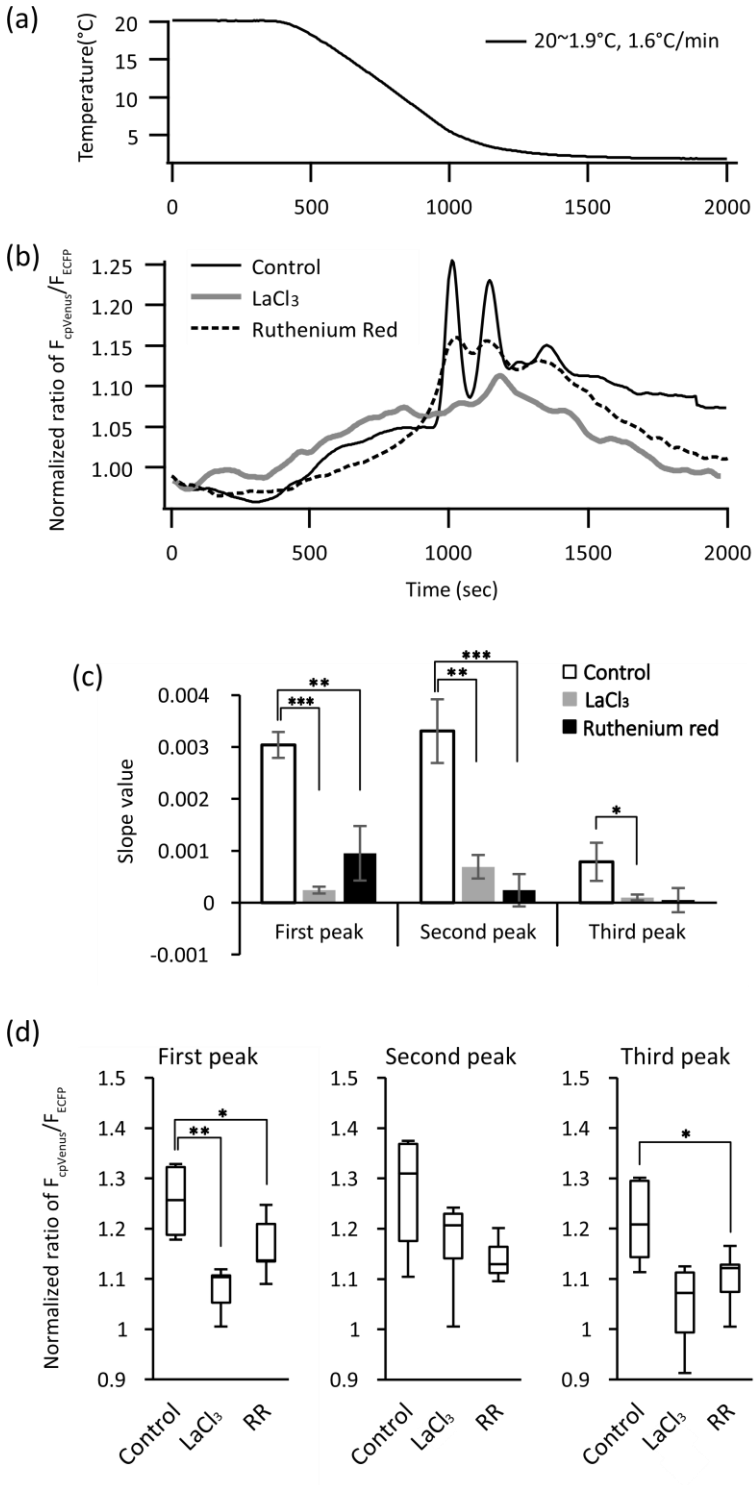

Figure 3.13. The effect of Ca^{2+} channel blockers on Ca^{2+} signals in leaf cells in the cryochamber. (a) The plants were cooled from 20°C to 1.9°C at a 1.6°C min^{-1} cooling rate. (b) The Ca^{2+} signals were induced by cooling with a chemical treatment: i.e., 0.05% of Triton X-100 solution was sprayed on the plants as control (black line), 1 mM $LaCl_3$ with 0.05% Triton X-100 solution (gray line), or 50 μM RR and with 0.05% Triton X-100 solution (broken black line) were sprayed on plants to inhibit their Ca^{2+} signals. Ratio values were normalized by the value at t = 0. Each plot of normalized FRET values represents the average of independent experiments (n = 5). (c) The slopes between peak time and 60 s before peak time were calculated to observe the effect of the chemicals. (d) The boxplots present the first to third quartile values and the bars represent the minimum and maximum values of the first to third Ca^{2+} signal peaks. Significant differences between each data set were analyzed using a *t*-test (***$p < 0.001$, **$p < 0.01$, *$p < 0.05$) (n = 4, 5).

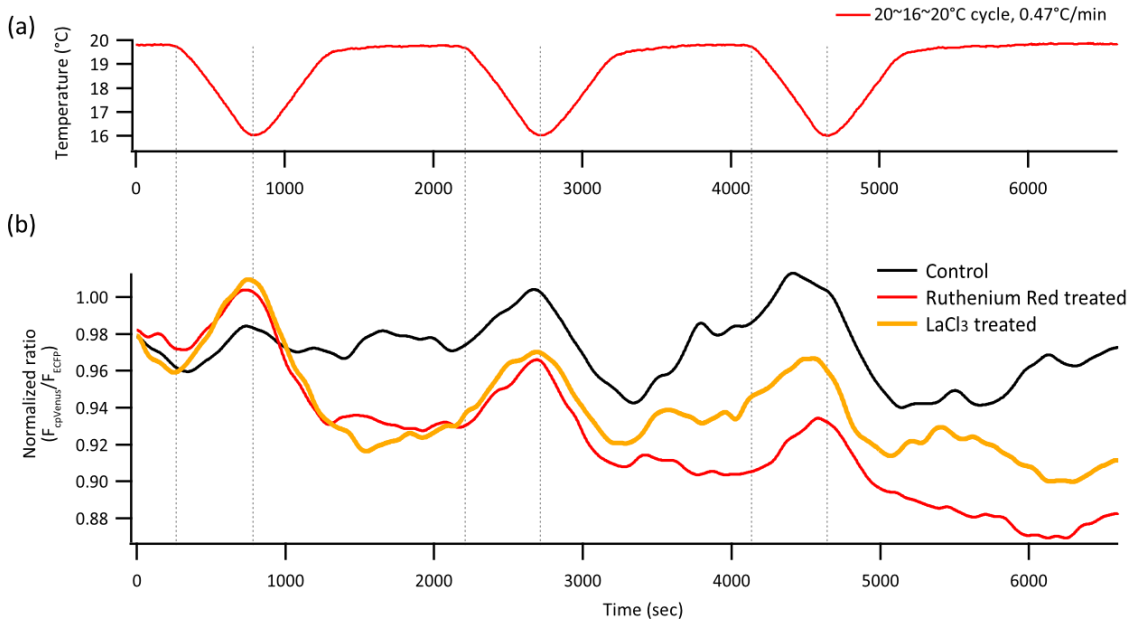

Figure 3.14. Effect of Ca^{2+} channel blockers on the small Ca^{2+} signals in leaf. (a) The temperature was changed from 20°C to 16°C to 20°C with 0.47°C min for three cycles. (b) 1 mM LaCl3 and 0.05% Triton X-100 mix solution, or 50 μM RR and 0.05% Triton X-100 mix solution sprayed to plants. Ca^{2+} signals were observed every 5 s (n = 5). All ratio values were normalized by the value at t = 0. Each plot of normalized FRET value represents the average of independent experiments.

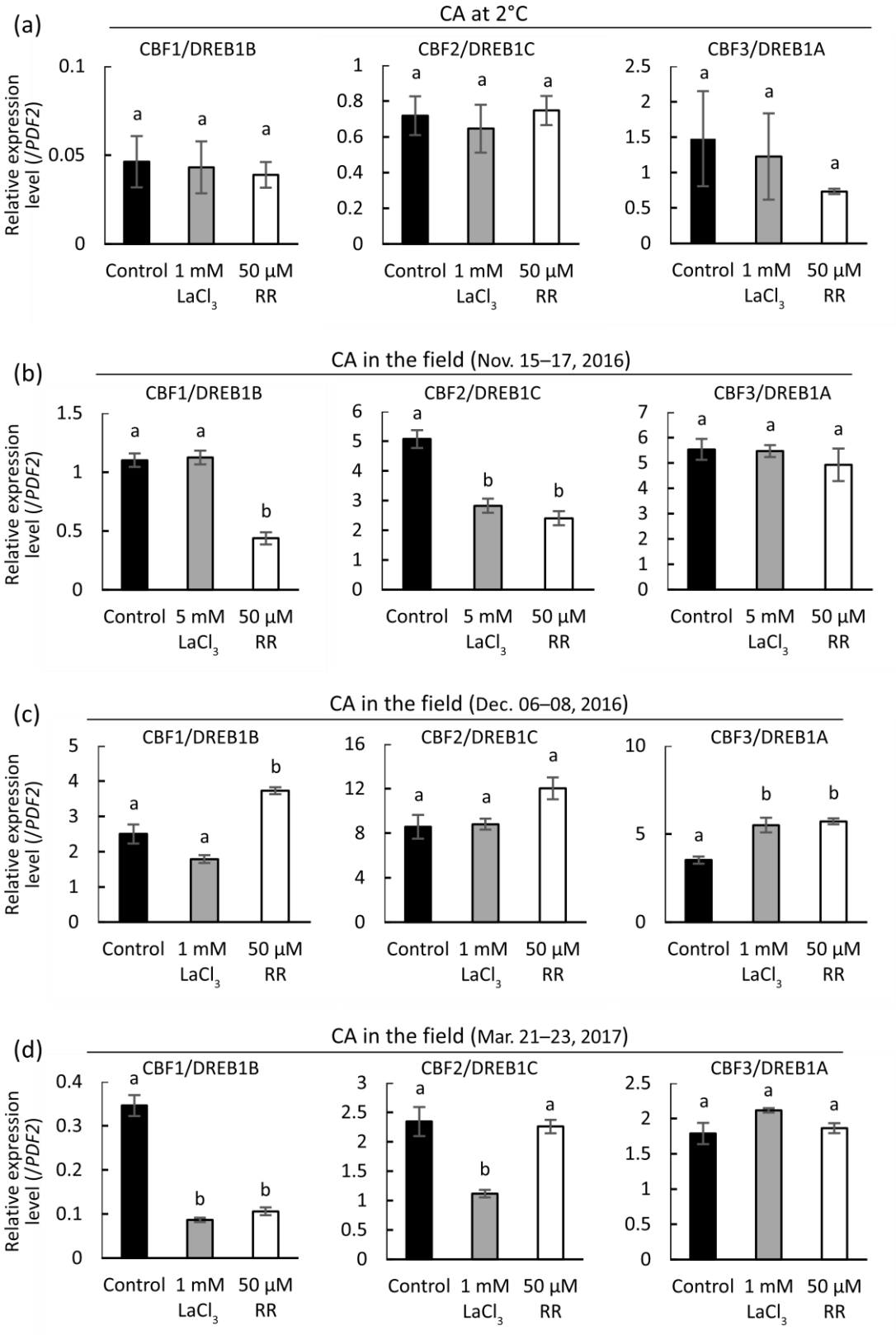

Figure 3.15. Inhibition of the expression levels of *CBF/DREB1s* by Ca^{2+} channel blockers at 46 h CA treatment. (a-d) The expression level of *CBF1-3* were measured in CA plants with 1 mM or 5 mM $LaCl_3$, or 50 μM ruthenium red. The chemicals were sprayed 1 hour prior to the initiation of CA treatment. (a) CA at 2°C in the chamber (b) CA in the field on November 15–17, 2016. (c) CA in the field, on December 6–8, 2016. (d) CA in the field on March 21–23, 2017. Significant differences between each value were analyzed using the Tukey–Kramer test ($p< 0.05$) (n = 3 or 4). The bars indicate the SE.

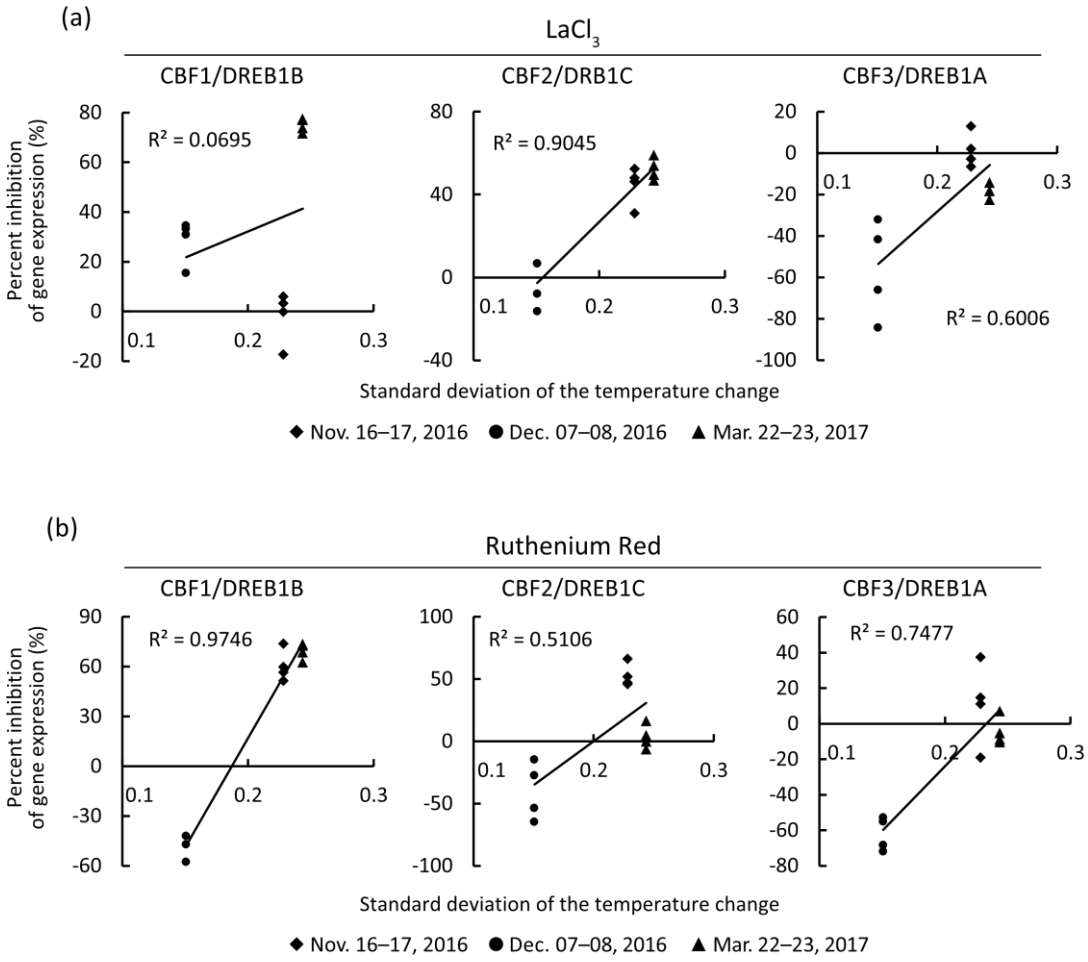

Figure 3.16. Correlation between the effect of Ca^{2+} channel blockers and fluctuation of temperature during CA treatment. (a and b) Standard deviations were calculated from the temperature change between 22 h and 46 h at the start of CA. The value of CA at 2°C was substituted as 0. Percent inhibition of gene expression was calculated by subtracting each gene expression level of chemical treated plants from the average value of gene expression level of control. (a) Effect of $LaCl_3$ on the expression of CBF1-3. (b) Effect by ruthenium red on the expression of CBF1-3 (n = 3 or 4).

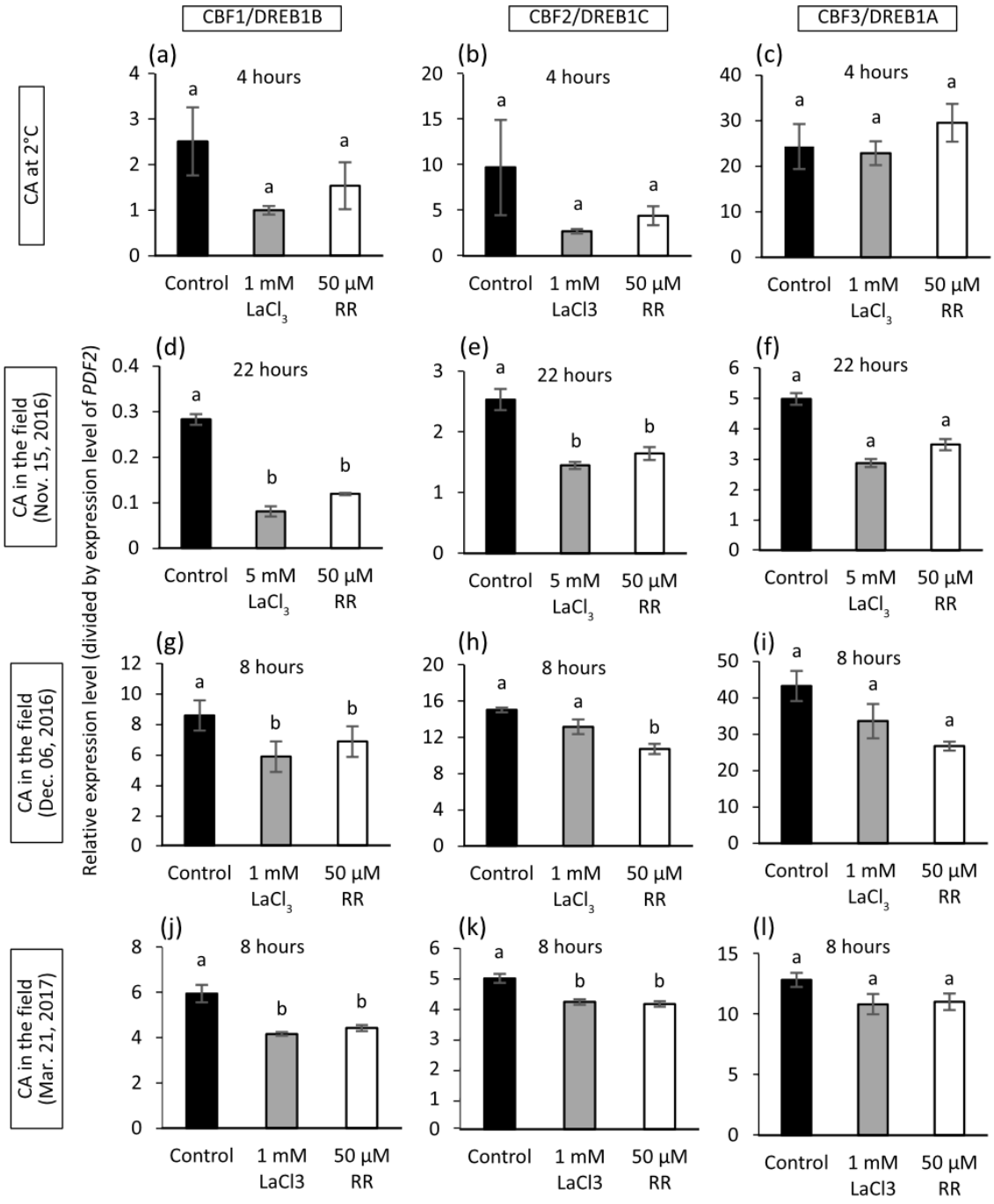

Figure 3.17. Inhibition of the first expression peak of CBF/DREB1s by Ca^{2+} channel blockers. (a-c) The expression level of CBF1-3 were measured in plants that cold-acclimated with 1 mM $LaCl_3$ or 50 µM Ruthenium Red at 4 h time point in 2°C constant chamber. The chemicals were sprayed 1 hour prior to the initiation of cold acclimation (CA) treatment. (d-f) CA in the field on November 15, 2016. Plants were sampled at 22 h after starting CA. (g-i) CA in the field on December 6, 2016. Plants were sampled at 8 h after starting CA. (j-l) CA in the field on March 21, 2017. Plants were sampled at 8 h after starting CA. Significant differences between each value were analyzed using the Tukey–Kramer test ($p < 0.05$) (n=3, 4). The bars indicate the SE.

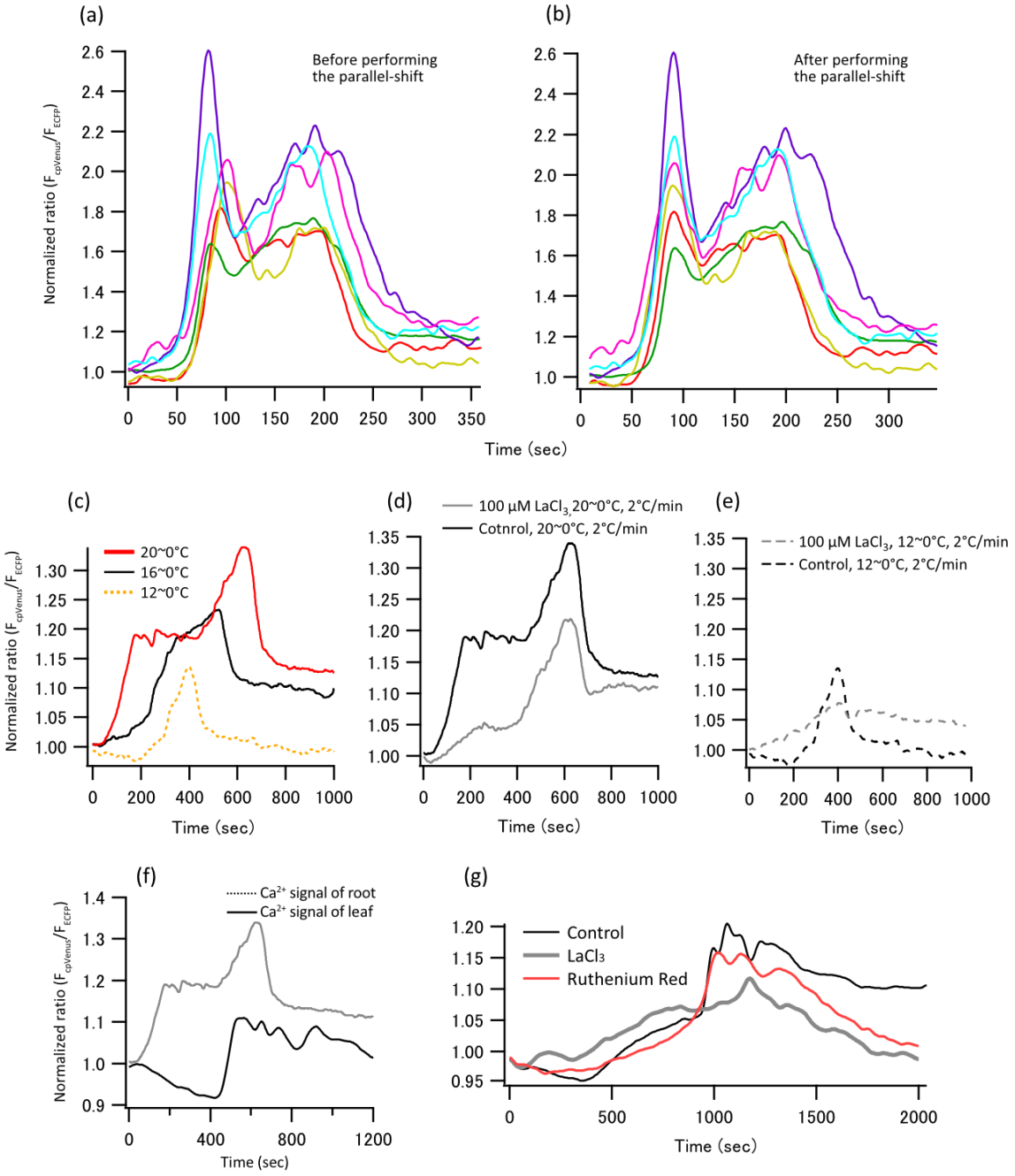

Figure 3.18. Example for parallel-shift among the x-axis of Ca^{2+} signals to visualize the averaged Ca^{2+} signal. (a) The left graph shows the data set which is not performed the parallel-shift. (b) Based on the averaged first peak time, the smoothed data were parallel-shifted along the x-axis and then averaged to show in the figures. (c) Untransformed data of figure 3.2b. (d) Untransformed data for figure 3.6b. (e) Untransformed data of figure 3.6d. (f) Untransformed data for figure 3.9c. (g) Untransformed data for figure 3.13b. Ratio values were normalized by the value at t = 0.

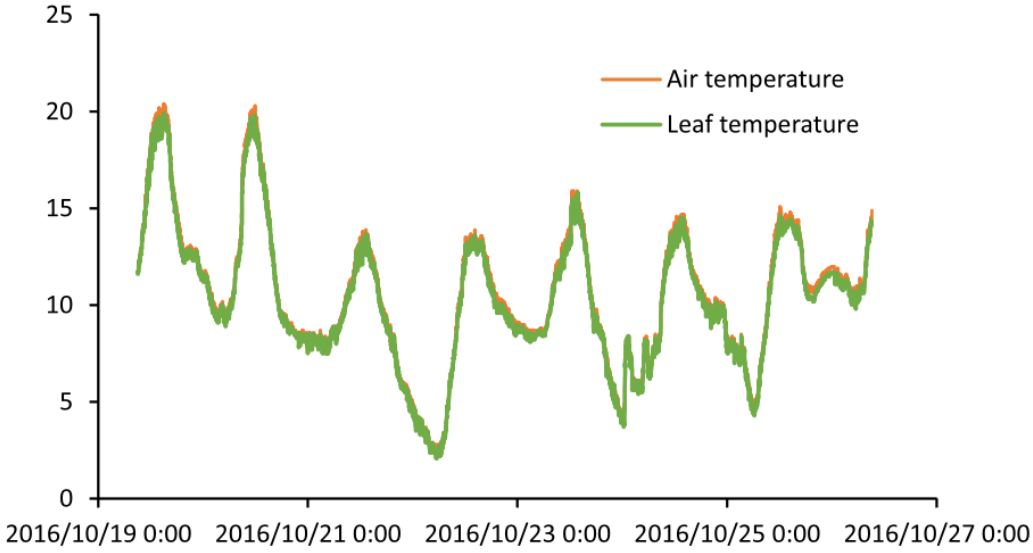

Figure 3.19. The temperature changes in leaves and air. The temperature of leaves (green) and air (orange) were measured every 1 min using a temperature logger.

Table 3.1. Primer arrangement

Primer Name	Primer Arrangement
CBF1_RT_FW	CCGCCGTCTGTTCAATGGAATCAT
CBF1_RT_RV	TCCAAAGCGACACGTCACCATCTC
CBF2_RT_FW	CGGAATCAACCTGTGCCAAGGAAA
CBF2_RT_RV	AGACCATGAGCATCCGTCGTCATA
CBF3_RT_FW	TTCCGTCCGTACAGTGGAAT
CBF3_RT_RV	AACTCCATAACGATACGTCGTC
PDF2_RT_FW	TAACGTGGCCAAAATGATGC
PDF2_RT_RV	GTTCTCCACAACCGCTTGGT

Chapter 4

Effect of the Temperature Cycle and Fluctuation during Cold Acclimation Treatment on Gene Expressions and Freezing Tolerance in Arabidopsis

Abstract

Plants increase stress tolerances depending on the environmental condition. For the study of cold acclimation (CA), molecular and physiological processes have been investigated by exposing plants to constant low-temperatures. However, to understand the CA in the field, the temperature cycle of day and night, and temperature fluctuation in minutes also should be discussed. Thus, I developed the experimental system which can maintain the temperature cycle and fluctuation during CA treatment: that is temperature fluctuating cyclic CA (FC–CA). FC–CA system was applied to three Arabidopsis accessions: Col-0, Fl-3, and Kas-1. Although the average temperature was higher in FC–CA than that of conventional CA (conv.–CA), both treatments tended to induce almost the same freezing tolerance. To observe the role of the Ca^{2+} signal during both CA treatments, Ca^{2+} channel blockers, ruthenium red and $LaCl_3$, were sprayed. Results demonstrated that the chemicals inhibited the increase of freezing tolerance, especially in FC–CA in Col-0 and Kas-1. These results suggest that FC–CA may induce more frequent Ca^{2+} signals and enhance freezing tolerance. Moreover, FC–CA revealed the possibility that the Ca^{2+} signaling pathway depends on the accessions. For the detailed analysis, three kinds of acclimation treatments are used: conv.–CA, CA with 10°C-day and 2°C-night of temperature cycles (C–CA), and FC–CA. Freezing tolerance of the plants after C–CA and conv.–CA was almost the same, but FC–CA resulted in the weakest freezing tolerance. On the other hand, the expression level of *CBF/DREB1s* was tended to be higher in order of conv.–CA, FC–CA and C–CA plants. In addition, the contribution of Ca^{2+} signal was higher in FC–CA and C–CA in freezing tolerance and FC–CA in gene expression level. Furthermore, the Ca^{2+} signal enhanced *CBF1/DREB1B*, *CBF2/DREB1C* and *CBF3/DREB1A* in FC–CA, but suppressed the expression of *CBF2/DREB1C* and *CBF3/DREB1A* in C–CA. It had not been reported that Ca^{2+} signaling inhibited the gene expression level of *CBF/DREB1s* so far. Therefore, the experiments of FC–CA and C–CA leaded the possibility of the existence of a novel Ca^{2+}-*CBF/DREB1s* pathway.

Introduction

Cold acclimation (CA) is the phenomenon that temperate plants enhance their freezing tolerance by exposure to the low-temperature to survive severe freezing temperature (see Levitt, 1980). Research on CA has been conducted for many decades around the world, and numerous transcriptional factors and cold-inducive genes have been identified. These studies have revealed the molecular mechanism of CA processes which increases freezing tolerance.

Each research group uses a slightly different CA condition. For example, there are reports using the following conditions: 2°C constant under a 12-h photoperiod (Yamazaki *et al*. 2008), 2°C constant at 8-h photoperiod (Uemura *et al*. 1995), 4°C constant under an 8-h photoperiod (Doherty *et al*. 2009), 4°C constant under a 12-h photoperiod (Dong *et al*. 2011), and 5°C-day and 2°C-night under a 12-h photoperiod (Uemura and Yoshida 1984). Gene expression induced by the difference in day length has been also studied. For example, in some trees such as white birch, cold-inducive gene expressions were induced by a short daylength (Puhakainen *et al*. 2004). Also, the expression of *CBF/DREB1s*, which are known as transcriptional factors of cold responsive genes, as mediated by the circadian rhythm (Franklin and Whitelam 2007). However, research on temperature change during the CA treatment has not progressed satisfactorily. There was a study which changed the temperature in the day and night (21°C and 1°C, or 1°C and 21°C), resulting that the light and low-temperature were needed to enhance the freezing tolerance (Wanner and Junttila 1999). Wanner and Junttila (1999) also mentioned that the accumulation of cold-inducive mRNA is not dependent on light and photosynthesis. Although they found the effect of the temperature cycle on freezing tolerance, further information is needed to understand the CA process in the natural environment.

We should know how our CA condition affects to the molecular level of CA process in plants. This is because the combination of the factors such as absolute temperature, day and night temperature cycle, photoperiod, temperature change rate and temperature fluctuation promotes CA process together in the natural environment. Therefore, understanding of the effect and role of each factor can be essential information for understanding CA process in the natural environment.

In plants, calcium ions (Ca^{2+}) function as a second messenger to regulate stress responses (Martí *et al*., 2013; McAinsh *et al*., 2009). Ca^{2+} signal is deeply involved in the low-temperature sensing, especially when the temperature decrease (Plieth *et al*. 1999; Kiegle *et al*. 2000; Knight and Knight 2000; Krebs *et al*. 2012; Hiraki *et al*., 2019a). I clearly showed that the Ca^{2+} signals were induced in the field-like cooling with slow cooling rate (Hiraki *et al*., 2019a). Additionally, *KIN1* and *KIN2*, known as cold responsive genes (Kurkela and Franck, 1990), are estimated to be regulated via Ca^{2+} signals induced by cold shock and/or low-temperature during cold acclimation (CA) (Knight *et al*., 1996; Tähtiharju *et al*., 1997; Chinnusamy *et al*., 2007;

McAinsh and Pittman, 2009; Chinnusamy *et al*., 2010; Miura and Furumoto 2013; Shi *et al*., 2015). Thus, it has been widely accepted that Ca^{2+} signaling regulates gene expression to enhance freezing tolerance. The Ca^{2+} signal is formed by the influx and efflux of Ca^{2+} from extracellular and intracellular pools such as vacuole (Knight *et al*. 1996; Knight and Knight 2009). The Ca^{2+} signal is received by calmodulin, binds to calmodulin-binding transcription activator (CAMTA) 3 and CAMTA5, and then these complexes induce the expression of transcription factors *CBF/DREB1* (Doherty *et al*. 2009; Kidokoro *et al*. 2017). In addition, in chapter 3, I revealed that the gene experession level of *CBF/DREB1s* was regulated depending on the amplitude of the temperature fluctuation via Ca^{2+} signaling (Hiraki *et al*., 2019a). *CBF/DREB1s* induce *COR* genes, a cold-responsive gene, and enhance the freezing tolerance (Fowler and Thomashow 2002; Wang and Hua 2009).

I focused on the temperature changes during CA to understand the effect of the temperature changes during CA treatment and the role of Ca^{2+} signals in the field. Especially, the temperature change of day and night, and temperature fluctuation in minutes were picked up. These two temperature changes are different in the temperature and time range, and the essential of the temperature change in the field. In artificial 2°C CA, the plants were cooled from 23°C to 2°C at a cooling rate of approximately or more than 1°C min^{-1} and were kept at 2°C for a few days or weeks. It has been reported that Ca^{2+} signals are induced by cooling (Plieth *et al*., 1999; Hiraki *et al*., 2019a) and disappear just after stopping the cooling (Hiraki *et al*., 2019a). Thus, in artificial CA, the Ca^{2+} signal may be induced only when the plant is transferred from room temperature to low temperatures, such as 2°C. It should be noted that a constant low temperature does not induce the Ca^{2+} signal (Plieth *et al*., 1999; Knight and Knight, 2000; Knight *et al*., 1996; Hiraki *et al*., 2019a); therefore, it means that the Ca^{2+} signal does not arise during a constant 2°C of artificial CA. In contrast, there are temperature changes from day to night, and a small temperature fluctuation is caused by the sun, cloud movements, and wind in the field. Plieth *et al.* (1999) reported that Ca^{2+} signals were induced several times by repeated steady cooling in root cells. Also, in leaf cells, I confirmed similar results under the slower cooling rate at approximately 0.5°C min^{-1}, which can occur sufficiently in the field (Hiraki *et al*., 2019a). Thus, this report suggests that the temperature fluctuation in minutes occurring in the field may cause the Ca^{2+} signals; and might regulate the gene expressions to enhance the freezing tolerance. Furthermore, based on this idea, the experiment of CA with temperature fluctuation can clarify the role of the Ca^{2+} signal not only in the initial step of CA process, but also during CA process.

In this study, I developed an experimental system that can make ~0.15°C min^{-1} of slow cooling from daytime to nighttime and about 1°C temperature fluctuation range during CA. By the combination of this experimental system and Ca^{2+} channel blockers, I verify the effect of Ca^{2+} signals induced in this experimental system. Using this system, I investigated the effect of these temperature condition in three Arabidopsis accessions; and analyzed in detailed in Col-0, and

estimated the role of Ca^{2+} signals.

Materials and Methods

Plant materials

Three *Arabidopsis thaliana* accessions were used: Columbia (Col-0), Frickhofen (Fl-3), and Kashmir (Kas-1). These plants were grown in petri dishes with modified Hoagland's nutrient solution with 1% agar (Minami *et al*., 2015) at 23°C under a 16-h photoperiod (photon flux rate: 80 μmol m^{-2} s^{-1}) for 2 weeks. Col-0 is used as a standard accession. Col-0 was established in USA, Fl-3 is native to Finland, and Kas-1 is from Kashmir, India.

Cold acclimation treatments

To maintain the temperature fluctuation during CA treatment, I developed the experimental system. The exterior of the device is a box of polystyrene foam (Figure 4.1a). A copper plate is laid on the bottom of the box (Figure 4.1b), and a silicone belt heater (SAKAGUCHI E.H VOC CO., Japan) is attached under the plate (Figure 4.1c). Heater is connected to temperature controller (KT4R; Panasonic Co., Japan) (Figure 4.1d) and power supply. The temperature controller was set for on / off mode to regulate the temperature, and it was set at 9°C in the daytime and 2°C in the night. Normally, the temperature of growth chamber is controlled by the method called as Proportional-Integral-Differential (PID) control so as not to make overshoot or temperature fluctuation. On this equipment, on / off control was adopted to maintain temperature fluctuation. Since this equipment has no cooling function and a lighting, it was placed in the growth chamber set at 1°C (Figure 4.1e).

Two types of CA treatments were used for the three Arabidopsis accessions experiment. One was the conventional CA at constant 2°C (conv.–CA) (Figure 4.2: black line). In the other treatment, day-and-night temperature cycles were generated. Basically, the temperature was set 9°C / 2°C (day / night), but the temperature was fluctuating during daytime. The temperature fluctuated at approximately 10°C with an amplitude of 1°C in the daytime. One cycle of the temperature fluctuation took approximately 10 min, and the nighttime temperature was kept at a constant 2°C (Figure 4.2: gray line). This acclimation treatment was named temperature fluctuating cyclic CA (FC–CA). In both treatments, the photoperiod was 12 h (6:00–18:00).

Three types of CA treatments were performed for the detailed analysis on Col-0. First is conv.–CA. The temperature was set at 2°C constant except defrost. Second is cyclic CA (C–CA). The temperature was set 9°C / 2°C (day / night). This temperature cycle was created by the temperature setting with PID control of the growth chamber. Third is FC–CA.

Chemical treatment

To evaluate the role of the Ca^{2+} signals during conv.–CA, C–CA and FC–CA, the Ca^{2+} channel blockers, 50 μM ruthenium red (RR) and 1 mM $LaCl_3$, were sprayed with 0.05% Triton X-100 onto the plants. Triton X-100 was used to penetrate the chemicals into the plant tissue. For control plants, 0.05% Triton X-100 solution was sprayed. Chemical treatment was performed 1 h before starting the acclimation treatments and 45 h after starting treatments (Figure 4.3).

Measurement of electrolyte leakage

After the chemical treatment, the freezing tolerance of each plant accession before and after CA treatments were evaluated by using the electrolyte leakage (EL) method. EL test was performed 1, 25, 73 or 169 h after the chemical treatment as a non-acclimated (NA), 1 d and 3 d acclimated plant for the three Arabidopsis accessions (see Figure 4.3), and 3 d and 7 d acclimated plant for Col-0 experiment. The EL values were measured with a conductivity meter (Twin Cond Conductivity Meter, B-173, HORIBA Ltd., Japan) according to the method used by Uemura *et al.* (1995). Normalized values were calculated using the following formula:

$$\text{Normalized EL} = \frac{EL_{-4} - EL_{nF}}{EL_{-80} - EL_{nF}} \quad \text{— (1)}$$

, where nF means the non-freezing temperature.

Measurement of survival rate

The survival rate was evaluated from the value of Fv/Fm, which is an indicator of photosynthetic activity, and the leaf measured by imaging chlorophyll fluorometer (FluorCam 800MF system, Photon Systems Instruments, Czech Republic). Fv/Fm was measured before and after starting the acclimation treatment, and after freezing test. Following formula was used to get the survival rate after freezing test. Significant differences between control and chemical treated value was analyzed using the t-test (***$p < 0.001$). Error bars indicate SE.

$$Survival\ rate = \frac{\left\{\left(\frac{Fv}{Fm}\right) \times Area\right\} after\ FT\ 1d}{\left\{\frac{Fv}{Fm} \times Area\right\} before\ CA} \quad \text{— (2)}$$

$$\text{Growth rate} = \frac{\left\{\frac{Fv}{Fm} \times Area\right\}\ after\ CA}{\left\{\frac{Fv}{Fm} \times Area\right\}\ before\ CA} \quad \text{— (3)}$$

$$Fixed\ survival\ rate \frac{(Survival\ rate)}{(Growth\ rate)} \quad \text{— (4)}$$

Measurement of mRNA accumulation level

Total RNA was isolated from the aerial part of the *Arabidopsis thaliana* (Col-0) using ISOSPIN Plant RNA (NIPPON GENE CO., LTD., Japan). ReverTra Ace qPCR RT Master Mix (TOYOBO Co.) was used for the cDNA synthesis. Real-time PCR was performed on the corresponding cDNA which were synthesized from each sample. *PDF2* used as a reference gene. The primers for real-time PCR are listed in Table 4.1.

Results

Freezing tolerance in the three Arabidopsis accessions

Influence of chemical treatment was observed by unfrozen plants maintained at non-freezing temperature of 0°C. While the EL value slightly increased by 0.05% Triton X-100, there was no difference between plants in the presence or absence of Ca^{2+} channel blockers (Figure 4.4A). Next, freezing tolerance tests were performed at −4°C before CA, and normalized EL values were calculated based on formula (1). In non-acclimated (NA) plants, the EL value was close to 100% in all samples (Figure 4.4B), suggesting that before CA all *Arabidopsis* accessions can hardly survive at −4°C in the condition of this study. Next, the effects of conv.–CA and FC-CA were tested in the presence or absence of channel blockers. During the conv.–CA, EL values in Col-0 tended to decrease each day; EL values decreased after 1 day of CA treatments in Fl-3 and Kas (Figure 4.4C); however, they did not change in 3 days (Figure 4.4D). A significant difference between control and chemical-treated plants in 3 days of FC–CA in Fl-3 and Col-0, and 3 days of CA treatments in Fl-3 was observed (Figure 4.4C).

Subsequently, I focused on the role of Ca^{2+} signals caused by the temperature fluctuation. The treatment with the RR and $LaCl_3$ inhibitors may have induced side effects (i.e., Triton X-100 in the solution may have direct negative effects on freezing tolerance and EL method). The side effect of these chemical treatments was removed by subtracting EL values of the control treatment without inhibitors. Both conv.–CA and FC–CA treatments included the Ca^{2+} signal, which was induced by the rapid cooling when the plant was transferred to each acclimation temperature (i.e., 10°C or 2°C) (Figure 4.2). To remove this effect from the results of FC–CA treatment, the EL value of conv.–CA was subtracted from that of FC–CA. Thus, the effect of Ca^{2+} signals induced

during FC–CA treatment on the enhancement of freezing tolerance was calculated using the following formula:

$$\begin{pmatrix}\text{Effect of calcium signal induced}\\ \text{by the temperature fluctuation}\end{pmatrix} = \{(\text{EL of FCCA, RL}) - (\text{EL of FCCA, Control})\} - \{(\text{EL of conv. CA, RL}) - (\text{EL of conv. CA, Control})\} \quad \text{— (5)}$$

, where RL means RR and $LaCl_3$ treatments. Figure 4.5 presents the data after calculation using the above formula from the results of Figure 4.4.

In Fl-3 plants, Ca^{2+} signal induced by temperature fluctuation did not increase the freezing tolerance in both plants temperature-treated for 1 and 3 days (Figure 4.5). This result indicates that Fl-3 may not use the Ca^{2+} signals induced by temperature fluctuation to enhance the freezing tolerance. In contrast, Col-0 plants exhibited a strong effect of the temperature-fluctuation-induced Ca^{2+} signaling on freezing tolerance in both 1 and 3 days (Figure 4.5). In Kas-1, there was no significant difference between control and chemical-treated plants in FC–CA (Figure 4.4). However, Ca^{2+} signaling tended to have a greater effect in Kas-1 than in Fl-3, particularly after 1 day but it could not maintain this responsiveness thereafter. In contrast, Col-0 could constantly respond to temperature fluctuation and exhibited the highest contribution of the temperature-fluctuation-induced Ca^{2+} signals to increase the freezing tolerance (Figure 4.5).

Temperature changes of the three cold acclimation treatments in Col-0

For the further analysis, I picked up the one Arabidopsis accession, Col-0. It showed the highest contribution of the Ca^{2+} signals during FC–CA treatment to the freezing tolerance (Figure 4.5). The temperature of inside of petri dish during the three kinds of acclimation treatments were measured by the thermocouples (Figure 4.6). These conditions were used to investigate the effect of temperature cycle of day and night, and the minute temperature fluctuations during the CA process. For the control, conv.–CA treatment at 2°C constant was used (Figure 4.6a). The temperature inside of the petri dish was slightly higher in daytime than in night time due to the light irradiation. Since this program included defrost setting, the transient temperature increases were observed. To investigate the effect of temperature cycle of day and night on freezing tolerance and gene expressions, the 10°C / 2°C (day / night) of cyclic cold acclimation (C-CA) was used (Figure 4.6b). Furthermore, to test the effect of the combination of temperature cycle and fluctuations FC–CA was performed (Figure 4.6c). The temperature range of fluctuation was between about 9°C and 12°C, and one fluctuation took about 12 to 18 minutes. The speed of temperature change was 0.14 to 0.2°C min^{-1}.

Effect of temperature cycle and fluctuation on the electrolyte leakage values

Electrolyte leakage (EL) values were measured after 3 d and 7 d of three acclimation treatment (i.e., FC–CA, C–CA and conv.–CA) with Ca^{2+} channel blockers, $LaCl_3$ and ruthenium red (RR) to investigate the effect of these acclimation treatments on increase of freezing tolerance. $LaCl_3$ blocks extracellular Ca^{2+} influx (Knight and Knight 2000) and ruthenium red blocks Ca^{2+} release from intracellular organelles (Knight *et al*. 1992; Monroy and Dhindsa, 1995). There tended to be a significant difference in EL value between control and chemical treated plants in FC–CA and C–CA (Figure 4.7). By contrast, there was no significant difference in EL value between control and chemical treated plants in conv.–CA in three condition of EL test (Figure 4.7). The values of EL of control plant on the treatment days 3 and 7 are almost same in FC–CA (Figure 4.7). On the other hand, in C–CA and conv.–CA treatment, the EL values of control tended to be higher in 3 d treatment than 7 d treatment (Figure 4.7). Comparison among the freezing tolerances after three type of acclimation treatment, FC–CA plant showed the weakest freezing tolerance (Figure 4.7d).

In order to visualize the contribution of the Ca^{2+} signal for enhancement of the freezing tolerance, the EL value of the control plant subtracted from the EL value of the plant treated with the Ca^{2+} channel blockers, $LaCl_3$ and ruthenium red (Figure 4.8). Focusing on the contribution of the Ca^{2+} signal to the increase of freezing tolerance for −4°C, the contribution of the Ca^{2+} signal was similar in FC–CA and C–CA at the 3 d of the acclimation treatment. In conv.–CA, the values of contribution of Ca^{2+} signal at 3 d was less than half of that of FC–CA and C–CA (Figure 4.9a). On the 7 d of the acclimation treatment, the contribution of the Ca^{2+} signal was almost same as that of the 3 d in FC–CA. However, in C–CA, it was about half of that of the 3 d of treatment. The effect of Ca^{2+} signal on the 7 d in conv.–CA was as low as on the 3 d (Figure 4.9a). In the contribution of the Ca^{2+} signal for the freezing tolerance at −6°C, the contribution was about three times of higher in FC–CA and C–CA at the 7 d of the acclimation treatment than that of the 3 d (Figure 4.9b). On the other hand, in conv.–CA, the contribution of Ca^{2+} signal was smaller in the 7 d of acclimation treatment than that of the 3 d (Figure 4.9b).

Gene expressions induced by three kinds of cold acclimation treatments

Gene expression level of *CBF1/DREB1B*, *CBF2/DREB1C,* and *CBF3/DREB1A* were analyzed by real-time PCR at 0, 8, 22, 32 and 46 h after starting the acclimation treatment, and showing the different gene expression changes in FC–CA, C–CA and conv.–CA. *CBF1/DREB1B* showed two expression peaks at 8 and 32 h from starting the acclimation treatment under all

conditions. In CA, the first expression peak of *CBF1/DREB1B* was larger than the second expression peak. By contrast, in FC–CA and C–CA, the magnitudes of the first and second expression peaks of *CBF1/DREB1B* were almost the same (Figure 4.10a). Comparison among the three acclimation treatments showed that the expression levels of *CBF1/DREB1B* in FC–CA and C–CA was on the one half to one tenth of that of conv.–CA (Figure 4.10a). *CBF2/DREB1C* had one peak of expression at 8 h and did not increase thereafter in conv.–CA (Figure 4.10b). The expression level of *CBF2/DREB1C* was the highest in conv.–CA. Almost no increase of expression of *CBF2/DREB1C* was observed in C–CA (Figure 4.10b). In FC–CA, there was two expression peaks at 8 and 32 h (Figure 4.10b). Expression of *CBF3/DREB1A* in conv.–CA had one peak at 8 h as in *CBF2/DREB1C*. Two expression peaks of *CBF2/DREB1C* were observed at 8 h and 32 h in C–CA and FC–CA (Figure 4.10c). Focused on the magnitude of the expression peak of *CBF3/DREB1A*, FC–CA induced 2 to 3 times higher expression peak in the first and second peak than that of C–CA (Figure 4.10c).

Inhibition of gene expressions by Ca^{2+} channel blockers in three acclimation treatments

Ca^{2+} channel blockers suppressed gene expressions in many cases. The role of Ca^{2+} signals in gene expression was evaluated by using $LaCl_3$, RR and its mixture. The time point at 32 h at which the second peak of the gene expression of *CBF/DREB1s* appears was picked up for further analysis to avoid the initial effect of the temperature decrease from room temperature to each temperature of acclimation treatment.

First, the expression of *CBF1/DREB1B* was significantly inhibited by $LaCl_3$ in FC–CA, C–CA and conv.–CA treatment (Figure 4.11a). Since the mixed solution also contained $LaCl_3$, the mixed solution tended to inhibit the gene expression as well as $LaCl_3$ solution (Figure 4.11a). RR tended to decrease the *CBF1/DREB1B* expression only in FC–CA ($p < 0.07$) (Figure 4.11a). Second, the expression of *CBF2/DREB1C* was inhibited by all chemical treatment in FC–CA (Figure 4.11b). Interestingly, RR upregulated the gene expression of *CBF2/DREB1C* in C–CA (Figure 4.11b). In conv.–CA, only $LaCl_3$ decreased the gene expression of *CBF2/DREB1C* (Figure 4.11b). Third, the expression level of *CBF3/DREB1A* was inhibited by the all chemical treatments in FC–CA (Figure 4.11c). $LaCl_3$ and mixed solution inhibited the expression of *CBF3/DREB1A*, but RR upregulated the expression of *CBF3/DREB1A* (Figure 4.11c). There was no significant difference among the control and chemical treated plants in expression level of *CBF3/DREB1A* in conv.–CA (Figure 4.11c) Gene expression level of *COR15A*, known as a CBF/DREB1s regulon cold inducive gene, was also measured with Ca^{2+} channel blockers. Although *COR15A* was suppressed under all chemical treatments in FC–CA, $LaCl_3$ and mixed solution inhibited the gene expression in C–CA and conv.–CA (Figure 4.11d). In summary, $LaCl_3$

inhibited almost all genes in all conditions. RR inhibited the gene expressions only in FC–CA, and upregulated *CBF2/DREB1C* and *CBF3/DREB1A* only in C–CA.

Discussion

Freezing tolerance in the three Arabidopsis accessions after conventional cold acclimation and temperature fluctuating cold acclimation treatment

Although the average temperature of FC–CA was higher than that of constant 2°C of conv.–CA, the EL value subjected to FC–CA treatment after freezing was approximately the same as that of conv.–CA (Figure 4.4). This result indicated that FC–CA had the potential to stimulate cold acclimation through Ca^{2+} signaling, which may be induced by the temperature fluctuation. Since the Ca^{2+} signals are induced by temperature changes (Knight *et al*., 1996; Plieth *et al*., 1999; Knight and Knight, 2000), it is conceivable that FC–CA induces more frequent Ca^{2+} signals during the acclimation treatment. In contrast, in conv.–CA, only a single Ca^{2+} signal was observed when the plants were transferred from room temperature (23°C) to 2°C (Figure 3.4j, k).

The plants were transferred from room temperature to each cold temperature (i.e., 10°C or 2°C), and then the transient Ca^{2+} peaks were induced. This rapid cooling enhanced the *CBF/DREB1s* pathway through the calmodulin binding transcription activators (CAMTA); CAMTA 3 and CAMTA 5 (Doherty *et al*., 2009; Kidokoro *et al*., 2017). Even the cooling range differed, the transient Ca^{2+} peaks were induced just after initiating the conv.–CA and FC–CA treatments. Therefore, the freezing tolerance of 1 d acclimated plants might be affected by the transient Ca^{2+} peak in both conv.–CA and FC–CA. On the other hand, since the *CBF/DREB1s* genes expressed within about 6 h from the rapid cooling and there was no expression increase (Kidokoro *et al*., 2017), this pathway (i.e., Ca^{2+}-CAMTA- *DREB1/CBF*) might act during the early stage of cold acclimation process. Moreover, there is a possibility that the Ca^{2+}-CAMTA- *CBF/DREB1* pathway may not be active in the late stage of cold acclimation, such as 3 days. Additionally, other factors might contribute to the increase in freezing tolerance. The use of Col-0 and Kas-1 accessions that have a large contribution to Ca^{2+} signals induced by temperature fluctuation may lead to the discovery of these factors.

Three acclimation settings and natural environment

The novel methods for the cold acclimation were established (Figure 4.6). One has the temperature cycle of day and night (10°C / 2°C) (C–CA), and the other has the temperature

fluctuation during day time in addition to the temperature cycle (FC–CA). Due to the defrost of low temperature chamber, the transient temperature increases and decreases occur in conv.–CA (Figure 4.6a). However, my previous study suggested that plants cannot increase Ca^{2+} concentration as a Ca^{2+} signal when plants transferred to unexpected higher temperature and was subsequently cooled from the high temperature (Hiraki *et al*., 2019a; Figure 3.7). Therefore, it is considered that the Ca^{2+} signal is not induced by the transient temperature change of defrost.

Since the cold responsive genes, *COR15A*, *COR15B* and *KIN1*, were induced even at 16°C with low red and far-red ratio (i.e., R/FR) (Franklin and Whitelam 2007), 10°C to 12°C of daytime temperature of C–CA and FC–CA may be cold enough to induce these genes (Figure 4.6b, c). In fact, the plant which was exposed to the constant 11°C for 7 days increased its freezing tolerance (Figure 4.12). In FC–CA, there were temperature fluctuations during daytime with about 0.2°C min^{-1} of temperature change speed. Temperature change speed of 0.2°C min^{-1} is common in the natural environment (Figure 4.13), and the temperature fluctuation maintained in my experiment system conforms to the natural environment (Figure 4.6c).

In the natural environment, temperature fluctuations are caused mainly by factors such as the movement of the sun and clouds, or wind and rain. Temperature fluctuations tend to be smaller in the winter than in the other seasons (Figure 4.14), because the sun light is weaker and the daytime is also shorter than the other seasons. In addition, when plants are covered with snow, the ambient temperature of plants became stable. Therefore, FC–CA, C–CA and conv.–CA can be used as the model of temperature change in fall to winter. By using FC–CA and C–CA which are considering the autumn conditions, and conv.–CA as the winter condition, I can study how cold acclimation process progresses in autumn to winter in natural environment.

Effect of temperature cycle and temperature fluctuation on freezing tolerance

Temperature fluctuations enhance the freezing tolerance through the Ca^{2+} signaling, but also suppress the cold acclimation process via unknown pathway. If the temperature fluctuation occurs daytime at about 10°C, the freezing tolerance of plant reached the upper limit by the 3 d (Figure 4.7). On the other hand, in C–CA and conv.–CA treatment, the freezing tolerance tended to be higher in 7 d treatment than in 3 d treatment, which is higher than that of plant subjected to FC–CA (Figure 4.7). Although the average temperature of FC–CA is almost the same as C–CA, the freezing tolerance tended to be lower in FC–CA than in C–CA (Figure 4.7a, b, d). These results indicate that the increase in freezing tolerance is inhibited by the temperature fluctuation. One of the candidates of the messenger for the temperature fluctuation is Ca^{2+} signal, because Ca^{2+} responds to the cooling (Knight *et al*. 1996; Plieth *et al*. 1999; Knight and Knight, 2000; Nagel-Volkmann *et al*. 2009; Hiraki *et al.*, 2019a). However, my results showed that Ca^{2+} signals did not

suppress the freezing tolerance but increased the freezing tolerance. This is because freezing tolerance decreases significantly in FC–CA when the plants were sprayed the Ca^{2+} channel blockers (Figure 4.7a, b, d). These results suggested that Ca^{2+} signals which are induced by the temperature fluctuation have the role to enhance the freezing tolerance. However, temperature fluctuation inhibited cold acclimation process through the unknown pathways.

Temperature cycle (C–CA) strongly increases the freezing tolerance. Interestingly, the average temperature was much higher in C–CA than in conv.–CA, but the freezing tolerance was almost the same or slightly higher in C–CA than in conv.–CA (Figure 4.7). The high contributions of Ca^{2+} signals in C–CA (Figure 4.9) that indicated Ca^{2+} signals induced by the temperature cycle enhance freezing tolerance. However, if there was temperature fluctuation along with temperature cycle, the increase of freezing tolerance was not induced (Figure 4.7). Therefore, the magnitude of the temperature fluctuation might be used as a kind of the indicator for sensing for the season in plants.

There are two kinds of Ca^{2+} signals which may increase the freezing tolerance. One is the Ca^{2+} signal which is induced by the temperature cycle of day and night. The other is the Ca^{2+} signal which in induced by the small temperature fluctuation. FC–CA included both Ca^{2+} signals, and C–CA included the Ca^{2+} signal induced by the temperature cycle of day and night. Since Ca^{2+} signals affected by the cooling rate, cooling duration, and absolute temperature and the shape of the Ca^{2+} signals changed dramatically depending on these parameters (Plieth *et al*. 1999; Nagel-Volkmann *et al*. 2009; Hiraki *et al*., 2019a), the Ca^{2+} signals caused by the cooling from day to night and the temperature fluctuation may be different each other in quality and quantity (Hiraki *et al*., 2019a; Figure 3.9). Focusing on the relationship between the Ca^{2+} signals and freezing tolerance, the contribution of Ca^{2+} signal on enhancement of the freezing tolerance was high even at 7 d FC–CA and C–CA. It means that Ca^{2+} signals caused by the temperature cycle of day and night and temperature fluctuation in minutes had a role to increase the freezing tolerance. By contrast, conv.–CA did not involve the contribution at 7 d (Figure 4.9). These results are consistent with the Ca^{2+} signals caused in each acclimation treatment.

Effect of temperature cycle and temperature fluctuation on gene expressions

Three different acclimation treatments induced the expression of the cold inducive transcriptional factors and their target genes in different manners. In conv.–CA plants, the expression level of *CBF/DREB1s* was higher than that of FC–CA and C–CA (Figure 4.10), because the genes are induced in a temperature dependent manner (Zarka *et al*. 2003). In the Conv.–CA treatment, plants were rapidly cooled the plants from room temperature to 2°C and placed at the lowest temperature among the three acclimation treatments. However, there was no

significant difference among the expression level of *COR15A*, which is CBF/DREB1s regulon gene, in three acclimation treatments at 32 h and 46 h (Figure 4.15). These results suggest two possibilities. One is that the small expression level of *CBF/DREB1s* is enough to induce the *COR15A*. The other is that *COR15A* was induced by the other pathway in FC–CA and C–CA.

The conv.–CA induced the first peak of *CBF/DREB1s* expression at 8 h and the second expression peak tended not to appear (Figure 4.10). On the other hand, since the second peak is induced in FC–CA and C–CA, the temperature cycle of day and night may be necessary for induction of the second peak. There have been reported that circadian rhythms and diurnal changes regulate expression of *CBF/DREB1s* (Dong *et al*. 2011). In addition, Millar (2003) reported that the circadian rhythms can be entrained by the warm/cold cycles. Likewise, the rhythm of temperature may have the effect of controlling the expression of *CBF/DREB1s* through the circadian in FC–CA and C–CA.

In FC–CA, expression level of *CBF/DREB1s* was higher than that of C–CA (Figure 4.10), but freezing tolerance was weaker in FC–CA than in C–CA (Figure 4.7). This suggests that the freezing tolerance may be increased by the pathway different from the Ca^{2+}-*CBF/DREB1s* in C–CA. The novel question is what factor does sense the temperature fluctuation, transduce signals, and inhibit the cold acclimation process in FC–CA. Possibilities include the 1 to 2°C higher highest temperature due to the temperature fluctuation and the novel signal transduction except Ca^{2+} signaling.

The Ca^{2+} signal is formed by the influx and efflux of Ca^{2+} from extracellular and intracellular pools such as vacuole (Knight *et al*. 1996; Knight and Knight 2009). $LaCl_3$ was used as a Ca^{2+} channel blocker to block the Ca^{2+} influx from the extracellular part (Knight and Knight 2000). RR was a putative Ca^{2+} channel blocker of organelles (Knight *et al*. 1992; Monroy and Dhindsa, 1995) and inhibited a part of Ca^{2+} signals caused by the cooling. I already showed and confirmed the effect of these Ca^{2+} channel blockers on the shape of Ca^{2+} signal with the cooling (Hiraki *et al*., 2019a; Figures 3.13 and 3.14). Especially, $LaCl_3$ strongly disturbed the first peak of Ca^{2+} signal (Knight and Knight 2000; Hiraki *et al*., 2019a), and RR decreased the three Ca^{2+} signal peaks halfway (Hiraki *et al*., 2019a). But there was no clear evidence showing each role of Ca^{2+} influx or efflux separately.

According to the results of the effect of Ca^{2+} signal inhibition on the gene expression, Ca^{2+} signals which may be induced by the temperature fluctuation induced *CBF/DREB1s* expression especially in FC–CA (Figure 4.11). On the other hand, RR upregulated the gene expressions only in C–CA, indicating that the Ca^{2+} efflux from intracellular pools in the Ca^{2+} signals induced by the temperature decrease from day to night suppressed the gene expression of *CBF2/DREB1C* and *CBF3/DREB1A* in C–CA (Figure 4.11). However, the suppression did not occur when there was the temperature fluctuation (i.e., in FC–CA) (Figure 4.11), but decreased freezing tolerance via unknown pathway which was activated in FC–CA. The temperature

fluctuation originally inhibited the cold acclimation process (Figure 4.7), but Ca^{2+} signal which was induced by the temperature fluctuation induced the expression of *CBF1/DREB1B*, *CBF2/DREB1C,* and *CBF3/DREB1A* (Figure 4.11). My previous study has reported that RR tended to inhibit the gene expression level of *CBF1/DREB1B* and *CBF2/DREB1C* when the amplitude of the temperature fluctuation was high, but decreased that of *CBF/DERB1s* when the amplitude of the temperature fluctuation was low in the field (Hiraki *et al*., 2019a; Figures 3.15 and 3.16). The results in this work and the previous report support the hypothesis that the Ca^{2+} signal regulates the gene expression level of *CBF/DERB1s* either positively or negatively dependent on the amplitude of the temperature fluctuation. Our results also support the idea that the role of Ca^{2+} influx and Ca^{2+} efflux was different depending on the temperature fluctuation. Since only Ca^{2+} efflux changed its role (i.e., positive or negative regulator), the gradation or the balance in Ca^{2+} concentration in the cell might affect the regulation of gene expession. In another possibility is that the Ca^{2+} signal which is induced by the rapid cooling during the day time may not suppress the gene expressions. It had been reported that the peak value of cold-induced Ca^{2+} signal was high during day time (Dodd *et al*. 2006). Also, the photoreceptors help the resetting of the internal clock (Devlin 2002), and the photoreceptors such as PHOTOTROPIN and PHYTOCHROME are mediated by the Ca^{2+} signal (Bowler 1994; Briggs and Olney 2001; Zhao *et al*. 2013). Therefore, the phenomenon that the role of Ca^{2+} signal varies with time might be prescribed by crosstalk with circadian and photoreceptor related factors.

Conclusion

Different acclimation treatments resulted in different level of freezing tolerance and Ca^{2+} signals which are induced in each acclimation affected the gene expression differently. Cold-induced Ca^{2+} signal was composed of the Ca^{2+} influx from the extracellular pools (can be blocked by $LaCl_3$) and the Ca^{2+} efflux from the intracellular pools (can be blocked by RR). In the Ca^{2+} signal caused by the cooling from day to night, Ca^{2+} influx from the extracellular pools tended to induce the gene expression of *CBF/DREB1s*, but Ca^{2+} efflux from the intracellular pools had the role of suppression of the gene expression of *CBF2/DREB1C* and *CBF3/DREB1A*. However, if there was temperature fluctuation with the temperature decrease, the suppressing did not occur. On the other hand, in the Ca^{2+} signal caused by the temperature fluctuation, both influx and efflux of Ca^{2+} tended to increase the gene expression of *CBF/DREB1s.* Since these Ca^{2+} signaling cannot be explained with only the Ca^{2+}-CAMTA3 or CAMTA5 pathway, there may be a novel Ca^{2+}-CBF/DREB1s pathway. Finally, I would like to emphasize that I found the cue for the novel pathway in cold acclimation by adding the temperature cycle and fluctuation to the conventional CA treatment.

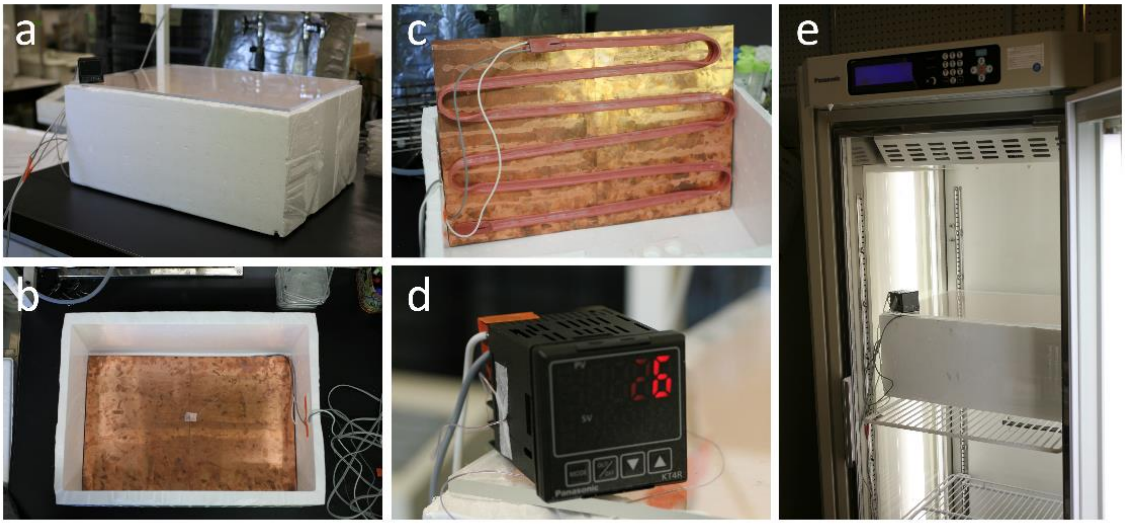

Figure 4.1. Setting of the chamber for temperature fluctuating cold acclimation. (a) The appearance of the chamber. (b) Cupper plate installed on the bottom of the chamber. (c) Silicone belt heater (SAKAGUCHI E.H VOC CO., Japan) attached to the back of the copper plate. (d) Temperature controller (KT4R; Panasonic Co., Japan). (e) For light and cooling, this chamber was installed into the growth chamber.

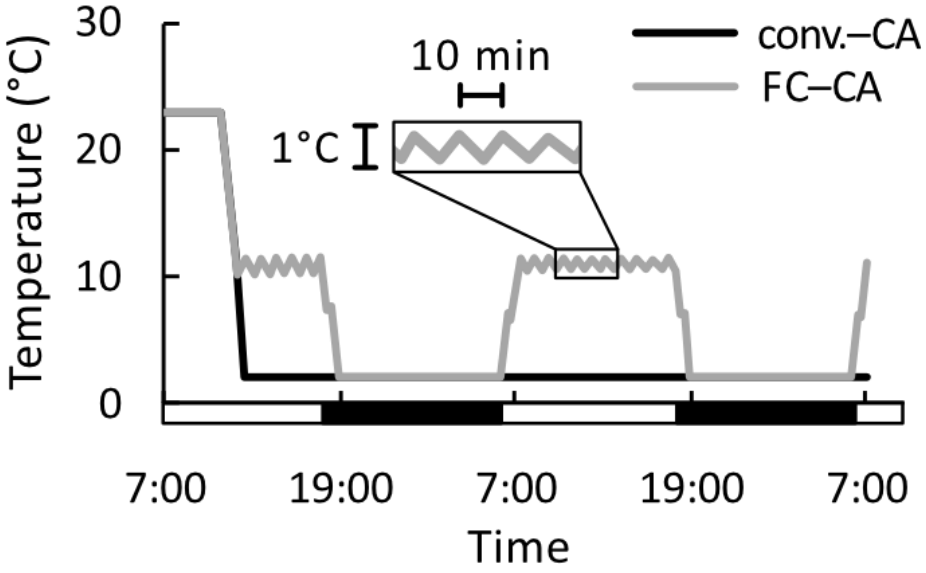

Figure 4.2. Diagrammatic illustration of the temperature changes in constant conv.–CA and FC–CA. The bar under the graph indicates the day (white) and night (black).

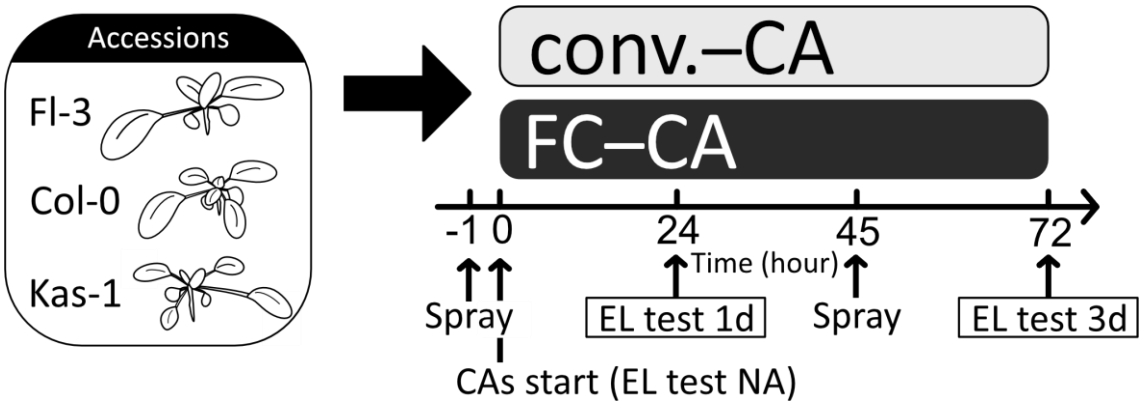

Figure 4.3 Experimental design. Three accessions of *Arabidopsis* plants were grown for 2 weeks at 23°C and then transferred to constant 2°C of conventional cold acclimation (conv.–CA) or temperature fluctuating cyclic cold acclimation (FC–CA). A solution of 0.05% Triton X-100 or 0.05% Triton X-100 + 50 µM ruthenium red + 1 mM $LaCl_3$, was sprayed at 1 h before and 45 h after starting the temperature treatments.

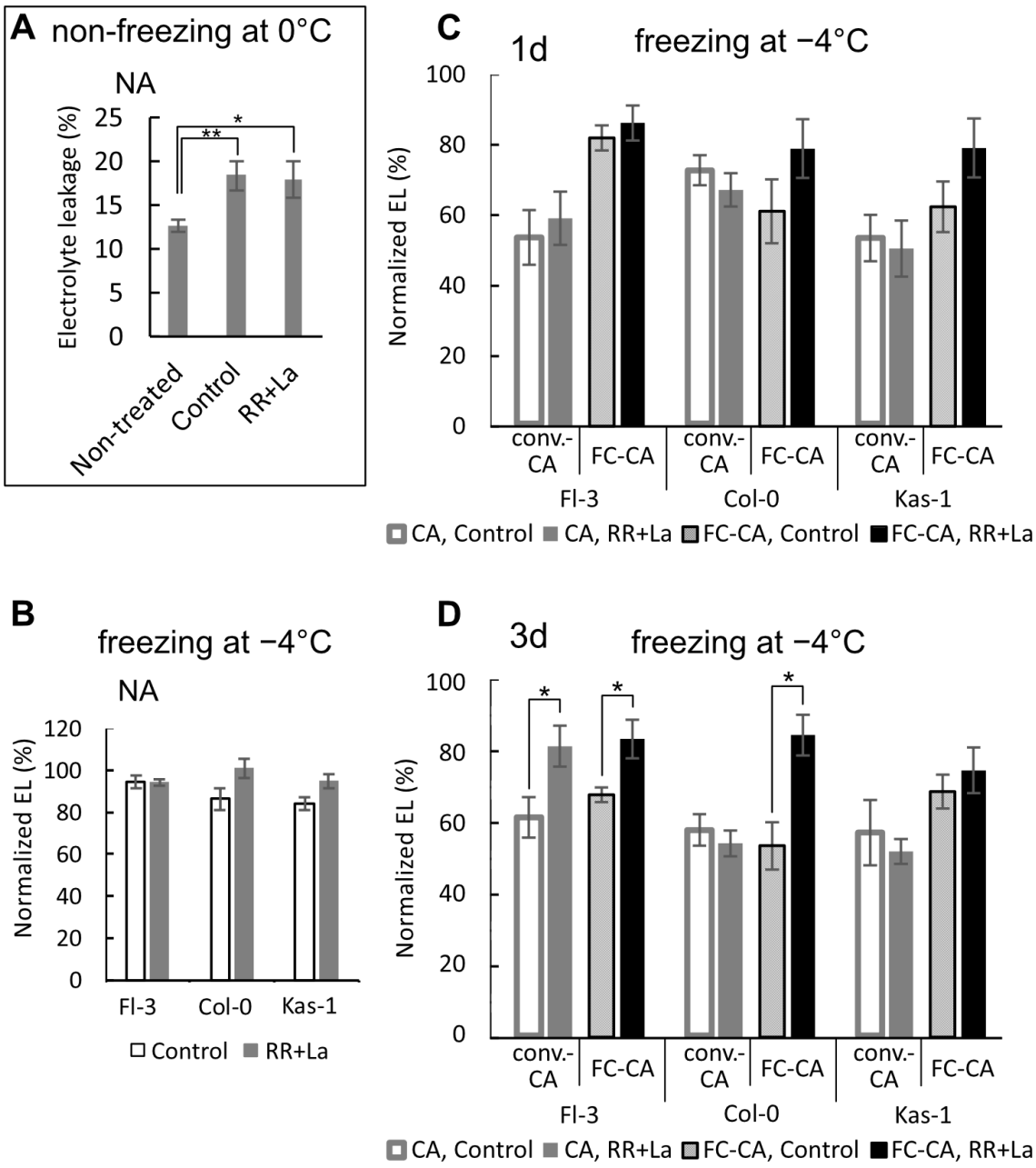

Figure 4.4. **Effect of the Ca^{2+} channel blockers on conventional cold acclimation (conv.–CA) or temperature fluctuating cyclic cold acclimation (FC–CA).** The freezing tolerance of plants before and after conv.–CA or FC–CA was estimated by electrolyte leakage (EL) methods. Before the freezing tolerance tests, the effect of the spray treatment of 0.05% Triton X-100 (control) or 0.05% Triton X-100 plus the Ca^{2+} channel blockers of ruthenium red and $LaCl_3$ (RR+La) was confirmed at a non-freezing temperature of 0°C using non-acclimated (NA) Col-0 (n = 12 to 18) (A). After three Arabidopsis accessions (Fl-3, Col-0 and Kas-1) were non-acclimated (n = 9) (B) or acclimated for 1 day (n = 6 to 9) (C) and 3 days (n = 6 to 8) (D), freezing tolerance tests were performed at −4°C. Error bars indicate SE. (*$p < 0.05$).

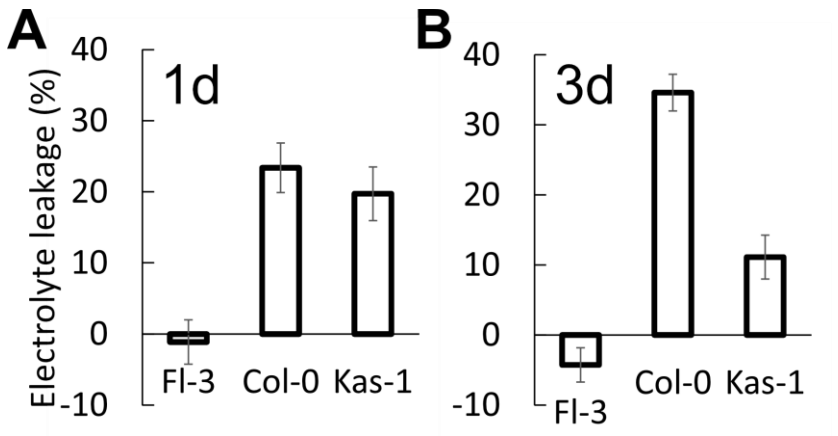

Figure 4.5. The contribution of the Ca^{2+} signals to the enhancement of freezing tolerance during temperature fluctuating cyclic cold acclimation treatment. The data in the figure were calculated using the formula (5) from the results of Figure 4.4. Error bars indicate SE.

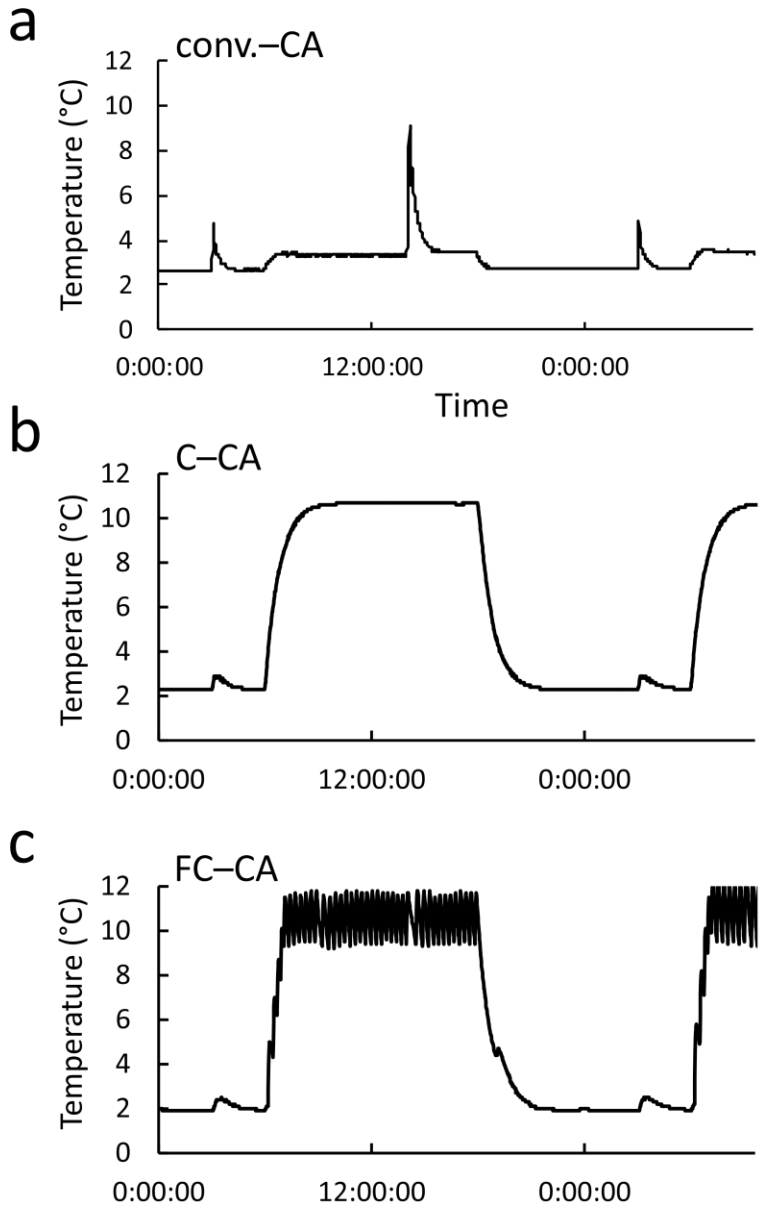

Figure 4.6. Temperature changes in three kinds of acclimation treatments. (a) The temperature changes of the conventional cold acclimation (conv.–CA). (b) Cyclic cold acclimation (C–CA) (c) Fluctuating cyclic cold acclimation (FC–CA). All temperature data were collected by using the temperature data logger, (TR-55i; T&D Co., Japan).

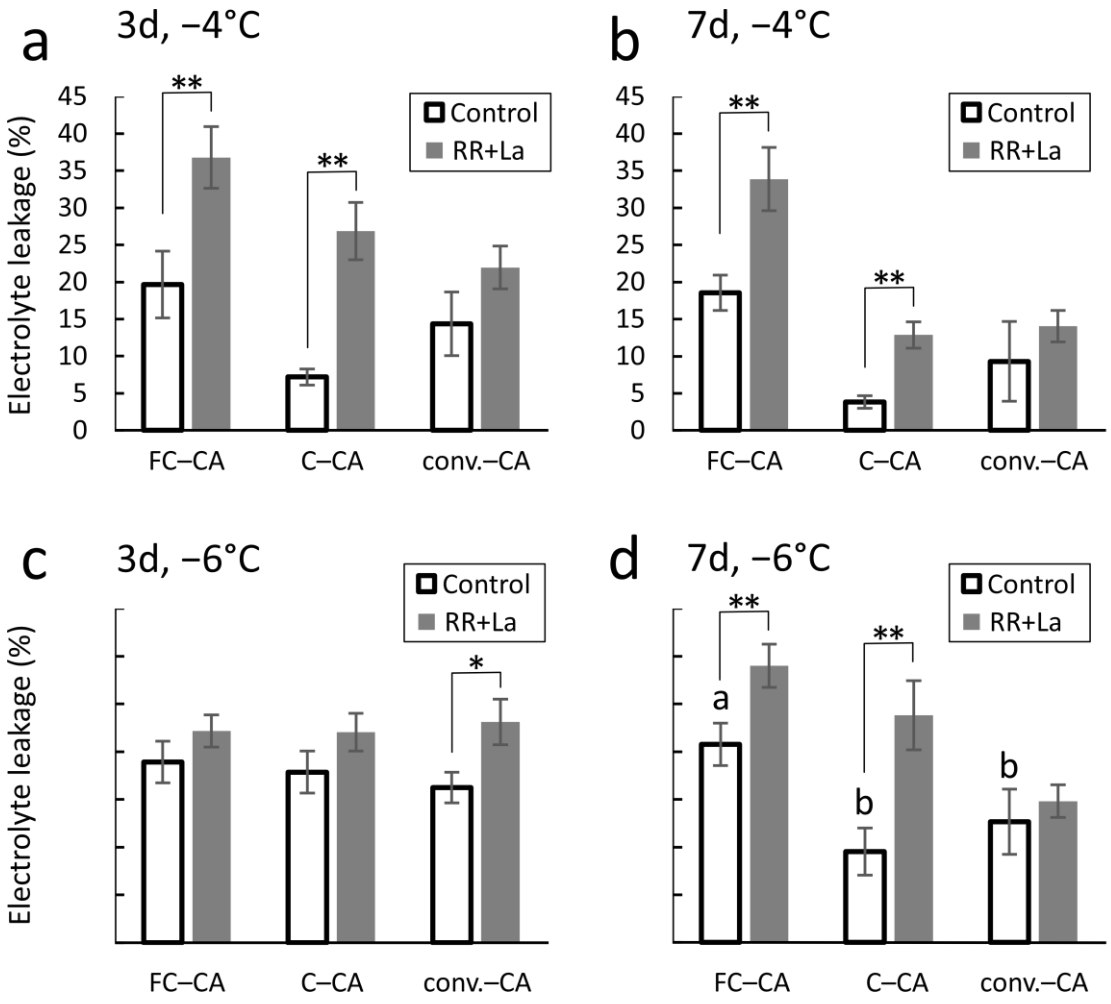

Figure 4.7. Electrolyte leakage (EL) in three acclimating treatments with Ca^{2+} channel blockers in Col-0. All plants were sprayed the mixed solution of 1 mM $LaCl_3$, 50 μM ruthenium red and 0.05% Triton X-100, or 0.05% Triton X-100 solution, 1 h prior to starting the acclimating treatments. (a) EL at −4°C freezing test after 3 day-acclimation in each condition. (b) EL at −6°C freezing test after 3 day-acclimation in each condition. (c) EL at −4°C freezing test after 7 day-acclimation in each condition. (d) EL at −6°C freezing test after 7 day-acclimation in each condition. Significant differences between control and chemical treated value was analyzed using the t-test (**$p < 0.01$, *$p < 0.05$) (n = 12 to 24). Significant difference among each value of control was analyzed by Tukey–Kramer test, and different letter indicated the significant difference ($p < 0.05$) (n = 12 to 24). The bars indicate the SE.

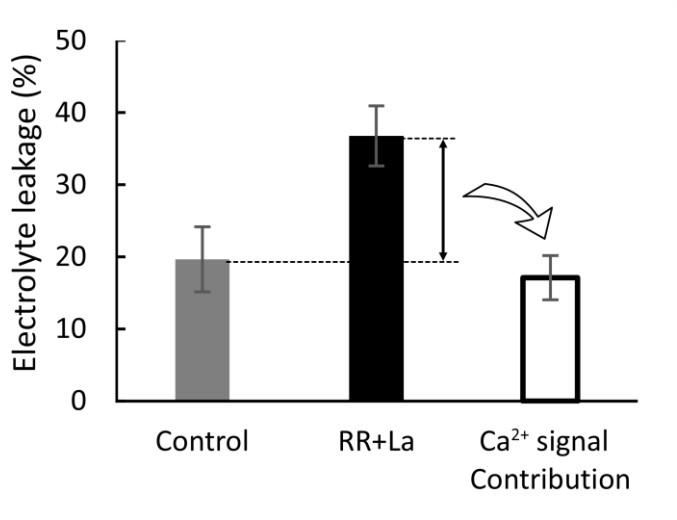

Figure 4.8 How to calculate the Ca^{2+} contribution in freezing tolerance based on the EL results. The EL value of the control plant subtracted from the EL value of the plant treated with the Ca^{2+} channel blockers, $LaCl_3$(La) and ruthenium red (RR). The error bars indicate SE. The SE value of the Ca^{2+} contribution was calculated by following formula.

$$\mathrm{SE}\ (\mathrm{a}+\mathrm{b}) = \sqrt{\frac{SE(a)^2 + SE(b)^2}{2}}$$

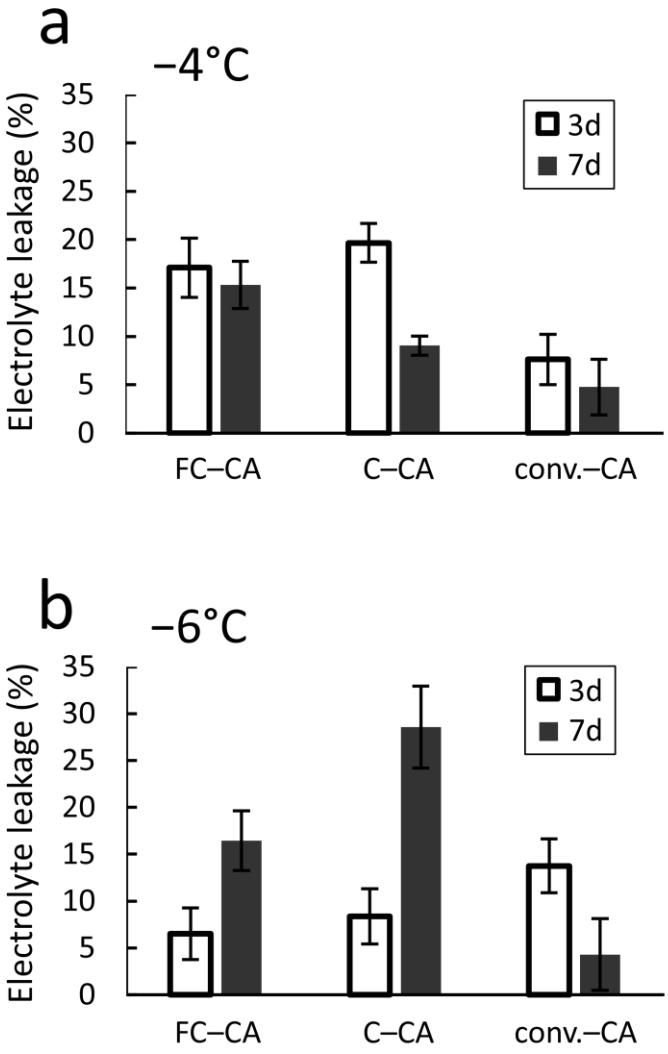

Figure 4.9. Contribution of Ca^{2+} signal on increase of freezing tolerance during the three acclimation treatments. The contribution was calculated by subtracting the value of EL in chemical treated plants from that of control. (a) Contribution of Ca^{2+} signal in EL values at −4°C freezing test after 3- and 7-day-acclimation treatments (b) Contribution of Ca^{2+} signal in EL values at −6°C freezing test after 3- and 7-day-acclimation treatments.

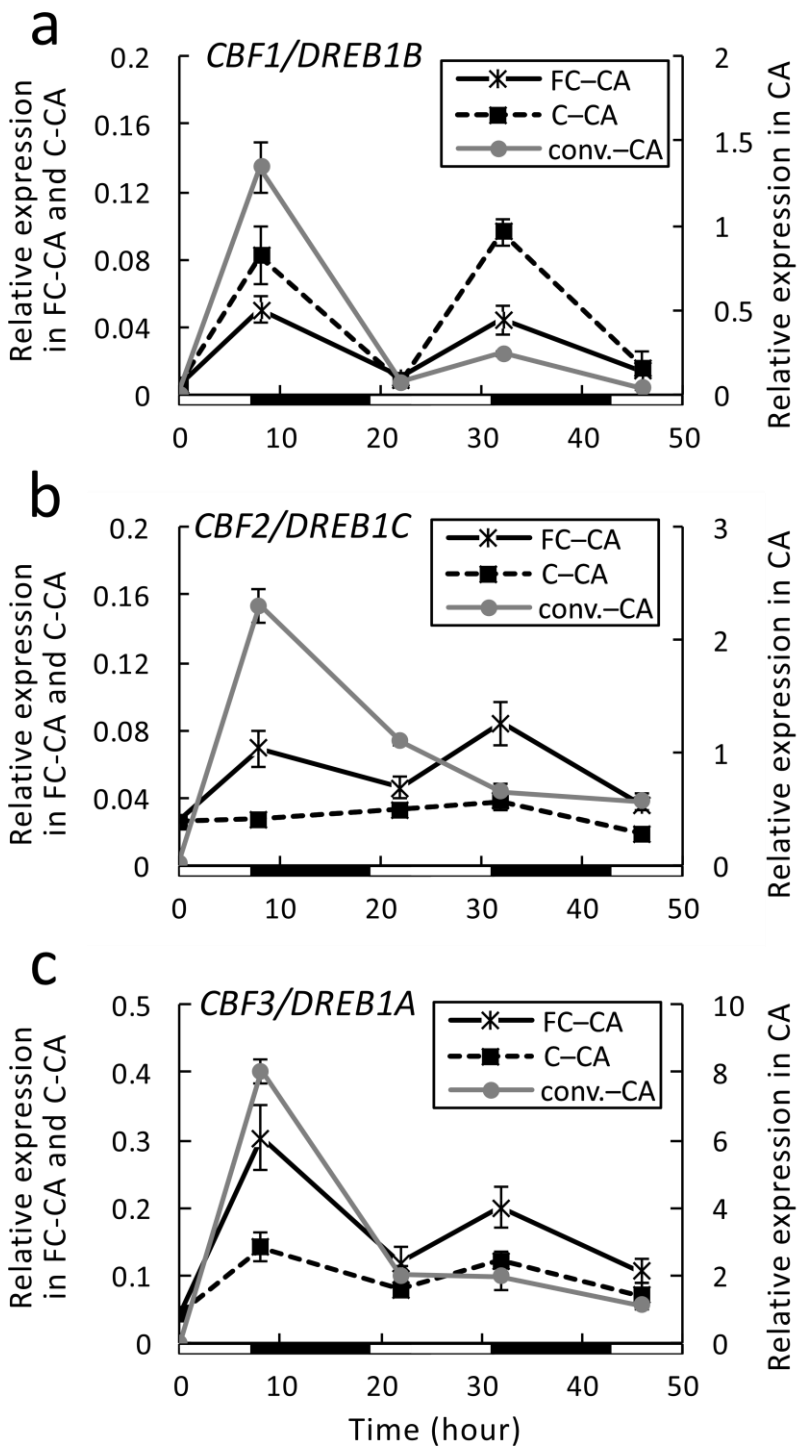

Figure 4.10. Expression levels of *CBF/DREB1s* during the three acclimation treatments. (a) The expression changes of *CBF1/DREB1B* was measured by real-time PCR at 0, 8, 22, 32 and 46 h after starting the acclimation treatments (n=3 to 6). (b) The expression changes of *CBF2/DREB1C* (n=3 to 6) (c) The expression changes of *CBF3/DREBA* (n=3 to 6). *PDF2* was used as a reference gene. The bars under the graph indicate day (white) or night (black) time. Error bars indicate SE.

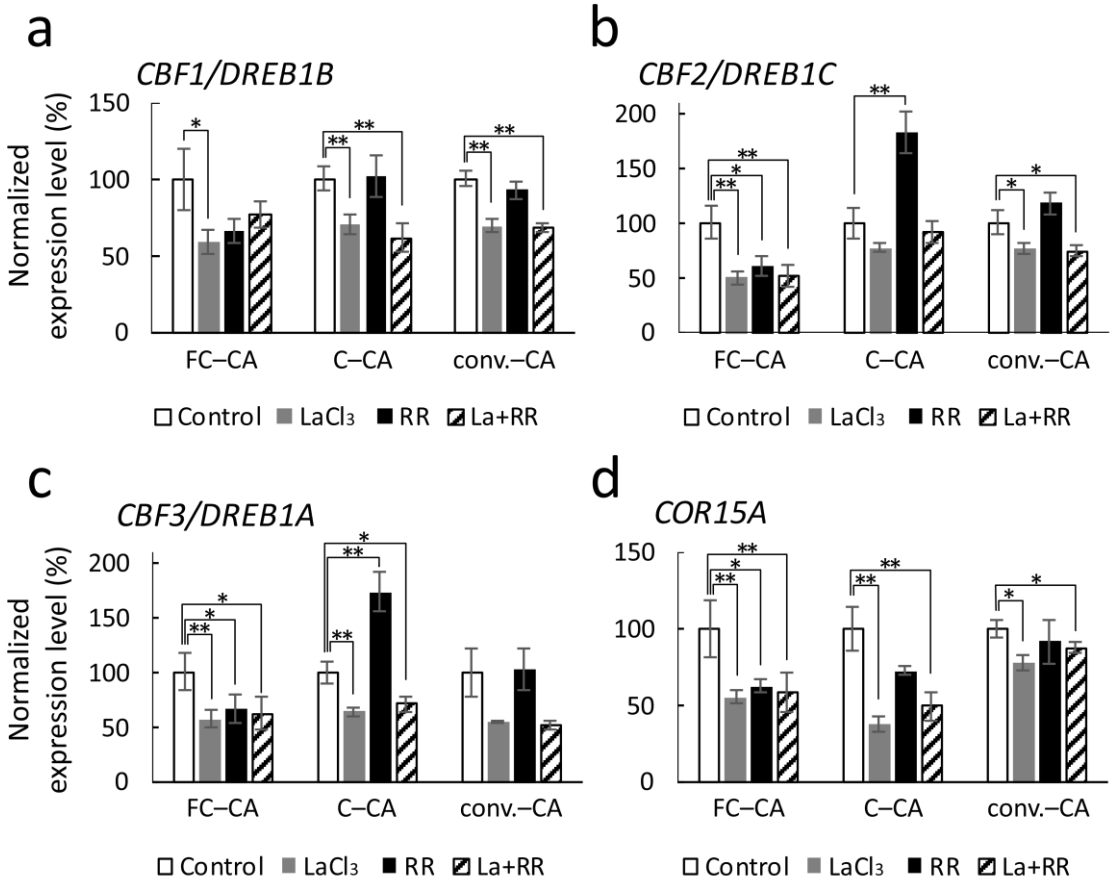

Figure 4.11. Effect of Ca^{2+} channel blockers on gene expression in three acclimation treatments at 32 h. Each expression level of gene in chemical treated plant was normalized to each control value. (a) Inhibition of expression level of *CBF1/DREB1B* by the Ca^{2+} channel blockers. (b) Inhibition of *CBF2/DREB1C* expression by the Ca^{2+} channel blockers. (c) Inhibition of expression level of *CBF3/DREBA* by the Ca^{2+} channel blockers. (d) Inhibition of *COR15A* expression by the Ca^{2+} channel blockers. Significant differences between control and chemical treated value was analyzed using the t-test (**$p < 0.01$, *$p < 0.05$). Error bars indicate SE.

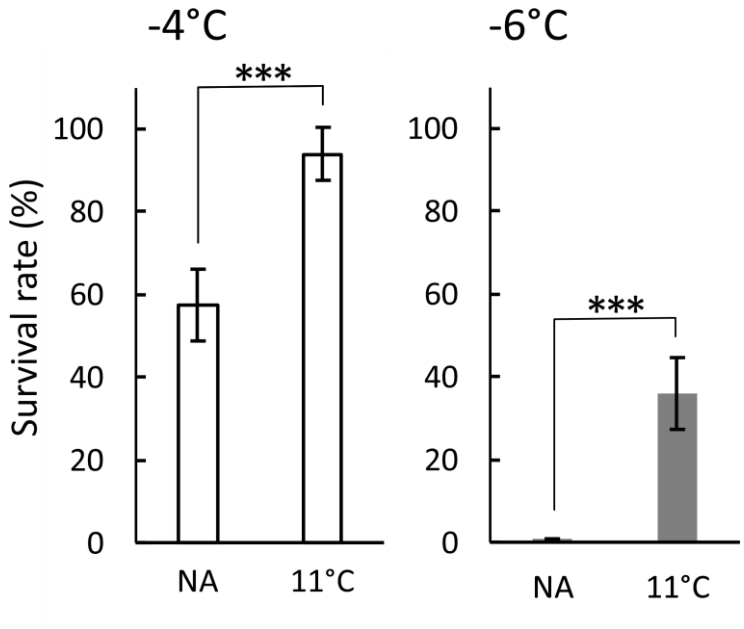

Figure 4.12. Effect of 11°C constant of acclimation on freezing tolerance. Two-week-old *Arabidopsis thaliana* (Landsberg) grown for 2 weeks (NA) and 7 d of 11°C acclimated plants were used for the freezing test. Plants were cooled from −2°C to −4°C or −6°C at 2°C h^{-1} of cooling rate.

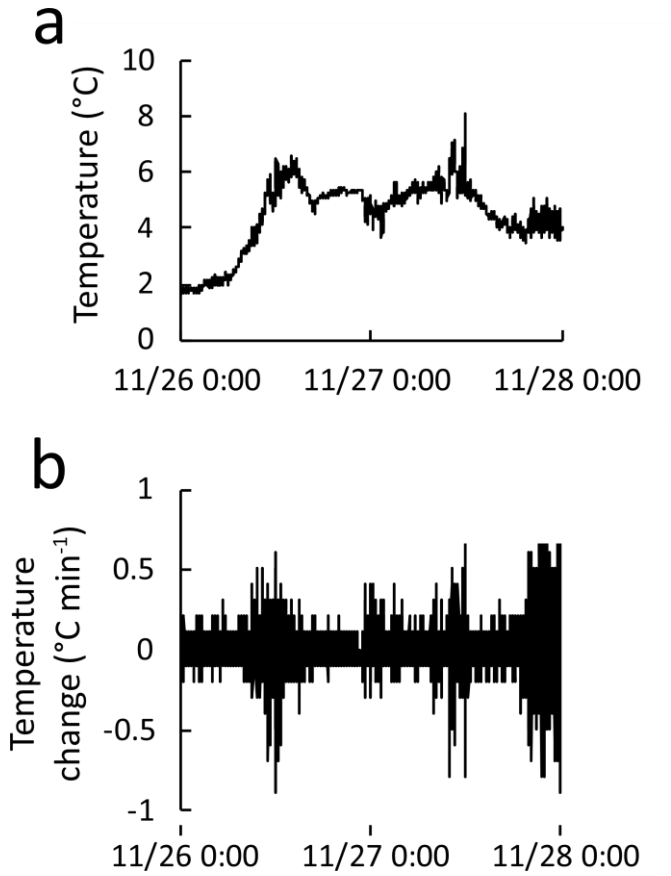

Figure 4.13. An example of air temperature change in Morioka, Japan. (a) The temperature data were collected between November 26th to 28th, 2015 by using the temperature data logger (TR-55i; T&D Co., Japan) (b) The rate of temperature change (°C min^{-1}) was calculated.

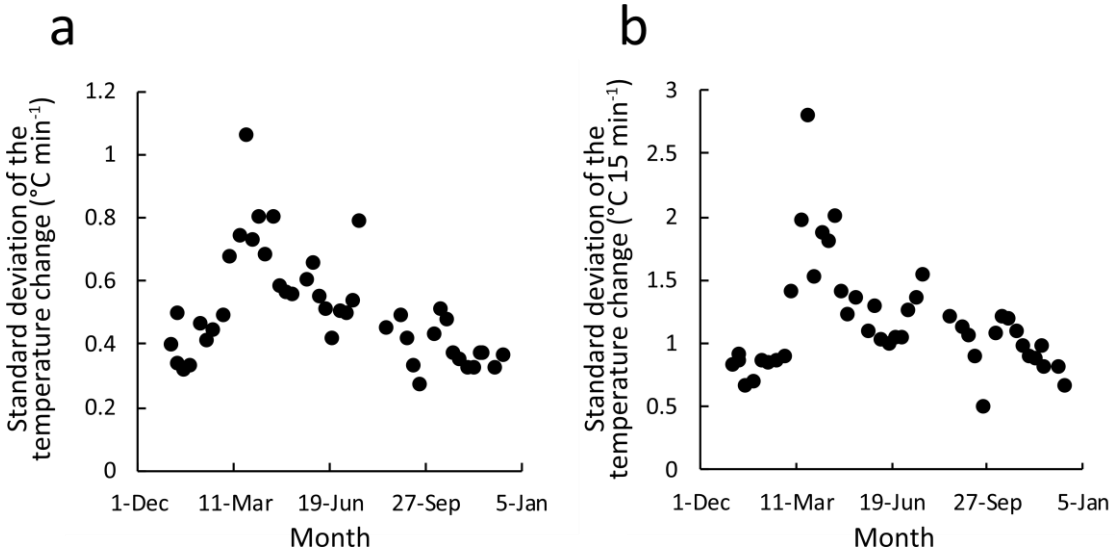

Figure 4.14. Standard deviation of temperature changes. The temperature data were collected during November 25th, 2015 to January 17th, 2017. (a) Temperature difference between every 1 min was calculated and the standard deviation was calculated from the temperature change and plotted. (b) Temperature difference between every 15 min was calculated and the standard deviation was calculated from the temperature change and plotted.

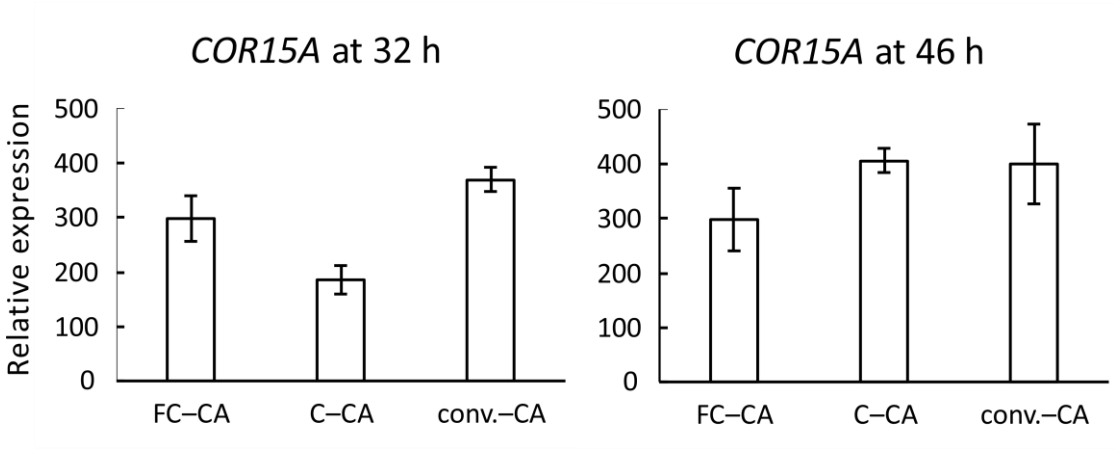

Figure 4.15. The expression level of *COR15A* at 32 and 46 h after starting the acclimation treatment (n =3 to 6). *PDF2* was used as a reference gene. Error bars indicate SE.

Table 4.1. Primer arrangement

Primer Name	Primer Arrangement
CBF1_RT_FW	CCGCCGTCTGTTCAATGGAATCAT
CBF1_RT_RV	TCCAAAGCGACACGTCACCATCTC
CBF2_RT_FW	CGGAATCAACCTGTGCCAAGGAAA
CBF2_RT_RV	AGACCATGAGCATCCGTCGTCATA
CBF3_RT_FW	TTCCGTCCGTACAGTGGAAT
CBF3_RT_RV	AACTCCATAACGATACGTCGTC
COR15A_RT_FW	AACGAGGCCACAAAGAAAGC
COR15A_RT_RV	CAGCTTCTTTACCCAATGTATCTGC
PDF2_RT_FW	TAACGTGGCCAAAATGATGC
PDF2_RT_RV	GTTCTCCACAACCGCTTGGT

Chapter 5

Season Specificity in the Cold-Induced Calcium Signal and the Volatile Chemicals in the Atmosphere

Abstract

Cold-induced Ca^{2+} signals in plants are widely accepted to be involved in cold acclimation. Surprisingly, despite using Arabidopsis plants grown in a growth chamber, we observed a clear seasonal change in cold-induced Ca^{2+} signals only in roots. Ca^{2+} signals were captured using Arabidopsis expressing Yellow Cameleon 3.60. In winter, two Ca^{2+} signal peaks were observed during a cooling treatment from 20°C to 0°C, but in summer only one small peak was observed under the same cooling condition. In the spring and autumn seasons, an intermediate type of Ca^{2+} signal, which had a delayed first peak and smaller second peaks compared with the those of winter type, was observed. Volatile chemicals and/or particulates in the air from the outside may affect plants in the growth chamber; this idea is supported by the fact that incubation of plants with activated carbon changed the intermediate-type Ca^{2+} signal to the summer-type. There was also a weak correlation between the seasonal characteristics of the Ca^{2+} signal and the solar radiation intensity. It has been reported that the ethylene concentration in the atmosphere seasonally changes depending on the solar radiation intensity. Ethylene gas and 1-aminocyclopropane-1-carboxylic acid treatment affected the Ca^{2+} signals, the shape of which became a shape close to, but not the same as, the winter type from the intermediate type or the summer type, indicating that ethylene in the atmosphere may be one of several factors influencing the cold-induced Ca^{2+} signal.

Introduction

To better understand the plant cold acclimation process, I have been studying the mechanism of cold sensing involving transient increases in Ca^{2+} concentration (i.e., Ca^{2+} signals). Although plants were grown in a growth chamber in our laboratory, the plant cells clearly presented seasonal changes in the pattern of cold-induced Ca^{2+} signals during the course of this study. These seasonal changes were completely unexpected.

Almost all researchers who work on plant physiology use a growth chamber or phytotron in their laboratory to maintain a stable environment. A growth chamber provides a homogeneous experimental environment regardless of the season. However, even in a chamber that is installed indoors, the environment changes by season. Many growth chamber models can adjust the temperature, humidity, and light conditions, but do not control any other factors, such as volatile chemicals in the air. In the field, temperature, humidity, day length, and volatile chemicals change depending on the season. The seasons are deeply related to sunlight intensity and day length. The UV (280–400 nm) level of the sun is also important for biogeochemical cycles (Zepp *et al*., 2007). For example, UV-B (280–315 nm) radiation accelerates the transformation of organic matter into dissolved inorganic carbon and nitrogen (Zepp *et al*., 2007). According to data from the Japan Meteorological Agency, the UV level in Japan is high in July and August, decreases during the autumn season, is low from late November to early January, and gradually increases in the spring.

Allelopathy is the phenomenon by which plants affect neighboring plants by releasing compounds. The role of allelopathy is mainly to inhibit neighboring plant growth to gain a competitive advantage. There has not been enough evidence to describe growth inhibition by volatile compounds as allelopathy (Inderjit *et al*., 2006). However, transgenic plants deficient in the production of volatile chemicals or phytohormones show growth inhibition by volatile compounds (Baldwin *et al*., 2006). Experiments using transgenic plants that cannot release or sense ethylene suggested that ethylene produced by one plant can affect the growth and establishment of neighboring plants under laboratory conditions (Inderjit *et al*., 2009). This is an example of plants responding to chemicals and compounds in the environment (including from other plants). Ethylene is a phytohormone (Gane, 1934) that is well known as a promoter of fruit ripening and seed germination (Abeles *et al*., 1992). Ethylene also regulates senescence and responses to stresses such as flooding, abscission, wounding, and pathogen attack (Abeles *et al*., 1992). The pathway of ethylene biosynthesis is known, and 1-aminocyclopropane-1-carboxylic acid (ACC) has been identified as the precursor of ethylene in higher plants (Adams and Yang, 1979).

Plants enhance their cold and freezing tolerance through exposure to low temperatures. This phenomenon is called cold acclimation (see Levitt, 1980). In the first step of

this process, plants must sense cold or a temperature decrease. It has been reported that a transient cytosolic Ca^{2+} concentration increase is induced by cooling (Knight *et al*., 1991; Plieth *et al*., 1999; Knight and Knight, 2000). This is called a Ca^{2+} signature and/or Ca^{2+} signal. Several reports support that a Ca^{2+} signal acts as a second messenger in biotic and abiotic stresses (McAinsh and Pittman, 2009; Martí *et al*., 2013). Ca^{2+} signal is induced by the cooling depending on the cooling rate, absolute temperature, cooling duration and state of the plant (e.g., cold acclimated or non-acclimated) (Plieth *et al*., 1999; Knight and Knight, 2000; Hiraki *et al*., 2019). We also reported that Ca^{2+} signals may regulate the gene expression level of C-repeat (CRT)-binding factor/dehydration-responsive element binding protein 1 (*CBF/DREB1)* depending on the minute temperature fluctuation (Hiraki *et al*., 2019). Moreover, even at room temperature, artificial Ca^{2+} signals activate cold-responsive promoter motifs (Whalley *et al*., 2011; Whalley and Knight, 2013), suggesting that Ca^{2+} signals encode information to regulate gene expression. Therefore, production of a Ca^{2+} signal is one of the first steps of cold acclimation and reflects how plants sense cold.

To study Ca^{2+} signaling behavior, I developed an experimental system to observe the Ca^{2+} concentration in living cells under temperature changes. Our cryostage can control the temperature of samples under a microscope. Arabidopsis expressing Yellow Cameleon 3.60, which is a Ca^{2+} sensor fluorescence protein, was used to image the concentration changes of Ca^{2+}. I observed seasonal changes in the Ca^{2+} signal induced by the same cooling conditions even when the plants were grown in a growth chamber installed in our laboratory. To understand these unexpected observations, I tried to identify the factor that changed the Ca^{2+} signal.

Materials and Methods

Plant materials

Arabidopsis thaliana plants expressing Yellow Cameleon 3.60 were grown in Petri dishes containing modified Hoagland's nutrient solution solidified with 1% agar (Uemura *et al*., 1995). The plants were incubated in a vertical position for a week at 23°C under a 16-h photoperiod (photon flux rate: 80 μmol m^{-2} s^{-1}).

Ca^{2+} signal measurement under the cooling

An Arabidopsis seedling expressing Yellow Cameleon 3.60 (Nagai et al., 2004) was set to the cryomicroscope (Hiraki *et al*., 2019a). Ca^{2+} signals were measured according to changing temperatures, and data were analyzed according to the methods used by Hiraki et al. (2018).

Data analysis

All Ca^{2+} signals were smoothed to analyze the peak time with the IGOR-pro 6.3 software (WaveMetrics, Inc.; https://www.wavemetrics.com/). To generate the averaged Ca^{2+} signals for Figure 5.4A, FRET values were extracted or inserted with a function for complementing missing values in the IGOR-pro 6.3 software when the interval times differed. The time interval was fixed at 2 s.

Treatment

To reduce atmospheric humidity or chemicals, silica gel or activated carbon, respectively, was added to the petri dishes just after seeding. A piece of aluminum foil was set between the medium and silica gel or activated carbon. For ethylene treatment, a banana was put with a petri dish in a glass box and covered with plastic wrap. For the control, the banana was replaced with a tube filled with wet soil (a mixture of vermiculite and perlite). For ACC treatment, Hoagland's medium containing 1 μM 1-aminocyclopropane-1-carboxylic acid was used. One-week-old Arabidopsis seedlings were transferred to the ACC plates and incubated for one day. Hoagland's medium without ACC was used as a transfer control.

Results

I focused on the cold-induced Ca^{2+} signals that may precede cold acclimation. On December 16, 2013, 1-week-old Arabidopsis seedlings grown at 23°C in the growth chamber installed in our laboratory were cooled from 20°C to 0°C with a 2°C min^{-1} cooling rate on the cryostage of a laser scanning confocal microscope. The cooling was started at 30 s. The Ca^{2+} signal was observed in the plant roots during cooling. The Ca^{2+} signal showed two peaks as reported in previous studies (Figures. 5.1A and 5.2: winter type; Knight and Knight, 2000; Hiraki *et al*., 2019a). The peaks appeared at 170 s and 630 s. On August 04, 2015, a similar experiment was performed using the same equipment and the same growth chamber. The only difference was that the temperature was changed from 20°C to 2°C with a 2°C min^{-1} cooling rate, but the conditions were exactly the same until the temperature reached 2°C (i.e., at 570 s). Unexpectedly, there was no Ca^{2+} increase at around 170 s, and only one small peak was observed at about 570 s (i.e., just after stopping the cooling) (Figures. 5.1B and 5.2: summer type).

The fact that the first experiment was performed in the winter and the second one was in the summer triggered us an idea that the different Ca^{2+} signaling might be caused by factors that exhibit seasonal changes. To test this, I decided to repeat the Ca^{2+} measurement for

approximately five years, thus including five winters and four summers. In all experiments, the temperature was changed from 20°C to 0°C with a 2°C min^{-1} cooling rate. It should be emphasized that all samples were grown in the same growth chamber installed in our laboratory. There was no difference in growth temperature, day length, or light intensity during the growth period. In the winter season, Arabidopsis tended to show Ca^{2+} signals with two Ca^{2+} peaks at about 200 s and 600 s in the roots (Figure 5.2, left column). This type of Ca^{2+} signal was named the winter type. Conversely, in summer, Ca^{2+} signals with only one peak at about 600 s were observed (Figure 5.2, middle column). This type was called the summer type. In addition, an intermediate type of Ca^{2+} signal was observed, mainly in the spring and autumn seasons, which had two peaks; the first peak was small and appeared at about 400 s. In other cases, some samples showed summer-type or winter-type Ca^{2+} signals in the spring and autumn seasons. These Ca^{2+} signals were categorized as the intermediate-type Ca^{2+} signals (Figure 5.2, right column). This phenomenon was observed only in the plant roots. When the aerial part of the plant was cooled from 20°C to 0°C at about 1.4°C min^{-1}, there was no difference in the height or number of Ca^{2+} signal peaks in winter (November–December) and summer (July) (Figure 5.3). To show the characteristics of the summer, winter, and intermediate Ca^{2+} signals in the roots, each group of averaged Ca^{2+} signals was averaged again (Figure 5.4A). The August 4, 2015 samples were excluded because of the different cooling scheme (20°C–2°C). The signal height tended to be higher in winter types, followed by intermediate and finally summer types. All averaged first peak times for the Ca^{2+} signals are shown in Figure 5.4B.

Furthermore, all Ca^{2+} signals categorized as the winter, intermediate, or summer type are summarized in Figure 5.5A. The cumulative solar radiation in Morioka for one week in which the plants grew was calculated from the Japan Meteorological Agency database. The higher cumulative solar radiation tended to result in the summer-type Ca^{2+} signals, while lower solar radiation induced winter-type Ca^{2+} signals (Figure 5.5A). I found a correlation between the cumulative solar radiation and the first peak time of each Ca^{2+} signal ($R = 0.5918$) (Figure 5.5B).

Humidity changes by season (less than 70% from winter to spring and 80% in summer in Morioka, Japan; see the Japan Meteorological Agency database). This could be one of the candidate factors that altered the cold-induced Ca^{2+} signal by season. To reduce the humidity, on August 15, 2016, 15 g of silica gel balls were added directly to the petri dishes with growing plants for one week. The silica gel removed the internal condensation in the petri dish (Figure 5.6A). Under these conditions, a summer-type Ca^{2+} signal was induced by cooling from 20°C to 0°C at 2°C min^{-1}, which is similar to the Ca^{2+} signals of the control (Figure 5.6B). Furthermore, because the biggest difference in the seasonal changes of Ca^{2+} signals was the time shift of the first peak (Figures 5.2 and 5.4), statistical analysis of the first peak time was performed between the Ca^{2+} signals of the control and silica gel-treated samples. Again, there was no significant

difference (Figure 5.6C). Thus, I concluded that seasonal change in humidity is not a decisive factor for the seasonal changes of the Ca^{2+} signal.

Another candidate factor was a volatile chemical. To remove or reduce the chemicals in the air, 15 g of activated carbon tips were put into the petri dishes during the 1-week growth period (Figure 5.7A). This experiment was performed on September 26, 2016. The plants were cooled from 20°C to 0°C at 2°C min^{-1}, and the Ca^{2+} signals were observed during cooling. The Ca^{2+} signal in the control was categorized as intermediate type. In contrast, activated carbon treatment changed the Ca^{2+} signal to the summer type (Figure 5.7B). Peak time analysis also indicated that the activated carbon treatment significantly changed the peak time (Figure 5.7C).

In further experiments, I tried to identify the causative chemical. To expose 1-week-old Arabidopsis seedlings to ethylene gas, a banana and petri dish were packed together in a plastic-wrapped glass box for 2 days. For the control, a 50-mL tube filled with wet soil (vermiculite and perlite) was packed with the petri dish as a mock of banana (Figure 5.8A). It has been reported that bananas produce ethylene gas at 0.0017 µL/L h^{-1} (McGlasson, 1969; Liu *et al*., 1999). In fact, the concentration of ethylene in the petri dish was approximately 3.5 µL/L (Figure 5.9D). The measurement of ethylene was performed according to the methods used by Suzuki *et al*. (1997). The root length was shorter in the ethylene-treated plants than in the control (Figure 5.9B), indicating that ethylene gas produced by the banana inhibited root elongation. In the control, the Ca^{2+} signals observed on September 27, 2017 were classified as the intermediate type upon cooling from 20°C to 0°C at 2°C min^{-1}. Conversely, the ethylene-treated Arabidopsis showed the winter-type Ca^{2+} signals (Figure 5.8B), and a significant difference was found in the peak time between the control and ethylene treatment (Figure 5.8C). To confirm that ethylene enhanced the level of the Ca^{2+} signal and induced the first peak, an experiment was performed with 1 µM ACC, which is the precursor of ethylene (Adams and Yang, 1979). One-week-old Arabidopsis seedlings were transferred from normal Hoagland's nutrition medium to a medium with or without ACC (Figure 5.8D). After 1 day, root hairs increased in number (Figure 5.9A, C) and the root length was shorter in ACC-treated Arabidopsis seedlings (Figure 5.8D), indicating the ACC treatment affected the Arabidopsis seedlings; and then Ca^{2+} signals were observed (on July 4, 2018). In response to the cooling from 20°C to 0°C at 2°C min^{-1}, the control Arabidopsis seedlings showed the summer-type Ca^{2+} signals in response to cooling from 20°C to 0°C at 2°C min^{-1}, while the ACC-treated Arabidopsis seedlings showed the intermediate- or winter-type Ca^{2+} signals (Figure 5.8E). The analysis of peak time also indicated that there was a significant difference between the control and treatment (Figure 5.8F). The results from ACC-treated plants were similar to those with ethylene (Figure 5.8). Thus, experiments with ethylene gas and ACC clearly show that ethylene gas can be an important factor inducing seasonal changes in the Ca^{2+} signals upon cooling.

Discussion

Seasonal changes in Ca^{2+} signals and cold acclimation

My study uses Arabidopsis seedlings grown under a controlled environment in a laboratory growth chamber. That is, the Arabidopsis seedlings are supposed to be grown under the same conditions. However, surprisingly, my detailed observation over 5 years showed differences in cooling-induced Ca^{2+} signals depending on the season (Figures 5.1, 5.2, 5.4 and 5.5).

The Ca^{2+} signals were categorized into three types of shape. The first was the winter type. This type had two Ca^{2+} signal peaks during the cooling from 20°C to 0°C and tended to be observed in autumn and winter seasons. The second was the "summer type," which had just one small Ca^{2+} signal peak during cooling. The single peak in the summer-type Ca^{2+} signal was observed at the same time as the second peak in the winter type. The third type was the "intermediate type"; this had two peaks, but the first and second peaks were smaller than those of the winter type (Figure 5.4A), and the first peak time was widely distributed between 100 and 400 s (the winter type had a first peak at about 200 s). In addition, not all samples showed the intermediate type on the same day; some samples still showed the summer type. Therefore, the standard errors were large in the spring to summer and autumn to winter seasons (see Figure 5.4B; October 5, 2015; September 6, 2016; October 9, 2016; July 10, 2017; September 26, 2017; and May 19, 2018). This result suggested that the Ca^{2+} signal gradually changed from the winter to summer types and vice versa (Figure 5.4).

Many reports support the hypothesis that a Ca^{2+} signal acts as a second messenger during cold stress (Knight et al., 1996; Chinnusamy et al., 2010; Shi et al., 2015). In the case of cold stress, the Ca^{2+} influx and efflux come from extracellular and intracellular sources respectively, and are received by calmodulin. Calmodulin binds to the calmodulin binding transcription activator (CAMTA) 3 and CAMTA 5, and then positively regulates the expression levels of the CBF/DREB1s transcription factors (Doherty et al., 2009; Kidokoro et al., 2017). In the early process of cold acclimation, CBF/DREB1 transcription factors induce the expression of DRE/CRT ciselement and induce cold-responsive (*COR)* genes and consequently enhance freezing tolerance (Fowler et al., 2002; Wang and Hua, 2009). In our recent study, it has been shown that Ca^{2+} signals may regulate *CBF/DREB1* gene expression during cold acclimation, especially, under field conditions in winter (Hiraki et al. 2019). Thus, from the perspective of gene expression, it is reasonable that plants enhance Ca^{2+} signals in the winter season.

On the other hand, this seasonal response of cold-induced Ca^{2+} signals was observed only in the root cells. In leaf cells, a similar pattern of Ca^{2+} signals was observed in both summer and winter, and the number of peaks was not changed by the season (Fig. S1). This

difference between root and leaf may be related to the fact that the temperature of aerial part changes frequently compared with the soil temperature. Air temperature suddenly drop even in the summer and, for example, in June at Morioka (ca. 40°N in Japan) it often drops below 10°C while maximum temperature is over 30°C. In addition, the leaf temperature drops sharply by the cloud movement, wind and rain. Plants can suffer from chilling stress even in summer. Interestingly, it is known that an Arabidopsis mutant impaired in the expression of *CBF/DREB1* genes is sensitive to chilling stress, and that overexpression of *CBF3/DREB1A* gene restores chilling resistance to the mutant (Gong et al. 2002). Thus, throughout the year, the aerial part of plants needs to sense air temperature drop and regulates *CBF/DREB1* gene expression by cold-induced Ca^{2+} signals.

Estimation of candidate factors which cause the seasonal changes of Ca^{2+} signal

Even though the humidity was supported to be controlled in the growth chamber, humidity differs dramatically between winter and summer in Japan, where I have a large amount of precipitation in the spring-autumn period. Thus, silica gel was used to decrease the humidity in the petri dishes in the summer season. The results indicated that humidity did not contribute to cold-induced Ca^{2+} signaling (Figure 5.6). Next, to test the possibility that other volatile chemicals affected the cold-induced Ca^{2+} signals, activated carbon was used to decrease the chemicals in the air. This experiment was done in the autumn season, and an intermediate type of Ca^{2+} signal was observed in the control. Because the first peak observed in the control disappeared in the activated carbon treatment (Figure 5.7), the chemicals adsorbed on the activated carbon may increase from autumn to winter and affect cold-induced Ca^{2+} signals. Additionally, although activated carbon also absorbs moisture (Horikawa *et al*., 2010), this possibility was excluded based on the results in Figure 5.6.

To narrow down possible candidates, my 5-year observations of cold-induced Ca^{2+} signal gave us further hints. That is, the cumulative solar radiation during each growing period (i.e., 1 week) in Morioka (Figure 5.5A) showed the correlation to the peak time of Ca^{2+} signal (Figure 5.5B). For example, the Ca^{2+} signal observed in July 26, 2018 categorized as intermediate type despite being in the summer. However, the cumulative solar radiation was 89.7 in July19–25, 2018 (i.e., experiment day: July 26, 2018), and it was much lower than that of 144.1 and 124.0 in July 2–9, 2018 (July 10, 2018) and July 26 to August 1, 2018 (August 2, 2018), respectively. These results indicated that the factors which cause the seasonal changes of Ca^{2+} signal might be dissolved by the sunlight. The decrease of ethylene concentration depends on sunlight, because ethylene reacts with nitric oxides to produce ozone and other oxidants under the UV radiation of the sun (Altuzar *et al*., 2001). This suggests that stronger sunlight in the summer season tends to

decrease the concentration of ethylene in the atmosphere. In fact, the concentration of ethylene was higher in winter (48 ppb) than in other seasons (average: 5.27 ppb) in Yokohama, Japan (Hanai *et al*., 1983). In addition, the fact that activated carbon can adsorb ethylene gas (Relch *et al*., 1980), consistent with the result of Figure 5.7. Thus, ethylene was considered as one of the main candidates. In addition, since there was no correlation between the cumulative solar radiation of one or a few days before the experiment day and the peak time of the Ca^{2+} signals, accepting ethylene for a long time might be important for seasonal sensing in case of a lower concentration of ethylene in the field. This mechanism is useful for sensing seasonal changes without being influenced by short-term weather. On the other hand, low solar radiation did not always result in winter-type Ca^{2+} signaling (e.g., November 20, 2015; December 9, 2015).

Assuming that the causative chemical is ethylene, it is easy to explain why there were a few unseasonable types of Ca^{2+} signals in my results (Figure 5.5). A few studies have monitored the concentration of ethylene in the atmosphere. In Los Angeles, the median concentration of ethylene was 0.0107 μL/L, and the maximum was 0.5005 μL/L (Schinfeld, 1989). In Mexico City, a higher concentration of ethylene (~0.035 μL/L) was measured in the morning than in the afternoon (~0.007 μL/L) (Altuzar *et al*., 2001). The authors suggested that a large ethylene emission was caused by the inefficient combustion of vehicles in the morning, and found that a high density of traffic tended to increase the concentration of ethylene. In Washington D.C., the ethylene concentration was also high in areas of heavy traffic (~0.6 μL/L) (Abeles and Heggestad, 1973). According to another report, the concentration of ethylene can change day by day even in the same location (Zhang and Huang, 2010). Therefore, it is conceivable that the concentration of ethylene varies depending on the sunlight even in the same season; and therefore, the unseasonal Ca^{2+} signals can be observed in each season.

Ethylene is one of the candidate substances

I focused on ethylene, a gasiform phytohormone, as one of the potential Ca^{2+} signal modifier. In my results, ethylene gas changed the shape of the Ca^{2+} signals in the summer season, suggesting that ethylene gas was the chemical that changed the Ca^{2+} signals to the winter type in the laboratory. To confirm that ethylene acts as a Ca^{2+} signal modifier, I used ACC, which is the precursor of ethylene (Adams and Yang, 1979). Since both ethylene gas and ACC treatment resulted in similar Ca^{2+} signals changes, I concluded that ethylene could change Ca^{2+} signals to the winter type.

Ethylene is related to many physiological responses (Abeles *et al*., 1992). Ethylene gas is released in response to wounding, fruit ripening, pathogen infections, auxins, and cytokinins (Abeles *et al*., 1992). Extractable ethylene from the leaves and fruits of several apple cultivars were measured from June to October, and the highest level of ethylene was observed in October

in most cultivars (Blanpied, 1972). It was also reported that un-stressed Arabidopsis released ethylene gas without wounding under the control of the circadian clock (Thain *et al*., 2004). While there has been no report that ethylene is involved in Ca^{2+} signaling, it was reported that abscisic acid (ABA) of a phytohormone induces Ca^{2+} release from intracellular Ca^{2+} via inositol 1,4,5-trisphosphate (IP_3)-dependent Ca^{2+} channels (Knight *et al*., 1996; Zhu, 2002; Xiong *et al*., 2002).

It has been reported that ethylene negatively regulates the *CBF/DREB1* pathway and decreases freezing tolerance (Zhang and Huang, 2010; Shi *et al*., 2012). In addition, from the perspective of allelopathy, ethylene is used as a growth inhibitor for neighboring plants (Inderjit *et al*., 2006). Therefore, exogenous ethylene functions as an effector that acts as a kind of "stress" for plants. Knight and Knight (2000) and Hiraki *et al*. (2018) reported that cold acclimation treatment (i.e., low-temperature stress) changed the shape of the Ca^{2+} signal induced by cooling. In particular, it showed a higher second peak in cold-acclimated Arabidopsis than in non-acclimated plants (Knight and Knight, 2000); and the higher responsiveness to the cooling in cold-acclimated Arabidopsis than in non-acclimated plants (Hiraki *et al*., 2019a). Knight *et al*. (1996) and Knight and Knight (2000) suggested that while the first peak included a significant contribution from extracellular Ca^{2+} sources, the second peak of the Ca^{2+} signal represented efflux from the vacuole and endoplasmic reticulum. My results showed that ethylene gas and ACC treatment at room temperature increased the first peak of the cold-induced Ca^{2+} signal. This suggests that external ethylene increased the Ca^{2+} influx from extracellular sources and changes the height and timing of the first peak of the Ca^{2+} signal without cold acclimation treatment. On the other hand, because my ethylene treatments did not completely change the Ca^{2+} signal to the winter type (Figure 5.8), there is a possibility that other seasonal factors act in conjunction with ethylene. The fact that activated carbon can adsorb ethylene gas (Relch *et al*., 1980) consistent with the result of Fig. 5.7. However, activated carbon also absorbs other low-molecular-weight organic compounds. In order to sense the season, plants integrate multiple conditions such as low temperature, temperature decrease, light and day length, and regulate the cold acclimation process (Knight *et al*., 1996; Puhakainen *et al*., 2004; Lee and Thomashow, 2012; Legris *et al*., 2016). Likewise, it is thought that there are multiple factors that determine the seasonal type of Ca^{2+} signals to regulate cold acclimation process in specific season. As one of them, we suggest low-molecular-weight organic compounds such as ethylene gas which are decomposed by sunlight act as a Ca^{2+} signals modifier.

Conclusion

Taken together, my results strongly suggest that plants integrate the seasonal factors

influencing Ca^{2+} signaling. Even plants grown in the laboratory growth chamber showed seasonal changes in their Ca^{2+} signals in response to cooling. I concluded that the main candidate which caused the seasonal changes in cold-induced Ca^{2+} signals was ethylene. This hypothesis was supported by the Ca^{2+} signal observation with ethylene gas and ACC. Since the cold-induced Ca^{2+} signal act as a second messenger in cold acclimation process, seasonal change of the ethylene and the other factors concentration may contribute the in cold-acclimation process. (Figure 5.10).

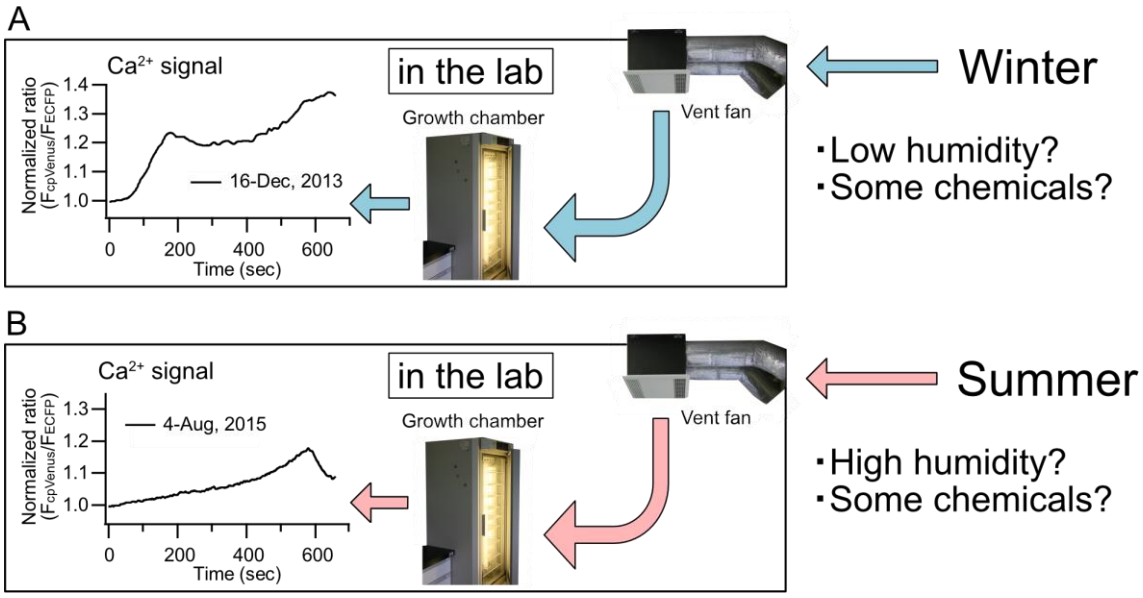

Figure 5.1. Effect of seasons on cold sensing of plants grown in a growth chamber. (A) On December 16, 2013, Ca^{2+} signals were measured under a cryomicroscope. FRET values (i.e., ratio of fluorescence intensity of cpVenus/ECFP) indicate the Ca^{2+} concentration. The roots were cooled from 20°C to 0°C with a 2°C min^{-1} cooling rate. The cooling was started at 30 s. (B) Ca^{2+} signals observed on August 4, 2015. The roots were cooled from 20°C to 2°C with a 2°C min^{-1} cooling rate. In both experiments, the Ca^{2+} signals were averaged, smoothed, and normalized by the value at $t = 0$ ($n = 4–5$).

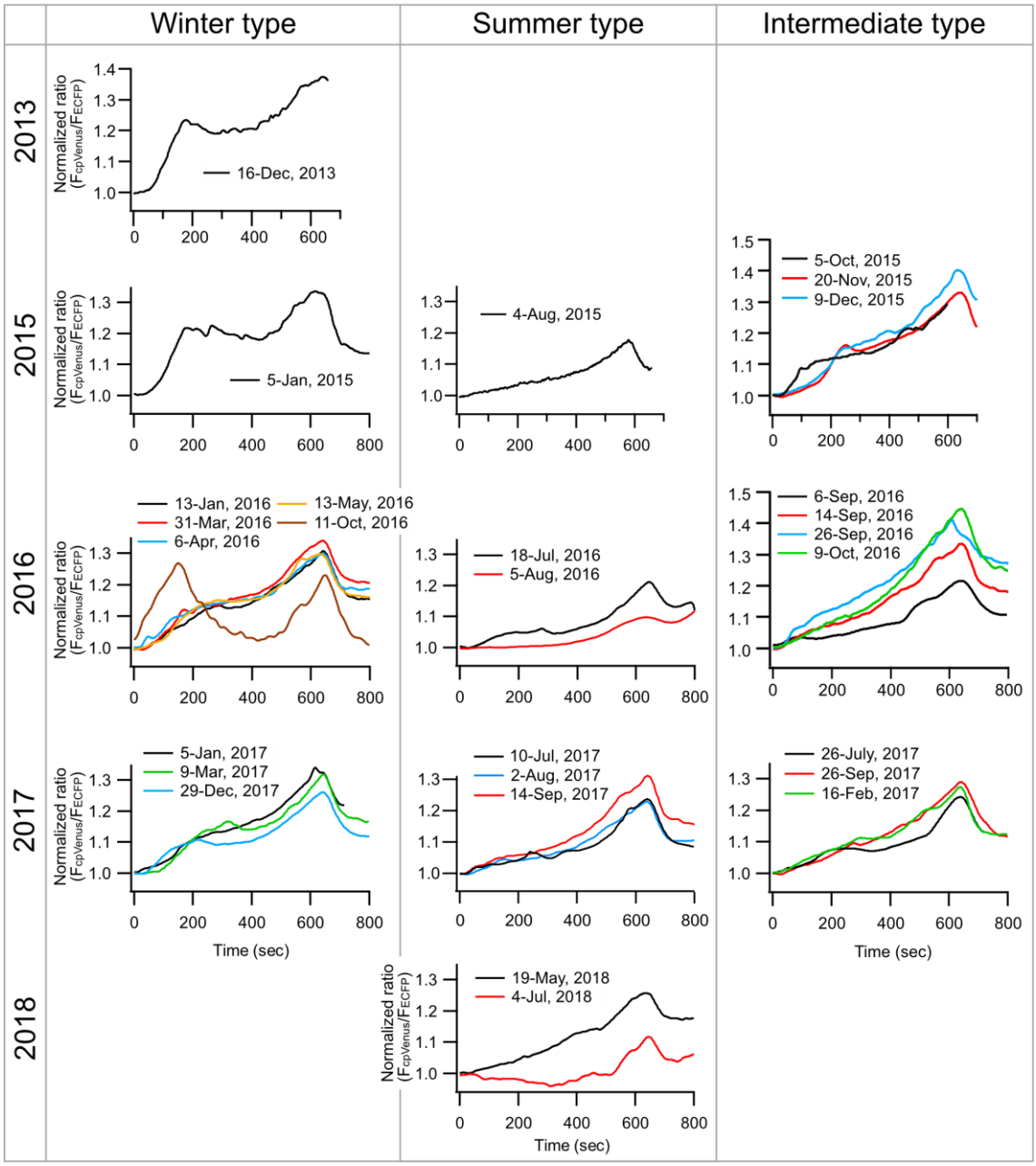

Figure 5.2. Seasonal changes of Ca^{2+} signals in the roots of Arabidopsis expressing Yellow Cameleon 3.60 grown in a growth chamber. FRET values indicate the Ca^{2+} concentration. The Ca^{2+} signals in the elongating part of the root were captured every 2–15 s on December 16, 2013; January 5, August 4, October 5, November 20, and December 9, 2015; January 13, March 31, April 6, May 13, July 18, August 5, September 6, September 14, September 26, October 9, and October 11, 2016; January 5, February 16, March 9, December 29, July 10, July 26, August 2, and September 14, 2017; and May 19 and July 4, 2018. The Ca^{2+} signals were averaged, smoothed, and normalized by the value at $t = 0$ ($n = 3$–7). The roots were cooled from 20°C to 0°C with a 2°C min^{-1} cooling rate. The cooling was started 30 s after starting capture and stopped at 630 s. The temperature was maintained at 2°C from 630 s to the end. Note that on August 4, 2015, the temperature was changed from 20°C to 2°C.

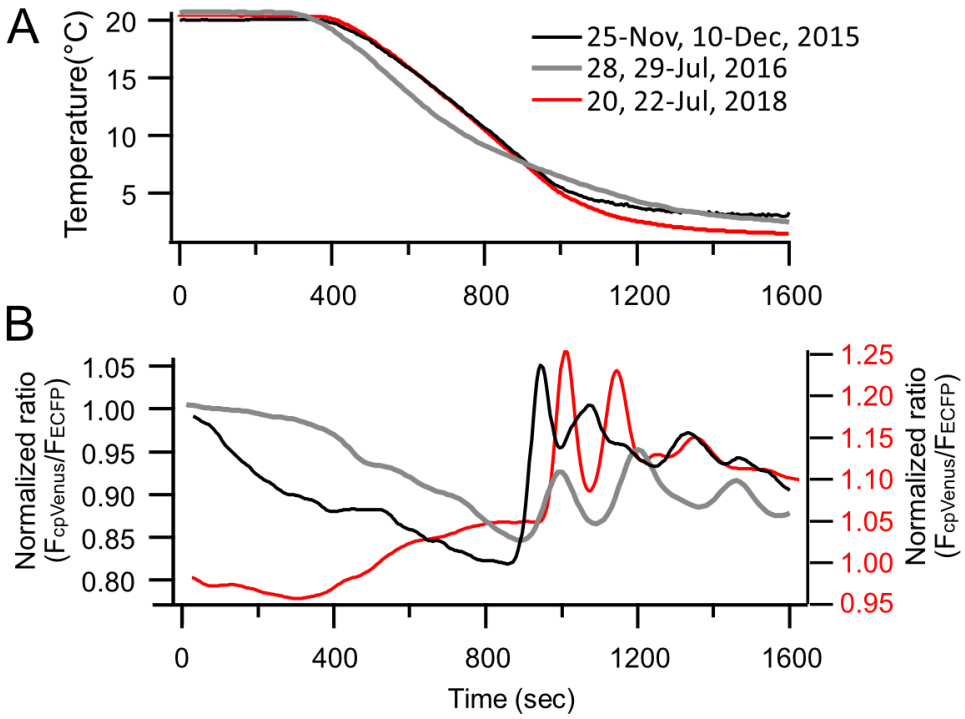

Figure 5.3. Ca^{2+} signal of leaves in winter and summer. (A) Two-week-old whole plants were cooled in the cryochamber of a microscope. The cryomicroscope for the leaves consisted of a confocal microscope, cooling circulator (Ministat 230 with Pilot ONE; Huber Kältemaschinenbau GmbH, Germany), glass-jacketed beaker [Asahi Glassplant Inc (as a cooling chamber)], objective inverter, adjustment cylinder (to extend the objective inverter), and iron plate. Temperature changes in the medium and air near the aerial part of the plant were measured by a thermocouple data logger (MCR-4TC; T&D Co., Japan) and averaged. (B) The Ca^{2+} signals of the fifth leaf were observed in each plant on 28 and 29 Jul 2016, 25 Nov and 10 Dec 2015, and 20 and 22 Jul 2018. The plants were sprayed with 0.05% Triton X-100 1 h prior to observation only on 20 and 22 Jul 2018. Because the microscope settings and treatments (spray and cooling setting) were different, the data for 20 and 22 Jul 2018 are shown using the second y axis (right). Fluorescence images were captured every 5–10 s (n = 4–5).

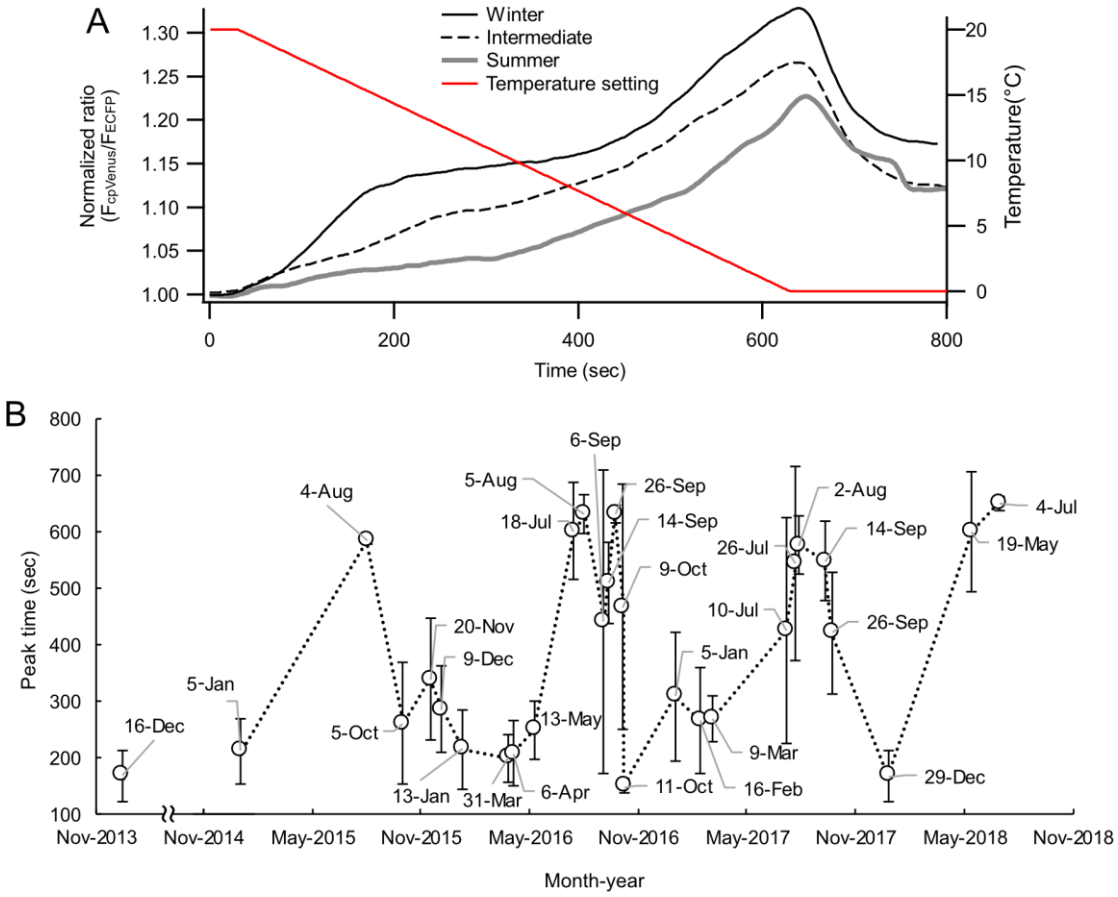

Figure 5.4. Overview of seasonal changes of Ca^{2+} signals in root cells. (A) Averaged winter-type, summer-type and intermediate-type Ca^{2+} signals. Each day the averaged Ca^{2+} signals shown in Fig 2, except for those from August 4, 2015, were averaged for each Ca^{2+} signal type (n = 7–10). (B) The first peak time of each experiment from December 16, 2013 to May 19, 2018 (n = 3–7). Error bars indicate SD.

A

Day of the experiment	Peak time (sec)	SD of peak time	Type of the Ca^{2+} signal	Cumulative solar radiation (MJ/m^2)
2013/12/16	167.4	45.1	Winter	30.4
2015/1/5	210.2	56.6	Winter	45.7
2015/8/4	573.3	6.6	Summer	131.6
2015/10/5	257.5	106.2	Intermediate	108.4
2015/11/20	333.1	105.5	Intermediate	44.9
2015/12/9	281.0	74.8	Intermediate	45.3
2016/1/13	212.4	69.5	Winter	54.0
2016/3/31	196.8	40.0	Winter	112.9
2016/4/6	205.1	56.8	Winter	93.0
2016/5/13	245.7	49.4	Winter	106.7
2016/7/18	590.5	84.3	Summer	110.2
2016/8/5	618.5	34.0	Summer	142.7
2016/9/6	433.8	263.1	Intermediate	121.6
2016/9/14	500.0	69.3	Intermediate	76.7
2016/9/26	619.3	16.4	Intermediate	82.4
2016/10/9	459.1	211.7	Intermediate	75.0
2016/10/11	150.2	12.0	Winter	71.4
2017/1/5	304.7	111.4	Winter	36.8
2017/2/16	261.4	91.0	Intermediate	61.3
2017/3/9	266.1	39.8	Winter	77.6
2017/7/10	417.8	194.5	Summer	144.1
2017/7/26	534.3	169.2	Intermediate	89.7
2017/8/2	565.8	51.0	Summer	124.0
2017/9/14	537.7	69.3	Summer	93.3
2017/9/26	414.4	105.1	Intermediate	108.5
2017/12/29	166.4	44.8	Winter	39.3
2018/5/19	589.4	103.9	Summer	96.8
2018/7/4	638.2	11.0	Summer	128.4

B

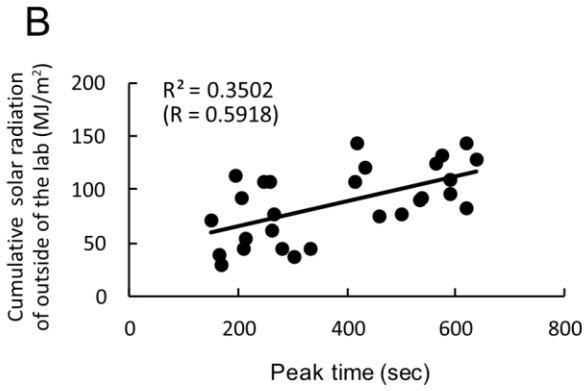

Figure 5.5. Outside solar radiation and Ca^{2+} signaling. (A) Each peak time and its standard deviation of the Ca^{2+} signals was extracted from the data set which are used in Figure 5.2. The cumulative solar radiation value includes solar radiation during 7 days of growth were calculated from the data base of Japan Meteorological Agency. (B) The correlation between the cumulative solar radiation and the peak Ca^{2+} signal time.

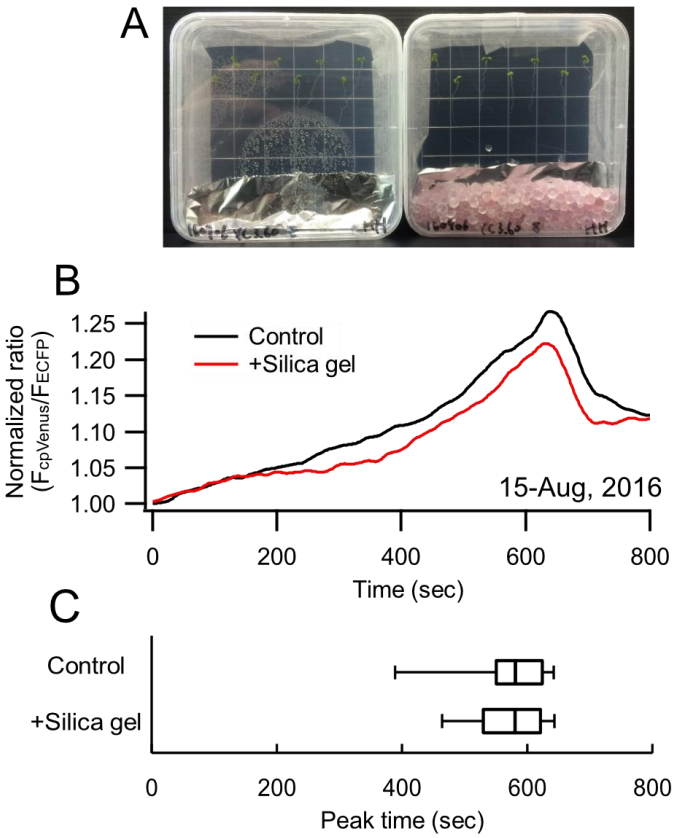

Figure 5.6. Effect of humidity on cold-induced Ca^{2+} signals in Arabidopsis roots on August 15, 2016. (A) Fifteen grams of silica gel balls were put into the petri dish (right) to reduce the humidity. (B) Averaged Ca^{2+} signals with or without silica gel (n = 4). (C) Boxplots were used to indicate the timing of the Ca^{2+} signal peaks. The boxplots present the first to the third quartile values, and the bars represent the minimum and maximum values (n = 4). Significant differences between each data set were analyzed using the t-test (*$p < 0.05$).

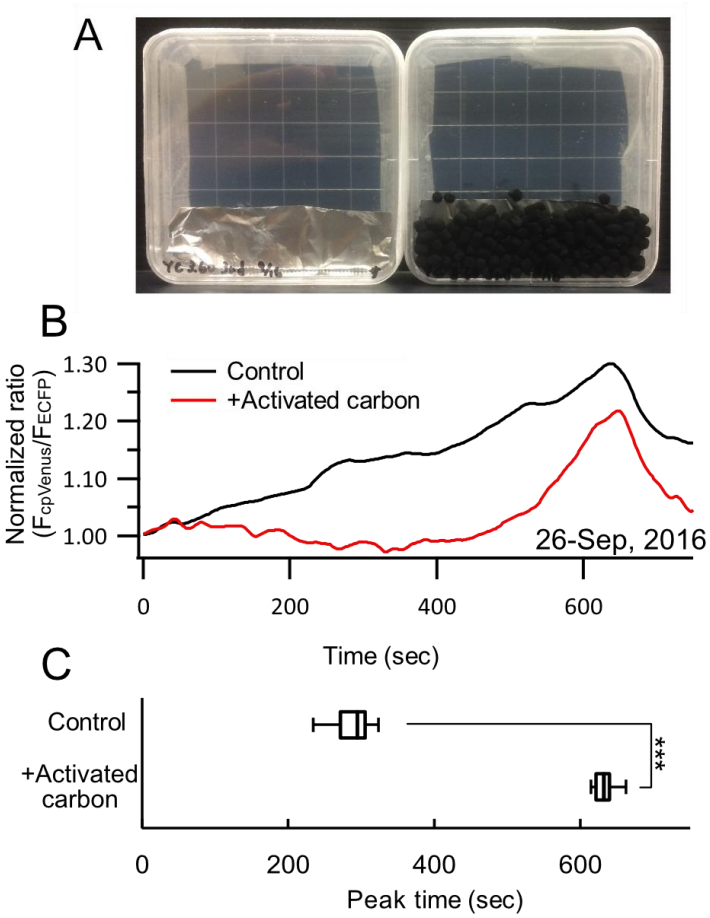

Figure 5.7. Effects of the activated carbontips on cold-induced Ca^{2+} signals in Arabidopsis roots on September 26, 2016. (A) Fifteen grams of activated carbon tips were put into the petri dish (right) to reduce the chemicals in the air. (B) Averaged Ca^{2+} signals with or without activated carbon (n = 4–5). (C) Boxplots indicate the timing of the Ca^{2+} signal peaks. The boxplots present the first to the third quartile values, and the bars represent the minimum and maximum values (n = 4–5). Significant differences between each data set were analyzed using the t-test (***$p < 0.001$).

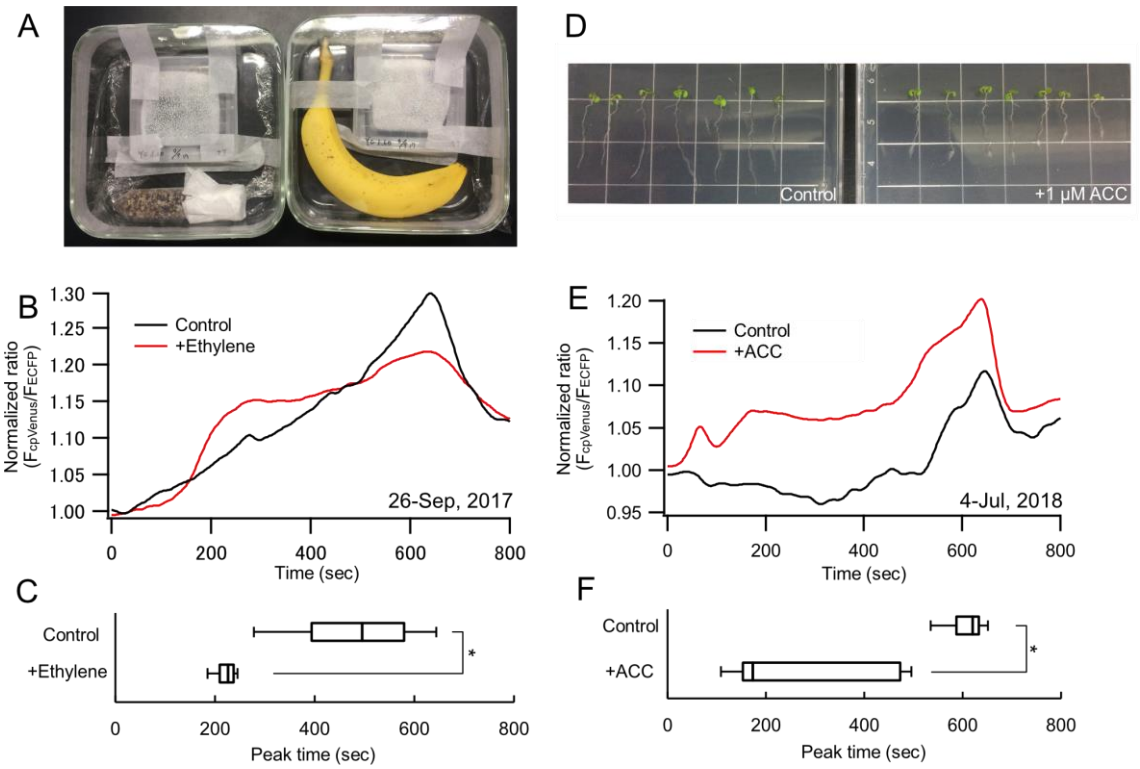

Figure 5.8. Effect of ethylene on cold-induced Ca^{2+} signals in Arabidopsis roots. (A) Seven-day-old Arabidopsis seedlings were packed with banana in a glass box for 2 days. (B) Averaged Ca^{2+} signals with or without banana on September 26, 2017 ($n = 4$). (C) Boxplots indicate the timing of the Ca^{2+} signal peaks. The boxplots present the first to the third quartile values, and the bars represent the minimum and maximum values ($n = 4$). Significant differences between each data set were analyzed using the *t*-test ($*p < 0.05$). (D) Seven-day-old Arabidopsis seedlings were transferred to Hoagland's medium in the presence or absence of 1 μM ACC and grown for one day. (E) Averaged Ca^{2+} signals with or without ACC treatment on July 4, 2018 ($n = 5$). (F) Boxplots indicate the timing of the Ca^{2+} signal peaks ($n = 5$). Significant differences between each data set were analyzed using the *t*-test ($*p < 0.05$).

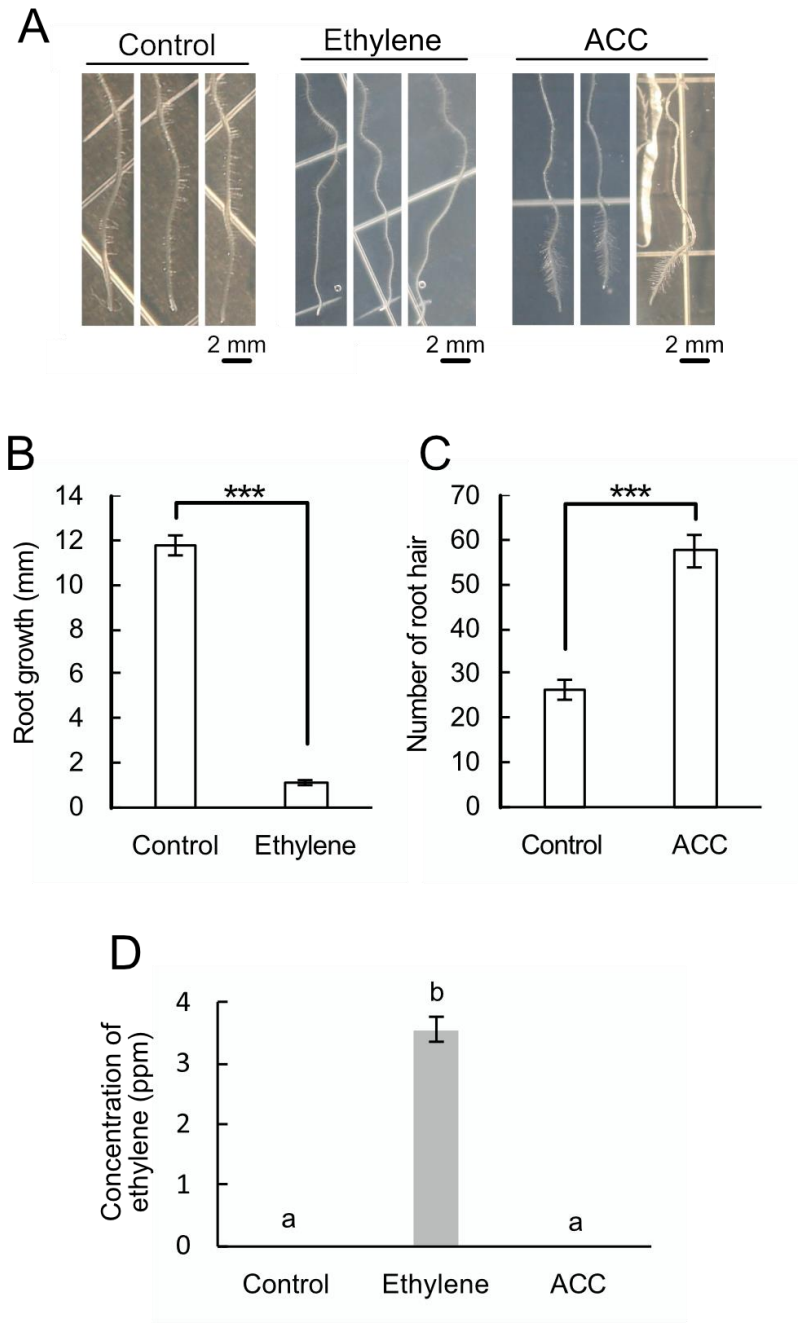

Figure 5.9. Effect of ACC and ethylene treatments. (A) Morphological change of the root before and after ACC or ethylene treatments. (B) Root growth during two days in control and ethylene treated plants. Significant differences between each data set were analyzed using the *t*-test (***$p < 0.001$) ($n = 15$–19). (C) The number of root hair within 10 mm from the root cap in control and ACC treated plants ($n = 13$) (D) Concentration of ethylene was measured in each petri dish by using a gas chromatography. Significant differences between each data set were analyzed using the *Tukey-test*. Different letter indicates significant difference ($p < 0.001$) ($n = 3$).

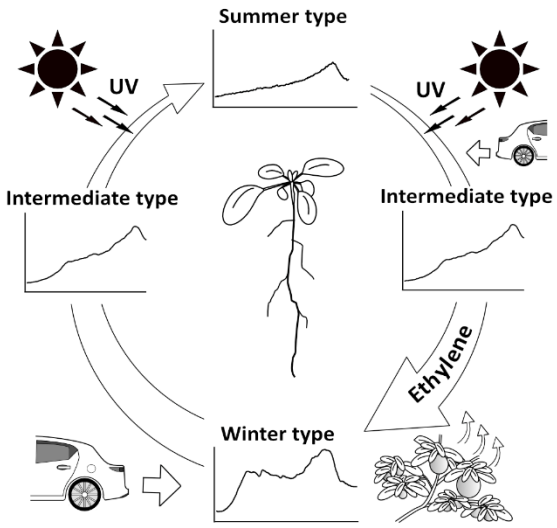

Figure 5.10. Seasonal changes of the calcium signal type and concentration of ethylene in the atmosphere.

Chapter 6

Soft X-ray Spectromicroscopy: A Versatile Tool to Probe Plant Ion Distribution

Abstract

Cell wall acts as barriers to biotic and abiotic stresses. Ca^{2+} forms the cross linkage between pectins and increases the freezing tolerance. In addition, the extracellular space, between cell walls, is Ca^{2+} pool of plants. Vacuole is the largest and important intracellular Ca^{2+} pool in plant cells. To study the change of the accumulation level of Ca^{2+} in the Ca^{2+} pools before and after the cold acclimation (CA) treatments, the soft X-ray spectromicroscopy beamline at the Canadian Light Source equipped with a state-of-the-art Scanning Transmission X-ray Microscope (STXM) was used. This is the first study to map Ca^{2+} and biopolymers in the epidermal layers of Arabidopsis using STXM. Three Arabidopsis accessions showed the different accumulation change of Ca^{2+} after 2°C of conventional CA (conv.–CA) and the temperature fluctuating cyclic CA (FC–CA). The conv.–CA treatment induced the Ca^{2+} accumulation in the extracellular space and vacuole, where are the main Ca^{2+} pools. It is considered that the influx of Ca^{2+} channel may be enhanced by increasing the osmolarity difference between cytosol and Ca^{2+} pools. In addition, Ca^{2+} channel blockers, $LaCl_3$ and ruthenium red, were sprayed to investigate the role of Ca^{2+} signals for the Ca^{2+} accumulation. The Ca^{2+} channel blockers tended to decrease the Ca^{2+} accumulation after conv.–CA treatment, but increased after FC–CA. These results suggest that the cooling without the Ca^{2+} signals may induce the Ca^{2+} accumulation in the extracellular space and the vacuole to fix the Ca^{2+} signaling. Taken together, plants might adapt Ca^{2+} signaling to the ambient temperature by regulating the Ca^{2+} concentration in the Ca^{2+} pools.

Introduction

The cell wall and cuticular layer are the barriers to several biotic and abiotic stresses. For example, plant in temperate zone, ice formation occurs in extracellular space (apoplast) (Levitt, 1980). Ice formation also causes dehydration stress due to subsequent water migration from the symplast to the apoplast along its vapour pressure deficit. Thus, the cell wall acts not only as a barrier to the mechanical stress of ice propagation, but also as a barrier to water loss (Rajashekar and Burke, 1996) and may also have relevance to chilling injury (Bilska-Kos *et al.,* 2017). It is known that cold temperature induces changes of the cell wall improving the ability of plants to resist extracellular freezing (Solecka *et al*., 2008). In cell wall formation, Ca^{2+} forms cross linkages to the free carboxyl groups of acidic pectin residues under the catalysis of pectin methylesterase (Hepler, 2005). In addition, plants trigger the membrane resealing mechanism which involves Ca^{2+}-dependent SYT1 function in freezing and thawing (Yamazaki *et al.*, 2008). Furthermore, the extracellular space (i.e., between cell walls) is one of the main Ca^{2+} pools for the Ca^{2+} signals which act as a second messenger in cold acclimation process. Therefore, Ca^{2+} is largely involved in cold acclimation processes and enhancement of freezing tolerance. I here present a novel synchrotron-based mapping technique to investigate Ca^{2+} distribution in the apoplast and symplast of *Arabidopsis* leaf tissues.

Traditionally, scanning electron microscope (SEM) and transmission electron microscope (TEM) are used to study the presence of Ca^{2+} (Łabuz *et al.*, 2016) and Ca^{2+} crystal formation (Nakata, 2012) in *Arabidopsis* leaves at high spatial resolution. However, electron microscopy techniques require dehydration of the leaf samples through washing with alcohols and precipitation of Ca^{2+} with chemicals, both these procedures affect the quantitative and localization information.

Soft X-ray spectroscopy coupled with nano-scale microscopy has been shown to have advantages to study plant biopolymers and their distribution at sub-cellular resolution (~25 nm) (Karunakaran *et al,* 2015). The soft X-ray spectromicroscopy (SM) beamline at the Canadian Light Source (CLS) is equipped with a state-of-the-art scanning transmission X-ray microscope (STXM) that combines high resolution microscopy (25 nm) with X-ray absorption spectroscopy (XAS) from 130 to 2700 eV, enabling unique capabilities to study plant cell components and Ca^{2+} accumulation in the extracellular space. However, most plant cell walls are tens of microns in size and therefore, too thick for soft X-ray spectromicroscopy at the carbon and Ca^{2+} edges. Usually the samples are embedded in resins and cross-sectioned to 100 nm thick following similar protocols to electron microscopy.

In this study, I present a novel approach to study Ca^{2+} localization and quantification in *Arabidopsis* leaf cells using the STXM at 20 nm spatial resolution. To my knowledge, this is the first study to map Ca^{2+} and biopolymers in the epidermal layers of *Arabidopsis* using STXM.

Materials and Methods

Plant materials

Three *Arabidopsis thaliana* accessions were used: Columbia (Col-0), Frickhofen (Fl-3), and Kashmir (Kas-1). These plants were grown in petri dishes with modified Hoagland's nutrient solution with 1% agar (Uemura *et al*., 1995) at 23°C under a 16-h photoperiod (photon flux rate: 70 µmol m^{-2} s^{-1}) for 2 weeks. Col-0 was established in USA, Fl-3 is native to Finland, and Kas-1 is from Kashmir, India.

Acclimation treatments

Two types of CA treatments were used. One was the conventional constant 2°C of CA treatment (conv.–CA) (Figure 4.2: black line). In the other treatment, day-and-night temperature cycles were generated. In addition, the temperature fluctuated at approximately 10°C with an amplitude of 1°C in the daytime. One cycle of the temperature fluctuation took approximately 10 min, and the nighttime temperature was kept at a constant 2°C (Figure 4.2: gray line). This acclimation treatment was named temperature fluctuating cyclic CA (FC–CA). In both treatments, the photoperiod was 12 h (6:00–18:00).

Measurement of Ca^{2+} accumulation

Epidermal layers of the leaves harvested from *Arabidopsis* plants grown in agar solution in a petri dish (Figure 6.1a) were peeled using forceps (both from the abaxial and adaxial sides) of the three accessions (Col-0, Fl-3 and Kas-1) used in the study. The epidermal layers were floated on water, transferred onto the TEM grids (Figure 6.1b) and mounted into the STXM sample holder. The air inside STXM chamber was replaced by He since evacuating the air through the roughing pump ruptured the hydrated or partially air-dried cells on the TEM grids. A region of interest was chosen by selecting a single layer of intact cells (Figure 6.1c) and two images, one before Ca^{2+} absorption (350.5 eV; Figure 6.2a) and one on the absorption peak of Ca^{2+} (352.4 eV; Figure 6.2b) were recorded at 100 nm resolution from 30 µm area per sample and two biological replicates were used in the study.

Results and Discussion

Role of Ca^{2+} accumulation in the extracellular space and the vacuole

Since there was no significant difference in accumulation level of Ca^{2+} between adaxial side and abaxial side of the leaf (Hiraki *et al*., 2018; Figure 6.3), abaxial side was used for further experiment to compare among the three accessions including Col-0 which cannot peal the adaxial side. The accumulation level of Ca^{2+} were measured in the extracellular space and the cytoplasm in three *Arabidopsis* accessions, Fl-3, Col-0, and Kas-1. Since the major part of the epidermal cells is vacuole (see Endler et al., 2006), the results of cytoplasm tend to indicate the Ca^{2+} accumulation level in vacuole. Thus, the results indicate the Ca^{2+} accumulation level in two major Ca^{2+} pools, the extracellular space and the vacuole.

After 4 days of conv.–CA treatment, the three accessions tended to increase the accumulation level of Ca^{2+} in the extracellular space and the vacuole (Figure 6.4). FC–CA tended to increase the accumulation level of Ca^{2+} only in Kas-1, but decreased in FL-3 and Col-0 in both extracellular space and vacuole (Figure 6.4). However, there was no significant difference among these three accessions and acclimation treatments in the accumulation level of Ca^{2+}. Since it takes long time to observe one sample by the synchrotron, the repeat number was small and make it difficult to show the significant difference.

Ca^{2+} plays an important role in determining the structural rigidity and stabilization of the cell wall (Wyn Jones and Lunt, 1967; Burström, 1968) through forming Ca^{2+} bridges with pectin molecules (Chang *et al*., 1995). Suutarinen *et al.* (2000) showed that, $CaCl_2$ pre-freezing treatments stabilized the pectin in strawberry tissues. Since the cell wall acts as barrier for ice propagation and the water loss (Rajashekar and Burke, 1996), the accumulation level of Ca^{2+} in the cell wall might be a kind of indicators of the freezing tolerance. Therefore, results of the weaker freezing tolerance in FC–CA than that of conv.–CA (Figure 4.7) is consistent with the accumulation level of the Ca^{2+} (Figure 6.4).

To investigate the role of Ca^{2+} signals during the cold acclimation treatments in the Ca^{2+} accumulation, the Ca^{2+} channel blockers, $LaCl_3$ and ruthenium red (RR), were sprayed. Only Col-0 was used for the experiment with the Ca^{2+} channel blockers. In 4 days of conv.–CA treatment, the Ca^{2+} channel blockers tended to decrease the Ca^{2+} accumulation in the extracellular space and vacuole, and there was a significant difference in vacuole between the control plant and the Ca^{2+} channel blockers treated plant (Figure 6.5). Despite $LaCl_3$ and RR do not chelate Ca^{2+} directly, these chemicals decreased the accumulation level of Ca^{2+} in both extracellular space and vacuole. Therefore, the transient cytosolic Ca^{2+} increase which is induced by the initial temperature change of conv.–CA treatment might contribute the

accumulation of Ca^{2+} in vacuole through the restoring of Ca^{2+} (Jian *et al.*, 1999). On the other hand, there is a possibility that low temperature (e.g., 2°C) induces the increase of Ca^{2+} accumulation independent from the Ca^{2+} signaling.

In the 4 days of FC–CA treatment, the Ca^{2+} channel blockers tended to increase the Ca^{2+} accumulation in the extracellular space and the vacuole, and there was a significant difference in the Ca^{2+} accumulation in the extracellular space (Figure 6.5). The different effect of the Ca^{2+} channel blockers in conv.–CA and FC–CA might be caused by the different Ca^{2+} signal. In conv.–CA, one large Ca^{2+} signal was induced just after the conv.–CA treatment started (Figure 3.9j, k). On the other hand, temperature fluctuation like FC–CA induce many small Ca^{2+} signals (Figure 3.9h, i), and the Ca^{2+} signals were inhibited by the Ca^{2+} channel blockers (Figure 3.14). If the chemicals block the Ca^{2+} channels, the concentration of Ca^{2+} in the cytosol does not increase; and therefore, the plant might increase the accumulation level of Ca^{2+} in the Ca^{2+} pools (i.e., extracellular space and vacuole) to fix the disturbed Ca^{2+} signals by increase the osmolarity difference between cytosol and Ca^{2+} pools as a kind of the feedback of Ca^{2+} signaling in FC–CA treatment.

The experimental system

Even in the "cytoplasm part" of the images in this experiment, it was including the cell wall of the surface and undersurface of the epidermal cells. To obtain the accurate intensity of the Ca^{2+} accumulation of the cytoplasm, the background should be removed. For example, EGTA treatment may decrease the accumulation level of Ca^{2+} in the cell wall. The difference between this value and the control is background. Then I can obtain the accurate values of accumulation level of Ca^{2+} in the cytoplasm region. In addition. the area of the extracellular space and cytoplasm was separated by using the function of the threshold (Figure 6.2d, e). Since the concentration of Ca^{2+} was similar between the extracellular space and the vacuole, the value of threshold was decided depending on the bright field images in this study. If I can separate the smaller region such as the cytosol by using the better method, it leads a more detailed discussion with more information.

Conclusion

I developed the experimental methods to measure the accumulation level of Ca^{2+} in the extracellular space and vacuole in the epidermal cells of Arabidopsis. The results suggested the possibilities that: (1) the accumulation change of the Ca^{2+} in the extracellular space and the vacuole may be different among the accessions; (2) the accumulation level of Ca^{2+} pools might be mediated by the cold-induced Ca^{2+} signals or low-temperature; and (3) there may be the

feedback between Ca^{2+} accumulation in the pools and Ca^{2+} signaling.

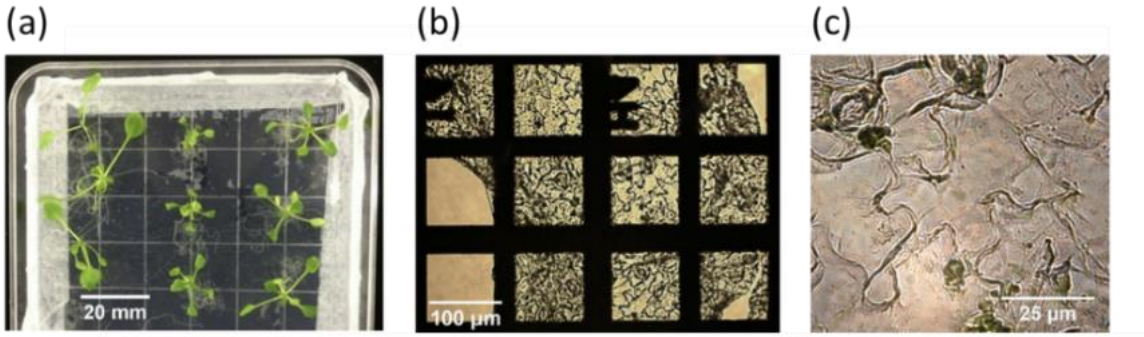

Figure 6.1. Materials and observation. (a) Arabidopsis accessions Fl-3, Col-0 and Kas-1 were grown in the petri dish with agar medium. (b) The epidermal cell layer was put on the TEM grids (SPI; 200 mesh). (c) Intact single cell layer was chosen under the optical microscope.

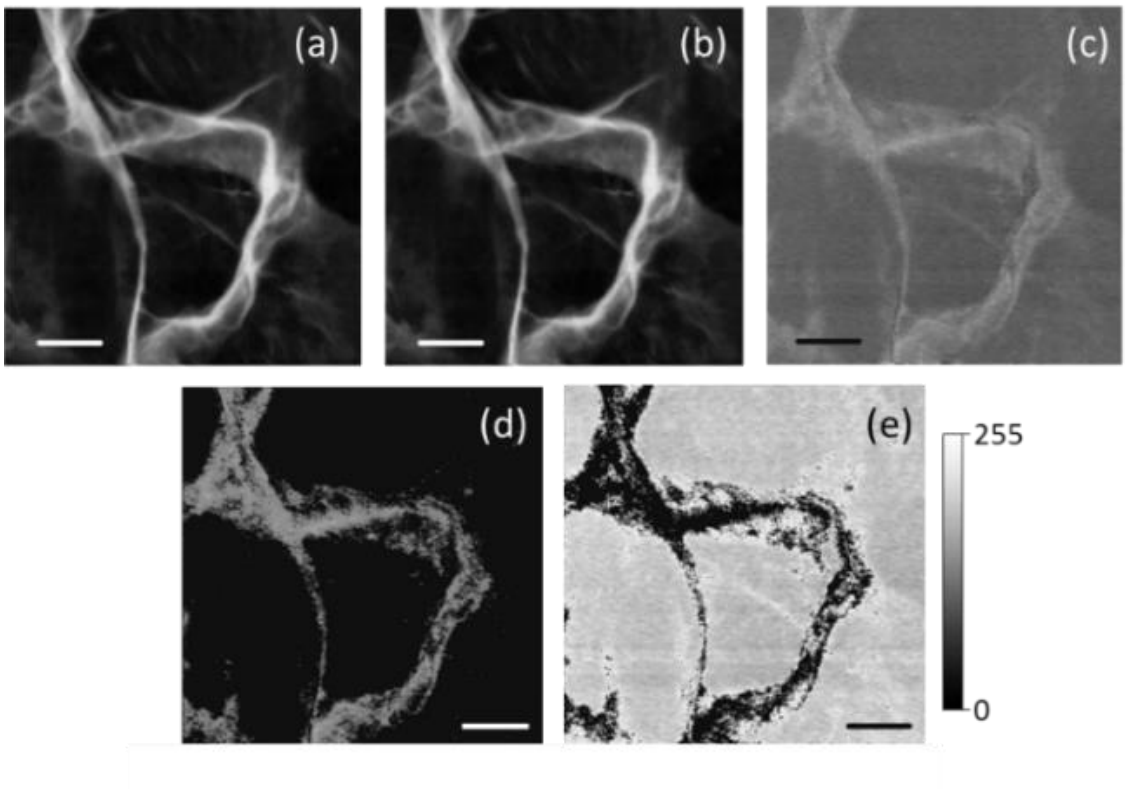

Figure 6.2. STXM image analysis. (a) The image of before Ca^{2+} absorption (350.5 eV). (b) The image of absorption peak of Ca^{2+} (352.4 eV). (c) The difference between the before absorption and absorption peak of Ca^{2+}. (d) The map of Ca^{2+} on the extracellular space. The intensity shows the density of Ca^{2+}. (e) The map of Ca^{2+} in cytoplasm (vacuole). Each region of the extracellular space and cytoplasm (vacuole) were respectively separated by the "generate mask" function (aXis2000, IDL). Each scale bar indicates 5 μm.

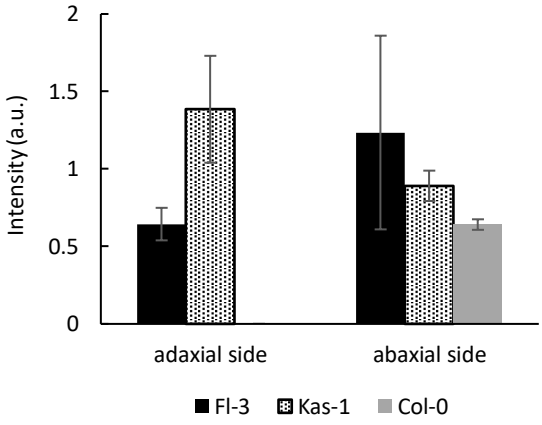

Figure 6.3. Ca^{2+} density of cell wall in peeled epidermal cells from the abaxial and adaxial sides in three accession (Fl-3, Col-0 and Kas-1). Error bar indicate SE. n = 2.

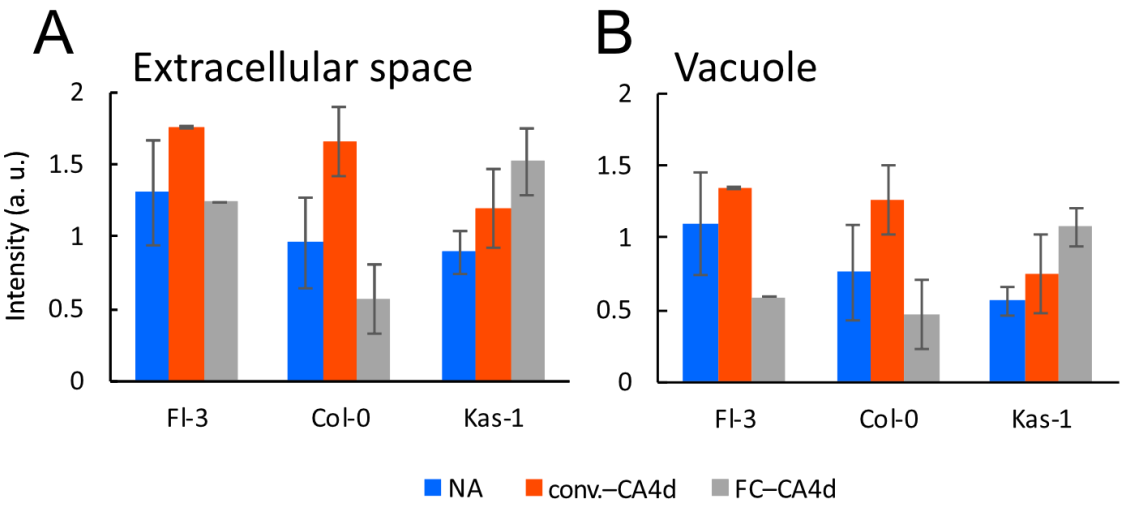

Figure 6.4. Ca^{2+} accumulation level in extracellular space and vacuole in three *Arabidopsis* accessions. Non-acclimated plant (NA), 4 d of conventional cold acclimated plant (conv.–CA4d) and 4 d of the temperature fluctuating cyclic cold acclimation (FC–CA) were used. (A) Ca^{2+} accumulation level which was calculated from the cell wall. (B) Ca^{2+} accumulation level which was calculated from the cytoplasm area. The statistical analysis was performed by using the Turkey-test. Error bars indicate SE (n = 3).

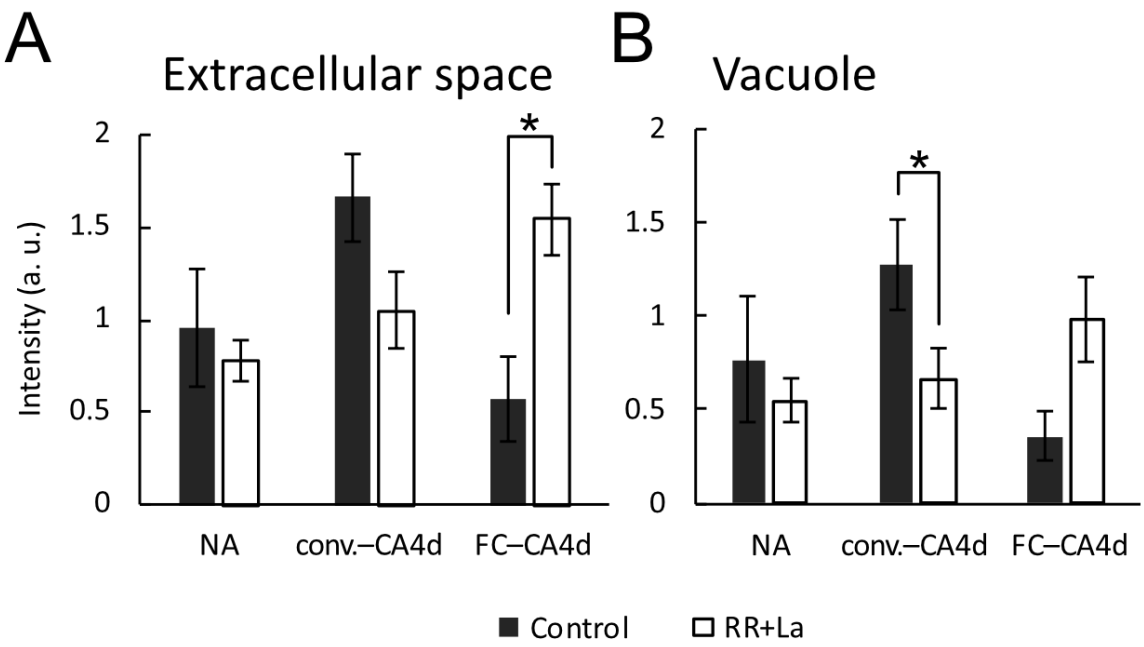

Figure 6.5. Ca^{2+} accumulation level in extracellular space and vacuole in Col-0 with the Ca^{2+} channel blockers. Non-acclimated plant (NA), 4 d of conventional cold acclimated plant (conv.–CA4d) and 4 d of the temperature fluctuating cyclic cold acclimation (FC–CA) were used to investigate the effect of the Ca^{2+} channel blockers, 50 μM ruthenium red (RR) and 1 mM $LaCl_3$ (La) (A) Ca^{2+} accumulation level which was calculated from the cell wall. (B) Ca^{2+} accumulation level which was calculated from the cytoplasm (vacuole) area. Significant difference between each data was analyzed by using a t-test (*$p < 0.05$) Error bars indicate SE ($n = 3$).

Chapter 7

General discussions

Advantage and originality of Ca^{2+} signal observation

Small range of cooling and slow cooling rate

The Ca^{2+} signal observation under field-like condition was succeeded in this study. I used the temperature change of 20~16~20ºC cycle with a cooling rate of 0.47ºC/min (Figure 3.9h, i). There has been no information on Ca^{2+} signal behavior associated with CA in the field. A few reports have shown that the cold shock induced the transient Ca^{2+} increase (Knight *et al*., 1997; Plieth *et al*., 1999, Knight and Knight, 2000). These results, though the conditions of cold shock (i.e., cooling very rapidly) never happen in the field, have supported that Ca^{2+} signals can be used as a second messenger for cold sensing in plants. To experimentally consider the role of the Ca^{2+} signals during CA in the field, I examined Ca^{2+} signals at the 0.47ºC/min of cooling rate, and succeeded in observing the occurrence of Ca^{2+} signal under this condition (Figure 3.9h, i). This result simply supports the hypothesis that Ca^{2+} signal is induced in the field.

Plieth *et al*. (1999) used several patterns of the cooling, and the minimum cooling was 4ºC cooling with 4ºC min^{-1} of cooling rate. They observed the transient Ca^{2+} signals by each cooling. On the other hand, I succeeded in observing the Ca^{2+} signal in the 1ºC cooling with 4ºC min^{-1} in root cells (Figure 3.7) and 4ºC cooling with about 0.5ºC min^{-1} in leaf cells (Figure 3.9). The cyomicroscopic system I developed which can control the temperature accurately following the program allows the smaller range of cooling and slower cooling rates compared with the previous studies. Furthermore, by performing the temperature correction, I could detect the hidden Ca^{2+} signal peaks caused by the small range of cooling and slow cooling rates (see Chapter 2). Besides, since I used the intact plants for the Ca^{2+} signal observation, the artifact effect may be reduced compared with the experiments by Plieth *et al*. (1999).

Direct observation of the effect of the Ca^{2+} channel blockers

It had been reported that the expression of *CBF/DREB1s* genes were regulated by calmodulin-binding transcription activator (Doherty *et al*., 2009; Kidokoro *et al*., 2017). They suggested that Ca^{2+} signals may mediate the expression of the cold responsive genes through calmodulin. However, these reports lack to show evidence of the direct connection between Ca^{2+} signals (which are induced under the field or the artificial cooling) and the *CBF/DREB1s* gene expression. In this aspect, I provided evidences **i)** the Ca^{2+} signals under field-like condition in the leaf (Figure 3.9h, i) for the first time in leaf cells, **ii)** the effect of Ca^{2+} channel blocker on Ca^{2+} signals (Figures 3.13 and 3.14), **iii)** the inhibition of *CBF/DREB1s* gene expression in the field by the channel blockers (Figure 3.15), and **iv**) the enhancement of *CBF/DREB1s* gene expression through the Ca^{2+} signals under temperature fluctuations (Figure

3.16). These results support the hypothesis that Ca^{2+} signals are used to regulate the cold acclimation process in the natural environment.

Eighteen facts in cold-induced Ca^{2+} signal in plant cells

1. The Ca^{2+} signal is induced by the cooling.
2. Continuous cooling is needed to sustain the Ca^{2+} signal.
3. The faster cooling rate induces the shorter time interval between Ca^{2+} signal peaks in root and leaf cells, and larger Ca^{2+} signal peaks in root cells.
4. In root cells, two peaks are induced by the continuous cooling (e.g., 20ºC to −10ºC).
5. In leaf cells, three peaks are induced by the enough cooling duration.
6. In root cells, the latent phase of the Ca^{2+} signal is longer in the lower start temperature.
7. In leaf cells, the latent phase of the Ca^{2+} signal turns to the increase phase just after the cooling rate starts to decrease from its maximum value.
8. In root cells, the basic shape of the Ca^{2+} signal is the same if the cooling range is the same.
9. In leaf cells, the basic shape of the Ca^{2+} signal is the same if the cooling duration is the same.
10. The first peak of the Ca^{2+} signal is composed of the Ca^{2+} influx from extracellular, and the second and the third peak of Ca^{2+} signal are composed of the Ca^{2+} efflux from the intracellular pool.
11. $LaCl_3$ can decrease the height of the first peak of Ca^{2+} signal in root cells, and tends to decrease all peaks in leaf cells.
12. Ruthenium red can decrease the all Ca^{2+} signal peaks halfway.
13. Even if the latent phase is delayed, the first peak of the Ca^{2+} signal is mainly composed of the influx of Ca^{2+} from extracellular space.
14. One Ca^{2+} signal peak is composed of the Ca^{2+} influx and efflux through several Ca^{2+} channels.
15. Changes in plant responsiveness to low-temperature depend on the ambient temperature.
16. In root cells, the first peak of Ca^{2+} signal appears only in the winter season.
17. Root can sense 1ºC of cooling with 2ºC min^{-1} of cooling rate.
18. Leaf can sense 4ºC of cooling with about 0.5ºC min^{-1} of cooling rate.

Detailed explanation of the 18 facts of cold-induced Ca^{2+} signal in plant cells

1. **The Ca^{2+} signal is induced by the cooling.**
2. **Continuous cooling is needed to sustain the Ca^{2+} signal.**

It had been reported that the cold-shock and low-temperature treatment induced Ca^{2+} signal (Knight *et al*. 1991; Plieth *et al*., 1999; Knight and Knight, 2000; Nagel-Volkmann *et al*., 2009; Krebs *et al*., 2012). I also confirmed this in both root and leaf cells in Arabidopsis by using many cooling regimes in chapter 3. In previous studies, they focused on the cooling rate and Ca^{2+} signals, but did not focus on after stopping the cooling. I showed that the cooling stoppage decrease Ca^{2+} signal not depending on the prior condition in both root and leaf cells (Figures 3.2, 3.4, 3.7, 3.9 and 3.10). Since the cryochamber could not stop the cooling immediately like the cryostage (Figure 3.9b, e), I could not stop cooling in the middle of the first and second peaks in leaf cells (Figure 3.9d-f). However, the heating decreased Ca^{2+} signal in leaf cells (Figure 3.9h, i) as well as in root cells (Figure 3.7). The reason why nobody showed the effect of stoppage of cooling may be that no one could stop the cooling accurately. As plants can sense temperature changes very accurately, it is thought that Ca^{2+} signal stops by sensing the changing of the temperature change rate from minus to plus. Because Ca^{2+} signal is a messenger that conveys complex temperature changes, observing the Ca^{2+} signal shows "how plants sense cold".

3. **The faster cooling rate induces the shorter time interval between Ca^{2+} signal peaks in root and leaf cells, and larger Ca^{2+} signal peaks in root cells.**

It had been reported that the faster cooling induced the larger peak height of Ca^{2+} signal in Arabidopsis and wheat (Plieth *et al*., 1999; Nagel-Volkmann *et al*., 2009). I found that the faster cooling rate induced shorter time interval between first and second peak in root and leaf cells (Figures 3.4g and 3.10d). By combining the first and the second Ca^{2+} peak, plant makes a large Ca^{2+} peak and might induce the gene expression to the rapid cooling.

4. **In root cells, two peaks are induced by the continuous cooling (e.g., 20ºC to −10ºC).**

Since the cooling stoppage decreases the Ca^{2+} signal immediately, the second peak of the Ca^{2+} signal in root started to decrease due to the stopping of the cooling in Figure 3.2. But when the plants were cooled from 20ºC to −10ºC, the second peak of Ca^{2+} signal appear during the cooling (at about −5ºC) (Figure 3.5). Since the cooling rate changes the duration of Ca^{2+} signal, but did not changed the basic shape (Figure 3.4), the cooling range is important for inducing the second peak of Ca^{2+} signal in root cells. It meant that a 25ºC of

continuous cooling range is needed to induce the full cold-induced Ca^{2+} signal in root cells not depending on the cooling rate. On the other hand, such a large and continuous cooling does not occur in the field. Therefore, this Ca^{2+} signal is just the result in the laboratory.

5. **In leaf cells, three peaks are induced by the enough cooling duration.**

The enough duration of cooling induced the peaks of the three Ca^{2+} signals not dependent on the cooling range and the cooling rate in leaf cells (Figures 3.9d-f and 3.10). Both the cooling of 20 to 2.5ºC and 12 to 1.5ºC induced three Ca^{2+} signal peaks in leaf cells (Figure 3.9d-f). Besides, all three cooling rates, 1.6, 0.85 and 0.47ºC min^{-1}, induced the three Ca^{2+} signal peaks in leaf cells (Figure 3.10). Therefore, only the cooling duration (continuous cooling) is important for inducing the three peaks in leaf cells.

6. **In root cells, the latent phase of the Ca^{2+} signal is longer in the lower start temperature.**
7. **In leaf cells, the latent phase of the Ca^{2+} signal turns to the increase phase just after the cooling rate starts to decrease from its maximum value.**

In root cells, Ca^{2+} concentration increases just after the temperature begins to fall. The latent phase is dependent on the absolute temperature of start temperature (Figure 3.2a-c, h, i). On the other hand, in leaf cells, the timing of Ca^{2+} signal increase is dependent on the time point where the cooling rate starts to decrease from its maximum value (Figure 3.9g). Campbell *et al*. (1996) reported that there was a difference in sensitivity to low-temperature between root and aerial part in Tobacco. They mentioned that aerial part needed the longer time to increase Ca^{2+} concentration. The reason may be the different switch to start Ca^{2+} concentration increase in root and leaf cells. Each characteristic of Ca^{2+} signal may indicate differences in cold sensing and freezing tolerance to optimize in different environment.

8. **In root cells, the basic shape of the Ca^{2+} signal is the same if the cooling range is the same.**
9. **In leaf cells, the basic shape of the Ca^{2+} signal is the same if the cooling duration is the same.**

Cooling rate changes the peak height and time interval between peaks of Ca^{2+} signal in root cells (Figure 3.4). Low-temperature induced the longer latent phase in root cells (Figure 3.2b, c, h, i). These two factors do not change the number of peaks, but if the cooling range is changed, the peak number and the peak height changed dramatically in root cells (Figures 3.2c and 3.7). By contrast, leaf cells have another characteristic. Cooling rate decides the length of the latent phase as mention above. Absolute temperature did not change anything. However, if the cooling duration is different, the three peaks were not

induced (Figure 3.9h, i). On the other hand, if the cooling duration is same, almost same shape of Ca^{2+} signal is induced even the cooling range and starting temperature are different each other (Figure 3.9d-f).

10. The first peak of the Ca^{2+} signal is composed of the Ca^{2+} influx from extracellular, and the second and the third peak of Ca^{2+} signal are composed of the Ca^{2+} efflux from the intracellular pool.

11. $LaCl_3$ can decrease the height of the first peak of Ca^{2+} signal in root cells; and tends to decrease all peaks in leaf cells.

12. Ruthenium red can decrease the all Ca^{2+} signal peaks halfway.

Knight *et al.* (2000) reported that $LaCl_3$, a Ca^{2+} channel blocker of plasma membrane, suppress the increase of the first peak of Ca^{2+} signal. In addition, Knight *et al*. (1992) and Monroy and Dhindsa (1995) have reported that RR acts as intracellular Ca^{2+} channel blocker. In my result, $LaCl_3$ decreased the height of the first peak of Ca^{2+} signal in both root and leaf cells (Figures 3.6 and 3.13). In leaf cells, $LaCl_3$ also tended to decrease the second and third peak (Figure 3.13). RR tended to decrease not only the second and the third peak of Ca^{2+} signal, but also first peak weakly in leaf cells (Figure 3.13). However, we should not decide the role and effect of the chemicals because the effect of these chemicals are not completely clear in plant cells. The important thing is that these chemicals can disturb the Ca^{2+} signals different way.

13. Even if the latent phase is delayed, the first peak of the Ca^{2+} signal is mainly composed of the influx of Ca^{2+} from extracellular space.

It has been reported that the first peak of Ca^{2+} signal is mainly composed of the influx of Ca^{2+} from extracellular (Knight and Knight, 2000). Lower-temperature caused the longer latent time and sometime the peak appears between the first and second peak which is induced by the cooling from room temperature (Figure 3.2b, c). But the delayed first peak due to the low-start-temperature also composed of the influx of Ca^{2+} from extracellular space (Figures 3.6 and 3.8). The second and the third peak may be composed of the Ca^{2+} efflux from intracellular pools. It has been reported that the slow vacuolar ion channels release Ca^{2+} from vacuoles depending on the increase in the cytosolic Ca^{2+} concentration (Ward and Schroeder, 1994; Bewell *et al*., 1999) Therefore, Ca^{2+}-induced Ca^{2+} channels may contribute the increase of the second and third peak of Ca^{2+} signals.

14. One Ca^{2+} signal peak is composed of the Ca^{2+} influx and/or efflux through several Ca^{2+} channels.

Cold-induced Ca^{2+} signal seems to have two or three peaks in root and leaf,

respectively. However, the analysis by the software IGOR pro indicated that even one peak contains a few peaks in it (Figure 3.3). This result suggests that several Ca^{2+} channels are contributing to make one Ca^{2+} peak. If each type of Ca^{2+} channel open and close depending on the specific condition, plant might encode the detailed temperature information into the Ca^{2+} signal.

15. Changes in plant responsiveness to cooling depend on the ambient temperature.

NA plants can increase Ca^{2+} concentration for the response to the cooling from 20°C. But after CA, they cannot increase the Ca^{2+} concentration. In contrast, NA plants cannot increase Ca^{2+} concentration in the cooling from 2°C, but CA plant can (Figure 3.7). These results suggest that plant changes its cold responsiveness to cooling regarding to Ca^{2+} signals dependent on the ambient temperature. One of the candidates which change plant cold responsiveness depending on the ambient temperature is membrane fluidity. Benzyl alcohol and dimethyl sulfoxide were used to increase or decrease the membrane fluidity, and reproduce the fluidity of the plasma membrane before and after the CA treatment, but the cold responsiveness to the cooling did not change in the most cases based on the Ca^{2+} signals (Figure 7.1). The increase in membrane fluidity in NA plants induced the CA plant-like Ca^{2+} signals by the cooling from 20ºC to 16ºC (Figure 7.1C), and showed the faster increase of Ca^{2+} signals to the cooling from 2 ºC to −2 ºC, but the peak height was not so high as actual CA plants (Figure 7.1E). On the other hand, the decrease of membrane fluidity in 7 d CA plants did not show de-acclimate effect (Figure 7.1D, F). These results suggest that not only the change of membrane fluidity due to the modification of component in membrane lipids but also other factors may be involved in the formation of Ca^{2+} signals after CA.

16. In root cells, the first peak of cold-induced Ca^{2+} signal appears only in the winter season.

Interestingly, only in root cells, the Ca^{2+} signal shows seasonal change. Since the ethylene gas and ACC treatments increased the first peak of Ca^{2+} signal even in the summer, ethylene may cause the seasonal change of cold-induced Ca^{2+} signal in root cells. This is a reasonable phenomenon because the freezing tolerance is needed only in the winter season in root and leaf, and leaf needs chilling tolerance even in summer season.

17. Root can sense 1ºC of cooling with 2ºC min^{-1} of cooling rate.

18. Leaf can sense 4ºC of cooling with about 0.5ºC min^{-1} of cooling rate.

I tested 1ºC of cooling with 2ºC min^{-1} of cooling rate as the minimum cooling in root cells. This cooling finished within 30 s but root cells could sense this small cooling (Figure

3.7). Since the leaf cells increase the Ca^{2+} signal slower than root cells, 4ºC of cooling with 0.47ºC min^{-1} of cooling rate was used as the minimum cooling. About 0.5ºC min^{-1} of cooling rate was used to show whether the Ca^{2+} signal surely act in the field or not (Figure 3.9h, i). In previous studies, 3ºC min^{-1} was the smallest cooling rate, and showed prolonged Ca^{2+} signal without any Ca^{2+} signal peaks (Plieth *et al*., 1999). Therefore, the 2ºC min^{-1} of cooling rate for root cells and 0.5ºC min^{-1} of cooling rate for leaf cells are smallest cooling rate now on. My results showed that these slow cooling rates and small range of temperature changes induced Ca^{2+} signals. This suggest that the Ca^{2+} signal can sense the temperature changes in the natural environment.

These 18 facts of cold-induced Ca^{2+} signals were found by using the simple cooling changes. The facts 1, 4, 10 and 11 are based on the previous studies, but other 14 facts were found through my work. Since, these experiments are not complete all the characteristics of Ca^{2+} signal, the further study is needed. For example, in the fact 12, the effect of ruthenium red should be tested in root cells. Also, for the facts 17 and 18, I can pursue the limit of cooling range and cooling rate that plants can perceive by using the smaller cooling range and the slower cooling rate. I believe that it is possible to establish a simulation of Ca^{2+} signal by accumulating such detailed experimental data of the Ca^{2+} signals. Once the simulation is established, more research group can discuss and work on the study related to Ca^{2+} signals without observing the Ca^{2+} signals by themselves.

Ca^{2+} signal and the balance of Ca^{2+} channel and Ca^{2+} pump

The Ca^{2+} signal is a result of increasing or decreasing of Ca^{2+} concentration by changing the balance between the amount flowing through the Ca^{2+} channel and the amount of release by the Ca^{2+} pump (Keener and Sneyd, 1998). Therefore, understanding of the characteristics of the Ca^{2+} channels and Ca^{2+} pumps are important information to establish the simulation of the cold-induced Ca^{2+} signals.

Focusing on one Ca^{2+} channel by the patch-clamp technique, it was observed that a Ca^{2+} channel turned from the closed state to opened state without taking more than 0.01 sec, and vice versa (see Hedrich, 1989; Ward and Schroeder, 1994). On the vacuole, which is one of the main intracellular Ca^{2+} pools (Knight and Knight, 2000), has two types of Ca^{2+} channels. One is slow-vacuolar (SV) channel, which is stimulated by the high Ca^{2+} concentration in cytoplasm (>0.3 μM) (Ward and Schroeder, 1994). The kinetics of the activation of the current was slow, and therefore it was termed slow-vacuolar (SV) channel (Hedrich and Neher, 1987). The other is

fast-vacuolar (FV) channel. This is activated by the decrease in cytoplasmic Ca^{2+} (<0.3 μM). Since the kinetic was fast, it termed as fast-vacuolar (FV) channel (Ward and Schroeder, 1994). It also had been reported that the current through SV and FV channels at physiological membrane potentials and density in tracer-flux experiments. According to their measurement, the speed of ion movement was 0.1 fmol vacuole^{-1} s^{-1} (Colombo *et al*., 1988; Martinoia *et al*., 1985; Martinoia *et al*., 1986).

The speed at which the Ca^{2+} concentration increase in a cytosol is depending on whether the increase in the number of opened Ca^{2+} channels or the increase of flow rate of individual Ca^{2+} channels. To determine which factor contribute to the Ca^{2+} signaling, I must determine an *I-V* curve of the opened Ca^{2+} channel by the patch-clamp technique (Keener and Sneyd, 1998). However, it is difficult to determine an *I-V* curve of all types of Ca^{2+} channels which contributing the cold-induced Ca^{2+} signaling, because it is not certain which Ca^{2+} channel is activating at specific timing.

In case of Ca^{2+} channels, the ion movement was caused by the concentration difference between inside and outside of the membranes. On the other hand, Ca^{2+} transporter uses energy such as adenosine triphosphate (ATP) to efflux Ca^{2+} from cytosol. Ca^{2+} ATPase and Ca^{2+}/nH^{+} antipoters mediate Ca^{2+} efflux. The estimated *Km* values of Ca^{2+} ATPase was 0.07 μM to 12 μM (Liss *et al*., 1991; Ping *et al*., 1992; Bush, 1995). It also had been reported that the *Km* values in wheat aleurone cells was from 0.15 μM for an ATPase associated with the tonoplast to 2 μM for an ATPase associated with the plasma membrane (Bush and Wang, 1994).

Here, I discuss whether these findings can be used for the analysis of my experimental results and useful for establishing the simulation of cold-induced Ca^{2+} signaling. The information of the speed of ion movement and the Ca^{2+} concentration which stimulate the channels and pumps are useful for deciding the parameter of a simulation. Besides, the information helps the understanding of the Ca^{2+} signals. The cooling from 20°C to 0°C induced the Ca^{2+} signal which had two peaks, but the two peaks were composed of four hidden peaks (Figure 3.3b). Since 0.3 μM is a kind of threshold for activating the FV channel and SV channel, the hidden Ca^{2+} peak number 2 and 3 might include the Ca^{2+} efflux through FV channel and SV channel, respectively (Figure 3.3b). Furthermore, one of my results of the cold-induced Ca^{2+} signals in root and leaf showed the complex dynamics in the speed of Ca^{2+} concentration change (Figure 7.2). The graph indicates how the speed of increase or decrease changed during the Ca^{2+} signal observation in Figure 3.9c. This analysis was performed to find out when and how many Ca^{2+} channels and pumps were activated. However, even after performing the smoothing process, increase and decrease in the speed of Ca^{2+} concentration change are occurring repeatedly, especially in root (Figure 7.2). Since it is difficult to pick up the meaningful peaks in the graph, the reduction of the noise is needed. In addition, although it cannot be determined whether these increases and decreases in the speed of Ca^{2+} concentration

change are due to an increase in the number of Ca^{2+} channels or pumps, or due to an increase of the flow rate of the channel or pumps, it can be sufficiently reproduced as a simulation as a phenomenon.

Moreover, there is a problem regarding the concentration of Ca^{2+}. If I do not know the actual Ca^{2+} concentration, I cannot calculate the actual speed of the Ca^{2+} concentration change. To calibrate the Ca^{2+} concentration from the ratio value of Yellow Cameleon 3.60, R_{max} (Maximum ratio value of the FRET) and R_{min} are needed. The Ca^{2+} chelator, EGTA and BAPTA-AM reduced the Ca^{2+} concentration, and R_{min} value was calculated (R_{min} = 0.508). However, I could not increase Ca^{2+} concentration satisfactory even if I use any kinds of Ca^{2+} ionophore chemicals and any concentration of chemicals (data not shown). The Ca^{2+} concentration induced by the rapid cooling was higher than the R_{max} in my experiment. In fact, any researchers succeed in obtaining R_{max} in plant cells. Even I used the protoplast, I could not observe the high ratio value (the value increased by the chemical treatment, but not enough). Thus, many researchers published using ratio data (Fluorescence of cpVenus/ECFP) (Yuan *et al*., 2014; Krebs *et al*., 2012; Behera *et al*., 2015). Therefore, an experimental technique which can solve the problem of R_{max}, or another fluorescence / luminescence protein which can calculate the Ca^{2+} concentration should be used to determine the Ca^{2+} concentration to establish the detailed simulation of cold-induced Ca^{2+} signaling for the understanding of the Ca^{2+} signaling and cold sensing of plants.

Ca^{2+} signal in several plant species

There are many reports related on cold-induced Ca^{2+} signals in Arabidopsis. On the other hand, there are very few studies are reported in other plant species. Originally, cold-induced Ca^{2+} signal has been reported in tobacco (Knight *et al*., 1991; Campbell *et al*., 1996) and Arabidopsis (Knight *et al*., 1996; Plieth *et al*., 1999; Knight and Knight, 2000) after discovering the cold-induced Ca^{2+} signal in plant cells. Though detailed investigation and analysis were performed in Arabidopsis, both tobacco and Arabidopsis could response to the cooling immediately.

Nagel-Volkmann *et al*. (2009) has reported the cold-induced Ca^{2+} signals in winter wheat. Nagel-Volkmann *et al*. found that the concentration of Ca^{2+} signals was more dependent on the cooling rate than on the absolute temperature in winter wheat as well as in Arabidopsis (Nagel-Volkmann *et al*. 2009). This result suggests a commonality in cold-induced Ca^{2+} signal of winter wheat and Arabidopsis (Plieth *et al*., 1999). In addition, since they could not observe the Ca^{2+} signal by only at cooling rates higher than 8ºC min^{-1}, they concluded that the Ca^{2+} signal was minor relevance as a messenger in cold acclimation process in the field in winter

wheat (Nagel-Volkmann *et al*. 2009). It is true that the same experimental system could not observe the clear Ca^{2+} signal by the cooling at 3ºC min^{-1} in Arabidopsis root (Plieth *et al*., 1999), but I succeeded in observing the Ca^{2+} signal by the cooling at 0.47ºC min^{-1} in Arabidopsis leaves and roots (Figures 3.9h, i, 3.10a-c). Therefore, I hypothesized that winter wheat is also able to induce Ca^{2+} signals to slower cooling rate even in the field.

Ma *et al*. (2015) revealed that *COLD1*, quantitative trait locus, which enhance chilling tolerance, influences cold-induced Ca^{2+} signal in rice. The Ca^{2+} signal which was caused by the cold shock in rice was similar to that in tobacco, Arabidopsis and winter wheat in shape (Knight *et al*., 1991; Campbell *et al*., 1996; Knight *et al.*, 1996; Plieth *et al*., 1999; Knight and Knight, 2000; Nagel-Volkmann et al. 2009). However, there is no report which focus on the Ca^{2+} signals caused by the slow cooling rate, so we do not sure whether slow cooling rate also induces the similar Ca^{2+} signal in different plant species.

Since every report uses different cooling rates and cooling methods, it is difficult to compare each Ca^{2+} signal. The length of periods in Ca^{2+} signal (see Figure 3.2d) is dependent on the cooling rate and absolute temperature (Hiraki *et al*., 2019a). Therefore, it is necessary to compare the Ca^{2+} signals in multiple plant species by using the same experimental equipment under the same cooling condition. Although it was not cold-induced Ca^{2+} signal, a comparison of Ca^{2+} signals which are induced by the hyperpolarization / depolarization cycles in rice and Arabidopsis has been reported (Behera *et al*., 2015). They concluded that rice had a lower maximal signal amplitude but greatly increased signal duration when compared with Arabidopsis (Behera *et al*., 2015). Therefore, we have to compare multiple plant species to understand the Ca^{2+} signaling in many plant species because similar characteristics might be found in the response to the cold.

Arabidopsis get the maximum freezing tolerance by exposure to low temperature such as 2ºC for 7 d (Uemura *et al.*, 1995). On the other hand, wheat and rye need about 50 d to enhance their freezing tolerance to the maximum level (Fowler *et al.*, 1995). This means that the time duration of which Ca^{2+} signals act is longer in wheat and rye than in Arabidopsis. Fowler *et al*. (1995) used the cold acclimation treatment at 4 ºC constant. Thus, Ca^{2+} signal might not be induced by the acclimation treatment except starting the treatment. Perras and Sarhan (1989) used the cold acclimation condition of 6 ± 1°C day (10 h photoperiod) and 2 ± 1°C night and for 10 d or 40 d for wheat and found the specific proteins in 40 d. Therefore, even though there was a temperature cycle, wheat needed 40 d to proceed the cold acclimation process. In addition, the response speed of *CBF/DREB1* gene to cold was almost same among Arabidopsis, wheat and rye (Jaglo *et al*., 2001), but wheat and rye required much longer time to enhance the freezing tolerance. Thus, the Ca^{2+}-CBF/DREB1 pathway may not be dominant in cold acclimation process in wheat and rye, or Ca^{2+} signals may act different way in wheat and rye from Arabidopsis. Ca^{2+} signal sometimes suppresses the expression of *CBF* genes even in

Arabidopsis (Figures 3.15, 3.16 4.11), and therefore there is a possibility that Ca^{2+} signal mainly suppress the cold acclimation process in wheat and rye. The response to low-temperature should be different and the role (regulation) of Ca^{2+} signal also might be different, because each plant species has each level of cold tolerance. What we can mention now is, the Ca^{2+} signal which responds to low temperature quickly and transfers the information into the cell may be widely used for low temperature sensing in many plant species to regulate gene expression.

Although it is necessary to observe the Ca^{2+} signal in other plant species, the observation of Ca^{2+} signals is difficult. However, physiological experiments and analysis of gene expression with Ca^{2+} channel blockers can be easily performed. I showed that the role of Ca^{2+} signal can be evaluated indirectly by the experiment with the Ca^{2+} channel blockers (i.e., $LaCl_3$ and RR), and temperature cycle and fluctuation (Chapter 3 and 4). Therefore, it is considered that the role of Ca^{2+} signal in each plant species can be estimated by conducting the same experiment with many plant species.

Role of the Ca^{2+} signal in cold acclimation process: from the aspect of the gene expression and freezing tolerance

There are two kinds of Ca^{2+} signals in plant for response to cooling. One is a large Ca^{2+} signal induced by cooling with a large temperature range such as day and night. The other is a small Ca^{2+} signal that appears in response to temperature fluctuation in a few minutes. Although these Ca^{2+} signals have not been distinguished in previous studies so far, this study suggests that these two types of the Ca^{2+} signal may stimulate another cold acclimation pathway.

The Ca^{2+} signal decreases when the cooling stops (include heating) not depending on the prior condition in root and leaf cells (Figures 3.2, 3.4, 3.7, 3.9 and 3.10). Although the constant cooling rarely occurs in the field, the Ca^{2+} signal which has two or three peaks were induced by the constant cooling, and had function in the cold acclimation process (Knight *et al*., 1996; Tähtiharju *et al*., 1997; Doherty *et al*, 2009; Kidokoro *et al*., 2017). Thus, I observed both the Ca^{2+} signals which are caused by the rapid cooling and the field-like cooling (Figures 3.2, 3.4, 3.5, 3.7, 3.9 and 3.10). To study the role of these Ca^{2+} signals, I sprayed the Ca^{2+} channel blockers, $LaCl_3$ or RR, and then observed each Ca^{2+} signal (Figures 3.13 and 3.14). These results suggested that $LaCl_3$ tended to inhibit the Ca^{2+} signal which was induced by the rapid and large temperature range of cooling rather than slow and small range of cooling, and RR inhibited the Ca^{2+} signal which was induced by the slow and small cooling rather than the rapid and large temperature range of cooling (Figures 3.13 and 3.14).

To figure out the role of the two different types of Ca^{2+} signals, the specific setting of the cold acclimation was established. I made a small chamber which can maintain the temperature

fluctuation in minutes during cold acclimation (see Figures 4.1 and 4.6). This allowed us to investigate the role of the two type of Ca^{2+} signals. $LaCl_3$ may inhibit the Ca^{2+} signal which is induced by the "rapid cooling" and "constant long duration of cooling." Following three types of acclimations were used: constant 2ºC, 10ºC day / 2ºC night of cyclic CA (C–CA) and temperature fluctuating CA (FC–CA). All CA treatments include the rapid cooling when the treatment starts; that is the rapid cooling. C–CA and FC–CA also had the temperature cycle of day and night (Figure 4.6). This temperature change was the "constant and long duration of cooling" Thus, $LaCl_3$ tended to inhibited gene expression of *CBF/DREB1s* and *COR15A* in all acclimation treatments (Figure 4.11). On the other hand, RR inhibited the gene expression of *CBF/DREB1s* only in FC–CA (Figure 4.11). RR tended to inhibit the small Ca^{2+} signal, such as the Ca^{2+} signal induced by the temperature fluctuation in FC–CA (Figure 3.14). Comparing with the peak values, the Ca^{2+} signal induced by the "constant and long duration of cooling" had about 3 to 7 times larger Ca^{2+} signal peak than the Ca^{2+} signal induced by the "temperature fluctuation" (Figure 3.9). However, when the small Ca^{2+} signals were inhibited by RR in FC–CA, the expression level of *CBF/DREB1s* was inhibited to about 40% compared with the control (Figure 4.11). Since RR did not inhibit the gene expression of *CBF/DREB1s* in C–CA, I concluded that the small Ca^{2+} signals induced by the "temperature fluctuation" contributed to the approximately 40% of gene expression of *CBF/DREB1s* in FC–CA (Figure 4.11). Taken together, this study supports the hypothesis that a small Ca^{2+} signal (e.g., induced by the temperature fluctuation) is also generated during the cold acclimation process as well as a large Ca^{2+} signal (e.g., induced by the "rapid cooling" and "constant and long duration of cooling").

Extracellular space and the vacuole are the major Ca^{2+} pools of the Ca^{2+} signaling (Knight *et al*., 1996). I tried to develop the experimental system to measure the accumulation level of Ca^{2+} in the extracellular space and vacuole in the epidermal cells of Arabidopsis (see Chapter 6). The results suggested that conventional CA treatment tended to induce the accumulation of Ca^{2+} in the extracellular space and the vacuole (Figures 6.4 and 6.5). In CA plant, the responsiveness to cooling was enhanced compared with NA plant (Figure 3.7). Accumulation of Ca^{2+} in the Ca^{2+} pools may lead the large difference in osmotic pressure between the cytosol and Ca^{2+} pools; and the speed of outflow from the Ca^{2+} pools to the cytosol may be enhanced. Interestingly, FC–CA did not induce the accumulation of Ca^{2+} in both extracellular space and vacuole, but FC–CA with Ca^{2+} channel blockers increased the accumulation level of Ca^{2+}, especially in the extracellular space (Figure 6.5). In FC–CA treatment, the temperature of the daytime is about 10ºC and the temperature is fluctuating (Figures 4.2 and 4.6). The higher temperature in FC–CA might not induce the Ca^{2+} accumulation. On the other hand, if the Ca^{2+} signaling is disturbed by the Ca^{2+} channel blockers, plant may accumulate Ca^{2+} in extracellular space and vacuole to fix the Ca^{2+} signaling. Taken together, there might be a kind of feedback interaction between the Ca^{2+} signaling and accumulation level of Ca^{2+} in Ca^{2+} pools.

It had been reported that there was a difference between cold-sensitive plants and cold-insensitive plants in the Ca^{2+} signaling (Jian *et al*., 1999). Therefore, the difference of the Ca^{2+} signaling and its signal transduction may be one of the important factors in CA process and enhancement of the freezing tolerance. However, it is difficult to find the different Ca^{2+} signal contribution on CA process by using the conventional CA treatment, because it induced just one Ca^{2+} signal. Here, I used the FC–CA treatment in three Arabidopsis accessions: Col-0, Fl-3 and Kas-1. Three Arabidopsis accessions showed different levels of freezing tolerance after FC–CA (Figure 4.4). The contributions of the Ca^{2+} signal, which is caused by the temperature fluctuation, was dependent on the accessions (Figures 4.4 and 4.5). This indicates that the Ca^{2+} signaling pathway and signal transduction might be specific in each accession. For the further analysis, performing FC–CA treatment on a number of Arabidopsis accessions and analyzing by using next generation sequencer technique may lead the finding of the novel factors on the Ca^{2+} signaling in CA process.

The temperature fluctuation induced the decrease of the freezing tolerance compared with that of conv.–CA and C–CA (Figure 4.7). The temperature fluctuation during the daytime was the only one difference between FC–CA and C–CA, but 3 and 7 d of FC–CA plants tended to result in the weaker freezing tolerance than that of C–CA (Figure 4.7). Since the temperature fluctuation may cause the Ca^{2+} signals (Figure 3.9h, i), Ca^{2+} signal was the candidate which inhibited the increase of freezing tolerance, but Ca^{2+} channel blockers decreased the expression level of *CBF/DREB1s* and *COR15A* (Figure 4.11) and the freezing tolerance (Figure 4.7). It means that Ca^{2+} signal which induced by the temperature fluctuation enhances the gene expression and increase of the freezing tolerance. Therefore, there was an unknown factor which suppresses the cold acclimation process stimulated by the temperature fluctuation independent from Ca^{2+} signaling. On the other hand, if there is no temperature fluctuation but temperature cycle of day and night, the Ca^{2+} efflux from intracellular pool induced by the cooling from day-temperature to night-temperature inhibited the gene expression of *CBF2/DREB1C*, and *CBF3/DREB1A* (Figure 4.11b, c). I also tried the analysis of the gene expression with the Ca^{2+} channel blockers in the field condition during winter in Morioka, Japan. On the early December, 2016, there were less temperature fluctuations compared with other experiment days (Figure 3.12c). Thus, the temperature condition on the early December in 2016 was similar to the condition of C–CA. Focus on the gene expression, the expression level of *CBF/DREB1s* in the early December tended to be upregulated by the RR treatment as well as C–CA (Figure 3.15c). These two results lead to the hypothesis that the Ca^{2+} signal not only has a function of inducing gene expression but also has a role of inhibition a CA pathway depending on the temperature condition (Figure 7.3). Whalley *et al*. (2011) and Whalley and Knight (2013) also has reported that different shape of the Ca^{2+} signal induced different gene expression. Thus, the Ca^{2+} signal may regulate the gene expression positive and negative way according to the

encoded information.

In addition, the seasonal change of the Ca^{2+} signal was observed in root cells (see Chapter 5). In the winter, the rapid cooling induced the Ca^{2+} signal which had two signal peaks from the cooling to stoppage of the cooling. However, in the summer, the same rapid cooling induced Ca^{2+} signal with just one small peak (Figures 5.1, 5.2 and 5.4). Since the Ca^{2+} signals which were induced by the rapid cooling strongly induce the gene expression of *CBF/DREB1s* (Figure 3.17) (Kidokoro *et al.,* 2017), plants may have the function to avoid inducing the Ca^{2+} signal to increase the freezing tolerance in the summer.

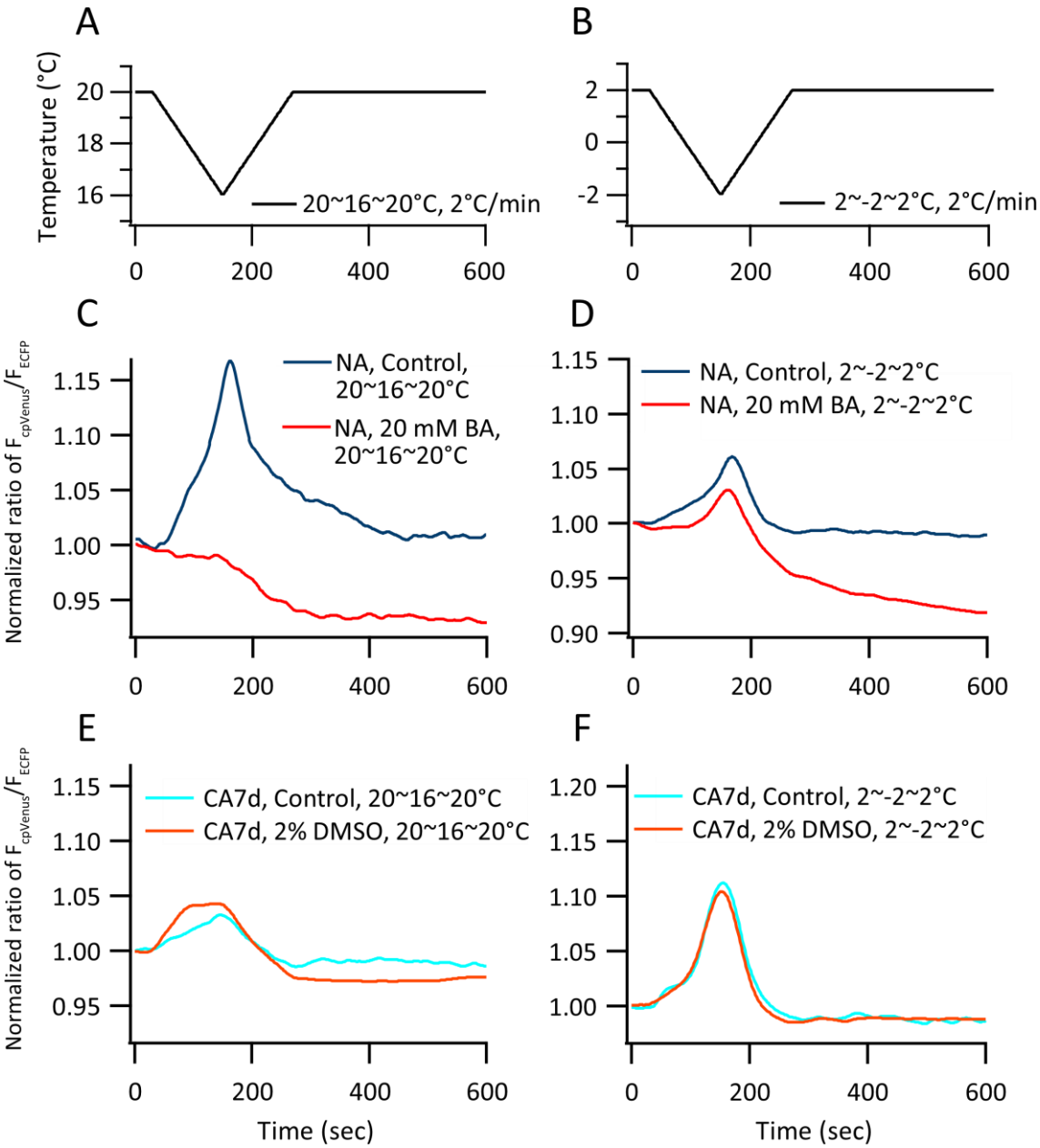

Figure 7.1. Ca^{2+} signals and fluidity of membrane in YC3.60-expressing *Arabidopsis* roots. (A) The temperature changed from 20°C to 16°C and then to 20°C or (B) 2°C to −2°C to and then 2°C. Samples in both experiments were cooled/heated at a rate of 2°C min^{-1}. (C and D) The non-cold acclimated (NA) plants were treated with 20 mM of benzyl alcohol (BA) to increase membrane fluidity. (E and F) The 7 d cold-acclimated (CA7d) plants treated with 2% of dimethyl sulfoxide (DMSO) to decrease membrane fluidity. The FRET values were calculated and normalized against the initial values (n = 4, 5).

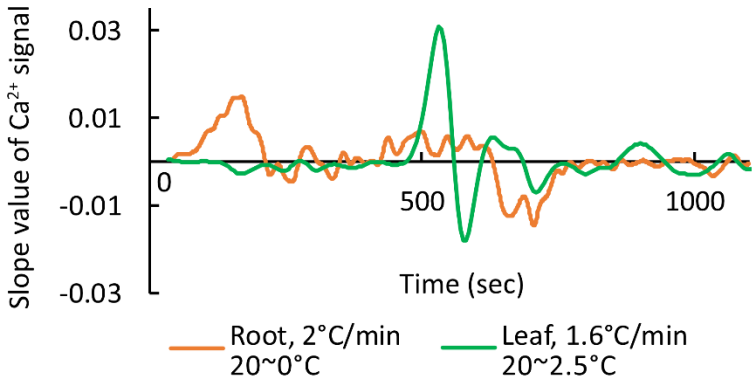

Figure 7.2. The speed of the Ca^{2+} concentration changes in leaf and root. The slope values were calculated from the averaged Ca^{2+} signal data set in Figure 3.9c. Every 5 s of slope values were plotted.

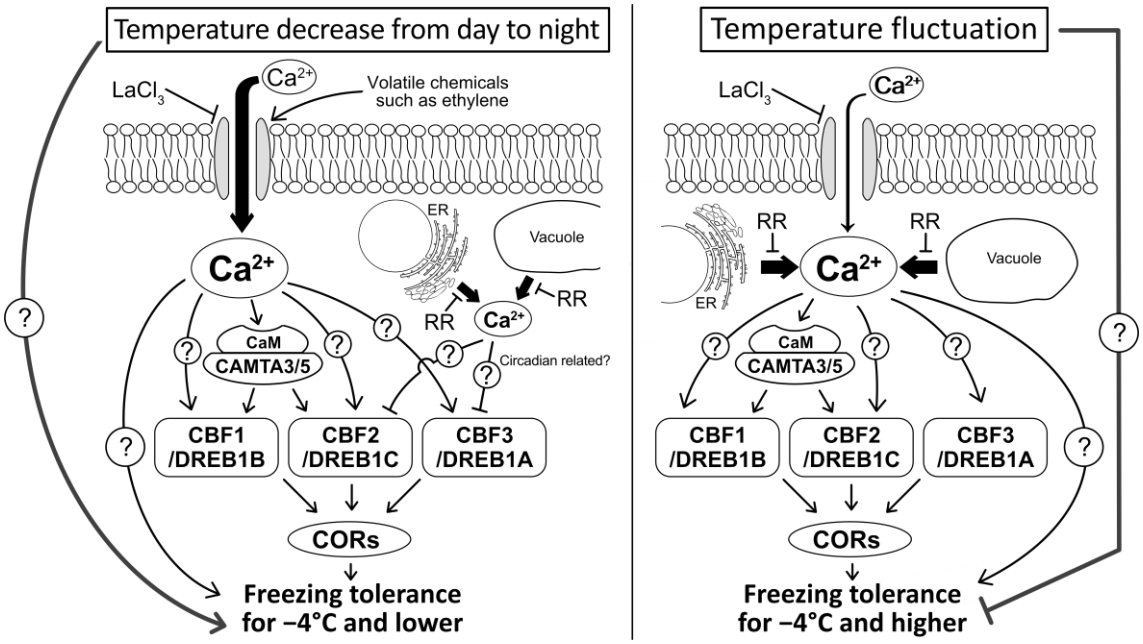

Figure 7.3. Summary of the effect of temperature cycle and temperature fluctuation.

Conclusion

Field-like cooling induced the Ca^{2+} signal. This result clearly shows that the Ca^{2+} signal acts in the field. The temperature fluctuation in minutes tended to induce the *CBF/DREB1s* in the field via the Ca^{2+} signals. By using the special chamber which can maintain the temperature fluctuation resulted in the observation that the temperature fluctuation induced *CBF/DREB1s* through the Ca^{2+} signals as well as in the field. In both field CA and FC–CA, low amplitude of the temperature fluctuation suppresses the *CBF2/DREB1C* and *CBF3/DREB1A* by the Ca^{2+} efflux from the intracellular pool. By contrast, conventional CA did not induce Ca^{2+} signal except for the one induced by the initial temperature change from room temperature to the acclimation temperature, and did not enhance the gene expression through the Ca^{2+} signal. These results suggest that conventional CA treatment is not a sufficient treatment from the views of the Ca^{2+} signaling which is induced by the temperature fluctuations and temperature cycle. Using the field CA, FC–CA and C–CA treatments, the novel role and pathway of the Ca^{2+} signal were revealed. The experiment of FC–CA also suggested the possibility that there is a feedback mechanism to fix the disturbed Ca^{2+} signal by modifying the accumulation level of Ca^{2+} in Ca^{2+} pools. In addition, although the Ca^{2+} signals which are induced by the temperature fluctuation increased the expression level of *CBF/DREB1s* and the freezing tolerance, the temperature fluctuation tended to inhibit the cold acclimation process independent from the Ca^{2+} signaling. This result suggests that there is the pathway which inhibits expression of *CBF/DREB1s* and the freezing tolerance when the temperature is fluctuating. Since the amplitude of the temperature fluctuation is low in the winter and high in the summer, the pathway may be useful to avoid an unnecessary cost. The Ca^{2+} signal also has the similar function. Especially the first peak of the Ca^{2+} signal is suppressed in the summer and increased its responsiveness and height of peak by exposure to the volatile chemicals, such as ethylene. In fact, it had been reported that the concentration of ethylene was the highest in winter. Taken together, the Ca^{2+} signal plays an important role not only in promoting the CA process but also in suppressing the CA process by the seasonal sensing in plant cells in the field. On the other hand, the temperature fluctuation and the temperature cycle of day and night cause enhancement and suppression of the freezing tolerance independent from the Ca^{2+} signal. Therefore, the further study on CA process including the Ca^{2+} signal in the natural condition (i.e., with the temperature fluctuation and cycle) is needed, and this study strongly suggested that there is a large difference between the artificial CA treatment and CA in the field. The study with field-like CA helps our understanding of “how plants sense cold in natural environment” and may help the future agriculture.

Acknowledgements

First of all, I would like to express thank to Dr. Yukio Kawamura (Iwate University) for supervising for 6 and half years since I was undergraduate student. I am proud that I am the Dr. Kawamura's first Ph.D. student. I grateful to Dr. Matsuo Uemura (Iwate University), Dr. Michiko Sasabe (Hirosaki University), Dr. Wataru Mitsuhashi (Yamagata University) and Dr. Jun Kasuga (Obihiro University of Agriculture and Veterinary Medicine) for co-supervising. I would like to thank Dr. Abidur Rahman and Dr. Uzuki Matsushima for their helpful advice.

I am grateful to Dr. Karin Schumacher (Heidelberg University, Germany) for *Arabidopsis* plants expressing YC3.60. I would thank Dr. Shoji Mano and Dr. Etsuko Watanabe for *Arabidopsis* accessions, Kas-1 and Fl-3.

I thank Ms. Mei Ogata for the data of the air temperature in the field (Figure 3.11b, c) and Ms. Maki Kanaya for the data of survival rate (Figure 4.12).

I express my thanks to Dr. Karen Tanino (University of Saskatchewan, Canada) and her students for accepting me in her laboratory for three weeks in 2015 and three months in 2018. I also appreciate the financial support of Embassy of Canadian, Tokyo and Japanese Society for the Promotion of Science (JSPS) for my study in Saskatoon in 2015 and 2018, respectively. In addition, I grateful to Dr. Chithra Karunakaran, Dr. Na Liu, Dr. Jian Wang and Dr. Jarvis Stobbs (Canadian Light Source, Canada) for operating and helping my synchrotron work.

I thank Dr. Manabu Watanabe (Iwate University) for measuring the concentration of ethylene, and Mr. Mohammad Arif Ashraf (Iwate University) for helping the ACC experiment in Chapter 5. I appreciate very much the support from Ms. Yuko Suzuki, Ms. Michiko Saito and Ms. Nozomi Yokota in our laboratory, and Ms. Valsala Gowribai in Dr. Tanino's laboratory in the University of Saskatchewan for technical assistance.

I particularly thank Dr. Karen Tanino for reviewing a part of this manuscript. I also express my thank to my father, Tatsumi Hiraki (Iwate University) for editing a part of this manuscript. I am grateful to the member of Cryobiofrontier Research Center, Iwate University, for their supports and discussions. Finally, I would like to thank my family and friends for their encouragements and supports.

A part of this work was supported by JSPS Kakenhi [grant number 25292205 and 18K19319 to Y. K. and grant number 22120003 to M. U.]; JSPS Overseas Challenge Program for Young Researchers to H. H.; and Dean's Fund of UGAS, Iwate University (to H. H.).

Copyrights

Chapter 2 and 3 of this thesis were based on the manuscript of Hiraki *et al*., (2019a) in *Plant and Cell Physiology*. The section entitled “Freezing tolerance in the three Arabidopsis accessions” and “Freezing tolerance in the three Arabidopsis accessions after conventional cold acclimation and temperature fluctuating cold acclimation treatment”, in Chapter 4 and figure 4.2-4.5 was the reprint of the manuscript of Hiraki *et al*. (2019b) in *Cryobiology and Cryotechnology* 65, (in press). “Introduction” and “Materials and Methods” in chapter 4 also including the reprint of the manuscript of Hiraki *et al*. (2019b) in *Cryobiology and Cryotechnology* 65*,* (in press). Chapter 6 of this thesis includes the manuscript and figures of Hiraki *et al*. (2018) in Microscope and Microanalysis 24 (Suppl 2) 356-357, especially in “Introduction” and “Materials and Methods”.

References

Abeles, FB. and Heggestad, HE. (1973) Ethylene: an urban air pollutant. *J. Air Pollut. Control Assoc.* 23, 517-521.

Abeles, FB., Morgan, PW. and Salveit, ME. (1992) Ethylene in Plant Biology. *San Diego. Academic Press*. 1992.

Adams, DO. and Yang, SF. (1979**)** Ethylene biosynthesis–identification of 1-aminocyclopropane-1-carboxylicacidasanintermediateintheconversion of methionine to ethylene. *Proc. Natl. Acad. Sci. USA.*76, 170–174.

Agarwal, M., Hao, Y., Kapoor, A., Dong, CH., Fujii, H., Zheng, X. and Zhu, JK. (2006) A R2R3 type MYB transcription factor is involved in the cold regulation of *CBF* genes and in acquired freezing tolerance. *J. Biol. Chem*. 281, 37636-37645.

Allen, GJ., Chu, SP., Harrington, CL., Schumacher, K., Hoffmann, T., Tang, YY., Grill, E. and Schroeder, JI. (2001) A defined range of guard cell calcium oscillation parameters encodes stomatal movements. *Nature* 411, 1053-1057.

Altuzar, V., Pacheco, M., Tomás, SA., Zelaya-Angel, O. and Sánchez-Sinencio, F. (2001) Analysis of ethylene concentration in the Mexico City atmosphere by photoacoustic spectroscopy. *Anal. Sci.* 17, s541-s543.

Asada, K. (1996) Radical production and scavenging in the chloroplasts. In NR. Baker ed., Photosynthesus and the Environment, *Netherlands: Kluwer Academic Publishers*, 123-150.

Baldwin, IT., Halitschke, R., Paschold, A., von Dahl, CC. and Preston, CA. (2016) Volatile signaling in plant-plant interactions: "Talking trees" in the genomics era. *Science* 311, 812–815.

Behera, S., Wang, N., Zhang, C., Schmitz-Thom, I., Strohkamp, S., Schültke, S., Hashimoto, K., Xiong, L. and Kudla, J. (2015) Analyses of Ca^{2+} dynamics using a ubiquitin-10 promoter-driven Yellow Cameleon 3.6 indicator reveal reliable transgene expression and differences in cytoplasmic Ca^{2+} responses in Arabidopsis and rice (*Oryza sativa*) roots. *New Phytol.* 206, 751-760.

Bilska-Kos, A., Solecka, D., Dziewulska, A., Ochodzki, P., Jończyk, M., Bilski, H. and Sowiński, P. (2017) Low temperature caused modifications in the arrangement of cell wall pectins due to changes of osmotic potential of cells of maize leaves (Zea mays L.). *Protoplasma*, 254, 713-724.

Blanpied, GD. (1972) A study of ethylene in apple, red raspberrv, and cherry. *Plant Physiol*. 49, 627-630.

Bowler, C., Heuhaus, G., Yamagata, H. and Chua, NH. (1994) Cyclic GMP and calcium mediate phytochrome phototransduction. *Cell* 77, 73-81.

Braam, J., Sistrunk, ML., Polisensky, DH., Xu, W., Purugganan, MM., Antosiewicz, DM., Campbell, P. and Johnson, KA. (1997) Plant responses to environmental stress: regulation and functions of the Arabidopsis TCH genes. *Planta* 203, S35–S41.

Briggs, WR. and Olney, MA. (2001) Photoreceptors in plant photomorphogenesis to data. Five phytochromes, two cryptochromes, one phototropin, and one superchrome. *Plant Physiol.* 125, 85-88.

Bush, DS. (1995) Calcium regulation in plant cells and its role in signaling. *Annu. Rev. Plant Physiol. Plant Mol. Biol.* 46, 95–122.

Bush, DS. and Wang, T. (1994) Diversity of calcium transporters in wheat aleurone cells. *Plant Physiol.* 105 (Suppl.): 149.

Burström, HG. (1968) Calcium and plant growth. *Biol. Rev. (Cambridge)* 43, 287-316.

Campbell, AK., Trewavas, AJ. and Knight, MR. (1996) Calcium imaging shows differential sensitivity to cooling and communication in luminous transgenic plants. *Cell Calcium* 19, 211-218.

Chang, CY., Lai, LR. and Chang, WH. (1995) Relationships between textural changes and the changes in linkages of pectic substances of sweet pepper during cooking processes, and the applicability of the models of interactions between pectin molecules. *Food Chem.* 53, 409-416.

Chen, WP. (2000) Regulation of calcium influx, free radical production and alternative pathway activity is associated with abscisic acid-improved chilling tolerance in maize (Zea mays L) cultured cells. Dissertation. University of Minnesota.

Chinnusamy, V., Schumaker, K. and Zhu, JK. (2003) Molecular genetic perspectives on cross-talk and specificity in abiotic stress signalling in plants. *J. Exp. Bot*. 55, 225-236.

Chinnusamy, V., Zhu, JK. and Sunkar, R. (2007) Cold stress regulation of gene expression in plants. *Trends Plant Sci.* 12, 444-451.

Chinnusamy, V., Zhu, JK. and Sunkar, R. (2010) Gene regulation during cold stress acclimation in plants. *Methods Mol. Biol.* 639, 39-55.

Colombo, R., Cerana, R., Lado, P. and Peres, A. (1988) Voltage-dependent channels permeable to K^+ and Na^+ in the membranes of *Acer pseudoplatanus*. *J. Membr. Bioi.* 103, 227-36.

Dat, J., Vandenabeele, S., Vranova, E., Van Montagu, M., Inze, D. and Van Breusegem, F. (2000) Dual action of the active oxygen species during plant stress responses. *Cell Mol. Life Sci.* 57, 779-795.

Del Castillo, J. and Stark, L. (1952) The effect of calcium ions on the motor end-plate potenstials. *J. Physiol*. 116: 507-515.

Devlin, PF. (2002) Signs of the time: environmental input to the circadian clock. *J. Exp. Bot.* 53, 1535-1550.

Dodd, AN., Jakobsen, MK., Baker, AJ, Telzerow, A, Hou, SW., Laplaze, L., Barrot, L., Poethig, RS., Haseloff, J. and Webb, AAR. (2006) Time of day modulates low-temperature Ca^{2+} signals in Arabidopsis. *Plant J*. 48, 962-973.

Dodd, AN., Kudla, J. and Sanders, D. (2010) The language of calcium signaling *Annu. Rev. Plant Biol.* 61, 593-620.

Doherty, CJ., Van Buskirk, HA., Myers, SJ. and Thomashow, MF. (2009) Roles for Arabidopsis CAMTA transcription factors in cold-regulated gene expression and freezing tolerance. *Plant Cell* 21, 972-984.

Dong, MA., Farré, EM. and Thomashow, MF. (2011) Circadian clock-associated 1 and late elongated hypocotyl regulate expression of C-repeat binding factor (CBF) pathway in *Arabidopsis*. *Proc. Natl. Acad. Sci. USA*. 108, 7241-7246.

Ehlert, B. and Hincha, DK. (2008) Chlorophyll fluorescence imaging accurately quantifies freezing damage and cold acclimation responses in Arabidopsis leaves. *Plant Methods* 27, 4-12.

Endler, A., Meyer, S., Schelbert, S., Schineider, T., Weschke, W., Peters, SW., Keller, F., Baginsky, S., Martinoia, E. and Schmidt, UG. (2006) Identification of a vacuolar sucrose transporter in barley and Arabidopsis mesophyll cells by a tonoplast proteomic approach. *Plant Physiol.* 141, 196-207.

Felber, LM., Cloutier, SM., Kündig, C., Kishi, T., Brossard, V., Jichlinski, P., Leisinger, HJ. and Deperthes, D. (2004) Evaluation of the CFP-substrate-YFP system for protease studies, advantages and limitations. *BioTechniques* 36, 878-885.

Fowler, DB., Limin, AE., Wang, SY. and Ward RW. (1995) Relationship between low-temperature tolerance and vernalization response in wheat and rye. *Can. J. Plant Sci.* 76, 37-42.

Fowler, S. and Thomashow, MF. (2002) Arabidopsis transcriptome profiling indicates that multiple regulatory pathway are activated during cold acclimation in addition to the CBF response pathway. *Plant Cell* 14, 1675-1690.

Franklin, KA. and Whitelam, GC. (2007) Light-quality regulation of freezing tolerance in Arabidopsis thaliana. *Nat. Genet.* 39, 1410-1413.

Gane, R. (1934) Production of ethylene by some fruits. *Nature* 134, 1008.

Gong, Z., Lee, H., Xiong, L., Jagendorf, A., Stevenson, B. and Zhu, JK. (2002) RNA helicase-like protein as an early regulator of transcription factors for plant chilling and freezing tolerance. *Proc. Natl. Acad. Sci. USA.* 99, 11507-11512

Han, S., Tang, R., Anderson, LK., Woerner, TE. and Pei, ZM. (2003) A cell surface receptor mediates extracellular Ca2+ sensing in guard cells. *Nature* 425, 196–200.

Haswell, ES. and Meyerowitz, EM. (2006) MscS-like proteins control plastid size and shape in *Arabidopsis thaliana. Curr. Biol.* 16, 1-11.

Hedrich, R. and Neher, E. (1987) Cytoplasmic calcium regulates voltage-dependent ion channels in plant vacuoles. *Nature* 329, 833-35.

Hedrich, R. (1989) The physiology of ion channels and electrogenic pumps in higher plants. *Annu. Rev. Plant Physiol*. 40, 539-69.

Hepler, PK. (2005) Calcium: a central regulator of plant growth and development. *Plant Cell* 17, 2142-2155.

Hiraki, H., Liu, N., Wang, J., Stobbs, J., Karunakaran, C. and Tanino K. (2018) Soft X-ray spectromicroscopy: a versatile tool to probe pristine plant cell walls. *Microsc. Microanal*. 24 (Suppl 2), 356-357.

Hiraki, H., Uemura, M. and Kawamura, Y. (2014) Low-temperature sensing and the dynamics of cytoplasmic calcium in plant cells. *Cryobiol. Cryotechnol*. 60, 139-142. (in Japanese with English abstract)

Hiraki, H., Uemura, M. and Kawamura, Y. (2016) Calcium ion dynamics in plant caused by short time cooling. *Cryobiol. Cryotechnol*. 62, 65-68. (in Japanese with English abstract)

Hiraki, H., Uemura, M. and Kawamura, Y. (2019a) Calcium signaling-linked *CBF/DREB1* gene expression was induced depending on the temperature fluctuation in the field: views from natural condition of cold acclimation. *Plant Cell Physiol.* 60, 303-317.

Hiraki, H., Tanino, K., Watanabe, E., Mano, S., Uemura, M. and Kawamura, Y. (2019b) Effect of temperature fluctuating cyclic cold acclimation on freezing tolerance in three *Arabidopsis* accessions. *Cryobiol. Cryotechnol*. 65 (in press)

Hochmal, AK., Schulze, S., Trompelt, K. and Hippler, M. (2015) Calcium-dependent regulation of photosynthesis. *Biochem. Biophys. Acta*. 1847, 993-1003.

Huang, L., Berkelman, T., Franklin, AE. and Hoffman, NE. (1993) Characterization of a gene encoding a Ca^{2+}-ATPase-like protein in the plastid envelope. *Proc. Natl. Acad. Sci. USA.* 90, 10066-10070.

Hubbard, JI. (1961) The effect of calcium and magnesium on the spontaneous release of transmitter from mammalian motor nerve endings. *J. Physiol*. 159, 507-517.

Inderjit, von Dahl, CC. and Baldwin, IT. (2009) Use of silence plants in allelopathy bioassays: a novel approach. *Planta* 229, 569-575.

Jaglo, KR., Kleff, S., Amundsen, KL., Zhang, X., Haake, V., Zhang, JZ., Deits, T. and Thomashow, MF. (2001) Components of the Arabidopsis C-repeat/dehydration-responsive element binding factor cold-response pathway are conserved in Brassica napus and other plant species. *Plant Physiol.* 127, 910–917.

Jian, LC., Li, JH., Chen, WP., Li, PH. and Ahlstrand GG. (1999) Cytochemical localization of calcium and Ca^{2+}-ATPase activity in plant cells under chilling stress: a comparative study between the chilling-sensitive maize and chilling-insensitive winter wheat. *Plant Cell Physiol.* 40, 1061-1071.

Jonak, G., Kiergerl, S., Lighterink, W., Barker, PJ. and Huskisson, NS. (1996) Stress signaling in plants a mitogen-activated protein kinase pathway is activated by cold and drought. *Proc. Natl. Acad. Sci. USA*. 93, 11274-11279.

Karunakaran, C., Christensen, CR., Gaillard, C., Lahlali, R., Blair, LM., Perumal, V., Miller, SS. and Hitchcock, AP. (2015) Introduction of soft X-ray spectromicroscopy as an advanced technique for plant biopolymers research. *PloS ONE* 10, 1-18.

Kass, GEN. and Orrenius, S. (1999) Calcium signaling and cytotoxicity. *Environ. Health Perspect*. 107 (Suppl 1), 25-35.

Keener, J. and Sneyd, J. (1998) Mathematical Physiology. *New York*: *Springer-Verlag*.

Kiegle, E., Moore, CA., Haseloff, J., Tester, MA. and Knight, MR. (2000) Cell-type-specific calcium response to drought, salt and cold in the *Arabidopsis* root. *Plant J.* 23, 267-278.

Kidokoro, S., Yoneda, K., Takasaki, H., Takahashi, F., Shinozaki K. and Yamaguchi-Shinozaki, K. (2017) Different cold-signaling pathway function in the responses to rapid and gradual decrease in temperature. *Plant Cell* 29, 769-774.

Knight, H. and Knight, MR. (2000) Imaging spatial and cellular characteristics of low temperature calcium signature after cold acclimation in *Arabidopsis*. *J. Exp. Bot*. 51, 1679-1686.

Knight, MR. (2002) Signal transduction leading to low-temperature tolerance in *Arabidopsis thaliana*. *Philos. Trans. R. Soc. Lond B Biol. Sci*. 357, 871-875.

Knight, MR., Campbell, AK., Smith, SM. and Trewavas, AJ. (1991) Transgenic plant aequorin reports the effect of touch and cold-shock and elicitors on cytoplasmic calcium. *Nature* 352, 524-526.

Knight, MR., Smith, SM. and Trewavas, AJ. (1992) Wind-induced plant motion immediately increases cytosolic calcium. *Proc. Natl. Acad. Sci. USA.* 89, 4967-4971.

Knight, H., Trewaves, AJ. and Knight MR. (1996) Cold calcium signaling in *Arabidopsis* involves two cellular pools and a change in calcium signature after acclimation. *Plant Cell* 8, 489-503.

Krebs, M., Held, K., Binder, A., Hashimoto, K., Herder, GD., Parniske, M., Kudla, J. and Schumacher, K. (2012) FRET-based genetically encoded sensors allow high-resolution live cell imaging of Ca^{2+} dynamics. *Plant J.* 69, 181-192.

Łabuz, J., Samardakiewicz, S., Hermanowicz, P., Wyroba E., Pilarska M. and Gabryś, H. (2016) Blue light-dependent changes in loosely bound calcium in Arabidopsis mesophyll cells: an X-ray microanalysis study. *J. Exp. Bot.* 67, 3953-3964.

Lee, CM. and Thomashow, MF. (2012) Photoperiodic regulation of the C-repeat binding factor (CBF) cold acclimation pathway and freezing tolerance in *Arabidopsis thaliana*. *Proc. Natl. Acad. Sci. USA.* 109, 15054-15059.

Legris, M., Klose, C., Burgie, ES., Rojas, CC., Neme, M., Hiltbrunner, A., Wigge, PA., Schäfer, E., Vierstra, RD. and Casal, JJ. (2016) Phytochrome B integrates light and temperature signals in *Arabidopsis. Science* 354, 897-900.

Levitt, J. (1980) Responses of Plants to Environmental Stress, Chilling, Freezing and High Temperature Stresses. *New York: Academic Press*.

Liu, Q., Kasuga, M., Sakuma, Y., Abe, H., Miura., S., Yamaguchi-Shinozaki, K. and Shinozaki, K. (1998) Two transcription factors, DREB1 and DREB2, with an EREBP/AP2 DNA binding domain separate two cellular signal transduction pathways in drought- and low-temperature-respectively, in Arabidopsis. *Plant Cell 10*, 1391-1406.

Liss, H., Siebers, B. and Weiler, EW. (1991) Characterization, functional reconstitution and activation by fusicoccin of a Ca^{2+}-ATPase from *Corydalis sempervirens* Pers. cells suspension cultures. *Plant Cell Physiol.* 32, 1049-56.

Liu, X., Shiomi, S., Nakatsuka, A., Kubo, Y., Nakamura, R. and Inaba, A. (1999) Characterization of ethylene biosynthesis associated with ripening in banana fruit. *Plant Physiol*. 121, 1257-1265.

Logan, DC. and Knight MR. (2003) Mitochondrial and cytosolic calcium dynamics are differentially regulated in plants. *Plant Physiol*. 133, 21-24.

Love, J., Dodd, AN. and Webb, AAR. (2004) Circadian and diurnal calcium oscillations encode photoperiodic information in Arabidopsis. *Plant Cell* 16, 956-966.

Luan, S., Kudla, J., Rodriguez-Concepcion, M., Yalovsky, S. and Gruissem W. (2002) Calmodulins and calcineurin B–like proteins: calcium sensors for specific signal response coupling in plants. *Plant Cell* 14, S389-S400.

Lui, J., Whalley, HJ. and Knight, MR. (2015) Combining modelling and experimental approaches to explain how calcium signatures are decoded by calmodulin-binding transcription activators (CAMTA) to produce specific gene expression responses. *New Phytol.* 208, 174-187

Ma, Y., Dai, X., Xu, Y., Luo, W., Zheng, X., Zeng, D., Pan, Y., Lin, X., Liu, H., Zhang, D., Xiao, J., Guo, X., Xu, S., Niu, Y Jin, J., Zhang, H., Xu, X. and Li, L., Wang, W., Qian, Q., Ge, S. and Chong, K. (2015) *COLD1* confers chilling tolerance in rice. *Cell* 160, 1209-1221.

Martí, MC., Stancombe, MA. and Webb, AAR. (2013) Cell- and stimulus type-specific intracellular free Ca^{2+} signals in *Arabidopsis*. *Plant Physiol*. 163, 625-634.

Martinoia, E., Flügge, UI., Kaiser, G., Heber, U. and Heldt, HW. (1985) Energy-dependent uptake of malate into vacuoles isolated from barley mesophyll protoplasts. *Biochim. Biophys. Acta.*806, 311-319.

Martinoia, E., Schramm, MJ., Kaiser, G., Kaiser, WM. and Heber, U. (1986) Transport of anions in isolated barley vacuoles. I. Permeability to anions and evidence for a Cl-uptake system. *Plant Physiol.* 80, 895-901.

McAinsh, MR., Brownlee, C. and Hetherington, AM. (1997) Calcium ions as second messengers in guard cell signal transduction. *Physiol. Plant.* 100,16–29.

McAinsh, MR. and Pittman, JK. (2009) Shaping the calcium signature. *New Phytol.* 181, 275-294.

McAinsh, MR., Webb, AAR., Taylor, JE. and Hetherington, AM. (1995) Stimulus induced oscillations in guard cell cytosolic-free calcium. *Plant Cell* 7, 1207-1219.

McGlasson, WB. (1969) Ethylene production by slices of green banana fruit and popato tuber tissue during the development of induced respiration. *Aust. J. boil. Sci.* 1969; 22, 489-491.

Millar, AJ. (2004) Input signals to the plant circadian clock. *J. Exp. Bot.* 55, 277-283.

Miura, K. and Furumoto, T. (2013) Cold signaling and cold response in plants. *Int. J. Mol. Sci.* 14, 5312-5337.

Miwa, H., Sun, J., Oldroyd, GED. and Downie, JA. (2006) Analysis of calcium spiking using a cameleon calcium sensor reveals that nodulation gene expression is regulated by calcium spike number and the developmental status of the cell. *Plant J.* 48, 883–894.

Monroy, AF. and Dhindsa, RS. (1995) Low-temperature signal transduction: induction of cold acclimation-specific genes of alfalfa by calcium at 25°C. *Plant Cell* 7, 321-331.

Monroy, AF., Sangwan V. and Dhindsa RS. (1998) Low temperature signal transduction during cold acclimation protein phosphatase 2A as an early target for cold-inactivation. *Plant J.* 13, 653-660.

Monroy, AF., Sarhan, F. and Dhindsa, RS. (1993) Cold-induced changes in freezing tolerance, protein phosphorylation, and gene expression. *Plant Physiol.* 102, 1227-1235.

Nagai, T., Yamada, S., Tominaga, T., Ichikawa M. and Miyawaki, A. (2004) Expanded dynamic range of fluorescent indicators for Ca^{2+} by circularly permuted yellow fluorescent proteins. *Proc. Natl. Acad. Sci. USA.* 101, 10554-10559.

Nakata, PA. (2012) Engineering calcium oxalate crystal formation in Arabidopsis. *Plant Cell Physiol.* 53, 1275-.1282.

Nagel-Volkmann, J., Plieth, C., Becher, D., Lüthen, H. and Dörffling, K. (2009) Cold-induced cytosolic free calcium ion concentration changes in wheat. *Plant Physiol.* 166: 1955-1960.

Nomura, H., Komori, T., Kobori, M., Nakahira, Y. and Shiina, T. (2008) Evidence for chloroplast control of external Ca^{2+}-induced cytosolic Ca^{2+} transients and stomatal closure. *Plant J.* 53, 988-998.

Örvar, BL., Sangwan, V., Omann, F. and Dhindsa, RS. (2000) Early steps in cold sensing by plant cells: the role of actin cytoskeleton and membrane fluidity. *Plant J.* 23, 785-794.

Peltier, JB., Ytterberg AJ., Sun, Q. and van Wijk, KJ. (2004) New functions of the thylakoid membrane proteome of *Arabidopsis thaliana* revealed by simple, fast, and versatile fractionation strategy. *J. Biol. Chem*. 279, 49367-49383.

Perras, M. and Sarhan, F. (1989) Synthesis of freezing tolerance proteins in leaves, crown, and roots during cold acclimation of wheat. *Plant Physiol*. 89, 577-585.

Ping, Z., Yabe, I. and Muto, S. (1992) Identification of K^+, Cl^-, and Ca^{2+} channels in the vacuolar membrane of tobacco cell suspension cultures. *Protoplasma.* 171, 7-18.

Plieth, C., Hansen, UP., Knight, H. and Knight, MR. (1999) Temperature sensing by plants: the primary characteristics of signal perception and calcium response. *Plant J.* 18, 491-497.

Puhakainen, T., Li, C., Boije-Malm, M., Kangasjärvi, J., Heino, P. and Palva, T. (2004) Short-day potentiation of low temperature-induced gene expression of a c-repeat-binding factor-controlled gene during cold acclimation in Silver Birch. *Plant Physiol.* 136, 4299-4307.

Rajashekar, CB. and Burke, MJ. (1996) Freezing characteristics of rigid plant tissues (development of cell tension during extracellular freezing). *Plant Physiol*. 111, 597-603.

Rappaport, F., Vavasseur, A., Joyard, J., Richaud, P. and Rolland, N. (2005) HMA1, a new Cu-ATPase of the chloroplast envelope, is essential for growth under adverse light conditions. *J. Biol. Chem.* 281, 2882-2892.

Relch, R., Zlefier, WT. and Rogers, KA. (1980) Adsorption of methane, ethane, and ethylene gases and their binary and ternary mixtures and carbon dioxide on activated carbon at 212-301 K and pressures to 35 atmospheres. *Ind. Eng. Chem. Process Des. Dev.* 19, 336-344.

Rocha, AG. and Vothknecht, UC. (2012) The role of calcium in chloroplast—an intriguing and unresolved puzzle. *Protoplasma*. 249, 957-966.

Rudd, JJ. and Franklin-Tong, VE. (2001) Unravelling response specificity in Ca^{2+} signaling pathways in plant cells. *New Phytol*. 151, 7–33.

Sakai, A. and Larcher, W. (1987) Frost Survival of Plants: Responses and Adaptation to Freezing Stress. *Springer-Verlag*, Berlin.

Sangwan, V., Foulds, I., Singh, J. and Dhindsa, RS. (2001) Cold-activation of *Brassica napus BN115* promoter is mediated by structural changes in membranes and cytoskeleton, and requires Ca^{2+} influx. *Plant J*. 27, 1-12.

Schinfeld, JH. (1989) Urban air pollution: state of the science. *Science* 24, 745-752.

Seigneurin-Berny, D., Gravot, A., Auroy, P., Mazard, C., Kraut, A., Finazzi, G., Grunwald, D., Shi, Y., Ding, Y. and Yang, S. (2015) Cold signals transduction and its interplay with phytohormones during cold acclimation. *Plant Cell Physiol*. 56, 7-15.

Shi Y, Tian, S, Hou L, Huang X, Zhang X, Guo H, Yang S. (2012) Ethylene signaling negatively regulates freezing tolerance by repressing expression of *CBF* and type-A *ARR* gene in *Arabidopsis*. *Plant Cell* 24, 2578-2595.

Shimomura, O., Johnason, FH. and Saiga, Y. (1962) Extraction, purification and properties of aequorin, a bioluminescent protein from the luminous hydromedusan, Aequorea. *J. Cell. Comp. Physiol*. 59:223-239.

Sanders, D., Brownlee, C. and Harper, JF. (1999) Communicating with calcium. *Plant Cell* 11, 691-706.

Shirokova, N., Garcúa, J. and Rúos, E. (1998) Local calcium release in mammalian skeletal muscle. *J. Physiol.* 512.2: 377-384.

Short, EF., North, KA., Roberts, MR., Hetherington, AM., Shirras, AD. and McAinsh, MR. (2012) A stress-specific calcium signature regulating an ozone-responsive gene expression network in Arabidopsis. *Plant J*. 71, 948–961.

Solecka, D., Żebrowski, J. and Kacperska, A. (2008) Are pectins involved in cold acclimation and de-acclimation of winter oil-seed rape plants? *Ann. Biol.* 101, 521-530.

Steponkus, PL. (1984) Role of the plasma membrane in freezing injury and cold acclimation. *Annu. Rev. Plant Physiol.* 35, 543-584.

Steponkus, PL. and Webb, AM. (1992) Freeze-induced dehydration and membrane destabilization in plants. *Water and Life. Springer, Berlin, Heidelberg*, 338-362.

Suorsa, M., Scheller HV., Vener, AV. and Aro, EM. (2008) Light regulation of CaS, a novel phosphoprotein in the thylakoid membrane of *Arabidopsis thaliana*. *FEBS J*. 275, 1767-1777.

Suutarinen, J., Honkapää, K., Heiniö, RL., Autio, K. and Mokkila, M. (2000) The effect of different prefreezing treatments on the structure of strawberries before and after jam making. *Int. J. Food Sci. Technol.* 33, 188-201.

Suzuki, A., Kikuchi, T. and Aoba, K. (1997) Changes of ethylene evolution, ACC content, ethylene forming enzyme activity and respiration in fruits of highbush blueberry. *J. Japan. Soc. Hort. Sci.* 66, 23-27.

Tähtiharju, S., Sangwan, V., Monroy, AF., Dhindsa, RS. and Borg, M. (1997) The induction of *kin* genes in cold-acclimating *Arabidopsis* thaliana. Evidence of a role for calcium. *Planta* 203, 442-447.

Teardo, E., Formentin, E., Sefalla, A., Fiacometti, G.M. Marin, O., Zanetti, M., Lo Schiavo, F., Zoratti, M. and Szabò, I. (2011) Dual localization of plant glutamate recepror AtGLR3.4 to plastid and plasmamembrane. *Biochim. Biophys. Acta* 1807: 357-367.

Teige, M., Scheikl, E., Eulgem T., Doczi F., Ichimura K., Shinozaki, K., Dangl, JL. and Hirt, H. (2004) The MKK2 pathway mediates cold and salt stress signaling in Arabidopsis. *Mol. Cell.* 15, 141-152.

Thain, SC., Vandenbussche, F., Laarhoven, LJJ., Dowson-Day, MJ., Wang, ZY., Tobin, EM., Harren, FJM., Millar, AJ. and Van Der Straeten, D. (2004) Circadian rhythms of ethylene emission in Arabidopsis. *Plant Physiol.* 136, 3751-3761.

Thomashow, MF. (1999) Plant cold acclimation: freezing tolerance genes and regulatory mechanisms. *Annu. Rev. Plant Biol*. 50, 571-599.

Trewavas, AJ. and Knight, MR. (1994) Mechanical signaling calcium and plant form. *Plant Mol. Biol*. 26, 1329–1341.

Tuteja, N. and Mahajan, S. (2007) Calcium signaling network in plants. *Plant Signal. Behav.* 2, 79-85.

Tanino, K., Kobayashi, S., Hyett, C., Hamilton, K., Liu, J., Li, B., Borondics, F., Pedersen, T., Tse, J., Ellis, T., Kawamura, Y. and Uemura, M. (2013) *Allium fistulosum* as a novel system to investigate mechanisms of freezing resistance. *Physiol. Plant*. 147, 101-111.

Uemura, M., Joseph, RA. and Steponkus, PL. (1995) Cold acclimation of *Arabidopsis thaliana*: effect on plasma membrane lipid composition and freeze-induced lesions. *Plant Physiol.* 109, 15-30.

Uemura, M. and Yoshida, S. (1984) Involvement of plasma membrane alteration in cold acclimation of winter rye seedlings (*Secale cereal L. cv Puma*). *Plant Physiol,* 75, 818-826.

Vainonen, JP., Sakuragi, Y., Stael, S., Tikkanen, M., Allahverdiyeva, Y., Paakkarinen, V., Aro, E., Suorsa, M., Scheller, HV., Vener, AV. and Aro, EM. (2008) Light regulation of CaS, a novel phosphoprotein in the thylakoid membrane of *Arabidopsis thaliana*. *FEBS J*. 275, 1767-1777.

Wang, Y. and Hua, J. (2009) A moderate decrease in temperature induces COR15a expression through the CBF signaling cascade and enhances freezing tolerance. *Plant J*. 60, 340-349

Wanner, LA. and Junttila, O. (1999) Cold-induced freezing tolerance in Arabidopsis. *Plant Physiol*. 120, 391-399.

Ward, JM. and Schroeder, JI. (1994) Calcium-activated K^+ channels and calcium-induced calcium release by slow vacuolar ion channels in guard cell vacuoles implicated in the control of stomatal closure. *Plant Cell*. 6, 669-683.

Wasternack, C. (2007) Jasmonates: an update on biosynthesis, signal transduction and action in plant stress response, growth and development. *Ann. Bot*. 100, 681-697

Whalley, HJ. and Knight, MR. (2013) Calcium signatures are decoded by plants to give specific gene responses *New Phytol*. 197, 690-693.

Whalley, HJ., Sargeant, AW., Steele, JF., Lacoere, T., Lamb, R., Saunders, NJ., Knight, H. and Knight, MR. (2011) Transcriptomic analysis reveals calcium regulation of specific promoter motifs in Arabidopsis. *Plant Cell* 23, 4079-4095.

Wyn Jones, RG. and Lunt, OR. (1967) The function of calcium in plants. *Bot. Rev.* 33, 407-426.

Xiong, L., Schumaker, KS. and Zhu, JK. (2002) Cell signaling during cold, drought, and salt stress. *Plant Cell* 14, 165-183.

Yamazaki, T., Kawamura, Y., Minami, A. and Uemura, M. (2008) Calcium-dependent freezing tolerance in Arabidopsis involves membrane resealing via synaptotagmin SYT1. *Plant Cell* 20, 3389-3404.

Yoshida, S. (1983) Studies on freezing injury of plant cells. I. Relation between thermotropic properties of isolated plasma membrane vesicles and freezing injury. *Plant Physiol.* 75, 38-42.

Yuan, F., Yang, H., Xue, Y., Kong, D., Ye, R., Li, C., Zhang, J., Theprungsirikul, L., Shrift, T., Krichilsky, B., Johnson, DM., Swift, GB., He, Y., Siedow, JN. and Pei, ZM. (2014) OSCA1 mediates osmotic-stress-evoked Ca^{2+} increases vital for osmosensing in *Arabidopsis*. *Nature* 514, 367-371.

Zarka, DG., Vogel, JT., Cook, D. and Thomashow, MF. (2003) Cold induction of Arabidopsis *CBF* genes involves multiple ICE (inducer of *CBF* expression) promoter elements and a cold-regulatory circuit that is desensitized by low temperature. *Plant Physiol.* 133, 910-918.

Zepp, RG., Erickson, DJIII., Paul, ND. and Sulzberger, B. (2007) Interactive effects of solar UV radiation and climate change on biogeochemical cycling. *Photochem. Photobiol. Sci*. 6, 286-300.

Zhang, A. and Huang, R. (2010) Enhanced tolerance to freezing in tobacco and tomato overexpressing transcription factor TERF2/LeERF2 is modulated by ethylene biosynthesis. *Plant Mol. Biol.* 73, 241-249.

Zhao, X., Wang, YL., Qiao, XR., Wang, J., Wang, LD., Xu, CS. and Zhang, X. (2013) Phototropins function in high-intensity blue light-induced hypocotyl phototropism in Arabidopsis by altering cytosolic calcium. *Plant Physiol.* 162, 1539-1551.

Zhu, JK. (2002) Salt and drought stress signal transduction in plants. *Annu. Rev. Plant Biol.* 53, 247-73.

Zoratti, M. and Szabo, I. (2011) Dual localization of plant glutamate recepror AtGLR3.4 to plastid and plasmamembrane. *Biochem. Biophys. Acta.* 1807, 357-367.